



# UNIVERSITÀ DEGLI STUDI DI MILANO

PhD in Pharmacological biomolecular sciences,  
experimental and clinical  
XXXIV Cycle

Department of Pharmacological and Biomolecular Sciences  
BIO/16

PhD Thesis

## JNKs as therapeutic targets to tackle synaptic dysfunction in neurodevelopmental and neurodegenerative diseases

Candidate: Clara Alice Musi  
Student Number: R12324

Tutor: Prof. Tiziana Borsello  
Coordinator: Prof. Giuseppe Danilo Norata

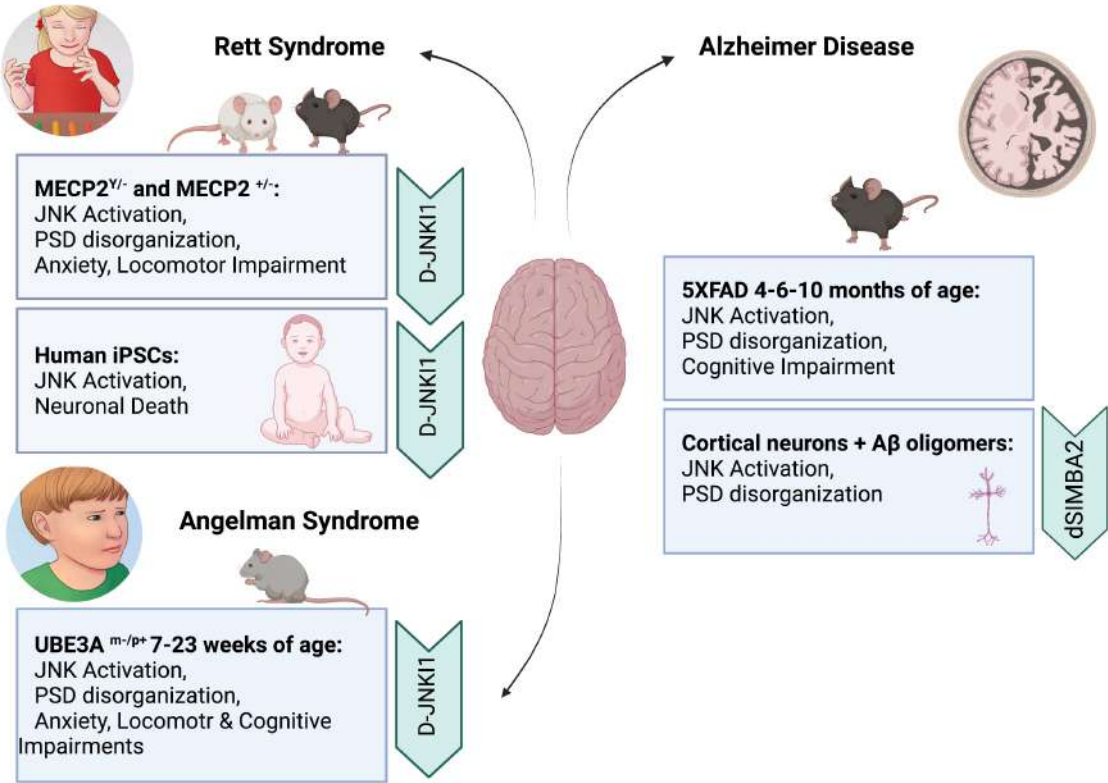
Academic Year: 2020/2021

# Graphical Abstract

---

Neurodevelopmental Diseases

Neurodegenerative Disease



# Abstract

---

Brain disorders are the first leading cause of disability and the second leading cause of death worldwide. Decoding the mechanisms of brain diseases is mandatory to improve diagnosis, neuroprotective strategies, and treatments.

Although there are many different pathological and clinical manifestations, as well as causes and molecular pathways underlying neurological disorders, increasing evidence suggest that synapses, having a crucial role in neuronal communication and brain functions, are the first station that degenerates and loses functionality in neurological diseases.

This concept has led to **the theory of brain disease**, from neurodevelopmental to neurodegenerative, **as synaptopathies**, in which the synaptic impairment is a shared pathogenic feature.

The main aim of this thesis was to dissect this concept, focusing on a specific pathway particularly involved in brain functions and dysfunctions: **the c-Jun N-terminal Kinase (JNK) signalling pathway**. More in details, we studied the role of JNK in two neurodevelopmental syndromes, Rett and Angelman, and in a chronic brain illness, Alzheimer disease, focusing on the synaptopathy as the first initial mechanism of many different brain diseases.

In **Rett Syndrome**, a rare severe developmental disease, we studied the synaptic dysfunction of two different murine models identifying JNK as an important actor downstream MECP2, the gene mutated in the pathology. We demonstrated that the specific inhibition of JNK, by D-JNKI1 treatment, strongly improved the symptoms and the molecular disorganization of the PSD region in both mice models. Then, we proved JNK activation in human neurons, differentiated from human MECP2-mutated iPSCs (**MECP2<sup>mut</sup>**), compared to the isogenic **control** expressing wild-type MECP2 allele (MECP2<sup>wt</sup>). The JNK signal was activated in the MECP2-mutated iPSCs and not in control iPSCs, and D-JNKI1 blocked the MECP2<sup>mut</sup> -induced neuronal death.

In **Angelman Syndrome**, we analysed the synaptic dysfunction in the UBE3A<sup>+/-</sup> mouse model. JNK was strongly activated in the brain of these mice, suggesting its important role also in this disorder. The D-JNKI1 treatment improved the behavioural defects, and this correlated with the stabilization of the synaptic biomarkers.

Finally, we focused on the **Alzheimer's synaptic dysfunction**, the most characterize synaptopathy, to study JNK role in a chronic illness.

Alzheimer mice model 5XFAD presented a powerful JNK activation together with synaptic dysfunction and cognitive impairment. We then centre our attention on the selective brain JNK isoform, JNK3, the most responsive to stress stimuli, finding that 5XFAD mice presented a powerful increase of JNK3 levels. Therefore, we decided to test the potential neuroprotective effect of the specific inhibition of JNK3. In fact, thanks to the collaboration with Prof. Falconi, we have in the laboratory the specific JNK3 inhibitor, dSIMBA2. Before testing this in-vivo, we studied the effect of JNK3 inhibition in an in-vitro model of synaptic dysfunction induced by A $\beta$  oligomers (ABO) to define the right dose and the neuroprotection against ABO-induced synaptic dysfunction, finding that dSIMBA2 prevents ABO toxicity and the induced-synaptopathy.

To summarize, the data obtained in this thesis participate in the reinforcement of **JNK as a central actor in the degeneration mechanisms of the synapses** that characterized both neurodevelopmental and neurodegenerative diseases. In addition, this work adds new elements to define **JNK3**, the most responsive JNK isoform to stress, as a key player in the AD, and an **important target for the treatment of synaptic injury**, potentially also in other brain illnesses. Developing new compounds able to inhibit one of the most responsive kinases to stress stimuli may be an intriguing field to explore to prevent synaptic dysfunction.



I disturbi cerebrali sono la prima causa di disabilità e la seconda causa di morte nel mondo. Lo studio dei meccanismi che sottendono queste malattie è quindi fondamentale per migliorare la diagnosi, le strategie neuroprotettive e i trattamenti.

Sebbene alla base dei disturbi neurologici vi siano manifestazioni patologiche e cliniche, nonché cause e determinanti molecolari diversi, prove crescenti suggeriscono che le sinapsi, che hanno un ruolo cruciale nella comunicazione neuronale e nelle funzioni cerebrali, sono la prima stazione che degenera e perde funzionalità nelle malattie neurologiche.

Questo concetto ha portato alla **teoria delle malattie cerebrali**, da quelle del neurosviluppo a quelle neurodegenerative, **come sinaptopatie**, in cui il danno sinaptico è una caratteristica condivisa.

Lo scopo principale di questa tesi è stato quindi quello di sezionare questo concetto, concentrandosi su una via di segnalazione cellulare specifica particolarmente coinvolta nelle funzioni e disfunzioni cerebrali: **il pathway della c-Jun N-terminal Kinase (JNK)**.

Più in dettaglio, abbiamo studiato il ruolo di JNK in due sindromi del neurosviluppo, Rett e Angelman, e in una malattia cerebrale cronica, il morbo di Alzheimer, concentrandoci sulla sinaptopatia come primo meccanismo iniziale di molte malattie cerebrali.

Nella **sindrome di Rett**, una malattia rara dello sviluppo, abbiamo studiato la disfunzione sinaptica in due diversi modelli murini identificando JNK come un importante attore a valle di MECP2, il gene mutato nella patologia. Abbiamo dimostrato che l'inibizione specifica di JNK, mediante il trattamento con D-JNKI1, migliora notevolmente i sintomi e la disorganizzazione molecolare della regione PSD in entrambi i modelli murini. Successivamente, abbiamo dimostrato l'attivazione di JNK anche nei neuroni umani, differenziati dalle iPSCs umane mutate (**MECP2<sup>mut</sup>**), rispetto al controllo isogenico che esprime l'allele MECP2 wt (**MECP2<sup>wt</sup>**). JNK è attivo nelle iPSCs con MECP2 mutato e non nelle iPSCs controllo e D-JNKI1 blocca la morte neuronale indotta da MECP2<sup>mut</sup>.

Nella **sindrome di Angelman**, abbiamo analizzato la disfunzione sinaptica nel modello murino UBE3A<sup>+/-</sup>. JNK è fortemente attivato nel cervello di questi topi, suggerendo il suo ruolo importante anche in questo disturbo. Il trattamento con D-JNKI1 migliora i difetti comportamentali e questo è correlato alla stabilizzazione dei marcatori sinaptici.

Infine, ci siamo concentrati sulla disfunzione sinaptica dell'Alzheimer, la sinaptopatia più caratterizzata, per studiare il ruolo di JNK in una malattia cronica.

Il modello murino di **Alzheimer** 5XFAD presenta una potente attivazione di JNK insieme a disfunzione sinaptica e deterioramento cognitivo. Abbiamo poi studiato l'isoforma di JNK selettiva del cervello, nonché la più responsiva agli stress, **JNK3**, trovando che i topi 5XFAD presentano un forte aumento dei suoi livelli. Pertanto, abbiamo deciso di testare il potenziale effetto neuroprotettivo dell'inibizione specifica di JNK3. Infatti, grazie alla collaborazione con il Prof. Falconi, abbiamo in laboratorio l'inibitore specifico di JNK3, dSIMBA2. Prima di testare questo in-vivo, abbiamo studiato l'effetto dell'inibizione di JNK3 in un modello in-vitro di disfunzione sinaptica indotta da oligomeri A $\beta$  (ABO) per definire la giusta

dose e la neuroprotezione contro la disfunzione sinaptica indotta da ABO, scoprendo che dSIMBA2 previene la tossicità e la sinaptopatia indotta da ABO.

Riassumendo, i dati ottenuti in questa tesi partecipano al rafforzamento di **JNK come attore centrale nei meccanismi di degenerazione delle sinapsi** che caratterizzano sia le malattie del neurosviluppo che quelle neurodegenerative. Inoltre, questo lavoro aggiunge nuovi elementi per definire **JNK3**, l'isoforma di JNK più reattiva allo stress, come un attore chiave nell'AD e un **bersaglio importante per il trattamento del danno sinaptico**, potenzialmente anche in altre malattie del cervello. Lo sviluppo di nuovi composti in grado di inibire una delle chinasi più reattive agli stimoli da stress può essere un campo interessante da esplorare per prevenire la disfunzione sinaptica.



<b>1. INTRODUCTION</b>	<b>13</b>
<b>1.1 SYNAPSES</b>	<b>14</b>
1.1.1 PRE-SYNAPTIC TERMINAL	15
1.1.2 POST-SYNAPTIC TERMINAL	16
1.1.3 INHIBITORY SYNAPSES	18
<b>1.2 SYNAPTIC DYSFUNCTION</b>	<b>22</b>
1.2.1 SYNAPTIC DYSFUNCTION IN NEURODEVELOPMENTAL DISORDERS	23
1.2.2 SYNAPTIC DYSFUNCTION IN NEURODEGENERATIVE DISEASES	30
<b>1.3 C-JUN N-TERMINAL KINASE</b>	<b>33</b>
1.3.1 MAPK	33
1.3.2 JNKs	34
1.3.4 JNKs ISOFORMS	41
1.3.5 JNKs IN NEURODEVELOPMENTAL DISORDERS	43
1.3.6 JNKs IN NEURODEGENERATIVE DISORDERS	43
1.3.7 JNKs INHIBITION	46
<b>2. AIMS</b>	<b>49</b>
<b>3. MATERIALS AND METHODS</b>	<b>52</b>
<b>3.1 ANIMAL PROCEDURES</b>	<b>53</b>
<b>3.2 BEHAVIOURAL TESTS</b>	<b>54</b>
<b>3.3 WHOLE-BODY PLETHYSMOGRAPHY (WBP) ANALYSIS</b>	<b>55</b>
<b>3.4 TRITON INSOLUBLE FRACTIONATION</b>	<b>56</b>
<b>3.5 WESTERN BLOT</b>	<b>56</b>
<b>3.6 LDH ASSAY</b>	<b>57</b>
<b>3.7 IPSCs AND IPSCs-DERIVED NEURONS</b>	<b>57</b>
<b>3.8 PRIMARY NEURONAL CULTURES</b>	<b>57</b>
<b>3.9 ALPHA SCREEN KINASE ASSAY</b>	<b>58</b>
<b>3.10 ABO PRODUCTION</b>	<b>58</b>
<b>3.11 TOXICITY STUDY AND MTT ASSAY</b>	<b>59</b>
<b>3.12 ABO TREATMENT</b>	<b>59</b>
<b>3.13 STATISTICAL ANALYSIS</b>	<b>59</b>
<b>4. RESULTS</b>	<b>60</b>
<b>4.1 JNK ACTIVATION IN IN-VIVO AND IN-VITRO MURINE AND HUMAN MODELS OF RETT SYNDROME</b>	<b>61</b>
4.1.1 MECP2 <sup>y/-</sup> BIRD MALE MICE MIMIC SEVERE AND ACUTE NEUROLOGICAL RTT SIGNS	61
4.1.2 MECP2 <sup>y/-</sup> BIRD MICE PRESENT ACTIVATION OF THE JNK PATHWAY AND PSD ALTERATIONS	63

4.1.3 THE SPECIFIC JNK INHIBITOR PEPTIDE D-JNKI1 RESCUES THE SEVERE AND ACUTE NEUROLOGICAL RTT SIGNS IN MECP2 <sup>y/-</sup> BIRD MALE MICE	63
4.1.4 THE SPECIFIC JNK INHIBITOR PEPTIDE D-JNKI1 RESCUES THE Milder NEUROLOGICAL RTT SIGNS IN MECP2 <sup>+/-</sup> JAE HETEROZYGOUS MICE	69
4.1.5 MECP2 <sup>+/-</sup> JAE HETEROZYGOUS MICE PRESENT ACTIVATION OF THE JNK PATHWAY AND ALTERATIONS IN THE PSD	71
4.1.6 FROM ANIMAL TO HUMAN iPSC MODELS: JNK PATHWAY ACTIVATION AND D-JNKI1 PROTECTIVE EFFECTS IN RETT MECP2 <sup>MUT</sup>	72
<b>4.2 JNK ROLE IN IN-VIVO MODEL OF ANGELMAN SYNDROME</b>	<b>75</b>
4.2.1 UBE3A <sup>M-/P+</sup> MICE PRESENT CHANGES IN JNK AND ERK SIGNALLING PATHWAYS ALTERATIONS AT 7 AND 23 WEEKS OF AGE	75
4.2.2 UBE3A <sup>M-/P+</sup> MICE SHOW CHANGES IN PSD BIOCHEMICAL MARKERS AND JNK ACTIVATION IN THE TIF AT 7 WEEKS OF AGE	77
4.2.3 UBE3A <sup>M-/P+</sup> MICE PRESENT BEHAVIOURAL IMPAIRMENTS AT 7 WEEKS OF AGE	79
4.2.4 UBE3A <sup>M-/P+</sup> MICE PRESENT CHANGES IN PSD BIOCHEMICAL MARKERS AND JNK ACTIVATION IN THE POST-SYNAPTIC ELEMENT AT 23 WEEKS OF AGE	81
4.2.5 UBE3A <sup>M-/P+</sup> MICE PRESENT BEHAVIOURAL IMPAIRMENTS AT 23 WEEKS OF AGE	83
4.2.6 SPECIFIC D-JNKI1 TREATMENT PREVENTS JNK SIGNALLING ACTIVATION IN 23 WEEKS OLD UBE3A <sup>M-/P+</sup> MICE	85
4.2.7 D-JNKI1 NORMALIZES BIOCHEMICAL PSD CHANGES IN 23 WEEKS OLD UBE3A <sup>M-/P+</sup> MICE	87
4.2.8 D-JNKI1 RESCUES COGNITIVE IMPAIRMENTS BUT NOT LOCOMOTOR DEFECTS	91
<b>4.3 JNK IN A CHRONIC DISEASE: TWO ALZHEIMER IN-VITRO AND IN-VIVO MODELS</b>	<b>94</b>
4.3.1 IN-VIVO MODEL-5XFAD MICE: JNK SIGNALLING PATHWAY ACTIVATION DURING TIME IN THE CORTEX AND HIPPOCAMPUS TOTAL HOMOGENATE	94
4.3.2 COGNITIVE IMPAIRMENT AND SYNAPTIC DYSFUNCTION IN 4 MONTHS OLD 5XFAD MICE	96
4.3.3 COGNITIVE IMPAIRMENT AND SYNAPTIC DYSFUNCTION IN 6 MONTHS OLD 5XFAD MICE	97
4.3.4 COGNITIVE IMPAIRMENT AND SYNAPTIC DYSFUNCTION IN 10 MONTHS OLD 5XFAD MICE	99
4.3.5 JNK3 CORRELATES WITH APP PHOSPHORYLATION AND COGNITIVE DECLINE	100
4.3.6 SPECIFICITY AND TOXICITY OF THE SPECIFIC JNK3 INHIBITOR PEPTIDE: D-SIMBA2	101
4.3.5 SET-UP OF THE IN-VITRO MODEL OF SYNAPTOPATHY INDUCED BY A $\beta$ OLIGOMERS (ABO)	103
4.3.6 DSIMBA2 NEUROPROTECTION IN-VITRO AGAINST ABO-INDUCED SYNAPTOPATHY	105
<b>5. DISCUSSION</b>	<b>107</b>
<b>5.1 RETT SYNDROME</b>	<b>109</b>
<b>5.2 ANGELMAN SYNDROME</b>	<b>112</b>
<b>5.3 ALZHEIMER DISEASE</b>	<b>114</b>
<b>6. REFERENCES</b>	<b>119</b>

# 1. Introduction

---

Neurosciences are the forefront of science, despite this, most of brain diseases are lacking effectively cure and extensive work is still needed to understand molecular, cellular and network functions of the brain to unravel the pathogenesis of complex diseases.

This challenge, probably, has its basis in the complexity of the brain that, with more than 100 billion neurons, with intricate connections forming at least 100 trillion synapses [1], is the most complex organ in biology [2,3].

## 1.1 Synapses

The synapses are the specialized site in which the communication between one neuron and another takes place, these are represented as separate pre- and post-synaptic components. The average neuron forms several thousand synaptic connections and receives a similar number. Many of these connections are highly specialized and the strength of synaptic transmission can be enhanced or diminished by neuronal activity. This plasticity is crucial for memory and other higher brain functions. There are two types of synapses: chemical and electric. Most synapses in the brain are chemical, mediating either excitatory or inhibitory action and amplifying the neuronal signals. At the chemical synapses pre- and post-synaptic terminal are separated by a small space, called synaptic cleft and there is not continuity between the cytoplasm of one cell and the next one. Cell adhesion molecules (CAMs) play the crucial role of connecting the two terminals. Among them, the most characterized are cadherins, Ig-CAMs, neuroligins, neuroligins (NLGNs), ephrins (Eph), and Eph receptors[4]. Their role is essential not only in the maintenance of the juxtaposition of pre- and post- synaptic terminal but also is required in the synaptogenesis[5].

Chemical transmission depends on the diffusion of a neurotransmitter across the synaptic cleft. The neurotransmitter is released from specialized swellings of the axons, the pre-synaptic terminal, which contain 100 to 200 synaptic vesicles each of which contains several thousand of molecules of neurotransmitter. The vesicles are clustered in a specialized region of the pre-synaptic membrane called active zone, in which the neurotransmitter is released after a depolarizing action potential. Neurotransmitter then diffuses in the synaptic cleft and binds their receptors in the post-synaptic terminal, in turn activating the receptors and leading to the opening or closing of ion channels.

It has been estimated that **synapses contain a number of proteins between ~1,900 to more than ~2,700**, including synaptic proteins involved in exocytosis and recycling of synaptic vesicles, receptors for neurotransmitters, ion channels, extracellular matrix proteins, cell adhesion molecules, cytoskeletal proteins, scaffolding proteins, membrane transporters, GTPases, phosphatases, and molecules involved in protein degradation[6,7].

### 1.1.1 Pre-synaptic terminal

Pre-synapses perform four principal functions in neurotransmitter release: they i) dock and prime synaptic vesicles, ii) recruit voltage-gated  $\text{Ca}^{2+}$  channels to allow fast synchronous excitation/release coupling, iii) contribute to the precise location of pre- and post-synaptic specializations exactly opposite to each other via transsynaptic cell-adhesion molecules iv) mediate short- and long-term pre-synaptic plasticity observed in synapses[8]. To do this, despite differences in shape and structure, the active zone of the pre-synaptic terminal is enriched in voltage-gated calcium channels and proteins mediating the exocytosis and endocytosis of vesicles. Also cytoskeletal-associated proteins, like Piccolo, Bassoon, Rab3a interacting molecule (RIM), and RIM-binding proteins are fundamental in organizing the dynamic changes occurring in this compartment[9,10] and anchoring pre-synaptic membrane proteins, such as ion channels and cell adhesion molecules[11].

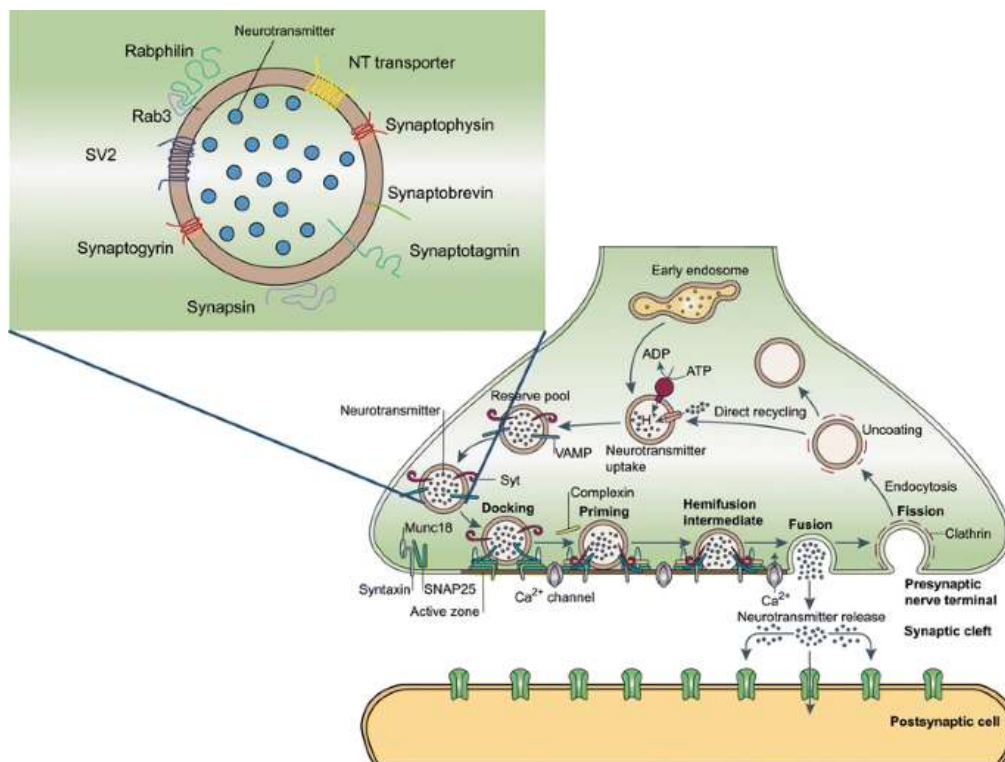


Figure 1. Schematic representation of the pre-synaptic terminal and vesicle release machinery [12].

Neurotransmitter release is mediated and facilitated by a group of highly conserved proteins, called SNAREs (soluble N-ethylmaleimide-sensitive fusion protein attachment protein receptors); particularly, v-SNAREs are associated with the vesicles while t-SNAREs contact the plasma membrane. Three or four SNARE proteins form the SNARE complex, generally syntaxin, VAMP and SNAP-25, and at least two of them must be anchored in the vesicle and target membranes through their carboxy-terminal transmembrane domains[13]. The identification and characterization of SNAREs lead to the conclusion that the mechanism of neurotransmitter release is universal a highly conserved. This allows spatial-temporal precision, accuracy, and speed of communication between neurons[14].

Since their direct role in synaptic transmission and consequently mental well-being, many clinical cases have been reported connected to SNAREs[14]. Investigating SNAREs and related proteins could shed new lights on the understanding of neuronal circuits and defects in communication, however this thesis is focalized on the other terminal of the excitatory synapses.

### 1.1.2 Post-synaptic terminal

Within the central nervous system, the majority of the post-synaptic terminal of the excitatory synapses is formed in the so-called dendritic spines: subcellular highly specialization of the dendrite compartment. In this compartment, with a relatively small volume, there is the highest concentration of neurotransmitter receptors, enzymes, scaffolding proteins, and cytoskeletal elements.

The relative length of the neck and the diameter of the head classify dendritic spines in five categories: mushroom, thin, stubby, filopodia, and branched cup-shaped spines[15,16].

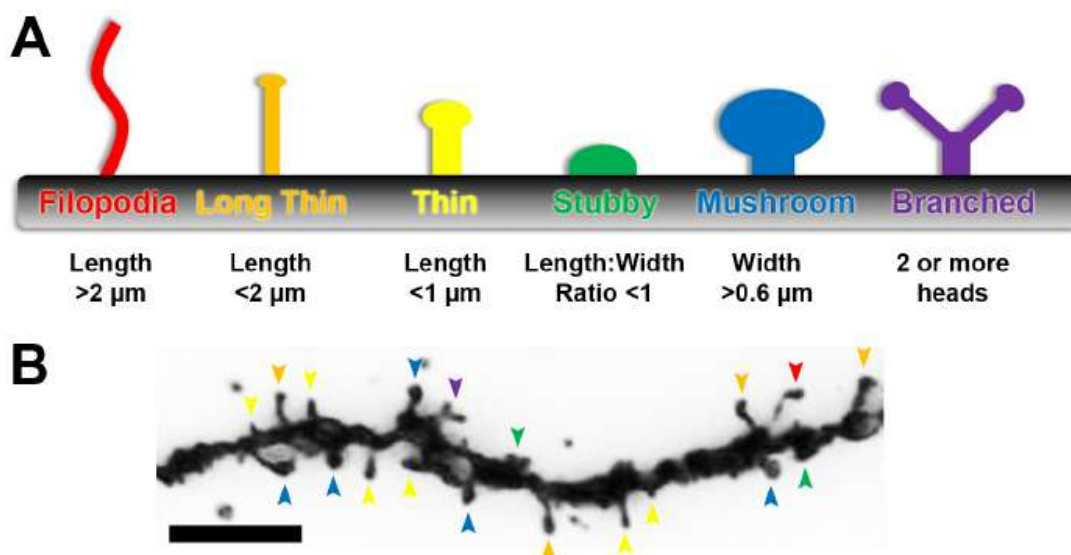
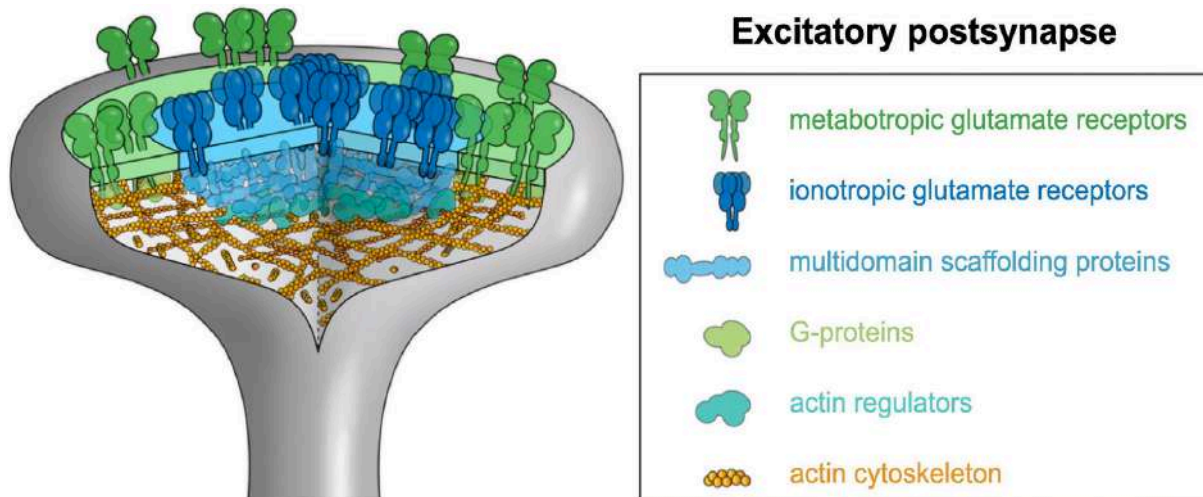


Figure 2. Classification of dendritic spines [17].

Spine head volumes range from 0.01 to 1  $\mu\text{m}^3$ , and spine necks vary between 50 and 500 nm in diameter and up to 3  $\mu\text{m}$  in length[16,18–20]. This static point of view, however, does not reflect the reality, in fact, dendritic spines are very dynamic structures that can modify size and shape within seconds to minutes and undergo more lasting changes in the time scale of hours to days. In fact, it was demonstrated that the size of the spine head correlates with the size of the post-synaptic density (PSD), and with the amplitude of the excitatory post-synaptic current (EPSC)[16,21,22].



*Figure 3. Organization of the PSD region [23].*

The PSD region is a protein-rich membrane specialization of the dendritic spines, containing more than 2000 proteins[24–26]. The communication among neurons is regulated by changes in the composition and organization of these proteins. Therefore, the isolation and quantification of synaptic proteins is a necessary and useful technique to gain insight into the ways that neurons respond to stimuli and alter synaptic function. Nowadays there are several protocols for the isolation of the PSD region, among them the centrifugation in Triton allows to isolate the insoluble fraction (TIF) in which it is possible to find an enrichment of post-synaptic proteins[27,28]. The main caveat of this technique is the impossibility of analysing dynamic variations of proteins in the PSD. However, the analysis of the TIF can give an idea of the biochemical composition of the proteins characterizing the PSD.

These proteins can be classified in i) cell-adhesion proteins, ii) cytoskeletal proteins, iii) scaffolding and adaptor proteins, iv) membrane-bound receptors and channels, v) G-proteins and modulators and vi) signalling molecules including kinases/phosphatases[15,29,30]. The major structural components of the PSD are scaffold proteins, working as a platform by binding to post-synaptic receptors, adhesion molecules, and cytoplasmic signalling proteins like kinases, phosphatases, and GTPases[31–33]. Among them, there are: -the discs large (DLG1–5) family belongs to the MAGUK superfamily which interacts with glutamate and other neurotransmitter receptors; -the SH3 and multiple Ankyrin repeat domains (SHANK1–3) protein family, which connects the system of scaffold and receptors to the cytoskeleton; -the DLG-associated proteins (DLGAP1–4) which connects the top and bottom layers of synaptic scaffolds[5,26,34–36].

The re-modelling of the PSD region, which consists in the regulation of the amount of neurotransmitter receptors and scaffold proteins, is the morphological correlate of the synaptic plasticity. The movement of neurotransmitter receptors is fine regulated between the plasma membrane and intracellular compartments[37], and they can also laterally diffuse within the plasma membrane[38]. This dynamic regulation of localization and numbers of neurotransmitters receptors depends on the synaptic plasticity, the cellular substrate for learning and memory. In fact, the long-term potentiation (LTP) and

long-term depression (LTD), have direct morphological correlates: spine head enlargement in LTP[39,40] and shrinkage of the spine head and decreased spines number in the LTD[41,42].

### **1.1.3 Inhibitory Synapses**

Inhibitory synapses are also known as asymmetrical or Type II synapses. In the CNS, the inhibition is mediated by gamma-aminobutyric acid (GABA) and glycine. Generally, inhibitory synapses are or GABAergic or glycinergic, although there are synapses that release both neurotransmitters[43].

The main scaffold proteins of inhibitory synapses is Gephyrin[44,45], that forms submembranous hexagonal macromolecular complexes[45] organizing protein-protein interactions among GABA Receptors, the cytoskeleton and several cell adhesion and signal transduction proteins[46].

Inhibitory and particularly GABAergic synapses are formed by interneurons (IN) that locally project with axonal arborization, dendritic or somatic compartments in the same anatomic structure[47,48]. Adult INs have a critical role in maintaining physiological activity levels, stabilizing and synchronizing neuronal networks preventing runaway excitation[49]. Similarly to glutamatergic synapses, also inhibitory synapses can dynamically change in response to the activity of the network with morphological reorganization of postsynaptic density or de novo formation and elimination of inhibitory contacts. However, compared to excitatory synapses, much less is known about inhibitory circuits.

**Since the focus of the thesis is the synaptopathy of the excitatory post-synaptic density, we dedicated the following chapters to the main markers analysed in this project.**

#### ***-Ionotropic Glutamate receptors***

Excitatory synapses are characterized by glutamate receptors (GluR). There are two classes of GluR: metabotropic and ionotropic. These last one, whose action is always excitatory or depolarizing, can, in turn, be classified in AMPA, Kainate and NMDA. AMPA receptors are encoded by four genes (GluA1-GluA4) and receptors are composed by two different subunits. NMDA receptors are coded by 5 genes divided into 2 groups: GluN1 and GluN2A-D. Each NMDAR has two GluN1 subunits and 2 different GluN2[50].

The subunit composition of glutamate receptors varies among different cell type and brain region and also during the development[51] and defines their functionality.

AMPA and NMDA receptors are concentrated in the middle of the PSD region, just opposite to the vesicle release site in the pre-synaptic terminal; on the contrary, metabotropic receptors are more lateral, in the pre-synaptic domains[52,53].

In particular, AMPARs are concentrated in the edge of the PSD region in order to allow a fast and efficient signal transmission[23,54,55]. The localization and function of AMPAR are fine regulated by remodelled actin cytoskeleton linked with the receptors through regulatory and adapters proteins[56–58]. NMDARs, instead, are enriched more towards the centre of the PSD[59,60]. Actin cytoskeleton plays a key role also in NMDAR stability[61], and, in turn, NMDAR activation influences cytoskeleton integrity[62].

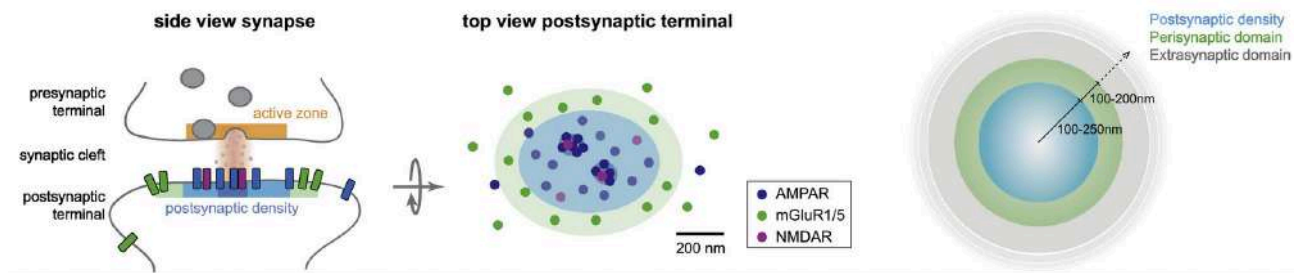


**Figure 4. Glutamate receptors localization in the PSD region[23].**

This different localization has also a functional meaning, central NMDAR allow AMPAR to turn over quickly at the periphery of the PSD, accounting for dynamic modulation of synaptic transmission[63]. In fact, AMPA receptors mediate the fast-depolarizing currents, whereas NMDA receptors are more important in modulating synaptic responses. In fact, they are voltage-dependent, higher permeable for  $Ca^{2+}$ , and coupled to intracellular signalling effectors, such as CaMKII[64]. A higher or lower increase in intracellular  $Ca^{2+}$  concentrations mediated by NMDA receptor is required for the expression of LTP or LTD.

### **-PSD95**

PSD95, a member of the membrane-associated guanylate kinase family (MAGUK), is the most abundant protein of the PSD region[29,65]. As a scaffold protein, it plays a crucial role in the trafficking, recruitment and stabilization of glutamate receptors (both AMPA and NMDA) in the membrane[66,67], controlling indirectly glutamatergic transmission and synaptic plasticity[68,69]. In particular, PSD95 directly binds NMDA via the PDZ binding domain[70], while indirectly through TARPs (like stargazing) AMPAs[66,71]. PSD95 is also implicated in the maturation of dendritic spines. Recent study demonstrates that, in-vitro, it takes at least 24 hours from the spine formation, to observe the accumulation of PD95, while other scaffold proteins like PSD-93, SAP102, and SAP97, appear early, facilitating AMPA recruitment. It seems that these proteins serve to the short-term stability of the spines, while PSD95 is essential for the long term stability[72,73]. Supporting these data, there are also studies on PSD95 knock-out mice, in which in hippocampal slices was observed increased spines turn-over and failure of spine stabilization after LTP induction[74]. On the contrary, over-expression of PSD95 increases spine stabilization, maturation[75], and AMPA transmission[74–76].

Due to its structure composed of different domains, PSD-95 undergoes to several post-translational modifications, modulating its post-synaptic localization within the dendritic spine. Among them, phosphorylation strongly modifies PSD95 stability, influencing receptors trafficking and clustering[77]. Several kinases can phosphorylate PSD95 in different Tyr, Ser and Thr residues; for instance, phosphorylation on Ser295 increases PSD-95 accumulation at the synaptic level[78,79], while in Thr19 reduced the stability of the protein in the post-synaptic membrane[80].

Effector agent	Location	Function
c-Abl kinase	Tyr <sup>533</sup>	Modulation of synapse formation by mediating PSD-95 clustering at postsynaptic sites
SrcPTKs	Tyr <sup>523</sup>	Upregulation of NMDAR function and synaptic transmission
CDK5	Tyr <sup>19</sup> , Ser <sup>25</sup> , Ser <sup>35</sup>	Regulation of PSD-95/NMDAR clustering at synapses
CK2	Thr/Ser	Regulation of the interaction of NMDARs with PSD-95 as well as surface NMDAR expression
JNK1	Ser <sup>295</sup>	Synaptic accumulation of PSD-95 triggering synaptic potentiation through the recruitment of AMPARs
SAPK3	Thr <sup>287</sup> , Ser <sup>290</sup>	Regulation of protein-protein interactions at the synapses in response to adverse stress- or mitogen-related stimuli
GSK-3 $\beta$	Thr <sup>19</sup>	Destabilization of PSD-95 within the PSD impairing AMPARs internalization and the induction of LTD
CaMKII	Ser <sup>73</sup>	Regulation of the signaling transduction pathway downstream of NMDARs and modulation of the spine growth and synaptic plasticity

**Figure 5. Main kinases involved in the phosphorylation of PSD95[77].**

### **-Drebrin**

Drebrin is an actin-binding protein, enriched in the dendritic spines that allow the formation of stable F-actin. Although F-actin is present also in the pre-synaptic terminals, Drebrin is preferentially trafficking in the post-synaptic side[81]. There are two isoforms of Drebrin: A and E. Expression of Drebrin A is neuronal specific, while Drebrin E is found in different tissues[82].

During the development, Drebrin A expression shows a profile similar to synapse formation and, indeed, it was demonstrated that Drebrin plays pivotal roles in spine formation and synaptic plasticity[82,83]. In particular, suppression of Drebrin A expression induces a delay in synapse formation and accumulation of other synaptic proteins like PSD95, CaMKII, and glutamate receptors[81,84], while its overexpression enhances spine elongation[85]. In fact, in-vitro, AMPA stimulation and intracellular Ca<sup>2+</sup> concentration increase the appearance of Drebrin A-decorated F-actin complexes at post-synaptic sites that function as a platform for the synaptic proteins[86].

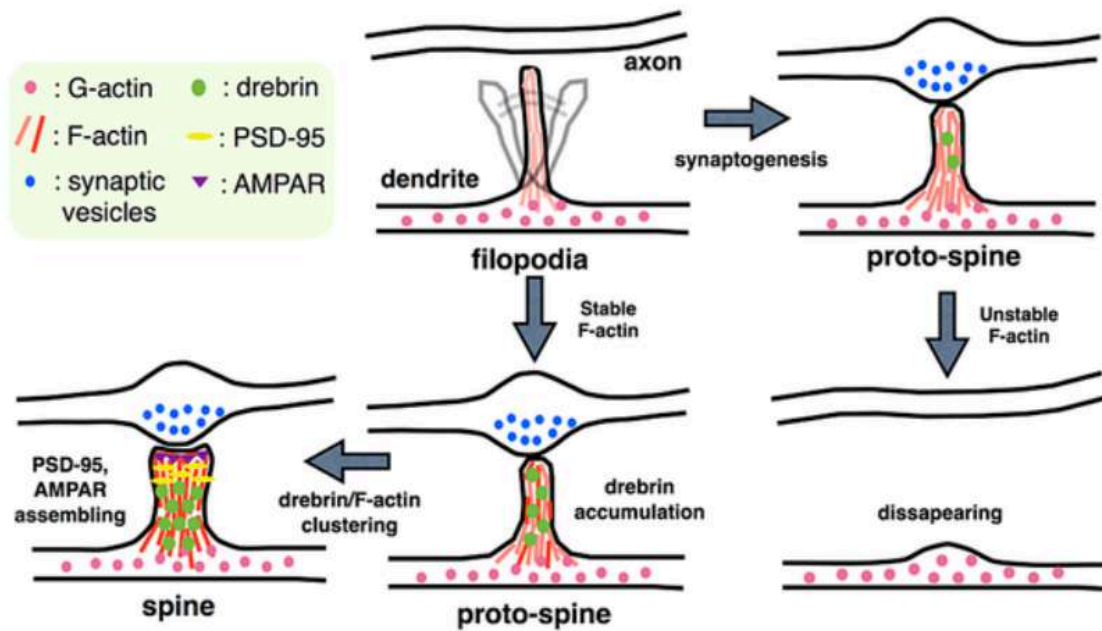


Figure 6. Schematic representation of Drebrin and F-actin as a platform for other synaptic proteins[87].

At least, 30 serine/threonine and 5 tyrosine phosphorylation sites have been found on Drebrin sequence. Despite this, phosphorylation effects on Drebrin stability are not well characterized. It is known that phosphorylation in Ser142 by cyclin-dependent kinase 5 (Cdk5) relieves the intramolecular inhibition of the actin binding domain, converting Drebrin from a single actin filament binding protein to a double actin filament binding protein co-operatively using both actin filament-binding domains[88].

### **-Shank**

Central PSD scaffolds are those belonging to the Shank family. There are three isoforms of SHANKs, coded by three different genes but with higher homology and with both overlapping and unique patterns of expression during time and spatial depending. Shank1 and Shank2 are increased during early postnatal development[89].

All Shanks can self-assemble into large scaffolds and form networks with other PSD proteins[88,90,91]; in fact, they are called “master organizing” molecules of the PSD[92,93] as they interact with large protein complexes, membrane-spanning, signalling proteins and cytoskeletal components[94]. Increased expression of Shank causes earlier maturation of the post-synapse and augmented dendritic spines dimensions. In addition, its overexpression induces the generation of spines in smooth neurons like cerebellar granule cells[95].

Ionotropic glutamate receptors (particularly GluR- $\delta$ 2 subunit) directly bind Shank[96], however, the majority of AMPA and NMDA subunits do not. NMDAr complexes bind Shank through SAPAP/GKAP, while Homer mediates the bond with metabotropic receptors. The interaction with AMPARs, on the contrary, occurs via stargazin/TARPs or SAP97 attached to the NMDA/SAP90/PSD-95 complex. Shank

serves also as a link between the receptors complex and the actin cytoskeletal. In fact, Shank can bind several classical actin-binding and modulating proteins of the PSD, such as brain  $\alpha$ -fodrin, cortactin or Abp1[67,97].

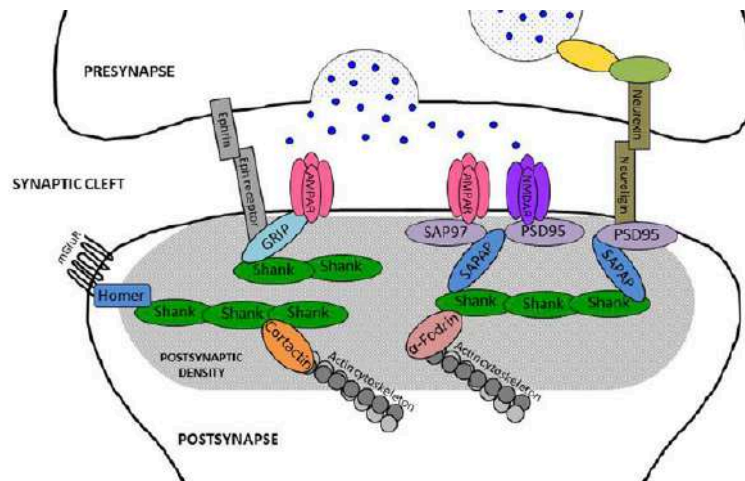


Figure 7. Shank in the post-synaptic density region[98].

## 1.2 Synaptic Dysfunction

Brain disorders represent 31,1% of all deaths worldwide, affecting 1 in 3 Europeans. The complexity of the molecular pathogenesis of this large variety of brain disorders made extremely difficult the diagnosis as well as the treatment of these diseases. Among them, neurodegenerative and neurodevelopmental disorders differ in time of onset, outcomes and pathological manifestations but, however, experimental and clinical evidence identified several shared points[99,100]. **One of them is the synaptic dysfunction: the first degenerative event of the excitatory synapses.**

Synaptopathies are therefore diseases characterized by subtle alteration of synaptic proteins, structure and function taking place at very early stages of brain diseases and include neurodegenerative disorders, such as Alzheimer Disease (AD) but also neurodevelopmental diseases like autism spectrum disorders (ASD). Of relevance, **synaptic dysfunction is closely related to behavioural impairments and occurs in an early stage of these pathologies**, implying that identification of key proteins/pathways underlining synaptopathies can lead to innovative approaches to rescue disease phenotype. Given the critical role synapses play in normal neurophysiology, it is not surprising that their dysfunction/loss may underlie many different brain diseases. Synapse dysfunction and loss has a devastating effect on neuronal communication, leading to wide ranging effects such as network disruption within central nervous systems and muscle wastage in the periphery.

“Synaptopathy” is therefore described as **the first degenerative event of the excitatory synapses**, which undergo a phase of “spine dysfunction/injury” common to **many brain diseases**. This process is dynamic and is composed by an **initial reversible phase**, during which synaptic function is impaired; in

***the second phase, the spine injury progresses in an irreversible stage***, associated with synaptic loss, and eventually neuronal death and cognitive impairment[101].

Because synaptic injury precedes neuronal death and surviving neurons possess a remarkable capacity of repair, understanding the cellular mechanism and intracellular pathways characterizing spine's injury, will allow preventing it and promoting synaptic plasticity and functional recovery.

Therefore, targeting a therapy to prevent synaptic dysfunction will have a great potential against many different brain illnesses.

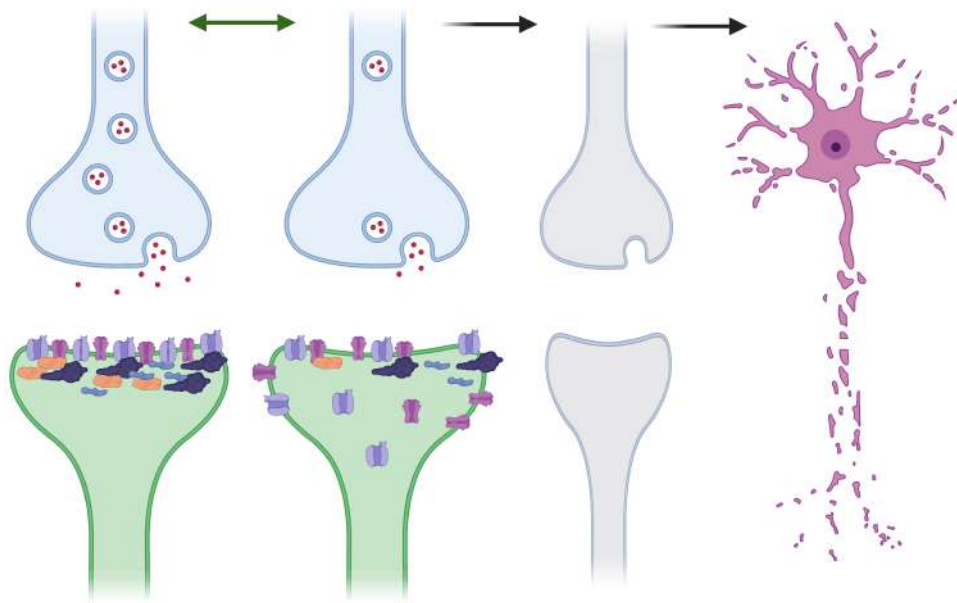


***Figure 8. Representation of the Synaptic Dysfunction process.***

**In this project, we studied and described synaptic injury before in neurodevelopmental diseases (Rett and Angelman Syndromes) and then in Alzheimer disease.** We chose to study these diseases because evidence in the literature suggests that they are all characterized by a dysfunction of the synapses. This dysfunction occurs at different stages in patients' lives, but we strongly believe that the underlying mechanisms are similar. To confirm this idea, we chose Rett, Angelman and Alzheimer as three prototypes of neurodevelopmental and neurodegenerative diseases for which robust animal models were available.

### **1.2.1 Synaptic Dysfunction in Neurodevelopmental Disorders**

Neurodevelopmental disorders (ND) are a class of diseases characterized by the impairment of one or more brain functions like cognitive, emotional, motor, and behavioural. Despite the great variety of symptoms, the most common ones are difficulties in social relationships and communication, inflexibility, and mentalizing[102]. Autism spectrum disorder (ASD) is the prototype for the

neurodevelopmental disorders, even if, some of them, including Rett syndrome, are not considered ASD but possess some autistic-like features. Despite the extensive research in this field, the common pathways underlying these disorders are still unknown. Nevertheless, the primary mechanisms of ASD are the disruption of synaptic connectivity[103].

Whether synaptic dysfunction is a reversible mechanism in ASD is still under investigation; this is an important point and may represent an important therapeutic window for reversing the pathological process. To obtain the proof of principle for reversion of a specific neuronal defect, mouse models carrying similar mutations to those identified in humans have been generated. These models are used to test the potential for reversibility and to discover the mechanisms underlying the pathologies, but species-specific differences might limit direct predictions in humans[104,105].

What is known is that ASD may start from deregulation of signalling pathways in the synapse, like post-translational modifications of synaptic proteins, altered gene transcription and translocation of mRNA in the synapses or impairment in neurotransmission in the early stages of the CNS development[106]. Several functional, anatomical and histological changes have been reported, also with contradictory results both in humans and animal models, but are relatively not understood, and may either weaken or intensify neuronal communication[107]. The two most studied ND are X fragile Syndrome (FXS) and Rett, **both suggesting that altered synaptic signalling is a key element in the pathophysiology of ASDs**. This altered neuronal activity is a reflection of disturbed synaptic integrity, which can be affected by abnormal morphology and expression of adhesion molecules, scaffolding proteins, as well as synaptic proteins like neurotransmitter transporters and receptors that in turn influence neuronal excitability and synaptic function[108].

In ND it seems that alterations in dendritic spines are due to abnormalities in synaptic pruning. Normally, during childhood and adolescence, the dendritic spine numbers decrease by 45%, on the contrary, in autistic patients, it is reduced only by 16%[109].

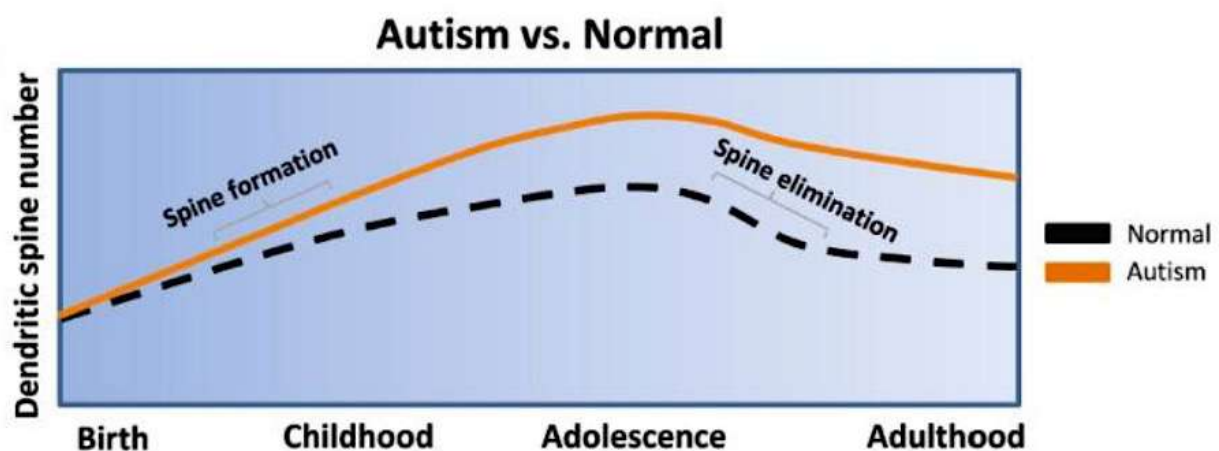


Figure 9. Comparison between normal and autism dendritic spines number[110].

This is confirmed by analysis on *post mortem* brain of autistic patients that reveal a higher average dendritic spine density in the frontal, temporal and parietal lobes associated with no epileptic seizure but with decreased brain weight and cognitive impairment[111]. In addition, recent works on iPSCs and mice models supported the hypothesis of synaptic dysfunction[112], showing altered white matter development of the tract related to cognitive, social and emotional functions, suggesting altered brain connectivity from childhood to early adulthood of ASD patients[113].

One of the shared symptoms in ND is the difficulty facing visual recognition and verbal expression, and these are probably due to the poor connections between frontal and temporal cortex[107,114]. Connectivity is also altered and characterized by low transmission and decreased connection in areas involved in the language processing, while it is particularly intense in primary paralimbic cortices[115]. This idea of loss of specialization of cortical regions[116] is in line with altered spatial relationships between cortical neurons and by alterations in shaping/size of the neuronal minicolumns grouping neurons with same receptive fields[117,118].

Another common feature in the autistic brain is the imbalance between excitatory/inhibitory transmission, resulting in the disruption of the formation of cortical networks and impairment in the information processing[108]. All the main neurotransmitters systems (nicotinic, glutamatergic, and GABAergic) seem to be impaired in ND.

Nicotinic receptors are reduced in cortex and cerebellum[119] of ASD patients, and particularly, Purkinje and granule cells show reduced affinity for the nicotinic receptor subunits alpha-3, alpha-4 and beta-2[120], however, how these reductions may be related to ASD neuropathology is unclear.

Concerning the GABA transmission, most of the studies report a decreased parvalbumin expression resulting from a lower number of PV neurons; accordingly with this observation there is a reduction of the levels of GABA receptors in parietal and frontal cortex and cerebellum of autistic patients compared to ctr[121,122]. This downregulation of GABA transmission may reflect an excitation/inhibition imbalance. In line, also receptors and transporters for the glutamate are deregulated[123], with decreased or increased levels of both ionotropic and metabotropic receptors levels depending on the age and area analysed[121,124]. In addition, results from magnetic resonance spectroscopy imaging (MRSI) confirm this E/I imbalance with lower GABA levels and higher glutamate levels in ASD subjects[125–127]. Overall, this imbalance influences the processes of information within the brain and behaviour like susceptibility of seizure. Also genetic mutation can contribute to the aberrant excitatory and inhibitory circuits[128].

Currently 910 genes are associated with ASD (Simons Foundation Autism Research Initiative, 2017) and include gene coding for proteins involved in protein translation and synaptic signalling[129,130].

Concerning the synapse, most of the candidate gene encode for typical PSD proteins[131] like scaffold proteins or ion channels. In fact, many of the mutations associated with ASD lead to alterations in excitatory or inhibitory neurotransmission that disrupt activity-dependent signalling and activity-dependent synapse development, maturation and refinement[132].

Among them, rare mutations associated with ASD have been found in Shank family[132]. In a screen of 226 families, particularly SHANK3 gene is mutated[133]. SHANK3 is a scaffold protein important in the direct regulation of both AMPA and NMDA signalling, but also in the regulation of the link between pre- and post-synaptic terminal binding neuroligins[134]. Data on patients are also confirmed by pre-clinical model, in which the knock-out of the gene results as reduced LTP in the hippocampus, mild autistic behaviour and reduced cognitive performances[133].

PSD-95 is another high-risk gene involved in autism-spectrum disorders[135], also proved in mice model. PSD-95 knock-out mice exhibit similar autism spectrum disorders behaviour and decreased vocalization[136].

Also rare mutations in multiple members of the neuroligin and neurexin families of synaptic adhesion have been found to be associated with ASD. Mice models carrying these mutation show alterations in excitatory or inhibitory neurotransmission[137]. All these genes encode for “supporting synaptic proteins” with a critical role in synaptic activity.

On the other hand, a substantial number of genes associated with ASD are also coding for of the NaV, CaV, and potassium channel families, as well as HCN channels[138] that have a direct detrimental effects on dendritic excitability.

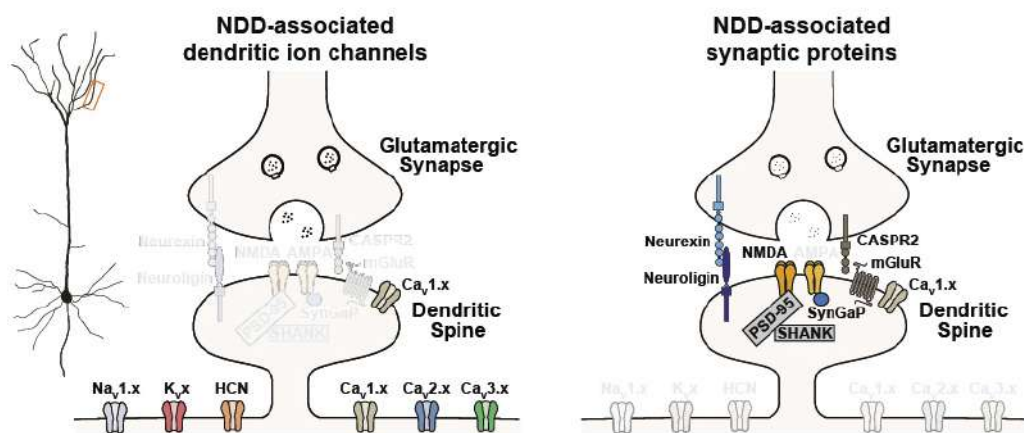


Figure 10. Schematic representation of synaptic proteins involved in ASD[138].

**We will here introduce synaptic dysfunction in neurodevelopmental diseases: Rett and Angelman Syndromes.**

### - Rett Syndrome

Rett syndrome (RTT) is a rare disease and is the second leading cause of genetic cognitive impairment in women[139], with an incidence of 1:10,000–20,000 live births; males are infrequent and rarely survive past birth[140]. 95% of cases are caused by de-novo loss-of-function mutations of the X-linked methyl-CpG binding protein 2 (MECP2) gene[141].

RTT is a progressive neurological disorder that evolves in different stages. After a pseudo-normal development in which patients usually achieve normal neurodevelopmental milestones, motor functions and communication skills, between 8 and 36 months of age regression starts and the with cognitive impairments that progress with many other severely disabling problems[142,143], including growth failure, epilepsy, gastrointestinal disorders, scoliosis and cardio-respiratory abnormalities[144–146], abnormal muscle tone and autistic features (20-50% of cases)[147,148]. Particularly, four manifestations are fundamental for the diagnosis: i) loss of language, ii) loss of fine motor coordination; iii) locomotive impairment and vi) hand stereotypes[149].

The first phase of the disease is the stagnation characterized by developmental delays followed by a rapid regression stage and the plateau stage during which the symptoms become more common, but the communicative skills may improve. The last phase is characterized by sever physical disability that led patients to become wheelchair dependent[150].

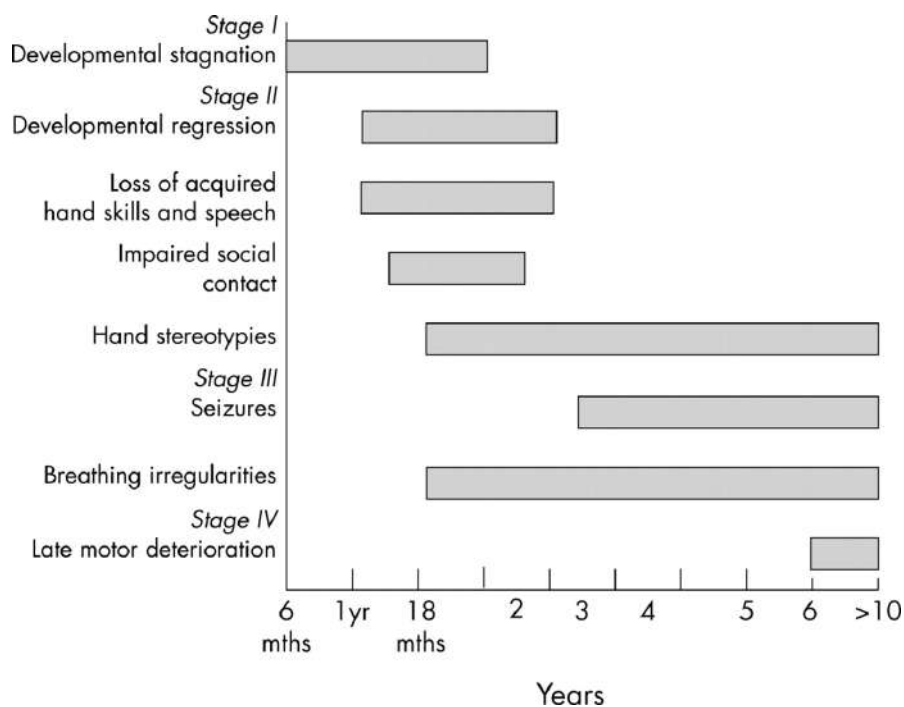


**Figure 11. Schematic representation of Rett Syndrome symptoms appearance during time**[151].

MECP2 expression in both human and mouse brains is correlated with the maturation and differentiations of neurons in the CNS[152]. In the normal brain, Mecp2 allows synapses formation, remodelling and stabilization and the effect of MECP2 deletion can be found at different levels in the brain: -firstly, in an increase of peri-somatic GABAergic terminal[153] and decrease excitatory projections[154]; -secondly, in specific synapses with changes in inhibitory and excitatory potency and excitability), -lastly the efficacy of synapse is impaired by the status of post-synaptic target neurons[149]. Recent studies report that subtle changes in connectivity and communication among neurons[155], density, stability and turnover of dendritic spines are altered in RTT brains[156]. There

is also a shift of the excitatory/inhibitory balance, observed both in murine and human models[157], in favour of excitation that helps to explain the RTT-brain defects and symptoms like seizures and hyperkinetic movements[158–160]. In particular, the brainstem, a brain area crucially involved in regulating autonomic functions, presents defects in synaptic transmission[161] with strongly depressed GABAergic synaptic transmission[162] and reduced expression of tyrosine hydroxylase [163,164] in line with the severe breathing abnormalities displayed by both mice and Rett patients[165]. There are also several evidence reporting reduced dendritic spines in different cortical and hippocampal region of Rett patients[166].

Rett is potentially treatable since Rett patients do not display neuronal death[150], despite the many efforts in the understanding of Rett pathogenesis, no treatments are available to cure this pathology. Interfering with key proteins downstream MeCP2, by bioactive tools, could lead to the development of effective therapeutic intervention in-vivo.

### **- Angelman Syndrome**

Angelman syndrome (AS) is a rare neurodevelopmental disorder[167]. The primary cause of Angelman syndrome is the selective loss of function of the maternal allele UBE3A, coding for E6AP protein, together with imprinting or silencing of the paternal chromosome 15q11-13 in the brain[168].

Both males and females are equally affected and the incidence of AS varies from 1 in 20,000 to 1 in 12,000 live births[169]. The developmental delay emerges around 6 months of age, becoming more apparent after 12 months[170] and reaching a plateau at 24–30 months[171]. Children with AS have strong deficits of fine and gross motor skills, absence of speech, intellectual disability and abnormal demeanour[170]. In addition, the 80% of the patients have epilepsy and sleep problems[170,172]. AS patients' life span could be quite long, around 60/70 years old. The early mortality is attributable to complications of seizures, or to accidental events due to their very inquisitive, hyperactive, and exploratory behaviours[173].

Consistent	Frequent	Occasional
Functionally severe intellectual disability	Microcephaly with flat occiput/occipital groove	Scoliosis
Movement/balance disorder	Seizures	Hypopigmentation
Speech impairment	Abnormal EEG	Increased sensitivity to heat
Behavioral phenotype (easily excited, happy, frequent laughter, hypermotoric)	Gastrointestinal difficulties (feeding problems, gastroesophageal reflux, constipation)	Growth disturbance depending on genotype
	Fascination with water or crinkly items	Ocular problems (refractive and alignment errors)
	Mouthing behavior	
	Ankle pronation	
	Sleep disturbance	

*Figure 12. AS Main symptoms and frequencies*[174].

Autopsy studies performed on the brains of AS patients have shown a decrease in brain size, with moderate brain atrophy. In particular, at the cerebellar level, the loss of Purkinje cells and granular cells and an extensive gliosis of Bergmann cells were found, while, at the cortical level, there was a decrease in the dendritic arborization of the pyramidal neurons of layers III and stratum V and abnormal genesis of the dendritic spines[168].

Growing literature evidence revealed a role for E6AP in neuron structural development as well as in dendritic spine development and plasticity[175,176]: Ube3A<sup>m-/p+</sup> AS mice displayed aberrant dendritic spines density and morphology, with variability in spine neck length and head size[177,178]. In addition, another key feature in AS brain, caused by loss of E6AP, is an E/I imbalance in the brains of Ube3A<sup>m-/p+</sup> mice, which may also contribute to seizure susceptibility[179]. However, little is known about the neuronal function of the UBE3A in control conditions and even less about the pathogenesis linked to UBE3A-related disorders, as well as the mechanisms that link UBE3A to dendritic spine are not clear yet.

To date, there is no cure for AS and therapeutic approaches are mostly based on genetic strategies[180]. Understanding synaptic injury in AS will help in the development of tailored synapse-targeted therapies. In fact, several strategies are focused on targeting specific cellular pathways altered by the lack of UBE3A, like dopaminergic pathways and phosphorylation of calcium/calmodulin-dependent kinase II (CaMKII), dendritic spine maturation, synaptic signalling pathways or mitochondrial dysfunction[181].

### 1.2.2 Synaptic Dysfunction in Neurodegenerative Diseases

Neurodegenerative diseases (NDD) are a class of different neurological disorders with a very large variety of clinical and pathological features, specifically affecting subgroups of neurons in specific brain regions[182]. Among them, the most frequent are Alzheimer's disease (AD), Parkinson's disease (PD), Multiple sclerosis (MS), and Huntington's disease (HD), all characterized by progressive and selective loss of functioning neurons associated with sensory, motor, and cognitive impairments[183]. Although neuronal death is the final stage of all these pathologies, it is difficult to think that neurons are functioning until the moment of the death, thus, neuronal death is the result of a pathological process already active and prolonged over time.

Another shared feature of NDD is the accumulation of aberrant misfolded proteins, different in different pathologies but with similar detrimental results[184]. Among them, alpha-synuclein ( $\alpha$ Syn) in PD[185], Tau and APP in AD[186] and Huntingtin (HTT) in HD[187] accumulate and mislocalize in neurons affecting synaptic terminal composition, organization and function[188–190].

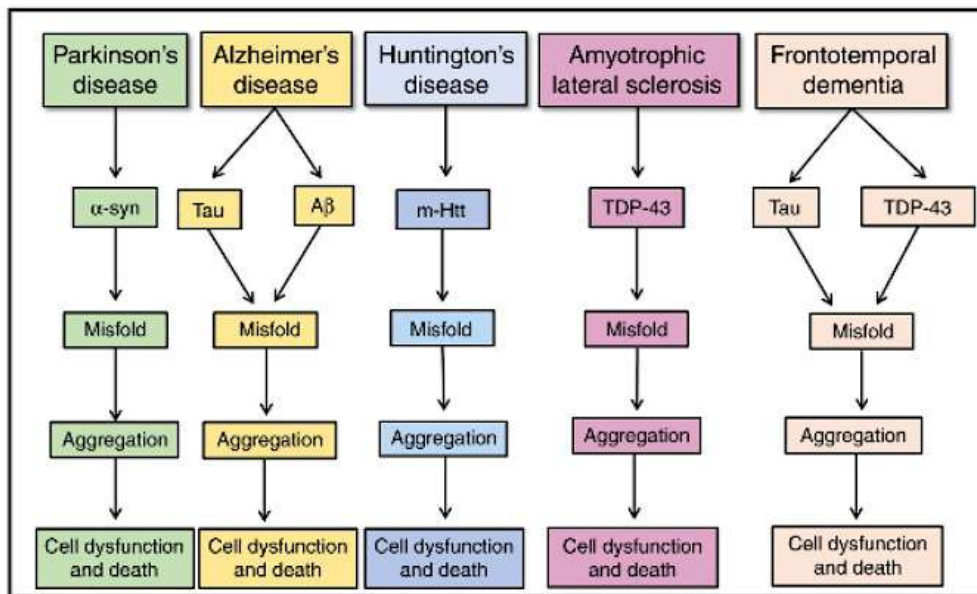


Figure 13. Neurodegenerative diseases common pathological hallmarks[191].

Understanding the initial phase of synaptic dysfunction in neurological disorders, however, is challenging because of limited and usually late-stage access to human tissues and of the long prodromal phase of these pathologies that delay the diagnosis.

In fact, some pioneering pharmacological strategies are targeting synaptic dysfunction by inhibiting key player interactions between proteins of the PSD region using cell-permeable peptides reveals strong therapeutic promise. For example, peptide disruption of PSD95 interactions with neuronal nitric oxide synthase (nNOS) or with the NMDA receptor results in decreased excitotoxic and ischemic damage in stroke models[192]. In particular, the PSD95-nNOS inhibitor peptide (Nerinetide) reduces ischemic

brain damage in patients undergoing endovascular repair of brain aneurysms and is now in phase III of the clinical trial against acute stroke[193].

With regards to neurodegenerative diseases, peptides that uncouple GluN2A binding to PSD-MAGUKs significantly reduced dyskinesias in PD rodent models[194]. In addition, the c-Jun N-terminal kinases (JNKs) inhibitor peptide, D-JNKI1, has been used in an increasing number of diseases animal models, including diabetes, stroke, neurotrauma, hearing loss and Alzheimer's disease, resulting in a potent neuroprotective compound. The efficacy of this peptide shows that JNK inhibition is a promising effective strategy for the treatment of these diseases and opens the possibility for testing whether JNK inhibition will have clinical perspective.

**AD is the most frequent among neurodegenerative diseases and has the most characterized synaptic dysfunction, for these reasons we focus on AD.**

### **- Alzheimer Disease**

Alzheimer's disease (AD) is an irreversible progressive neurodegenerative disorder characterized by learning and memory decline, intellectual retardation and emotional disturbances[195].

There are only 4 available Food and Drug Administration (FDA) approved treatments for AD that, however, have limited effects on cognitive improvement. Therefore, AD remains inexorable and incurable[196], representing the fifth leading cause of death globally[197]. 5.8 million people are affected by AD in the United States and 2,5% of 65-69 and 40% of 90-94 years population in Western Europe[198].

Despite in the last 25 years, several evidence demonstrate that the two main hallmarks of the disease are the accumulation of A $\beta$  and Tau insoluble species and plaques, the exact pathological cause for AD is still unknown[195]. In fact, 30% of over 75 population, medically normal, at the autoptoc analysis reveal neuropathological indications of AD[199,200].

Experimental data derived from studies on oligomers (the toxic species derived from the amyloidogenic cleavage of APP) derived from both humans and transgenic mice demonstrate that soluble, low-number oligomers can impair the activity-dependent modulation of synaptic strength and synaptic plasticity leading to synaptic loss and decrease in dendritic spine number. Larger aggregates of oligomers, like dodecamers, also exhibit neurotoxicity[201].

Therefore, intraneuronal accumulation of A $\beta$ , particularly the soluble and oligomeric A $\beta$  species, is considered more toxic than insoluble forms, that accumulate into plaques within the brain parenchyma[202]. The deposition of this plaques formation is followed by the formation of Neurofibrillary Tangles (NFTs), which would be more likely to cause the observed neuronal dysfunction

and degeneration since the spreading of tau pathology is highly correlated with the patterns of clinical symptoms and cognitive decline[203].

Pathological tau produced by posttranslational modifications, like phosphorylation, acetylation, ubiquitination and truncation, leads to conformational changes, aggregation, NFT formation and finally synaptic dysfunction[204,204]. The pathological tau induces synaptic dysfunction in several ways, including reducing the mobility and release of pre-synaptic vesicles, decreasing glutamatergic receptors, impairing the maturation of dendritic spines at post-synaptic terminals, disrupting mitochondrial transport and function in synapses, and promoting the phagocytosis of synapses by microglia[204].

Furthermore,  $\beta$ -amyloid and Tau are strongly related in fact, in 1/3 of synapses,  $A\beta$  and Tau co-localize in AD brain[205]; in addition, amyloid- $\beta$  promotes tau mislocalization in the dendrites, which in turn can affect the accumulation of  $A\beta$ [206].

Synaptic loss and synaptic dysfunction are the two key components of the neurodegenerative process of AD, especially in early AD. Synaptic dysfunction includes changes in the morphology and function of pre-synapses, dendrites, post-synapses, and synaptic clefts and synaptic loss is an early indicator of neuronal dysfunction[207].

In mild cognitive impairment patients (a condition that often evolves in AD), hippocampal synapses begin to decline[208]; then, patients in the middle phase of AD display a reduction of 25% in the pre-synaptic vesicle proteins[209]. With the progression of the disease, synapses are lost, and this loss is the best correlate with dementia[210–212].

These alterations affect all the main neurotransmitter systems in the brain, both cholinergic[213], GABAergic[214] and glutamatergic networks[215] resulting in the deregulation of neurotransmitter receptors levels, scaffold proteins, causing impairments in the mechanism of synaptic plasticity and imbalanced between excitatory and inhibitory transmission.

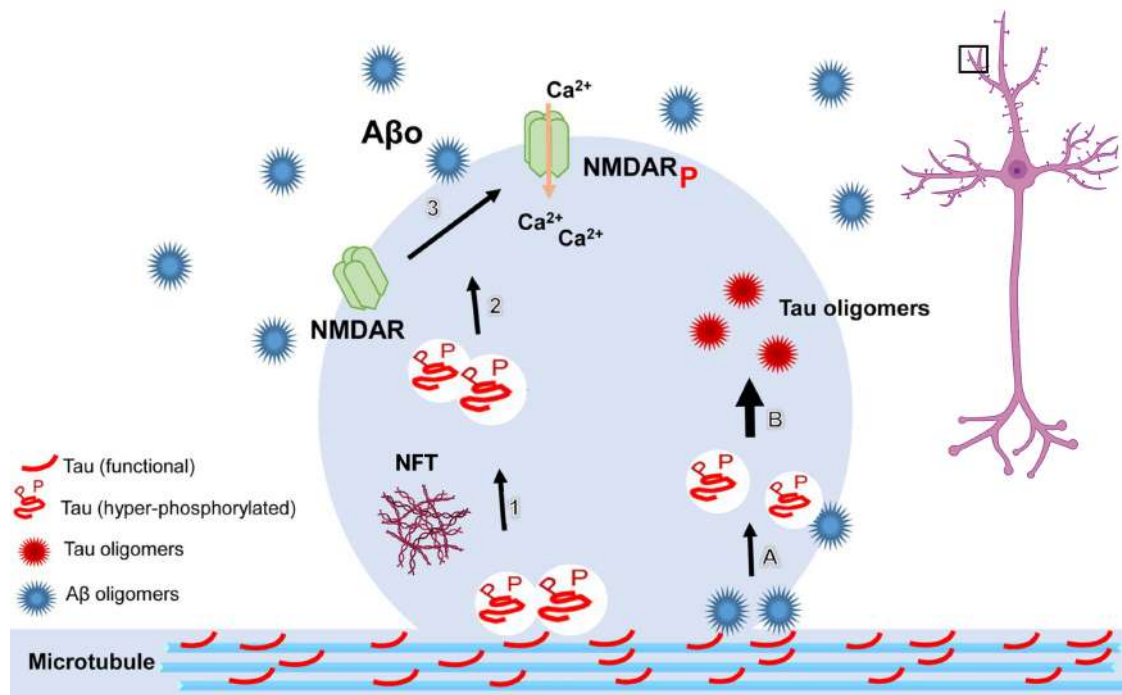


Figure 14. *Aβ and Tau Toxicity (Adapted)*[216].

Despite the efforts in drug discovery, no definitive cure for AD are available, and the majority of ongoing phase III clinical trials are focused on trying to stop or clearing Aβ plaques. Their failure leads to thinking of alternative intervention strategies downstream of Aβ and Tau, in the early events of synaptic dysfunction; being able to block this process, in the still reversible initial stages, would bring a huge improvement to the expectations and living conditions of AD patients.

**Among different stress signalling pathways involved in Synaptic diseases we focus on c-Jun N-Terminal Kinase that is a common key mediator in all the described pathologies.**

### 1.3 c-Jun N-Terminal Kinase

#### 1.3.1 MAPK

In mammals, the conventional MAPKs are classified into four specific classes: the ERK 1/2 module, the p38, the ERK5 and the JNK modules[217].

ERK1 and ERK2 are expressed in all tissues, with high levels in the brain, skeletal muscle, thymus, and heart[218] while ERK5 is expressed to various extents in all tissues, with particularly high levels in the brain, thymus, and spleen[219].

P38 is present in 4 different isoforms: p38α, p38β, ubiquitously expressed in all cells and tissues and p38γ, and p38δ with a more restricted expression and specialized functions[220]. Lastly, JNK family includes three isoforms (JNK1, JNK2 and JNK3).

ERK1/2 and ERK5 are involved in the mechanisms of cell proliferation, differentiation, and growth; instead, p38 plays a critical role in normal immune and inflammatory responses since it is activated by

chemo attractants, cytokines, chemokines and LPS and it can regulate cytokines expression[221]. JNKs cascade is triggered by several stress stimuli[222] and play a central role in apoptosis but also in migration and neuronal polarity, axogenesis, dendritic elongation and spines maturations[223]. Each MAPK is activated by dual phosphorylation mediated by a MAPK kinase (MAP2K) that is activated by the phosphorylation of another MAPKK kinase (MAP3K). The extent and timing of MAPK activation are also controlled by MAPK phosphatases (MKPs), which are highly conserved enzymes involved in the regulation of MAPK signalling. The regulation and balance between these physiological and/or pathological cellular mechanisms and the specificity of response to the signal are relevant processes within the signalling pathways involving MAPKs cascade.

### **1.3.2 JNKs**

JNKs are serine/threonine protein kinases belonging to the MAPKs mitogen-activated protein kinase (MAPK) displaying distinct patterns of subcellular localizations in neurons that underlie their pleiotropic actions, differentiated in two main categories: physiological and stress-inducible[224].

There are three genes, *Mapk8*, *Mapk9* and *Mapk10*, encoding for ten different JNK splicing variants. While JNK1 and JNK2 are widely expressed in all body tissues, JNK3 is expressed at very high levels only in the central nervous system (CNS), and less in cardiac smooth muscle and testis[101].

JNKs differ from classical MAPKs, because their activities are more potently induced in response to cellular stress rather than to mitogens[225]; in fact, they are activated in response to cytokines, heat shock, ionizing radiation, growth factors, oxidant stress and DNA damage, DNA and protein synthesis inhibition[226] and in response to endoplasmic reticulum stress[227].

JNKs, like all MAPKs members, are part of the modular cascade of the three-kinases signalling pathways (MAP3K – MAP2K – MAPK). For JNKs, mitogen-activated protein kinase kinases (MAP2K) are represented by MKK4 and MKK7 that directly activate JNKs phosphorylating them preferentially on tyrosine and threonine respectively. As both these phosphorylations are necessary for JNKs full activation, MKK4 and MKK7 likely co-operate to activate JNK[228]. In turn, they are activated in response to environmental stress[229]. On the contrary, there are at least 14 MAP3K kinases that allow a wide range of stimuli to activate the JNK pathway. Among them, known MAP3Ks in the JNKs signalling cascade are ASKs (apoptosis signal-regulating kinases), DLK (dual leucine zipper kinase), MEKKs (MAPK/extracellular-signal-regulated kinase kinase kinases), MLKs (mixed-lineage protein kinases), TAKs (transforming-growth-factor- $\beta$ -activated kinases) and Tpl2 (tumour progression locus 2)[230].

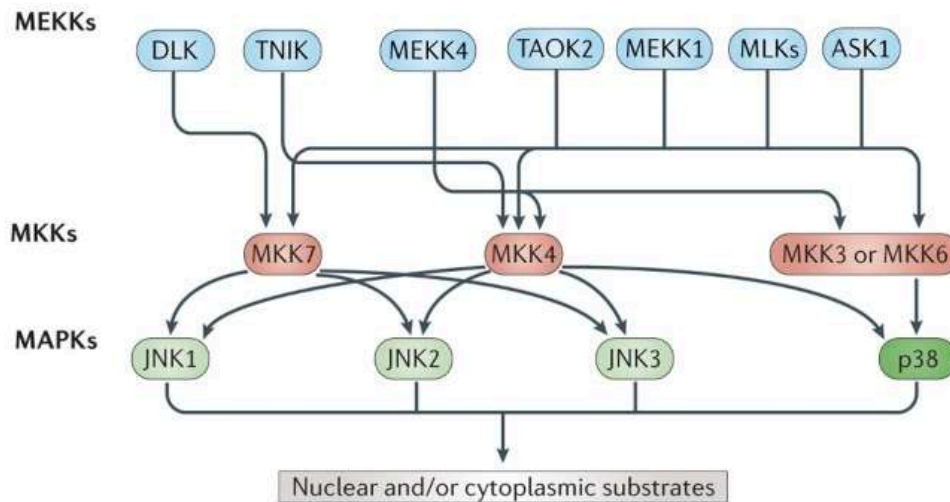


**Figure 15. The JNK cascade**[224].

As described in figure 15, some MAP3Ks and MAP2Ks are shared among MAPKs pathways, in particular between JNKs and P38, facilitating crosstalk and signal integrations among MAPKs. In this context, scaffold proteins, that do not have catalytic activities but organize the signalling module, play an important role in accelerating and isolating a single MAPK cascade, preventing crosstalk with other pathways and promoting signal specificity[101]. In fact, there are probably two coexisting types of MAPK/JNK cascade activation modules. In the first one, the simplest, MAPK members interact by direct protein-protein interactions[231]; in the second, the scaffold proteins that link the different MAP kinases, bringing them closer and accelerating the reaction cascade, assemble the module. In living cell, these two processes probably coexist, but the biological meaning is difficult to interpretate also due to scarce literature on the matter[101].

As cellular sensors, JNKs have signalling properties that allow processing and propagation of stimuli. Among them, there are -the ultrasensitivity, (a small increase in stimulus produces a very large response after a threshold is crossed); - the hysteresis, (a sort of memory reflected in the sustained activation of MAPK when the stimulus has disappeared); - digital response (all-or-none response at a single cell level)[232]. JNK cascade also exhibits switch-like responses to a variety of stimuli[233] .

Particularly in neurons, that have subcellular compartmentalization (cytoplasm and nucleus), but also functionally specialized compartments (axons, dendrites, and dendritic spines), JNKs play different roles depending on its localization and targets. More important, JNKs are not static in each cellular compartment and can be translocated along the cells.

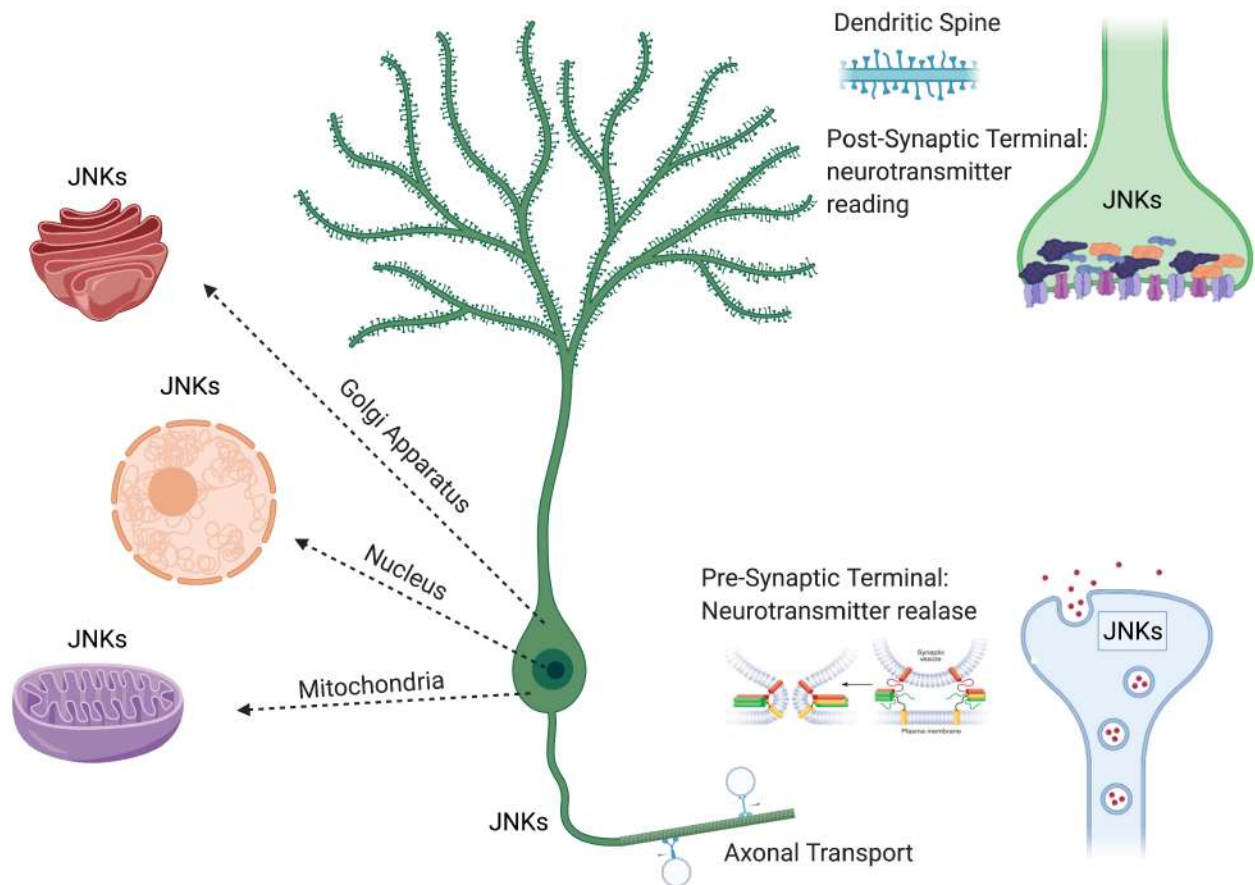


**Figure 16. JNKs localization in neurons.**

Several JNK substrates have been found in the cytoplasm, among them microtubule-associated proteins (MAPs) MAP1B, MAP2 and superior cervical ganglion 10 protein (SCG10)[224].

JNKs can also translocate to the mitochondria[234], where are involved in neuronal death in response to excitotoxic stress[235,236]. Here, the main JNKs targets are members of the BCL-2 protein family, BIM<sub>EL</sub> (BCL-2-interacting mediator of cell death extra-long), DP5 (also known as HRK) leading to BAX-dependent release of cytochrome *c* and apoptotic death[237–240].

Palmitoylation motif can address JNKs to Golgi complex[241], this modification is present on JNK1, JNK3 but not on JNK2. In particular, JNK3 is likely to be the major JNK isoform controlling secretory trafficking in neurons, whereas JNK1 may play a similar role in other cell types in which JNK3 is not expressed[242]. JNKs can also be transported by a kinesin-1 cargo in the axon where they regulate axonal formation, growth and the expression of axonal markers but not the axon fate, although these events are difficult to dissociate[243].

JNK isoforms regulate structural and neurophysiological aspects of synaptic plasticity. JNKs control spine stability, predominantly regulating spines with smaller head/neck length ratios, suggesting a major role in controlling thin spines, enriched during synapse formation[244]. To do this JNKs control actin dynamics[245]. In addition, it has been demonstrated that *Jnk1*<sup>-/-</sup> mice show decreased mushroom spine density and increased thin spine density in pyramidal neuron apical dendrites in

hippocampus CA3, with an overall decreased spine density in basal dendrites[246].

JNKs are also critically involved in regulating synaptic AMPA receptor trafficking during LTD[247] and contribute to metabotropic glutamate receptor-dependent LTD in the CA1, directly binding PSD95, AMPAR subunits[248–250], but also SHANK3[251]. Functionally, the JNK phosphorylation site in GluR2L controls reinsertion of internalized GluR2L back to the cell surface following NMDA treatment[249]. In addition, the JNK signalling pathway, through phosphorylation at serine 295, enhances the synaptic accumulation of PSD-95 and the ability of PSD-95 to recruit surface AMPA receptors and potentiate excitatory post-synaptic currents[248].

JNKs can also translocate to the nuclei in response to stressors such as excitotoxicity, withdrawal of trophic support, axotomy and hypoxia[252]. In this compartment, JNKs phosphorylate c-Jun and activate transcription factor 2 (ATF2)[224,253,254]. In turn, c-Jun–ATF2 dimers increase mRNA levels of proteins involved in signalling cell death[255,256] like pro-apoptotic genes MAPK phosphatase 1 (Mkp1), Dp5, Bim and Puma[224], the endoplasmic reticulum stress pathway genes Trib3 (tribbles homologue 3), Ddit3 (DNA damage-inducible transcript 3) and Txnip (thioredoxin interacting protein), a regulator of oxidative stress[257] contributing to the death of sympathetic neurons (in the absence of trophic support)[258], cortical neurons (following excitotoxicity)[259] and dopaminergic neurons (after axotomy)[254].

In addition, JNK directly targets chromatin modifiers, promoting histone phosphorylation and acetylation, influencing gene expression more profoundly[224].

Also at the peripheral level, JNK plays important role. Besides their role on the central synapses, JNK can act at the peripheral level (i.e. neuromuscular junctions, NMJs) as well. For example, it has been demonstrated that mice expressing catalytically inactive ubiquitin-specific protease 14 (USP14) displayed increased p-JNK that led to terminal swelling and sprouting at the NMJ, as well as motor deficits[260]. The inhibition of JNK (JNK inhibitor: SP600125) significantly improved motor function and synapse structure in these mice[260]. Moreover, Schellino and colleagues showed that the chronic administration of a specific JNK-inhibitor (D-JNKI1) in a spinal muscular atrophy (SMA) mouse model (SMN2<sup>+/+</sup>; SMN $\Delta$ 7<sup>+/+</sup>; Snn<sup>-/-</sup>) ameliorated the trophism of muscular fibres and the size of NMJs, leading to an improved innervation of muscles and motor performances[261].

### 1.3.3 JNK's scaffolds

Scaffold proteins coordinate different intracellular cell-signalling pathways; they lack of intrinsic catalytic activity but with other capacities able to influence the activity of the bound enzymes. Among others, scaffolds spatially and temporally organize kinases cascade. Basically, scaffolds perform three functions: i) increase the efficiency of information transfer between successive enzymes in a signalling cascade; ii) enhance the signal by reducing crosstalk between parallel cascades; iii) target effectors to specific subcellular locations. In the JNK's context, JIP and  $\beta$ -arrestin-2 are the two main signalling regulators[262]. They, in fact, assemble a specific triad of MAP3K, MAP2K and JNK, providing a physical

conduit for signal transduction assembly and amplifying different signals thanks to a “conveyor belt” mechanism[262,263].

### - JIPs

JNK interacting proteins (JIPs) are a family of scaffold proteins encoded by four genes[264] and composed of JIP-1, JIP-2, JSAP/JIP-3 and JIP/JLP. All the mammalian JIPs proteins are highly expressed in the brain[264,265] and regulate JNK signalling during many cellular responses.

JIPs coordinate the JNK-module and can also bind other proteins, including kinesin light chain (KLC)[266] and APP[267], influencing the cellular response to distinct stimuli, such as cytokines (IL1, IL6), UV, oxidative stress, ischemia, NMDA stimulation and Toll-like receptor 4, and regulating distinct and overlapping functions. JIP-proteins link both positive and negative JNK signalling regulators by activating, enhancing and accelerating the JNK phosphorylation/activation but also by mediating JNK dephosphorylation/inactivation[264].

More in detail, JIP-1 specifically binds all JNK isoforms and other actors of the JNK signalling cascade (MKK7, phosphatases, MEKK3, MLK3 and DLK), while JIP-2 interacts with JNK1, JNK2, MKK7, MLK2, MLK3 and DLK. However, while JIP-1 seems to bind only JNKs family members, on the contrary JIP-2 can also interact with p38[268]. Both scaffolds show augmented expression levels in neurons where they show a specific localization in cytoplasm, axons, dendritic growth cones and synapses[269]. Between JIP-1 and JIP-2, JIP-1 shows higher affinity for JNKs compared to JIP-2, but overexpression of JIP-1, as well as JIP-2, acts as an inhibitor of JNK signalling, probably because they sequester actors of the cascade[270].

JIP-3 shows a high affinity for JNK3[271], compared to JNK1 and JNK2, and acts as a JNK activator like JIP-1 and JIP-2, but it can also bind ERK, acting as an inhibitor. JIP-3 can also bind MKK7, MKK4, MEKK1, MLK3 and ASK1[268]. In addition, JIP-3 itself is a JNK target, since it can be phosphorylated only by JNK and not by p38 and ERK[272].

JIP-4 binds JNKs with a major affinity for JNK2 and JNK3[268]; it can also interact with KLC1 (kinesin light chain 1) but not with MKK7, MLK3, ASK1 and ERK, and, in fact, it does not appear to enhance JNK activation[264]. On the other hand, JIP-4 binds some isoforms of p38, and, in fact, it seems more involved in p38 signalling, probably representing a natural inhibitor of p38. Lastly, JIP-4 itself is a JNK and p38 target[265].

In neurons, JIPs play important roles in development and stress responses; they are mainly found in the cytoplasm, but nuclear localization has been reported under stress conditions[273]; in neurons, they localize also in the axon growth cones[274] as well as in both pre- and post-synaptic compartments[274,275]. In neurons, JIPs can translocate among cellular districts, are therefore very intriguing proteins that can be used as tools to modulate JNKs action.

Particularly, JIP1 was initially characterized as an inhibitor of JNK signalling, since its overexpression inhibits JNK phosphorylation on its elective target c-Jun preventing apoptosis[276]. The interaction

between JNKs and JIP1 is mediated by 20 aminoacids[277,278] of the JNK-binding domain (JBD) of JIP-1[279] and overexpression of JIP1 or JBD alone reduces JNK pathway activation[280,281]. Under normal conditions, JIP1 retains JNKs in the cytoplasm.

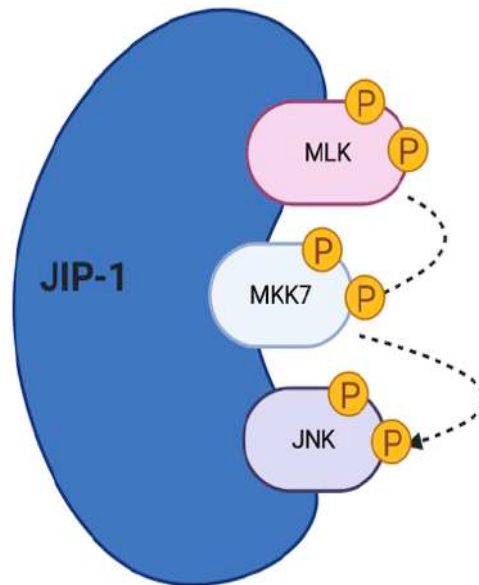


*Figure 17. JNK's scaffold protein JIP-1*[101].

With stress, reduced amounts of JIP1 after JNK activation may release phospho-JNKs to translocate into the nucleus where it activates c-Jun[273]. In fact, it is known that JIP1-JNK3 binding is highly increased in the brain 30 min after ischemia[282]. In addition, JIP1 can influence the kinesin-mediated localization of cargo molecules and organelles within the cell[283]. With in-situ hybridization, it was proved that JIP1 mRNA was found in different extent in cortex, hypothalamus, cerebellum, medulla, pituitary gland, olfactory bulb, and hippocampus. In particular, with immunofluorescence, in the cortex and cerebellum the prevalent staining was found in synaptic complexes in adult, and growth cones in developing nervous tissue[274]. These data are confirmed by biochemical and subcellular fractionation of neuronal cells that reveal its presence essentially in the cytosolic and membrane fractions[284].

#### **- $\beta$ -Arrestin-2**

$\beta$ -arrestins act as scaffold proteins for various components of clathrin-coated endocytosis[285], but they are also scaffolds for multiple kinases and phosphatases involved in cell signalling (such as the MAP kinase module)[286].

The arrestin family is composed of four members: arrestin-1,  $\beta$ -arrestin-1,  $\beta$ -arrestin-2 and arrestin-4. Arrestin-1 and -4 are also called visual-arrestins, because they are expressed in the photoreceptors of the retina, while  $\beta$ -arrestin-1 and -2 are ubiquitously expressed. Neurons express both  $\beta$ -arrestin-1 and -2, but adult neurons present 10/20-fold higher levels of  $\beta$ -arrestin-1 in most brain regions[287,288].

All arrestin isoforms bind JNK3, but only  $\beta$ -arrestin-2 serves as a scaffold, promoting JNK3 activation, independently of its interaction with G protein-coupled receptors (GPCRs).  $\beta$ -Arrestin2 can also facilitate the activation of JNK1 and JNK2[289]. What differentiates the bond between  $\beta$ -arrestin2 and JNK3 is the docking site. In fact, JNK3 binds to the C-terminus of  $\beta$ -arrestin-2 by its unique N-terminal region that is absent in other JNK isoforms[290].

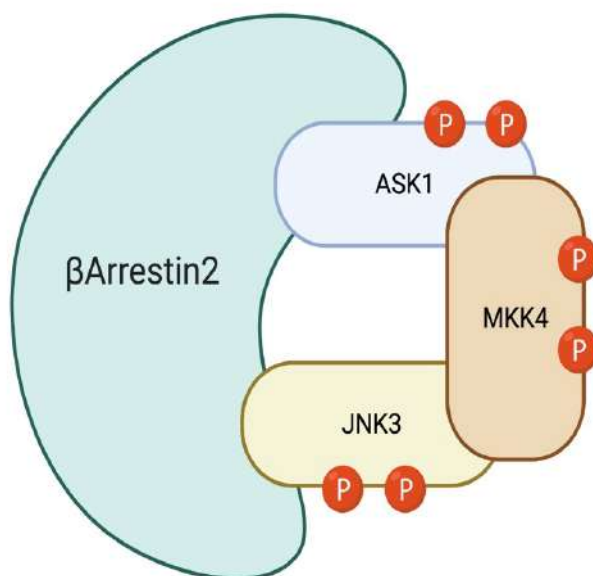


**Figure 18.  $\beta$ -Arrestin-2: JNK3 scaffold**[101].

The  $\beta$ -arrestin-2 is able to promote specifically the activation of JNK3, but not of JNK1 and JNK2, the other isoforms of the family JNK[291]. It has also been shown that mutations in this specification sequence may not only mediate the link between selective targets of JNK3, but also with JBD dependent partners[292]. Recent works showed that  $\beta$ -arrestin-2, by changing conformation, exposes different binding domains, which link and recruit certain proteins, in particular MAPK module components. In fact,  $\beta$ -arrestin-2 specifically associates with the JNK3, MKK4/MKK7 and ASK1 module, and also with JNK-phosphatase, the MAP kinase phosphatase 7 (MKP7)[293]. The  $\beta$ -arrestin-2 scaffold can amplify different signal modules/pathways, and how this module amplifies the signal is explained by the “conveyor belt” model previously described[119]. Concerning JNK3,  $\beta$ -arrestin-2 binds inactive-JNK3, thus bringing it close to MKK7/MKK4, which in turn can phosphorylate JNK3. A single phosphorylation of JNK3 reduces the strength of the bond with  $\beta$ -arrestin-2, while full phosphorylation leads to a higher decrease of its the interaction with the scaffold, resulting in the dissociation of P-JNK3, allowing another inactive JNK3 molecule to bind  $\beta$ -arrestin-2[290].

All these elements suggest an important role of  $\beta$ -arrestin-2 as another potential key modulator in neurodegeneration/neuroprotection, as for JIP-1.

### 1.3.4 JNKs Isoforms

There are 10 splice variants of the three human genes coding for JNK proteins. All JNK genes have been sequenced and structurally analysed. Among them, there is >80% of homology, however, they show some differences in their domain assembly, such as C-terminal extension, or different exon usage between subdomains which can be associated with functional specificity[294]. All the JNKs splice variants, in the human brain, have a molecular weight around 46 kDa or 54 kDa.

The proteins are characterized by the same structure, in particular, JNK3 shares 92% and 87% amino acid identity, with JNK1 and JNK2 respectively. However, there are two clusters of divergent regions, identified from the amino acid sequence alignment, that are located next to each other on the protein surface in the C-terminal lobe of JNK3[295]. The location of this non-conserved region suggests an extended substrate-binding site in JNK3 that may be important for substrate-binding specificity.

In mammals, JNK3 has two splice variants and shows limited expression in very few cell types, mostly in neurons, heart, and testes, whereas JNK1 and JNK2, each having four splice variants, are ubiquitously expressed[296].

In the brain, the highest JNK1, JNK2 and JNK3 mRNA levels are found in the neocortex, followed by the hippocampus, thalamus, and midbrain. JNK1 expression is regulated during the development: high levels of Jnk1 mRNA were found in the developing rat brain and decline postnatally. Despite this, Jnk1 mRNA levels remain high in the olfactory area throughout adulthood[297]. On the contrary, Jnk3 mRNA is the most highly expressed JNK transcript in the adult brain followed by Jnk2 and then Jnk1[297,298]. In mice, JNK3 is prominent in the nuclei of Purkinje and granule cells in the cerebellum and in the 30% of neurons of layers III and V of the cortex. By contrast, JNK1 expression is predominant in the cytoplasm and in both axons and dendrites in the cortex and is particularly enriched in cytosol and dendrites, of Purkinje and thalamic neurons[299]. In the hippocampus, JNK3 expression is found in ~90% of pyramidal layer neurons, whereas JNK1 expression is restricted to the CA3, CA4 and the hilus of the dentate gyrus[300]. JNK2 expression is comparatively low in most brain regions and is distributed in both the cytosol and nuclei[277,301]. Studies on JNK knock-out mice suggest that JNK1 is involved in most physiological JNK activity in the cortex and cerebellum, whereas JNK3 activity accounts for most JNK activity in the hippocampus and striatum[302,303]. In addition, it is known a compensatory increases in JNK isoform expression: JNK1 levels are increased in brain tissue from Jnk2<sup>-/-</sup> mice, whereas JNK2 levels are increased in the brains of Jnk3<sup>-/-</sup> mice[302,304].

	SAPK $\alpha$	SAPK $\beta$	SAPK $\gamma$
<i>Olfactory system</i>			
Olfactory tubercle	+	++	+
Granular layer of olfactory bulb	+	++	+
<i>Basal forebrain</i>			
Amygdaloid nucleus		++	+
Caudate putamen	+/-	++	+
Globus pallidus	+/-	++	+
<i>Cerebral cortex</i>			
	+	+++	+
<i>Hippocampus</i>			
Dentate gyrus	+/-	+++	++
Pyramidal layer	+/-	+++	+++*
<i>Thalamus</i>			
Medial/lateral habenula nucleus	+	+++	+
Reticular thalamic nucleus	+	+++	++
Subthalamic nucleus	+	++	+
Anteromedial and dorsal thalamic nucleus	+	++	++
<i>Hypothalamus</i>			
Dorsomedial hypothalamic nucleus	+/-	++	+
Paraventricular hypothalamic nucleus	+/-	+++	+
Periventricular hypothalamic nucleus		++	+/-
Arcuate nucleus hypothalamus		+++	+
<i>Mesencephalon</i>			
Substantia nigra compacta and reticular	+	++	+
Supramammillary nucleus	+/-	++	+/-
Dorsal raphe nucleus		+	+
<i>Cerebellum</i>			
Granular layer		++	+++*
Purkinje layer	+	+++	++
Deep cerebellar nucleus	++	+++	++
<i>Medulla and pons</i>			
Spinal nucleus of trigeminal	++	+++	+
Pontine reticular nucleus	++	++	+
Pontine nucleus	+	++	+
Motor trigeminal nucleus	+	++	+
Principal sensory nucleus of trigeminal	+/-	++	+
Dorsal cochlear nucleus	+	+++	++
Facial nucleus	++	+++	++
Vestibular nucleus	++	++	++
Hypoglossal nucleus	+	++	+

The relative density of labelling in cells is classified as very intense (+++), intense (++), weak but above background (+), and not clear (+/-).

\* Signal was confined to neurofibers or the site surrounding cell bodies of neurons.

**Figure 19. Summary of regional distribution of JNKs in the mouse brain.** SAPK $\alpha$  also known as JNK2, SAPK $\beta$  also known as JNK3, SAPK $\gamma$  also known as JNK1 [300].

To date, it is known that JNK1 and JNK2 are essential in physiological and homeostatic cell function and have redundant roles acting in a cooperative or synergistic way [305], both participating in apoptosis regulation during normal neurodevelopment [306]. However, they display specific functions playing opposite roles in fibroblasts and macrophages proliferation [305] or regulating T cell expansion during the viral lymphocytic choriomeningitis [307]. Moreover, *Jnk1*<sup>-/-</sup> mice showed abnormal cortical neuronal migration and anterior commissure degeneration during development [308]. On the contrary, *Jnk2*<sup>-/-</sup> mice show milder immune abnormalities [305]. Lastly, JNK3 is clearly associated with neuronal death and oxidative stress, representing the more responsive isoforms to stress stimuli in the brain and mainly involved in neurodegeneration [101]. In fact, *Jnk3*<sup>-/-</sup> mice show a decrease in c-Jun

phosphorylation in ischemia–hypoxia experimental models[309], in cytochrome-c (cyt-c) release after spinal cord injury[310], high resistance to kainic acid (KA)[311] and APP phosphorylation[312].

### 1.3.5 JNKs in neurodevelopmental disorders

Despite the majority of data on JNK role in pathological conditions is related to acute and neurodegenerative diseases, new evidence identified genes associated with the JNK pathway that seems to confer susceptibility to autism spectrum disorders, schizophrenia and intellectual disability[313].

In a model of Down-Syndrome, the Ts1Cje mice, JNK is strongly activated, participating, together with GSK3 $\beta$ , in the generation of mitochondrial dysfunction, over-production of ROS and tau hyperphosphorylation[314].

JNK was also found activated in a patient characterized by severe regressive autism, intellectual disability, and epilepsy carrying mutation in *PAK1* gene[315].

In addition, mice null for *Il1rap1* (interleukin-1 receptor accessory protein-like 1), implicated in monogenic forms of mental retardation and autism, show reduced JNK activity[316].

Lastly, expression profiling of autism genes identified a subset of highly expressed ASD (autism spectrum disorders)-candidate genes in which JNK, together with *NF $\kappa$ B* and *Tnf*, was central to ASD networks at multiple levels and cell-type specific expression[317].

These findings are in line with the identification of a de novo *MAPK10/JNK3* mutations in two un-related patients with a severe neurodevelopmental disorder[313] and complex physical and cognitive disorders, confirming that JNKs, and in particular *JNK3*, are candidates for mutation identification in patients with early-onset neurological disorders[251].

### 1.3.6 JNKs in neurodegenerative disorders

Several evidence demonstrate that JNK is involved in the pathogenesis of neurodegenerative disease like Alzheimer and Parkinson disease, but also in ischemia and stroke, acting on two different tightly link fronts: neuronal death and synaptic dysfunction.

Firstly, JNK, phosphorylating c-Jun, that, together with c-Fos and ATF, constitutes the activator protein 1 (AP-1) transcription factor, leads to the activation of caspases causing apoptotic cell death[318]. In this process, JNK can also phosphorylate pro-apoptotic and anti-apoptotic proteins: BIM (homologous to Bax) and BMF[239], Bcl-2 and Bcl-xL[239]. In addition, JNK promotes the autophagy by activating Beclin 1 and BIM[319]. All these mechanisms lead to neuronal loss and subsequent cognitive and memory impairments.

On the other hand, despite JNKs are essential in synaptic plasticity[246], prolonged JNK activation causes loss of synaptic protein function, in particular, decrease of important proteins levels in the post-synaptic density (PSD) region and mislocalization of glutamate receptors eventually driving the synaptic dysfunction[101,320].

In physiological conditions, JNK modulates memory consolidation via PSD-95 phosphorylation, promoting the reconstruction of neuronal cell structure and altering cytoskeletal dynamics[101,246]. On the contrary, under pathological conditions, JNK, by controlling PSD95 levels, induces the internalization of glutamate receptors both AMPA and NMDA, leading to LTP and LTD damage and spine loss[312,320–322].

In the frame of AD, JNK mediates the A $\beta$ -induced LTP impairment in the hippocampus[323], but not only. JNK promotes the production and accumulation of A $\beta$  protein via APP phosphorylation and, in turn, A $\beta$  peptide induces JNK activation, thus forming a positive feedback loop.

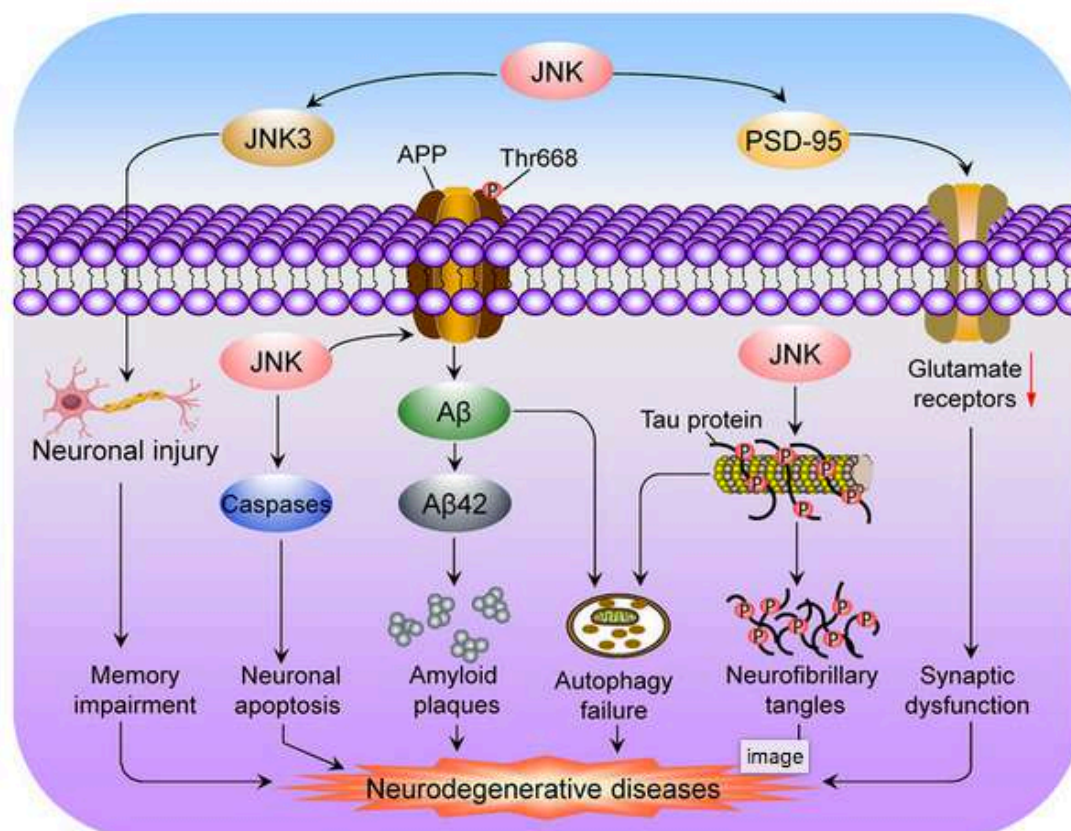


**Figure 20. JNK signalling in the pathogenesis of neurodegenerative diseases**[324].

All JNK1, JNK2 and JNK3 directly phosphorylate APP with different efficiency. JNK1 deficiency is not sufficient to induce any changes in the pathogenesis of AD in a preclinical model (APP/PS1)[325]. On the contrary, in primary neurons, as well as in-vivo, levels and activity of JNK3 directly correlate with APP phosphorylation on T668 confirming JNK3 as the major kinase involved in the abnormal phosphorylation of APP at T668[326]. It is in fact likely that A $\beta$  neurotoxicity is mainly due to JNK3 signal cascades[327] rather than JNK1/2 activation. In line with these observations, 5XFAD mice crossed with JNK3<sup>-/-</sup> showed dramatically reduced p-JNK signals. In addition, in these mice, insoluble A $\beta$ 42 levels were reduced dramatically compared to those in 5FAD/JNK3<sup>+/+</sup>[328]. Tau is extensively modified in-vivo by JNK at several conserved sites[329]. JNK's phosphorylation on Tau is not sufficient

to induce Tau dissociation from microtubules but may still contribute to neurotoxicity when Tau is released from the microtubules. In fact, JNK's phosphorylation on Tau occurs at the early stages of the pathology, in the phase of synaptic dysfunction and therefore before the cognitive decline[330]. In addition, Tau phosphorylation promotes Tau mislocalization at the dendritic spine level contributing to spine injury[331]. All three JNKs isoforms phosphorylate Tau at different sites. In particular, JNK2 was the best isoform at phosphorylating Tau, followed by JNK3 and JNK1, strongly reducing microtubule assembly[332,333].

JNK activation leads also to the phosphorylation of insulin receptor substrate 1 (IRS-1), which impairs downstream insulin signalling and leads to tau hyperphosphorylation. Moreover, affecting pancreatic  $\beta$ -cell function, JNKs induce insulin resistance[334]; this condition in the brain promotes A $\beta$  aggregation and tau hyperphosphorylation linking AD and diabetes. It is known, in fact, that diabetes can function as an accelerator of the dementia[335].

Several studies already demonstrated the JNKs key role also in AD human pathogenesis. In fact, phosphorylation of JNKs is markedly increased in AD and is closely associated with degenerating neurons, in particular with neurofibrillary tangles, senile plaque, neuropil threads and granulovascular degeneration structures[336]. More importantly, JNKs are not only activated, but also redistributed, from the nuclei to the cytoplasm in a manner that correlates with the progression of the disease[337]. Both JNK2 and JNK3 were related to neurofibrillary pathology in AD whereas JNK1 was exclusively associated with Hirano bodies[337]. In the cerebellum, an area that is less involved in AD pathology, there was no staining for phospho-JNK in both AD and control cases. Lastly, whereas JNK1 and JNK2 are increased in total brain homogenate in AD compared to control cases, JNK3 does not show increased protein levels[337]. On the contrary, in other studies, it was found that both JNK3 mRNA expression and protein levels were significantly up-regulated in the brain tissues of AD patients[338]. In the same study, no differences were observed for p-JNK and total JNKs levels. Similarly, the analysis of JNK1 and JNK2 did not show any variation between AD and control groups. But, importantly, a significant correlation between brain A $\beta$ 42 and JNK3 levels was observed. This correlation is also highlighted by colocalization between senile plaques and JNK3, suggesting that some JNK3 proteins may accumulate during the formation of amyloid aggregates[339]. JNKs were also analysed in the CSF of AD and controls. JNK1, JNK2 and p-JNK proteins were not detectable in the CSF by western blots but it was found a significant increase of JNK3 levels in AD patients compared to controls but not correlated with age, sex, A $\beta$ 1-42, T-tau/pTau, as well as MRI evaluations[340].

JNK is also associated with PD, in fact, in pre-clinical model of substantia nigra degeneration, JNK, c-Jun and MKK4 were strongly activated driving the loss of dopaminergic neurons[341]. Its inhibition has neuroprotective effects[324], supported by the fact that the expression of a dominant negative form of JNK in dopaminergic neurons improves survival, locomotor impairments and blocks neurodegeneration in PD[342]. In a model of MPTP-induced dopaminergic neurons degeneration, JNK3 also induces the expression of cyclooxygenase 2 (COX2), a key mediator DA neurotoxicity. In line, also in human PD brain,

P-JNK levels were increased[324].

Particularly JNK3 is strongly involved also in cerebral ischemia-induced neuronal apoptosis. Reperfusion significantly increases JNK3 phosphorylation, promoting neuronal damage in the hippocampus and leading to spatial learning and memory impairment[343].

### **1.3.7 JNKs inhibition**

Given the importance of JNK's role in disease, over the years several molecules have been proposed to selectively inhibit JNKs[256]. These molecules can be divided into chemical compounds and cell-permeable inhibitors peptides (CPP).

SP600125 is the first described chemical JNK inhibitor that blocks all isoforms activation. SP600125 is neuroprotective in animal models of stroke and in spinal cord injury in mice[344]. However, its action is not specific since it inhibits 74 kinases[224]. As other pyrimidine derivatives they block JNK by competitively inhibiting the active site responsible for the link with the ATP. In this way JNK it is no longer able to carry out its kinase activity[345].

On the other hand, CPPs are cargo bioactive capable of preventing the action of the kinase on its targets. CPPs are short fragments of approximately 50 amino acids composed of a CARGO peptide attached to an effector peptide. CARGO peptide is a fragment able to pass through cell membranes, including the blood-brain barrier (BBB), allowing bioavailable peptides in all tissues. One of the most used CARGO sequences is the TAT (Trans activating Regulatory Protein) domain of HIV-1. This domain is usually associated to an effector peptide responsible for the physiological response and therefore capable to block the JNKs action.

Of particular interest as a target for the synthesis of JNK inhibitors are scaffold proteins that can be used as competitive substrates. Following this strategy, D-JNKI1 was designed: a selective inhibitor of all three JNK isoforms capable of allosterically modulating the access of JNK to its "JBD dependent" targets[276,346,347]. D-JNKI1 was, in fact, drawn on the domain of JIP1 capable of binding JNK. By adding a molar excess of D-JNKI1, it is possible to prevent JNK's access to its cellular targets with a competitive substrate mechanism[347,348].

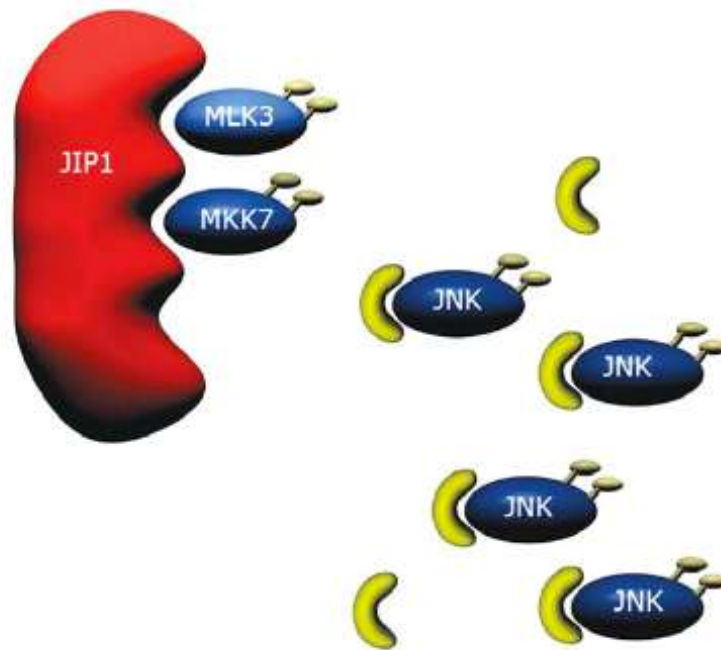


**Figure 21. Schematic representation of D-JNKI1 peptide (in yellow) mode of action[223].**

Numerous studies highlight the effectiveness of the D-JNKI1 treatment in both in-vitro and in-vivo models of AD[277,312,321,322,330]. Furthermore, D-JNKI is already in phase II and III of clinical trial for the treatment of eye diseases and inflammation of the inner ear (Auris Medical and Xigen). The main problem associated with the use of D-JNKI1 consists in the inhibition of all three isoforms of JNK throughout the body. The isoforms JNK1 and JNK2 are ubiquitously expressed, and they play important physiological roles. The inhibition of all JNK isoforms in all tissues it could therefore lead to even important side effects in the patient.

For these reasons, the strategy to inhibit JNK in specific cellular compartments has been used to selectively block JNK action in the nucleus, in the cytoplasm and at mitochondria[303,349].

Other feasible strategy is to take advantage of JNK3 isoform, mainly expressed in the CNS and the most involved in the stress response and in the induction of synaptic dysfunction[328,339]. Selectively inhibiting JNK3, keeping the other isoforms active in the various tissues, could therefore represent an adequate solution for the treatment of neurodegenerative diseases with low side effects[101,291,350]. Until now, there have been various efforts to pharmacologically inhibit JNK3, but not all of them have been successful. This is partly due to the high homology between the three isoforms of JNK. In fact, most of JNK drug discovery efforts are focused on the development of ATP-competitive inhibitors[351]. However, this is a challenging strategy to achieve specificity since the high homology in the ATP binding site among the different JNKs[352]. JNK3 shares 77% and 75% sequence identity with JNK2 and JNK1 and, in particular, the identity in the ATP-binding pocket is 98%[353]. For these reasons, most of the JNK3 inhibitors display very weak selectivity, interfering also with JNK1/2 and are not able to inhibit just the action of JNK3 on its targets[354]. On the contrary, strategies targeting the protein-protein

interactions that assure the specificity of the JNK3 response have a great potential and could be a more promising strategy in drug discovery[355] exhibiting a more specific pharmacological profile[356].

## 2. Aims

---

Defects in synapse organization, morphology and function are associated with both neurodevelopmental, psychiatric and neurodegenerative disorders[357]. Some of **the key mechanisms underlying these processes are known, but, to date, no treatments are available to cure these pathologies**. Therefore, some indications suggest that MAPKs regulate the stress mechanisms underlying “*synaptic dysfunction*”.

The overall aim of this work is to study **the role of JNK in both neurodevelopmental and chronic brain diseases focusing on the synaptopathy**, the first initial mechanism of many different brain diseases.

More in details, we dissected the JNK role in the synaptopathy associated with two neurodevelopmental disorders (Rett and Angelman Syndrome) and to a neurodegenerative pathology, Alzheimer disease, the most characterized form of dementia.

In Rett Syndrome we studied the synaptic dysfunction of two different Rett mouse models and we identified JNK as an important actor downstream MECP2.

We started from the *Mecp2*-knockout (***Mecp2*<sup>y/-</sup>**) male mice, displaying a **very severe phenotype**, discovering an important JNK activation in the total homogenate and in the post-synaptic elements. We then performed a chronic treatment of D-JNKI1, the specific inhibitor of JNK, demonstrating the key role of JNK. In fact, the treatment rescued the *Mecp2*-severe knockout phenotype.

We then tested this strategy in the **milder phenotype** of *Mecp2*-heterozygous female mice (***Mecp2*<sup>+/-</sup>** <sup>Ja</sup>), that mimics the random X-inactivation of Rett patients, characterizing the effects of JNK inhibition from a behavioural and biochemical point of view. Again, JNK inhibition offers an interesting tool to prevent some pathological defects of Jaenisch mice.

Lastly, knowing that the Rett is principally caused by point mutation in humans, to give a translational value to the results obtained in mice, we verified JNK activation in human neurons, differentiated from human MECP2-mutated iPSCs (**MECP2<sup>mut</sup>**), compared to the isogenic control expressing wild-type MECP2 allele (MECP2<sup>wt</sup>). The JNK signalling was activated in the MECP2-mutated iPSCs, inducing cell death, and D-JNKI1 blocked the MECP2<sup>mut</sup> -induced neuronal death of the **MECP2<sup>mut</sup>** iPSCs.

Concerning the Angelman Syndrome, another neurodevelopmental disorder, we analysed the synaptic dysfunction in the UBE3A<sup>m-/p+</sup> mouse model. Again, JNK signalling was strongly activated in the total homogenate, as well as in post-synaptic enriched protein fraction, suggesting an important role of JNK also in this disorder. To confirm this hypothesis, we treated UBE3A mice with D-JNKI1. The treatment improved the behavioural defects, and this correlated with the stabilization of the synaptic biomarkers. These results prove that JNK signalling plays a key role in Synaptic Dysfunction of the two neurodevelopmental diseases.

We therefore hypothesized that JNK may regulate a common pathway in the stressed synapse of many brain diseases. For this reason, we focused on the Alzheimer's synaptic dysfunction, the most characterize synaptopathy, studying JNK as a key modulator of this event also in a chronic illness.

We used the Alzheimer mice model 5XFAD. We considered three different time points representing the initial phase of the disease (4 months of age), the overt phase (6 months of age) and the late phase (10 months of age), finding JNK activation in two cellular compartments, the total homogenate, and the post-synaptic protein enriched fraction (TIF), together with synaptic dysfunction.

Since another team performed a treatment with D-JNKI1, in the same AD mice, with encouraging results[358,359], we switched to analyse just the selective JNK isoform for the CNS, JNK3, the most responsive to stress stimuli, finding that 5XFAD mice presented a powerful increase of JNK3 levels.

We therefore decided to test the potential neuroprotective effect of the specific inhibition of JNK3.

Thanks to the collaboration with Prof. Falconi, we designed the specific JNK3 inhibitor, dSIMBA2, proving its selectivity without any interaction with the other two JNK isoforms.

Before testing dSIMBA2 in in-vivo, we studied the effect of JNK3 inhibition in an in-vitro model of synaptic dysfunction induced by A $\beta$  oligomers (ABO) to define the dose and the neuroprotection against ABO induced synaptopathy. The dSIMBA2 inhibitor prevented A $\beta$  oligomers toxicity and now we have indications for the 5XFAD treatment. This work is now ongoing.

Importantly, we suggest that distant categories of brain disease shared the first neurodegenerative mechanism: the synapse dysfunction. We defined JNK as a key player in this process and we provided the first evidence that, among JNK isoforms, JNK3 is the most active in the synaptic stress-activated signalling. In addition, the performed treatment with the two JNK inhibitors proved that synaptic injury is reversible in two neurodevelopmental disorders and in a chronic disease. This induces to believe that preventing synaptic dysfunction is a winning strategy, which will have a great potential against many different brain illnesses.

## 3. Materials and Methods

---

### 3.1 Animal Procedures

- We used two mouse models of RTT:  $Mecp2^{tm1.1Bird}$  mice and  $Mecp2^{tm1.1Jae}$  mice (Jackson Laboratory, Bar Harbor, Maine). Knockout  $Mecp2^{tm1.1Bird}$  male mice were on a C57BL/6 background and age-compatible wild-type male mice (C57BL/6) served as controls. Heterozygous female  $Mecp2^{tm1.1Jae}$  mice with exon 3 deletion in *Mecp2* were crossed to C57BL6 for one generation, followed by breeding among offspring and then maintained on a mixed background; we used age-matched wild-type females as controls in all experimental conditions. Genotyping was done by PCR using a protocol provided by Jackson Laboratory and GoTaq@G2 Flexi DNA polymerase kit (Promega, Madison, USA). Mice were bred at IRCCS Mario Negri Institute for Pharmacological Research in a specific pathogen free (SPF) facility with a regular 12:12 h light/dark cycle (lights on 07:00 a.m.), at a constant room temperature of  $22 \pm 2^\circ\text{C}$ , and relative humidity  $55 \pm 10\%$ . Animals were housed in standard mouse cages with water and food ad libitum. Procedures involving animals and their care were in accordance with national and international laws and policies (Permit Number 43/03 PR).

The experimental scheme was composed by 8 groups: untreated wild-type and  $Mecp2^{y/-}$  male mice, D-JNK11 treated wild-type and  $Mecp2^{y/-}$  male mice, untreated wild-type and  $Mecp2^{+/-Jae}$  female mice and D-JNK11 treated wild-type and  $Mecp2^{+/-Jae}$  female mice. For behavioural tests we used:  $n=10$  wild-type male mice,  $n=10$   $Mecp2^{y/-}$  male mice,  $n=8$  wild-type female mice and  $n=8$   $Mecp2^{+/-Jae}$  female mice; for biochemical analysis (TIF and Western blots) we analysed  $n=10$  animals of Bird strain and  $n=10$  animals of Jaenisch strain for each experimental group. Animals ( $n=25$  wild-type male mice,  $n=25$   $Mecp2^{y/-}$  male mice) were monitored daily for wellbeing and welfare-related disease symptoms. Body weight was recorded weekly. Body weight loss was calculated as the difference (grams) from the maximum weight recorded for each animal. Based on previous works described in the D-JNK11 dose and paradigm of administration were decided. Animals were randomized assigning random numbers to experimental groups and also with respect to disease severity. In brief, all mice ( $Mecp2^{y/-}$  or wt) were injected intraperitoneally with D-JNK11 (22 mg/kg) every 28 days from 3 to 7 weeks of age [360]. Their weight was recorded before each treatment. Mice were always treated at the same time of day (9:00–10:00 A.M.) in randomized order in a specific room inside the animal facility. Each single mouse was our experimental unit. Heterozygous  $Mecp2^{+/-Jae}$  female and wt littermates were treated with D-JNK11 (22 mg/kg, i.p.) at 16 and 20 weeks of age.

The day after the treatment, mice, both male  $Mecp2^{y/-}$  or wt and female  $Mecp2^{+/-Jae}$  and wt, performed the behavioural trials. At the end of the tests they were euthanized, and brains were dissected for biochemical analysis.

- We used a model of Angelman Syndrome [361] B6.129S7-Ube3a<tm1Alb>/J - The Jackson Laboratory on a C57BL/6 background and age-matched wild-type mice (C57BL/6) served as controls. Heterozygous  $Ube3a^{tm1Alb}$  females were bred with wt males; this resulted in maternal transmission

of the *Ube3a* mutant allele and paternal transmission of the imprinted/silenced wt allele. Genotyping was done by PCR using a protocol provided by Jackson Laboratory. Mice were bred at IRCCS Mario Negri Institute for Pharmacological Research in a specific pathogen free (SPF) facility with a regular 12:12 h light/dark cycle (lights on 07:00 a.m.), at a constant room temperature of  $22 \pm 2^\circ\text{C}$ , and relative humidity  $55 \pm 10\%$ . Animals were housed in standard mouse cages with water and food ad libitum. Procedures involving animals and their care were in accordance with national and international laws and policies (Permit Number 565/2017-PR).

The experimental scheme comprised four groups: untreated wt and *Ube3a*<sup>m-/p+</sup> mice, D-JNK11 treated wt and *Ube3a*<sup>m-/p+</sup> mice. For behavioural tests we used male and female wt and *Ube3a*<sup>m-/p+</sup> mice; for biochemical analysis (TIF and Western blots) we analysed male and female mice as well, 10 mice per group. All mice (*Ube3a*<sup>m-/p+</sup> or wt) were injected intraperitoneally (i.p.) with D-JNK11 (22 mg/kg) every 28 days from 7 to 23 weeks of age. Their weight was recorded before and after each dose. Mice were always treated at the same time of day (9:00–10:00 A.M.) in randomized order in a specific room inside the animal facility. Each single mouse was our experimental unit. The day after the treatment, mice performed the behavioural trials. After behavioural tests the animals were euthanized, and brains were dissected for biochemical analysis.

- We used the 5xFAD model of Alzheimer Disease (B6SJL-Tg(APP<sup>S</sup>wFLon,PSEN1<sup>M146L</sup>\*L286V)<sup>6799</sup>Vas/Mmjax) on a B6SJL F1/J background and age-matched wild-type mice as controls. Hemizygous male mice were bred to B6SJL F1/J female mice. Genotyping was done by PCR using a protocol provided by Jackson Laboratory and GoTaq®G2 Flexi DNA polymerase kit (Promega, Madison, USA). Mice were bred at IRCCS Mario Negri Institute for Pharmacological Research in a specific pathogen free (SPF) facility with a regular 12:12 h light/dark cycle (lights on 07:00 a.m.), at a constant room temperature of  $22 \pm 2^\circ\text{C}$ , and relative humidity  $55 \pm 10\%$ . Animals were housed in standard mouse cages with water and food ad libitum. Procedures involving animals and their care were in accordance with national and international laws and policies (Permit Number 4/2021-PR).

The experimental scheme was composed by 2 groups: wild-type and 5XFAD tg male and female mice. For behavioural tests we used: n=10 wild-type male mice, n=10 5XFAD tg mice; for biochemical analysis (TIF and Western blots) we analysed n=10 animals of wild-type and n=10 5XFAD tg mice.

### 3.2 Behavioural tests

-Rotarod test:

Mice were tested for locomotor disability with a Rotarod test by the same operator. We used the accelerating Rotarod apparatus (Ugo Basile 7650 model). Once the animals were positioned on the rotating bar, time was started, and the rod was accelerated at a constant rate of 0.3 rpm/s from 3 rpm to 30 rpm for 5-min. The time (seconds) at which the animal fell from the bar was recorded. Three trials

were run for each animal, with a 5-min rest between them, and the longest retention time was recorded. The mean latency to fall during the session was calculated and used in subsequent analysis.

-Open Field and spontaneous locomotor activity:

After allowing the mice to acclimatize they were placed in the centre of the floor, defined as a 'starting point', and their behaviour was tracked with the activity monitoring system Ethovision (Noldus, Wageningen, Netherlands) for 5 min. This short time was chosen to avoid further stress to mutant mice. The parameters analysed as measures of spontaneous locomotor activity, exploratory activity, and state of anxiety were: the duration of movements divided into the number of internal (the nine central squares) and external (the sixteen peripheral squares) square crossed, the time spent in the central and outer areas of the open field, the overall distance travelled by the mice. These protocols were used to test the *Mecp2<sup>y/-</sup>* and *Ube3a<sup>+/-</sup>* and the relative control mice.

In heterozygous *Mecp2<sup>+/-</sup> <sup>1ae</sup>* females locomotor activity was recorded for 30 min. The behavioural parameters recorded were the overall distance travelled and the distance travelled in the periphery and in the centre of the open field arena.

- The novel-object recognition test (NORT):

The objects were randomly selected to avoid bias among animals and between groups. The time spent exploring the two objects was recorded for 10 min. Results were expressed as a discrimination index (DI) (seconds spent on novel - seconds spent on familiar)/(total time spent on objects). Animals with no cognitive impairment spent longer investigating the novel object, giving a higher DI. We used 30 animals for each experimental group.

- The Radial arm water maze (RAWM):

The radial arm water maze was performed as described in Alamed et al., 2006. Briefly, the maze is composed by 6 swim arms starting from a central area, with a submerged escape platform located at the end of one of the arms (the goal arm). To avoid water transparency titanium dioxide was suspended in it. On each trial, the mouse was initially placed in the centre of a randomly selected start arm and allowed to swim in the maze for up to 60 seconds to find the escape platform. The platform was in the same arm on each trial. On the first day, mice were given 15 trials alternating between a visible platform (above the water) and a hidden platform (below the water). The following day they were given 15 additional trials using the hidden platform only. Entry into an incorrect arm (all four limbs within the arm) was scored as an error. If a mouse failed to make an arm entry within 15 seconds, this also was scored as an error. The errors for blocks of 3 consecutive trials were averaged for data analysis.

### **3.3 Whole-body plethysmography (WBP) analysis**

Unrestrained *Mecp2<sup>y/-</sup>* and wt mice were placed in a WBP recording chamber (Emka Technology, Paris). After a habituation period of 15 min, a baseline recording was established for 30 min. Mice were then

removed from the chamber, injected intraperitoneally with the D-JNKI1 peptide (22 mg/kg). Two experimental protocols were followed to study the effect of D-JNKI1 on respiratory anomalies:

1. Preventive: D-JNKI1 was administered in those animals that at 6 weeks of age did not yet manifest apnea to verify its preventive power against respiratory anomalies
2. Curative: D-JNKI1 was administered to those animals that at 6 weeks of age already showed apnea to verify its curative power against respiratory anomalies.

For both paradigms, animals were recorded 24 hours after the injection and then once a week from 6 to 9 weeks of age. Analysis was performed using IOX2 software (EMKA Technologies, Paris). Apnea was considered only if the end expiratory pause was  $\geq 0.8$  sec. Only points of motion-free recording were analysed. The Periods of movement were removed automatically by the apnea software.

### **3.4 Triton Insoluble Fractionation**

Subcellular fractionation was as reported in the literature, with minor modification. Briefly, brain areas or neuronal culture were homogenized with a glass-Teflon Potter apparatus in 0.32 M ice-cold sucrose buffer containing the following concentrations (in mM): 1 HEPES, 1 MgCl<sub>2</sub>, 1 EDTA, 1 NaHCO<sub>3</sub>, and 0.1 PMSF, at pH 7.4, with a complete set of protease inhibitors (Complete; Roche Diagnostics, Basel, Switzerland) and phosphatase inhibitors (Sigma, St. Louis, MO). Samples were centrifuged at 1000  $\times g$  for 10 min. The supernatant (S1) was then centrifuged at 3000  $\times g$  for 15 min to obtain a crude membrane fraction (P2 fraction). The pellet was dissolved in buffer containing 75 mM KCl and 1% Triton X-100 plus protease and phosphatase inhibitors and centrifuged at 100,000  $\times g$  for 1 h. The supernatant was stored and referred to as TSF (S4). The final pellet (P4), referred to as TIF, was homogenized in a glass-glass Potter apparatus in HEPES 1mM with a complete set of protease and phosphatase inhibitors, and stored at  $-80$  °C until analysis.

### **3.5 Western blot**

Protein concentrations were quantified using the Bradford Assay (5000006, Bio-Rad Protein Assay Hercules, California, USA): 10  $\mu g$  of total homogenate and 5  $\mu g$  of TIF extracted proteins were separated by 10% SDS polyacrylamide gel electrophoresis. PVDF membranes (1620177, Bio-Rad, Hercules, California, USA) were blocked in Tris-buffered saline 5% no-fat milk powder (70166, Sigma-Aldrich, Darmstadt, Germany) and 0.1% Tween 20 (P1379, Sigma-Aldrich, Darmstadt, Germany) (1 h, RT). Primary antibodies were diluted in the same buffer (incubation overnight, 4°C) using: anti-P-JNKs (1:1000, BK9251S, Cell Signalling, Danvers, MA, USA); anti-JNKs (1:1000 BK9252S, Cell Signalling, Danvers, MA, USA); anti-p-c-Jun (1:1000, 06-659, Millipore, Bedford, MA, USA); anti-c-Jun (1:1000, BK9165S, Cell Signalling, Danvers, MA, USA); anti-NMDA Receptor 2A GluN2A (1:2000, BK4205S, Cell

Signalling, Danvers, MA, USA); anti-NMDA Receptor 2B GluN2B (1:2000, BK14544S, Cell Signalling, Danvers, MA, USA); anti-Glutamate Receptor 1 (AMPA subtype) GluA1 (1:1000, BK13185S Millipore, Bedford, MA, USA); anti-Glutamate Receptor 2 (AMPA subtype) GluA2 (1:1000, MAB397 Millipore, Bedford, MA, USA), anti-post-synaptic density protein 95 (1:2000, CAY-10011435-100, Cayman Chemical Company, Ann Arbor, Michigan, USA), anti PSD93 (1:1000, AB2930, Abcam, Cambridge, UK), anti Drebrin (1:1000, BSR-M05530, Boster, Pleasanton, CA, USA), anti Shank3 (1:1000, 64555, Cell Signalling, Danvers, MA, USA), anti-Actin (1:5000, MAB1501 Millipore, Bedford, MA, USA), anti-Tubulin (1:4000, Santa Cruz).

### **3.6 LDH assay**

The cell medium was collected and the release of LDH in the medium was quantified to assess cell viability, using the cytotoxic 96 non-radioactive cytotoxicity assay kit (Promega, Madison, USA, USA).

### **3.7 iPSCs and iPSCs-derived neurons**

We analysed three iPSCs clones derived from fibroblasts of a female patient with Thr158Met mutation in MECP2 gene: two clones expressing the mutated MECP2 allele (2271#22 and 2271#1) and one expressing the normal allele (2271#2) due to X-chromosome inactivation, which was used as a partial isogenic control [157]. An iPSCs line from a second MECP2-mutated patient with a p.Arg306 Cys mutation was obtained from James Ellis (University of Toronto) [362]. As additional controls, we used two iPSCs clones from a healthy new-born male and one healthy female child. All iPSCs lines were derived using the Yamanaka's classic retroviral approach [363] and characterized according to standard criteria [364]. Neurons were differentiated from mutated and control iPSCs lines as previously reported [157]. On day 30 of terminal differentiation, neurons for quantitative analyses were isolated by immuno-magnetic sorting using anti-CD24 antibodies (130-095-951, Miltenyi Biotec, Bergisch Gladbach, Germany) [365]. Based on previous in-vitro experiments described [366,367], control and mutated neurons were treated with D-JNKI1 at 2  $\mu$ M concentration starting on day 28 of terminal differentiation. On day 30, neurons were isolated as described above to obtain proteins for Western blot analysis.

### **3.8 Primary neuronal cultures**

Primary neuronal cultures were obtained from P1-P2 C57bl6 pups as described in Sclip et al., 2013 [322], with minor modification. In brief, after dissection hippocampi were incubated with 200U of papain (P3125, Sigma Aldrich, St Louis, USA) (30min, 34°C), with trypsin inhibitor (T-9253, Sigma

Aldrich, St Louis, USA) (45min, RT), and subsequently mechanically dissociated. Neurons were seeded on dish (300,000 cells/mL). Plating medium was B27/neurobasal-A (Gibco-Invitrogen) supplemented with 0.5mM glutamine (Gibco-Invitrogen), 100 U/ml penicillin, and 100 µg/ml streptomycin (Gibco-Invitrogen).

### **3.9 Alpha Screen Kinase Assay**

The AlphaScreen assay to detect JNK kinase phosphorylation was constructed as follows: a substrate peptide was biotinylated and coupled to streptavidin-coated AlphaScreen donor beads. Acceptor beads were coated with protein A coupled to specific anti-phosphosubstrate antibody. Kinase activity was detected by the interaction of donor and acceptor beads through the phospho-substrate-antiphosphosubstrate bridge, resulting in a close proximity of the donor and acceptor beads and the generation of an AlphaScreen fluorescence signal as described above. The kinase reaction was performed under the following assay buffer conditions: 20 mM Tris/HCl (pH 7.4), 10 mM MgCl<sub>2</sub>, 1 mM DTT, 100µM Na<sub>3</sub>VO<sub>4</sub>, and 0.01% Tween-20. Compounds (final concentration 5µg/mL, 1% DMSO) or vehicle control (final concentration 1% DMSO) were diluted in assay buffer and mixed with the JNK kinase (final concentration 5 nM). After an incubation time of 15 min at room temperature, biotinylated substrate (final concentration 6 nM) and ATP (final concentration 1 µM) diluted in assay buffer were added, followed by an incubation of the plates for 2 h at room temperature. After this incubation period, streptavidin donor and protein A/anti-phosphosubstrate antibody-coated acceptor beads were added (final concentration of each bead was 20 µg/mL) diluted in the following buffer: 20 mM Tris/HCl (pH 7.4), 200 mM NaCl, 80 mM ethylenediamine tetraacetic acid (EDTA), and 0.3% bovine serum albumin (BSA). After an overnight incubation, the assay was measured using the AlphaQuest reader. To avoid premature activation of the donor beads by environmental light exposure, the bead dispenses and reading steps were performed in a laboratory equipped with green room lighting (filter material Roscolux Chroma Green #389 from Rosco Labs: [www.rosco.com](http://www.rosco.com)).

### **3.10 ABO production**

Synthetic Aβ (1–42) peptide (Bachem) was dissolved in hexafluoro-2-propanol, incubated for 10 min in a bath sonicator at maximum power, centrifuged at 15,000 × g for 1 min, aliquoted, dried, and stored at –80 °C. Before use, the dried film was dissolved using DMSO and diluted to 100 µM in F12 Medium (Invitrogen, Waltham, MA). Oligomers were obtained by incubating the peptide for 16 h at 25 °C. Final Aβ oligomer concentrations were considered as monomer equivalents since the size of the oligomers is heterogeneous.

### **3.11 Toxicity study and MTT assay**

Toxicity studies were performed by treating neurons with increasing concentrations of dSIMBA2: 1  $\mu$ M, 1.25  $\mu$ M, 1.75  $\mu$ M and 2  $\mu$ M for 24h directly in the culture medium. The media was then removed and replaced with fresh media containing 0.4 mg/ml MTT ([3-(4,5-dimethyliazol-2-yl)-2,5-diphenyltetrazolium bromide]). Cells were incubated for 4 h at 37 °C. After this period, the media was removed and 100  $\mu$ l of a solution containing HCl:isopropanol 1:25 was added to each well to dissolve the formed formazan crystals. Cell viability was assessed by measuring the absorbance at 540 nm using a microplate reader.

### **3.12 ABO treatment**

In order to induce synaptopathy, the neuronal cultures were treated with A $\beta$  oligomers (Bachem) at 3 $\mu$ M concentration for 3h[368]. To verify the neuroprotective effect of SIMBA2, the cultures are pre-treated with dSIMBA2 1  $\mu$ M for 30 minutes and then the A $\beta$  oligomers are added 3  $\mu$ M for 3h.

### **3.13 Statistical Analysis**

Statistical analysis was done with the Graph Pad Prism 6 program. Data were expressed as mean  $\pm$  SEM with statistical significance  $p < 0.05$ . For comparison between multiple groups two-way ANOVA was used; for comparison between two groups T-test was used.

## 4. Results

---

## 4.1 JNK activation in in-vivo and in-vitro murine and human models of Rett Syndrome

### 4.1.1 Mecp2<sup>y/-</sup> Bird male mice mimic severe and acute neurological RTT signs

We used male Mecp2<sup>y/-</sup> to mimic a severe RTT model [369]. Mecp2<sup>y/-</sup> mice were monitored from 3 to 7 weeks of age, analysing their well-being conditions, focusing on the body weight growth curves. Body weight ( $p < 0.0001$ , Fig. 22a) dropped deeply in Mecp2<sup>y/-</sup> compared to wild-type (wt) mice, related to worsening of the neurological symptoms (Table 1 and Fig. 22a).

weeks	WT Body weight (g)	SEM	Mecp2 <sup>y/-</sup> Body weight (g)	SEM	Significance
3	9.12	0.3139	6.62	0.1678	****
4	15.3	0.5945	11.05	0.2949	****
5	20.16	0.2800	14.36	0.3556	****
6	21.52	0.2656	15.08	0.3430	****
7	22.96	0.3078	15.03	0.5646	****

*Table 1. Body weight of wt compared to Mecp2<sup>y/-</sup> from 3 to 7 weeks of age.*

Locomotion in Mecp2<sup>y/-</sup> mice was investigated in the Rotarod and Open Field Tests, repeated each week from 3 to 7 weeks of age. On the Rotarod Mecp2<sup>y/-</sup> mice had a shorten latency on the wheel than wt animals, with a significant decrease of locomotor ability at each time point ( $p < 0.0001$ , Fig. 22b). Locomotor performance was further investigated in the Open Field test by analysing the distance moved and the time spent immobile in the arena. Mecp2<sup>y/-</sup> mice spent significantly more time immobile ( $p = 0.0001$ , Fig. 22c) and consequently less distance moved ( $p = 0.0003$ , Fig. 22c) than wt mice. These data confirm the severe and well-detectable locomotor impairments in Mecp2<sup>y/-</sup> mice compared to age-matched wt mice. Breathing dysfunction in Mecp2<sup>y/-</sup> mice were tested by whole-body plethysmography to quantify frequency ( $f$ ), time of inspiration ( $T_i$ ) and expiration ( $T_e$ ) and apnea over 30 min of freely moving recording from 6- to 9-week-old Mecp2<sup>y/-</sup> mice. The onset and progress of respiratory dysfunction varied among Mecp2<sup>y/-</sup> mice examined. In the majority (13 out of 25) of mice, apnea appeared at 6 weeks of age, but 7 showed apnea at 7 weeks, 2 at 8 weeks, 2 at 9 weeks and 1 died without a single episode (Fig. 1d, table). Our results show that apnea started appearing at 6 weeks and became more frequent with age ( $p < 0.0001$ ; Fig. 22d).

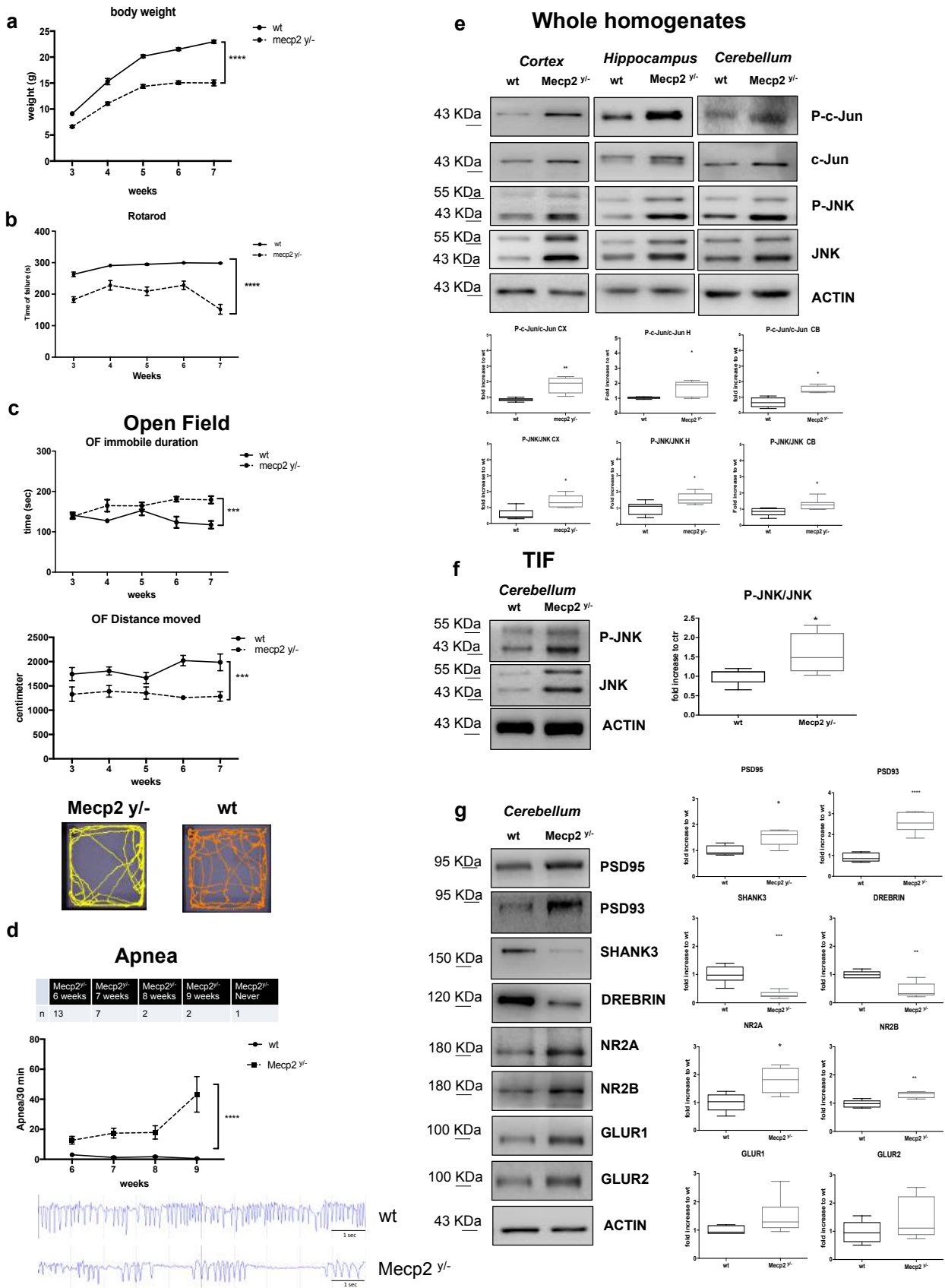


**Figure 22. JNK signalling activation in Mecp2<sup>y/-</sup> Bird male mice.** **a**) Growth curves of Mecp2<sup>y/-</sup> mice (n=25) compared to their wt littermates (n=25) from 3 to 7 weeks of age. **b-c**) Behavioural analysis of Mecp2<sup>y/-</sup> mice (n=10) compared to their control wt (n=10) from 3 to 7 weeks of age in the Rotarod (**b**) and Open field (**c**) tests (parameters shown: duration of immobility and distance moved). The distance moved by each experimental group was also presented in the arena-plots under the Open field

graphs. **d)** On-set and number of apnea in *Mecp2<sup>y/-</sup>* and wt mice at 6, 7, 8 and 9 weeks of ages in the table and the graphs, in the lower part, the representative plethysmographic traces of *Mecp2<sup>y/-</sup>* (n=15) vs wt (n=6) characterizing the respiratory patterns and breathing dysfunction. **e)** JNK signalling pathway activation in whole homogenate: Western blots and quantifications of P-c-Jun/c-Jun and P-JNK/JNK ratios in the cortex, hippocampus, and cerebellum of 7-weeks-old *Mecp2<sup>y/-</sup>* (n=10) and wt (n=10) mice. **f)** Western blots and quantifications of TIF fraction (post-synaptic elements) showed the JNK activation in cerebellum of 7-week-old *Mecp2<sup>y/-</sup>* (n=10) compared to wt (n=10) mice. **g)** Western blots and quantifications showed PSD alterations in *Mecp2<sup>y/-</sup>* (n=10) compared to wt (n=10) mice. Data were shown as mean  $\pm$  SEM. Significance was calculated using two-way ANOVA for repetitive measurements followed by Bonferroni post hoc test or Student's t-test followed by Tukey's post hoc test. Statistical significance: \*p<0.05, \*\*p<0.01, \*\*\*p<0.001, \*\*\*\*p<0.0001.

#### 4.1.2 *Mecp2<sup>y/-</sup>* Bird mice present activation of the JNK pathway and PSD alterations

To analyse the activation of the JNK stress pathway in *Mecp2<sup>y/-</sup>* Bird mice, we investigated the phosphorylation of c-Jun (P-c-Jun/c-Jun) and JNK (P-JNK/JNK) in three brain areas: cortex, hippocampus, and cerebellum. P-c-Jun/c-Jun and P-JNK/JNK ratios were significantly higher in *Mecp2<sup>y/-</sup>* than age-matched wt mice (Fig. 22e), indicating powerful activation of the JNK-stress pathway. In the *Mecp2<sup>y/-</sup>* mice the P-c-Jun/c-Jun ratio was 50% higher in the cortex (p=0.0055, Fig. 22e), 75% in the hippocampus (p=0.02, Fig. 22e) and 50% in the cerebellum (p=0.03, Fig. 22e) than in wild-type mice. Thus, in these brain regions the phosphorylation of JNK was significantly higher in *Mecp2<sup>y/-</sup>* than age-matched wt mice (cortex: p=0.013, hippocampus: p=0.03, cerebellum: p=0.028, Fig. 22e).

We then specifically assessed JNK activation at the PSD, by isolating the post-synaptic enriched protein fraction with the triton-insoluble fraction (TIF)[370] in the cerebellum because it regulates fine movements, motor-spatial memory, motor coordination and thus being relevant to RTT locomotor impairments.

The P-JNK/JNK ratio was significantly higher in *Mecp2<sup>y/-</sup>* than wt mice (p=0.027, Fig. 22f), indicating JNK activation in the post-synaptic protein enriched-fraction. To study the molecular organization of PSD region in *Mecp2<sup>y/-</sup>* mice, we quantified the levels of different post-synaptic markers. PSD95 (25%) and PSD93 (70%) levels were higher in *Mecp2<sup>y/-</sup>* mice (p=0.0149 and p<0.0001, Fig. 22g), while SHANK3 (70%) and Drebrin (60%) levels were lower than in wt mice (p=0.001, p=0.0016, Fig. 22g). In addition, N-methyl-D-aspartate receptor 2A (GluN2A) and 2B (GluN2B) levels were significantly higher in *Mecp2<sup>y/-</sup>* than in wt mice (60%, p=0.03 and 37%, p=0.01, Fig. 22g). Finally, the levels of GluA1 and GluA2, AMPA receptor subunits, presented a tendency not significant to be higher in *Mecp2<sup>y/-</sup>* than in wt mice (Fig. 22g). These results indicate abnormal organization of the PSD region in the absence of MeCP2.

#### 4.1.3 The specific JNK inhibitor peptide D-JNKI1 rescues the severe and acute neurological RTT signs in *Mecp2<sup>y/-</sup>* Bird male mice

*$\alpha$ -D-JNKI1 efficacy inhibits JNK pathway in *Mecp2<sup>y/-</sup>* mice.* The effectiveness and specificity of the cell-permeable peptide D-JNKI1 treatment was measured by its inhibitory effect on c-Jun in-vivo [371]. The

P-c-Jun/c-Jun ratio was therefore measured in the cortex, hippocampus, and cerebellum. D-JNK11 treatment powerfully prevented c-Jun phosphorylation in the cortex (84%), hippocampus (50%) and cerebellum (36%, Fig. 23e) in treated compared to untreated *Mecp2<sup>y/-</sup>* mice ( $p=0.0011$ ,  $p=0.0482$ ,  $p=0.0204$ , Fig. 23e). These results confirm the inhibitory specificity of D-JNK11's action.

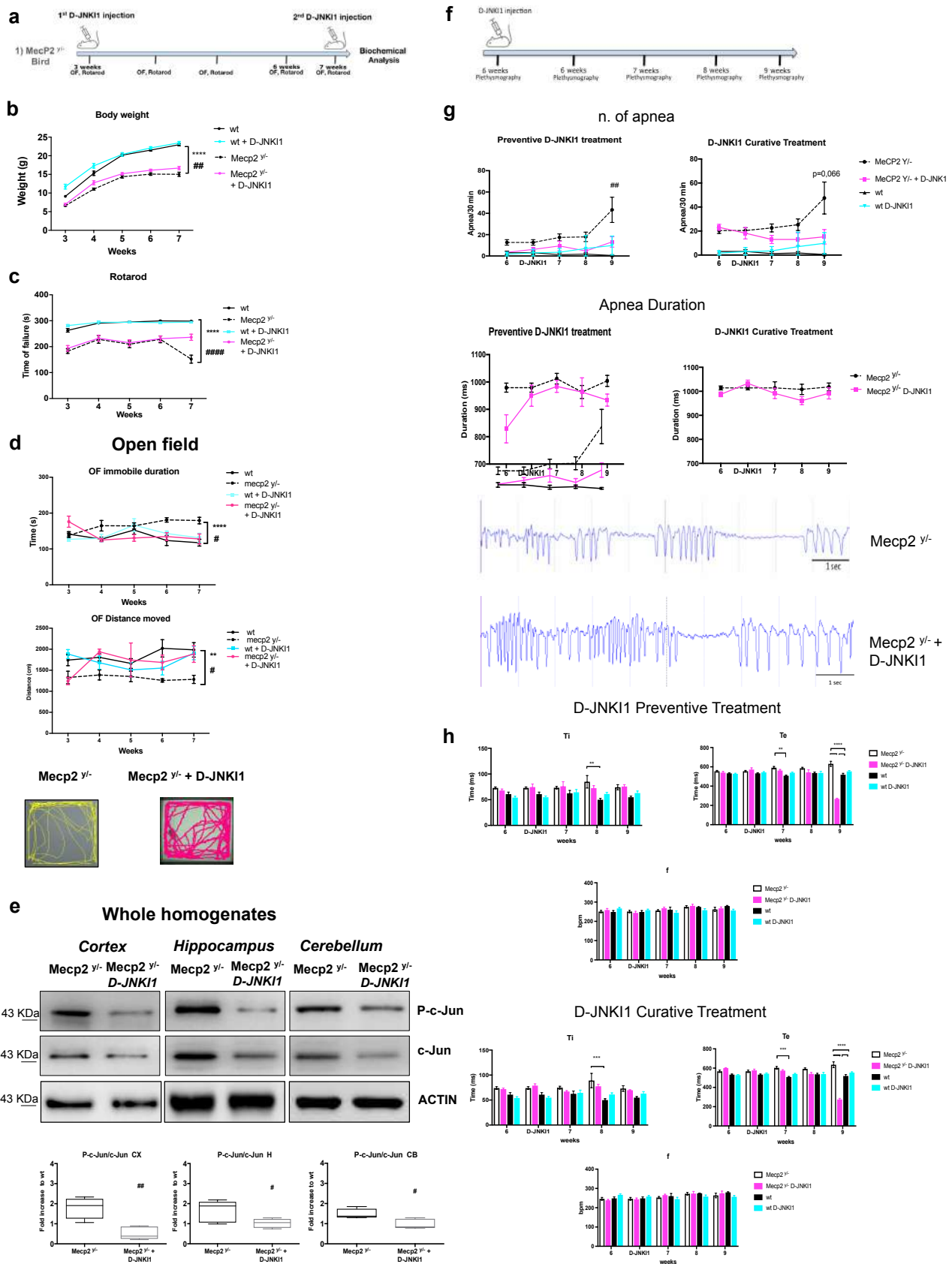


**Figure 23. D-JNK11 rescues well-being conditions, locomotor impairments and apnea numbers in Mecp2<sup>Y/-</sup> male mice. a)** Timeline of D-JNK11 treatment in Mecp2<sup>Y/-</sup> male mice. 24 h after the in D-JNK11 injection mice were tested for behavioural impairments. **b)** Growth curves of D-JNK11 treated (blue sky) and untreated (black) wild type, and D-JNK11 treated (fuchsia) and untreated (black dotted) Mecp2<sup>Y/-</sup> mice from 3 to 7 weeks of age (n=25 for each experimental group). **c-d)** Behavioural

analysis of D-JNK11 treated vs untreated wt and *Mecp2<sup>y/-</sup>* mice (n=10 for each experimental group) from 3 to 7 weeks of age in the Rotarod (c) and Open field (d) tests (parameters shown: time spent immobile, and distance moved, with relative Open field arena-plots). e) Western blots and the quantification P-c-Jun/c-Jun ratio in the whole homogenate of cortex, hippocampus, and cerebellum of 7-week-old D-JNK11 treated and untreated *Mecp2<sup>y/-</sup>* mice. f) Timeline of D-JNK11 treatment and plethysmography analysis. 24 h after the in D-JNK11 injection mice were tested for breathing abnormalities. g) Number and duration of apnea in preventive and curative D-JNK11 paradigm of treated (n=10) and untreated (n=6) wild type and *Mecp2<sup>y/-</sup>* mice (n=15) from 6 to 9 weeks of age. h) Breathing analysis in preventive (upper part) and curative (lower part) D-JNK11 paradigm of treated (fuchsia) and untreated *Mecp2<sup>y/-</sup>* (white) mice from 6 to 9 weeks of age and the treated (blue-sky) and untreated wild type (black) (parameters shown: Ti, Te and f). Data were shown as mean  $\pm$  SEM. Significance was calculated using two-way ANOVA for repetitive measurements followed by Bonferroni post hoc test or Student's t-test followed by Tukey's post hoc test. Statistical significance relative to control \*\*p<0.01, \*\*\*p<0.001, \*\*\*\*p<0.0001; D-JNK11 treated vs untreated *Mecp2<sup>y/-</sup>*: #p<0.05, ##p<0.01, #### p<0.0001.

**b- D-JNK11 improves the well-being conditions and rescues locomotor impairments.** The D-JNK11 peptide [371,372] was injected intraperitoneally from 3 to 7 weeks of age, every 28 days to prevent JNK hyper-activation in *Mecp2<sup>y/-</sup>* mice (Fig. 23a). By comparing the well-being conditions between treated and untreated *Mecp2<sup>y/-</sup>* mice, D-JNK11 chronic treatment did not cause any major toxic or side effects nor body weight loss, on the contrary induced a recovery in body weight (wt vs *Mecp2<sup>y/-</sup>* p<0.0001; D-JNK11 treated vs untreated *Mecp2<sup>y/-</sup>* p=0.0020 Fig. 23b).

Additionally, D-JNK11 treated *Mecp2<sup>y/-</sup>* mice had a significant lower latency to fall in the Rotarod test (p<0.0001, Fig. 23c) and also better open field test performances (Fig. 23d). The time spent in immobile state was shorter and the distance moved greater (p=0.018 and p=0.0237, Fig. 23d) in D-JNK11 treated compared to untreated *Mecp2<sup>y/-</sup>* mice. D-JNK11 did not show any toxic effects in wild-type mice and the curves of D-JNK11 treated and untreated wt animals overlapped with no significant differences (Fig. 23b-d).

**c- D-JNK11 reduces apnea numbers.** Due to the onset variability of apnea among *Mecp2<sup>y/-</sup>*, we used two different paradigms of D-JNK11 treatment: preventive and curative administration (Fig. 23f). In the first group, *Mecp2<sup>y/-</sup>* were treated at 6 weeks of age, before the onset of apnea, to analyse the potential preventive effect of D-JNK11; whereas, in the second group, mice received the treatment only after showing the first apnea, a protocol set to provide information on the potential curative effect of D-JNK11. All mice were recorded at 6 weeks of age and again the day after the D-JNK11 treatment.

Using whole-body plethysmography, we monitored breathing patterns (frequency (f), time of inspiration (T<sub>i</sub>) and expiration (T<sub>e</sub>) and apnea (end expiratory pause greater than 800 ms) in five different experimental mice groups: untreated *Mecp2<sup>y/-</sup>*, *Mecp2<sup>y/-</sup>* preventive-treated, *Mecp2<sup>y/-</sup>* curative-treated and treated and untreated wt mice from 6 up to 9 weeks of age. The preventive D-JNK11 treatment induces a significant decrease in apnea numbers (p=0.0047, Fig. 23g) but not in their duration, while the curative treatment exerts an almost significant effect in the reduction of apnea numbers but not in their duration in *Mecp2<sup>y/-</sup>* mice (p=0.066; Fig. 23g). We observed no significant differences among all groups in breathing rate (f). On the other hand, T<sub>e</sub> presented differences between

wt and *Mecp2<sup>y/-</sup>* at 7 weeks in both group of curative and preventive D-JNKI1 treatment ( $p=0.0002$ ,  $p=0.0035$ , Fig. 23h); this is in line with the fact that these mice already presented apnea. Genotypic differences of Ti were clear at 8 weeks in both groups ( $p=0.0002$  and  $p=0.0025$ , Fig. 23h) but both curative and preventive treatments were ineffective. Finally, at 9 weeks, the last time point tested, the genotypic effect was clear and both the curative and preventive D-JNKI1 treatments significantly reduced the Te ( $p<0.0001$ ; Fig. 23h). For Ti neither curative nor preventive D-JNKI1 treatments had any effect. Concerning the D-JNKI1 treatment in wt mice, this did not show any significant effect.

**d- D-JNKI1 effect on PSD alterations in *Mecp2<sup>y/-</sup>*.** In line with the behavioural and breathing results, the D-JNKI1 inhibitor rescued the changes in post-synaptic markers observed in *Mecp2<sup>y/-</sup>* mice. The treatment strongly lowered the P-JNK/JNK ratio in the post-synaptic enriched protein fraction (TIF) (equal to 40%) in *Mecp2<sup>y/-</sup>* ( $p=0.047$ , Fig. 24a) compared to untreated mice. The *Mecp2<sup>y/-</sup>* mice had high PSD95 and PSD93 levels ( $p=0.018$  and  $p<0.0001$  Fig. 24b), while SHANK3 and Drebrin decreased ( $p<0.0001$  and  $p=0.049$ , Fig. 24b); D-JNKI1 restored PSD95 ( $p=0.0002$ , Fig. 24b) and PSD93 ( $p<0.0001$ , Fig. 24b) level to 75% and 65% and SHANK3 and Drebrin level to 80% and 90% ( $p<0.0001$  and  $p=0.0121$ , Fig. 24b), normalizing the biochemical marker levels of *Mecp2<sup>y/-</sup>*.

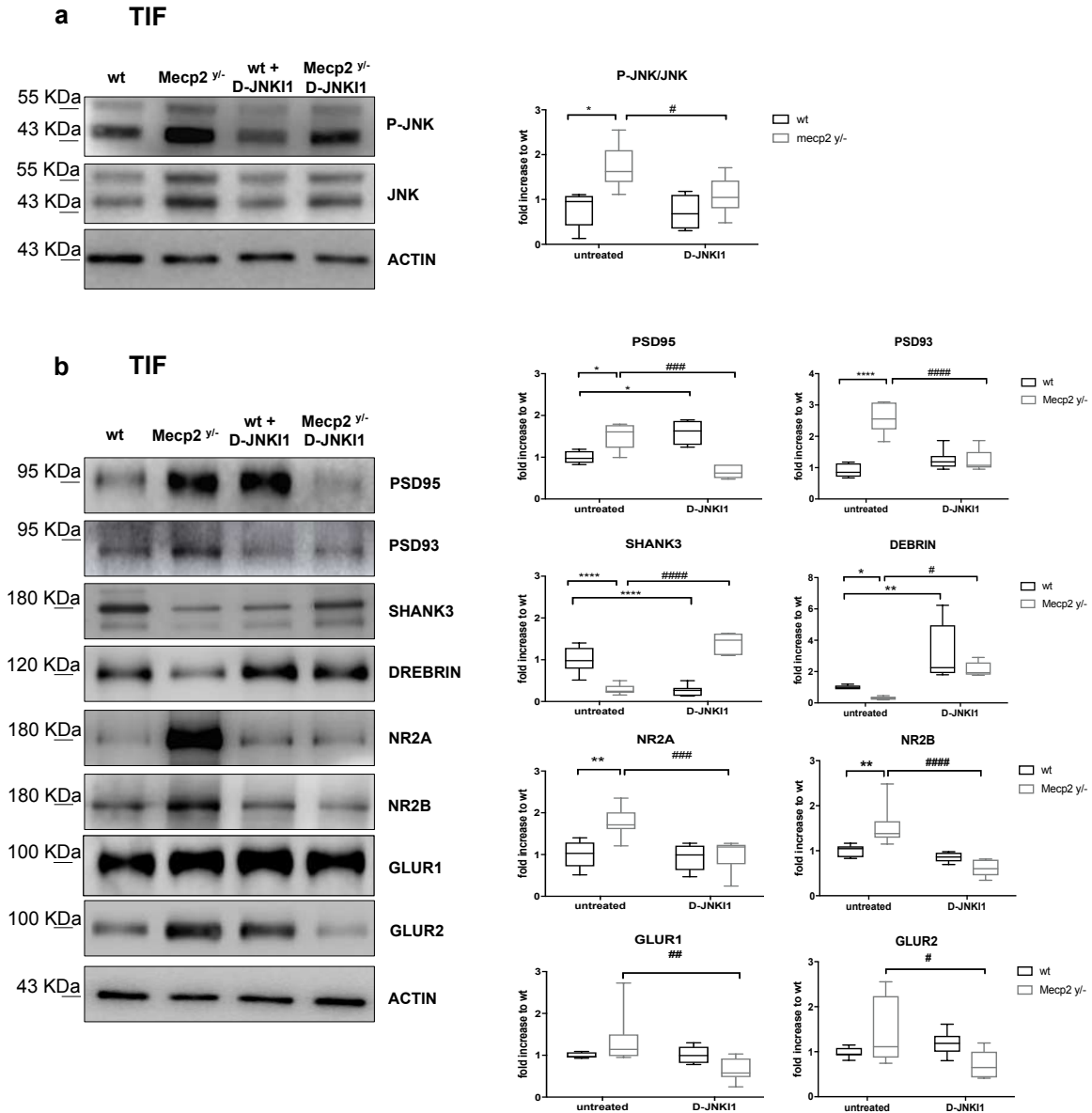


**Figure 24. D-JNKI1 effect against PSD alterations in *Mecp2*<sup>y/-</sup> male mice. a)** Western blots and quantifications in the cerebellum TIF (post-synaptic elements) of treated and untreated wt and *Mecp2*<sup>y/-</sup> mice to measure D-JNKI1 effect in-vivo. D-JNKI1 significantly reduced JNK activation in *Mecp2*<sup>y/-</sup> mice, but not in control wt mice. **b)** Western blots and quantifications of the post-synaptic elements in the cerebellum, showed normalization of the PSD markers levels to control level in D-JNKI1 treated compared to untreated *Mecp2*<sup>y/-</sup> mice (n=10 for each experimental group). Data were shown as mean ± SEM. Significance was calculated using two-way ANOVA followed by Bonferroni post hoc test for multiple comparisons. Significance relative to control \*p<0.05, \*\*p<0.01, \*\*\*p<0.0001. D-JNKI1 treated vs untreated *Mecp2*<sup>y/-</sup> #p<0.05, ##p<0.01, ###p<0.001, ####p<0.0001.

The inhibitor treatment induced recovery of NMDA and AMPA receptors to wt levels. GluN2A decreased 40% (p=0.0008, Fig. 24b), GluN2B 58% (p<0.0001, Fig. 24b), GluA1 50% (p=0.0082, Fig. 24b) and GluA2 50% (p=0.0113, Fig. 24b) compared to untreated *Mecp2*<sup>y/-</sup> mice. In wild-type treated mice, D-JNKI1 significantly increased PSD95 and Drebrin levels (p=0.0107, p=0.00021 Fig. 24b) and lowered SHANK3 (p<0.0001, Fig. 24b) however without any effect on glutamate receptors (AMPA and NMDA). The effects

of D-JNKI1 on PSD markers in wt mice did not modify their behavioural performances, thus excluding major toxic effects.

#### **4.1.4 The specific JNK inhibitor peptide D-JNKI1 rescues the milder neurological RTT signs in *Mecp2*<sup>+/-</sup> *Jae* heterozygous mice**

To assess the potential protective effect of JNK inhibition in female *Mecp2*<sup>+/-</sup> *Jae* mice, we treated them with D-JNKI1 depending on the developmental onset of their neurological symptoms. D-JNKI1 was delivered from 16 to 23 weeks of age, one injection every 28 days, and the behavioural tests were run every week for Rotarod test and at the end of the treatment for Open field test (Fig. 25a). Treatment did not cause any toxic side-effects on the wt and *Mecp2*<sup>+/-</sup> *Jae* mice metabolism, as indicated by the absence of body weight changes in each group of animals (Fig. 25b). Importantly, we found that D-JNKI1 rescued locomotor impairments in *Mecp2*<sup>+/-</sup> *Jae* mice. We also assessed motor coordination of female *Mecp2*<sup>+/-</sup> *Jae* mice with the Rotarod test, finding that these animals showed a significant impairment compared with wt controls demonstrated by a significant shorter latency to fall off the rod ( $p < 0.0001$ ; Fig. 25c).

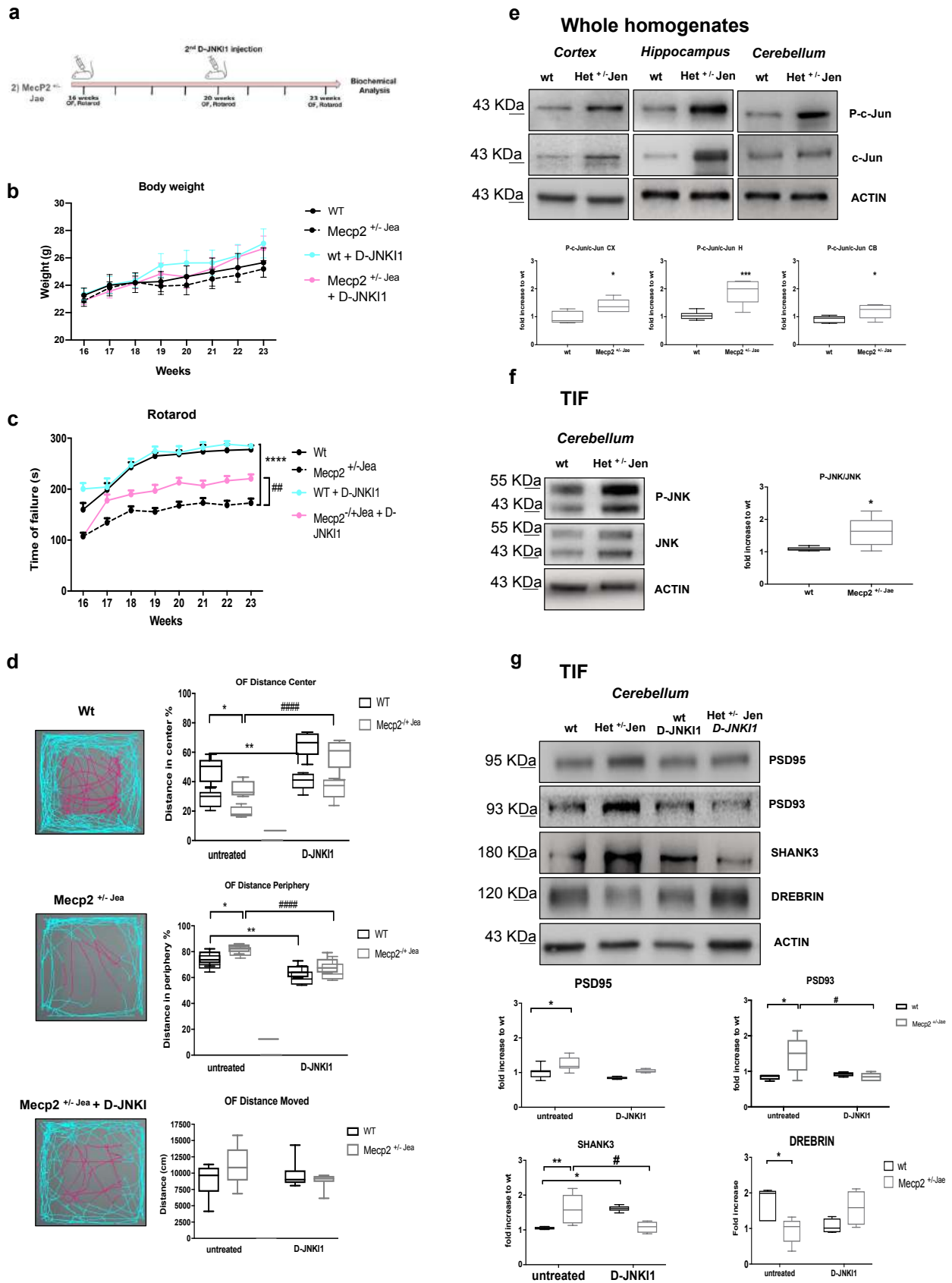


**Figure 25. Female *Mecp2*<sup>+/-</sup> Jaenisch neurological phenotype: JNK signalling activation and D-JNK11 treatment.** **a)** Timeline of D-JNK11 treatment in Female *Mecp2*<sup>+/-</sup> Jaenisch mice. 24 h after the in D-JNK11 injection mice were tested for behavioural impairments. **b)** Growth curves of D-JNK11 treated and untreated wt and *Mecp2*<sup>+/-</sup> Jea mice from 16 to 23 weeks of age. **c)** Rotarod Tests in D-JNK11 *Mecp2*<sup>+/-</sup> Jea treated mice (fuchsia line), *Mecp2*<sup>+/-</sup> Jea untreated (black dotted line), treated wt

(blue-sky line) and untreated wt (black line). **d)** Open Field test. D-JNKI1 improved the behavioural performance of *Mecp2<sup>+/-</sup>Jae* (see plots for central (fuchsia) and peripheral (blue sky) movements of wt and *Mecp2<sup>+/-</sup>Jae* treated and untreated mice). The last graph presented the distance moved: there were no genotypic differences. **e)** Western blots and quantifications of c-Jun activation in whole homogenate of cortex, hippocampus, and cerebellum in 23-week-old wt and *Mecp2<sup>+/-</sup>Jae* mice. **f)** Western blots and relative quantifications in the TIF cerebellum of 23-week-old wt and *Mecp2<sup>+/-</sup>Jae* mice confirmed JNK activation at the synaptic level in *Mecp2<sup>+/-</sup>Jae* mice. **g)** *Mecp2<sup>+/-</sup>Jae* presented alterations of the PSD-region and D-JNKI1 treatment normalised the biochemical alterations in treated vs untreated *Mecp2<sup>+/-</sup>Jae* mice. Each experimental group: n=8. Data were shown as mean  $\pm$  SEM. Significance was calculated using two-way ANOVA for repetitive measurements followed by Bonferroni post hoc test, Student's t-test followed by Tukey's post hoc test and two-way ANOVA followed by Bonferroni post hoc test for multiple comparisons (g). Significant differences from control \* $p < 0.05$ , \*\* $p < 0.01$ , \*\*\* $p < 0.001$ , \*\*\*\* $p < 0.0001$ ; D-JNKI1 treated vs untreated *Mecp2<sup>+/-</sup>Jae*: # $p < 0.05$ , ## $p < 0.01$ , ####  $p < 0.0001$ .

Intriguingly, after treatment, mutant females had a significantly longer latency to fall in the Rotarod test compared to untreated *Mecp2<sup>+/-</sup>Jae* mice ( $p = 0.0046$ ; Fig. 25c), while no effect was observed in wt mice. In addition, in the Open Field test, the total distance moved did not differ between genotypes at baseline (Fig. 25d), but *Mecp2<sup>+/-</sup>Jae* females moved less in the centre of the arena ( $p = 0.0134$ , Fig. 25d) and more in its periphery ( $p = 0.022$ , Fig. 25d) than wt mice. Intriguingly, D-JNKI1 treatment suppressed the differences in exploratory behaviour between mutant heterozygous mice and wt animals in the open field arena, as shown by the greater distance moved in the central area and a shorter distance in the peripheral area by D-JNKI1 treated than untreated *Mecp2<sup>+/-</sup>Jae* mice ( $p < 0.0001$ , Fig. 25d). In addition, in wild-type mice, the treatment significantly increased the distance travelled in the centre of the arena and reduced the distance travelled in the periphery ( $p = 0.0021$  and  $p = 0.0022$ , Fig. 25d). Thus, our data indicate that D-JNKI1 treatment improves both locomotor and exploratory defects in female *Mecp2<sup>+/-</sup>Jae* mice.

#### **4.1.5 *Mecp2<sup>+/-</sup>Jae* heterozygous mice present activation of the JNK pathway and alterations in the PSD**

*Mecp2<sup>+/-</sup>Jae* females showed JNK activation (Fig. 25e) and their P-c-Jun/c-Jun ratio was 30% higher in both cortex and cerebellum ( $p = 0.0141$  and  $p = 0.034$  Fig. 25e), and 50% in the hippocampus ( $p = 0.0015$ , Fig. 25e), compared to wt mice. The P-JNK/JNK ratio was significantly higher in the PSD region of *Mecp2<sup>+/-</sup>Jae* females than wt mice ( $p = 0.0345$ , Fig. 25f), indicating that *Mecp2<sup>+/-</sup>Jae* female mutants showed synaptic dysfunctions, as *Mecp2<sup>y/-</sup>* male mice. The pathology in heterozygous females, a previously unreported defect, involved increases in PSD95 (25%), PSD93 (50%) and SHANK3 (30%) levels ( $p = 0.0296$ ,  $p = 0.0308$ ,  $p = 0.0027$  Fig. 25g), with a decrease in Drebrin (46%,  $p = 0.0417$ , Fig. 25g) in the cerebellar post-synaptic enriched protein fraction. Importantly, D-JNKI1 significantly lowered both PSD93 and SHANK3 to control levels ( $p = 0.0174$  and  $p = 0.0134$ , Fig. 25g), while PSD95 and Drebrin only partially returned to normal level, with no significant effect. Finally, in wt mice D-JNKI1 did not have any

major effects on PSD proteins except for an increase of SHANK3 level ( $p=0.012$  Fig. 25g), without any effect on NMDA and AMPA receptors. In sum, our biochemical results show that, in line with their improved behavioural performance, D-JNKI1-treatment largely rescues the molecular organization of the PSD region in *Mecp2<sup>+/-Jae</sup>* mice.

#### **4.1.6 From animal to human iPSC models: JNK pathway activation and D-JNKI1 protective effects in Rett MECP2<sup>mut</sup>**

We next analysed JNK activation in human neurons differentiated from iPSCs (hiPSCs) derived from fibroblasts of RTT patients carrying a MECP2 mutation (MECP2<sup>mut</sup>) and from a normal control (MECP2<sup>wt</sup>). We analysed three iPSCs clones derived from fibroblasts of a female patient with Thr158Met mutation in MECP2 gene: two clones expressing the mutated MECP2 allele (2271#22 and 2271#1) and one expressing the normal allele (2271#2) due to X-chromosome inactivation, which was used as a partial isogenic control [157]. In addition, we analysed a second MECP2-mutated patient with a p.Arg306 Cys mutation. The hiPSCs expressing either the mutated or normal MECP2 allele (hMECP2<sup>wt</sup>) were differentiated in cortical neurons for 30 days as previously reported, generating mainly glutamatergic neurons [157] (Fig. 26a).

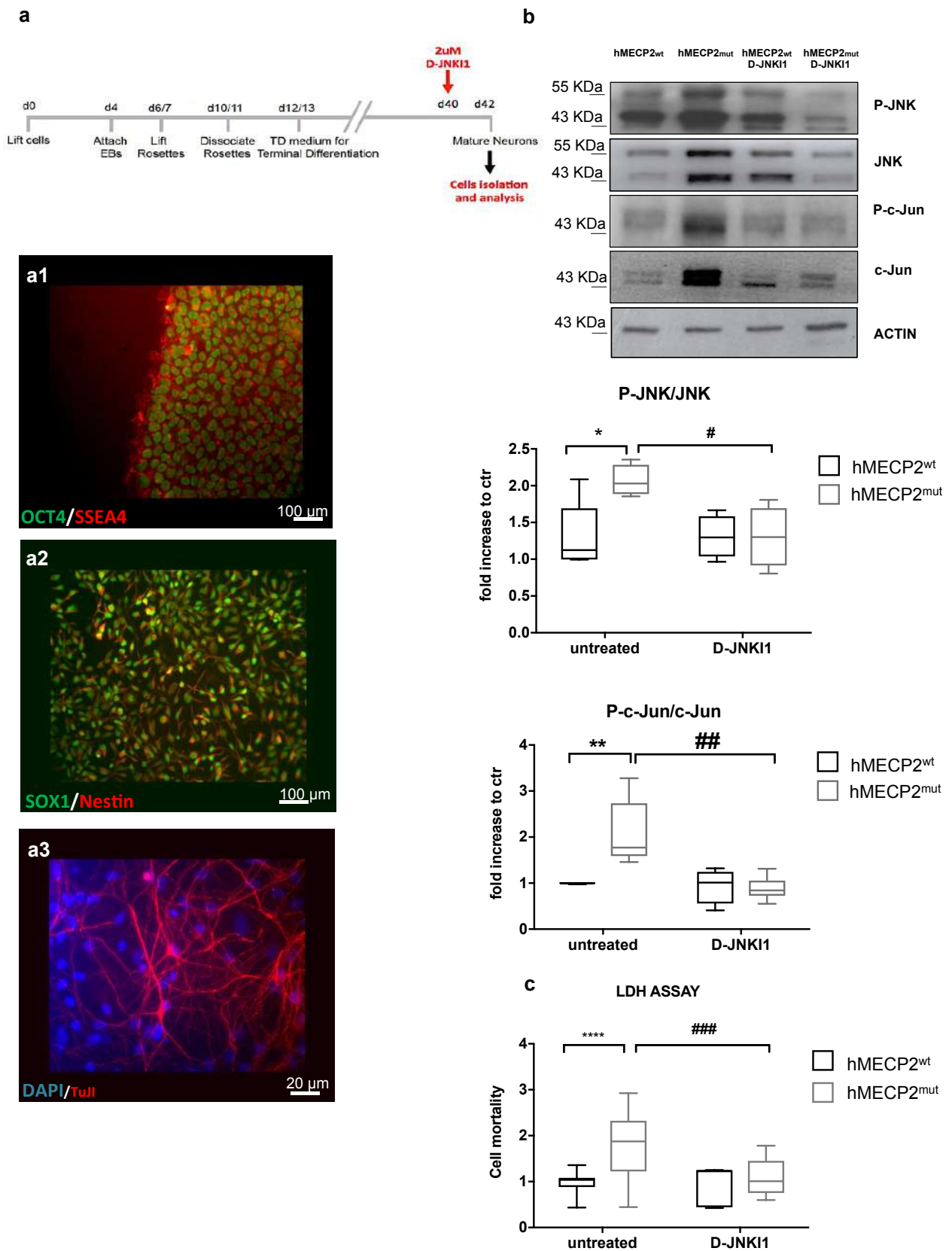


**Figure 26. JNK signalling activation and D-JNKI1's protective effects in Rett human iPSCs.** a) Neuronal differentiation of Human iPSCs. The upper panel showed the neuronal differentiation protocol. The timing of critical steps was indicated in days from day 0 (d0). At the end of the differentiation (red arrow, d40), neurons were exposed to 2 $\mu$ M D-JNKI1 for 48 hours before neurons were isolated for western blot analysis. Immunofluorescence was used to define cell identity (lower panel): **a1-**

OCT4/SSEA4 staining for iPSCs; **a2**- Nestin and SOX1 staining for telencephalic neural progenitors (d12/13); **a3**-  $\beta$ 3-Tubulin (TuJ1) staining for neurons in terminally differentiated cultures at day 40 and DAPI to stain nuclei. Scale bar: iPSCs and NPCs 100  $\mu$ m and neurons 20  $\mu$ m. **b**) Western blots and quantifications of JNK activation in neurons differentiated from hiPSCs clones expressing either the wild type (hMecp2<sup>wt</sup>) or the mutated (hMecp2<sup>mut</sup>); MECP2 allele and wt iPSCs were differentiated in neurons and isolated by immuno-magnetic sorting using anti-CD24 antibodies. The hMecp2<sup>mut</sup> displayed higher P-JNK/JNK and P-c-Jun/c-Jun ratios than to hMecp2<sup>wt</sup> neurons. D-JNKI1 reduced hMecp2<sup>mut</sup> activation to hMecp2<sup>wt</sup> levels; D-JNKI1 in hMecp2<sup>wt</sup> neurons did not change P-JNK/JNK and P-c-Jun/c-Jun ratios (n=4). **c**) Cell death in hMecp2<sup>wt</sup> and hMecp2<sup>mut</sup> neurons: the hMecp2<sup>mut</sup> showed greater cell death than to hMecp2<sup>wt</sup>. D-JNKI1 reduced induced-cell death in the hMecp2<sup>mut</sup> neurons (n=4; isolated by immuno-magnetic sorting using anti-CD24 antibodies) to the control level (hMecp2<sup>wt</sup>). Data were shown as mean  $\pm$  SEM. Significance was calculated using two-way ANOVA followed by Bonferroni post hoc test for multiple comparisons. Significance vs control \*p<0.05, \*\*p<0.01, \*\*\*\*p<0.0001; D-JNKI1 treated vs untreated mutated neurons #p<0.05, ## p<0.01, ###p<0.001.

Importantly, all the mutated allele hMECP2<sup>mut</sup> neurons showed a powerful increase in their P-JNK/JNK and P-c-Jun/c-Jun ratios compared to hMECP2<sup>wt</sup> neurons (p=0.0348, p=0.00473 Fig. 26b), providing strong evidence that MECP2 mutations activate the JNK pathway in hiPSCs derived neurons. In addition, hMECP2<sup>mut</sup> neuron media had higher level of LDH (50%) than hMECP2<sup>wt</sup> the internal control allele (p<0.0001, Fig. 26b), demonstrating that just the mutated allele induced cell death. D-JNKI1 treatment was able to reduce the P-JNK/JNK (50%) and P-c-Jun/c-Jun (70%) ratios in hMECP2<sup>mut</sup> neurons, reducing their ratios to wt neurons (p=0.0473 and p=0.0015, Fig. 26b). The JNK inhibition also prevented neuronal death in hMECP2<sup>mut</sup> neurons, as indicated by the significant reduction of the LDH in the media of treated compared to untreated hMECP2<sup>mut</sup> neurons (p=0.0001, Fig. 26b).

These data showed that the JNK signalling mediates pathological alterations in human neurons differentiated from MECP2<sup>mut</sup> hiPSCs. Importantly, D-JNKI1-treated control neurons did not show any increase in LDH or overt toxic effects, suggesting the safety of this treatment (Fig. 26b).

These results offer the first proof of principle that JNK is a key stress protein in human RTT and that its modulation produces therapeutic effects for this condition.

## 4.2 JNK role in in-vivo model of Angelman Syndrome

### 4.2.1 *Ube3a*<sup>m-/p+</sup> mice present changes in JNK and ERK signalling pathways alterations at 7 and 23 weeks of age

To investigate whether mutated-UBE3A induces JNK signalling pathway activation, we measured the p-JNK/JNK and p-c-Jun/c-Jun ratios in the total homogenate of cortex, hippocampus, and cerebellum of 7- and 23-week-old mice.

At 7 weeks, representing the early stage of the pathology, JNK activation was significantly higher in *Ube3a*<sup>m-/p+</sup> mice compared to age-matched wt mice. In *Ube3a*<sup>m-/p+</sup> mice the p-c-Jun/c-Jun ratio was 30% higher in the hippocampus ( $p < 0.001$ , Fig. 27B), 27% in the cortex ( $p < 0.05$ , Fig. 27A), and 43% in the cerebellum ( $p < 0.0001$ , Fig. 27C) than in wt mice.

The p-JNK/JNK and p-c-Jun/c-Jun ratios in the total homogenate of cortex, hippocampus and cerebellum were also measured at 23 weeks of age to determine the importance of stress signalling in the progression of *Ube3a*<sup>m-/p+</sup> pathology. JNK activity was significantly higher in *Ube3a*<sup>m-/p+</sup> mice than in age-matched wt mice (39% in the hippocampus, 27% in the cortex and 25% in the cerebellum,  $p < 0.0001$ ;  $p < 0.0001$ ;  $p < 0.0001$ , Fig. 27E, 27D, 27F). These findings illustrate that JNK activation persists until 23 weeks of age at an advanced stage of the AS pathology.

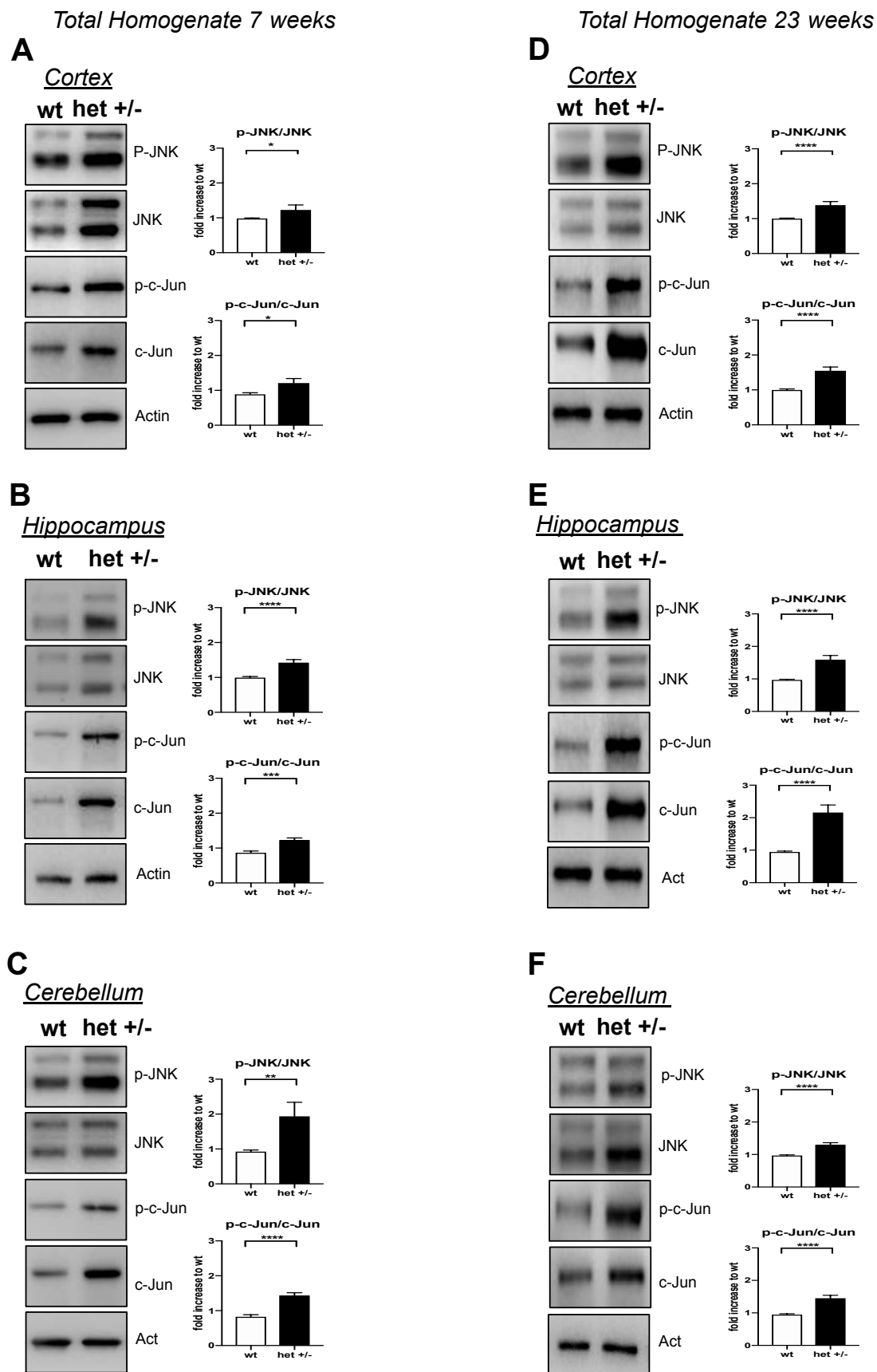


**Figure 27. Changes in JNK stress signalling pathway persist in the total homogenate from 7 to 23 weeks *Ube3a*<sup>m-/p+</sup> mice.** Representative western blots and relative quantifications of total homogenate of A) cortex, B) hippocampus, C) cerebellum of 7 weeks old mice and D), E), F) of 23 weeks old mice show higher level of p-JNK/JNK and p-c-Jun/c-Jun ratios in *Ube3a*<sup>m-/p+</sup> vs wt

mice.  $n=10$ . Genotypes are compared using  $t$ -tests. Statistical significance: \* $p<0.05$ , \*\* $p<0.01$ , \*\*\*\* $p<0.0001$ . Data are expressed as mean  $\pm$  SEM.

#### 4.2.2 $Ube3a^{m-/p+}$ mice show changes in PSD biochemical markers and JNK activation in the TIF at 7 weeks of age

To study the molecular organization of the PSD-region in  $Ube3a^{m-/p+}$  mice we isolated the post-synaptic enriched protein fraction (TIF) of hippocampus, cortex, and cerebellum.

We measured JNK activation in the PSD region, in  $Ube3a^{m-/p+}$  hippocampus compared to wt mice. The P-JNK/JNK ratio was significantly higher in  $Ube3a^{m-/p+}$  (50%,  $p<0.0001$ , Fig. 28) than wt mice. We also measured the p-PSD95/PSD95 ratio (Fig. 28), using a p-PSD95 antibody that recognizes the specific JNK phosphorylation site. The ratio was significantly higher in  $Ube3a^{m-/p+}$  (27%) than wt mice ( $p<0.01$ , Fig. 28). In addition, to analyse the molecular organization of the PSD region of  $Ube3a^{m-/p+}$  mice, we quantified Shank3, a scaffold protein strongly implicated in autism, Drebrin, a marker of mature spines and AMPA and NMDA glutamate receptors. Shank3 and GLUR2 levels were significantly higher in  $Ube3a^{m-/p+}$  (55% and 53%;  $p<0.01$ ,  $p<0.05$ , Fig. 28), while Drebrin was 23% lower than in wt mice ( $p<0.05$ , Fig. 28). NR2A, NR2B and GLUR1 levels showed no significant changes in  $Ube3a^{m-/p+}$  (Fig. 28). These results indicate abnormal organization of the PSD region in  $Ube3a^{m-/p+}$  mice.

#### Post-Synaptic Protein-enriched fraction of 7 weeks old mice

##### A Hippocampus

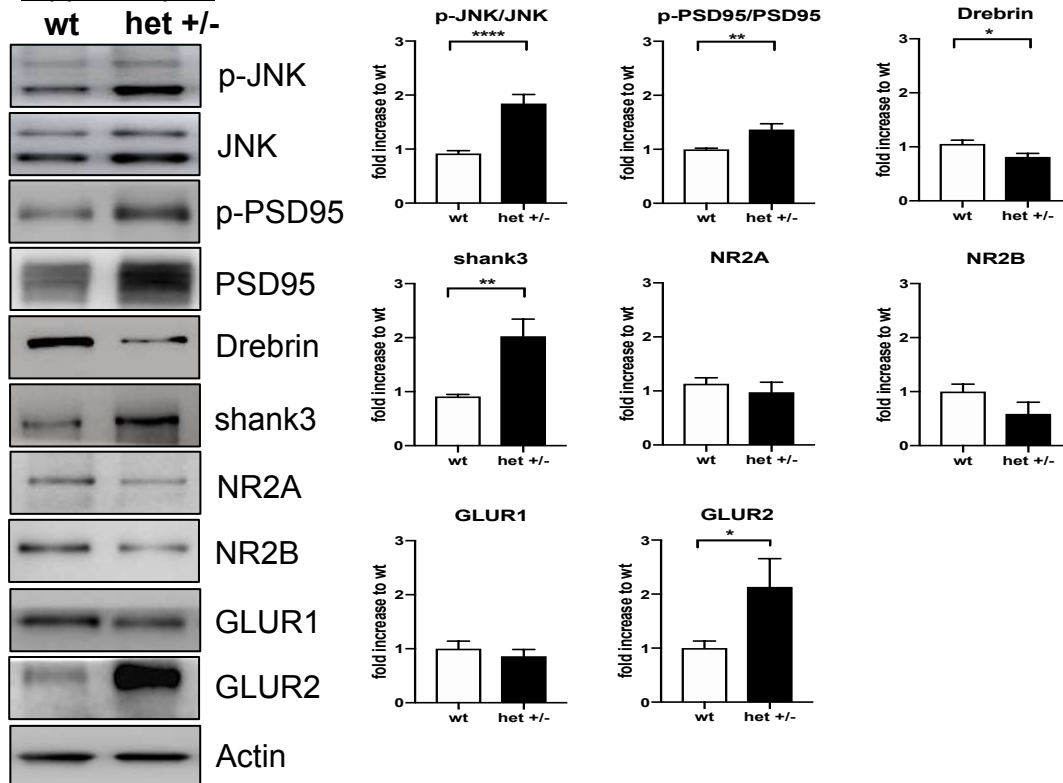


**Figure 28. Changes in JNK activation and PSD markers in the hippocampus of *Ube3a*<sup>m-/p+</sup> at 7 weeks of age.** A) Representative western blots and relative quantifications showed JNK activation followed by changes in biochemical marker levels. The p-PSD95/PSD95 ratio, Shank3 and GLUR2 levels are higher in *Ube3a*<sup>m-/p+</sup> mice than wt, while Drebrin level is lower. NR2A, NR2B and GLUR1 level do not differ in *Ube3a*<sup>m-/p+</sup> and wt mice. n=10. Genotypes are compared using t-tests. Statistical significance: \*p<0.05, \*\*p<0.01, \*\*\*\*p<0.0001. Data are expressed as mean ± SEM.

We analysed JNK activation at the PSD region in the cortex as well. The p-JNK/JNK ratio was significantly higher (45%) in *Ube3a*<sup>m-/p+</sup> than wt mice (p<0.0001, Fig. 29), indicating JNK activation in the post-synaptic compartment also in this brain area. The p-PSD95/PSD95 ratio was significantly higher in *Ube3a*<sup>m-/p+</sup> (28%) than wt mice (p<0.0001, Fig. 29). In *Ube3a*<sup>m-/p+</sup> the Shank3 level was 51% higher and Drebrin 43% lower than in wt mice (p<0.001 and p<0.01, Fig. 29). In addition, NR2A (45%) and AMPA receptor subunits GLUR1 (30%) were significantly lower in *Ube3a*<sup>m-/p+</sup> than in wt mice (p<0.05, p<0.05, Fig. 29), while NR2B and GLUR2 levels showed no changes (Fig. 29).

### Post-Synaptic Protein-enriched fraction of 7 weeks old mice

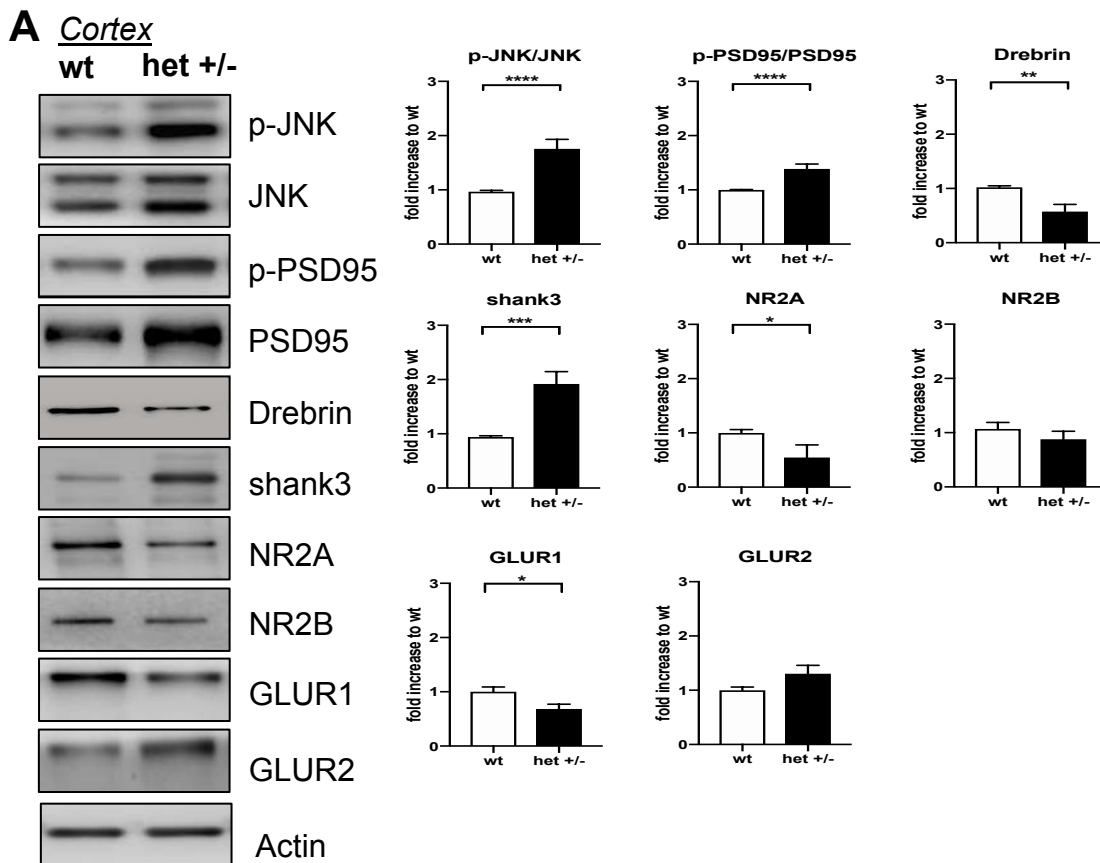


**Figure 29. Changes in JNK activation and PSD markers in the cortex of *Ube3a*<sup>m-/p+</sup> at 7 weeks of age.** A) Representative western blots and relative quantifications showed JNK activation followed by changes in biochemical marker levels. The p-PSD95/PSD95 ratio and Shank3 levels are higher in *Ube3a*<sup>m-/p+</sup> mice than wt, while Drebrin, NR2A and GluR1 levels are lower. NR2B and GLUR2 levels do not differ in *Ube3a*<sup>m-/p+</sup> and wt mice. n=10. Genotypes are compared using t-tests. Statistical significance: \*p<0.05, \*\*p<0.01, \*\*\*\*p<0.0001. Data are expressed as mean ± SEM.

Finally, we also examined JNK activation in the PSD region in the cerebellum, in *Ube3a*<sup>m-/p+</sup> compared to wt mice. At this stage there is only a tendency for an increase of p-JNK/JNK ratio in *Ube3a*<sup>m-/p+</sup> compared to wt, meaning that JNK activation is not as strong as in the other areas. The p-PSD95/PSD95 ratio (29%) and Shank3 level (46%) were significantly higher in *Ube3a*<sup>m-/p+</sup> than wt ( $p < 0.05$ ,  $p < 0.001$ , Fig. 30) while Drebrin (59%), NR2A (70%), NR2B (71%), GLUR1 (41%) and GLUR2 (58%) levels were significantly lower ( $p < 0.001$ ,  $p < 0.05$ ,  $p < 0.01$ ,  $p < 0.05$ ,  $p < 0.01$ , Fig. 30).

### Post-Synaptic Protein-enriched fraction of 7 weeks old mice

#### B Cerebellum

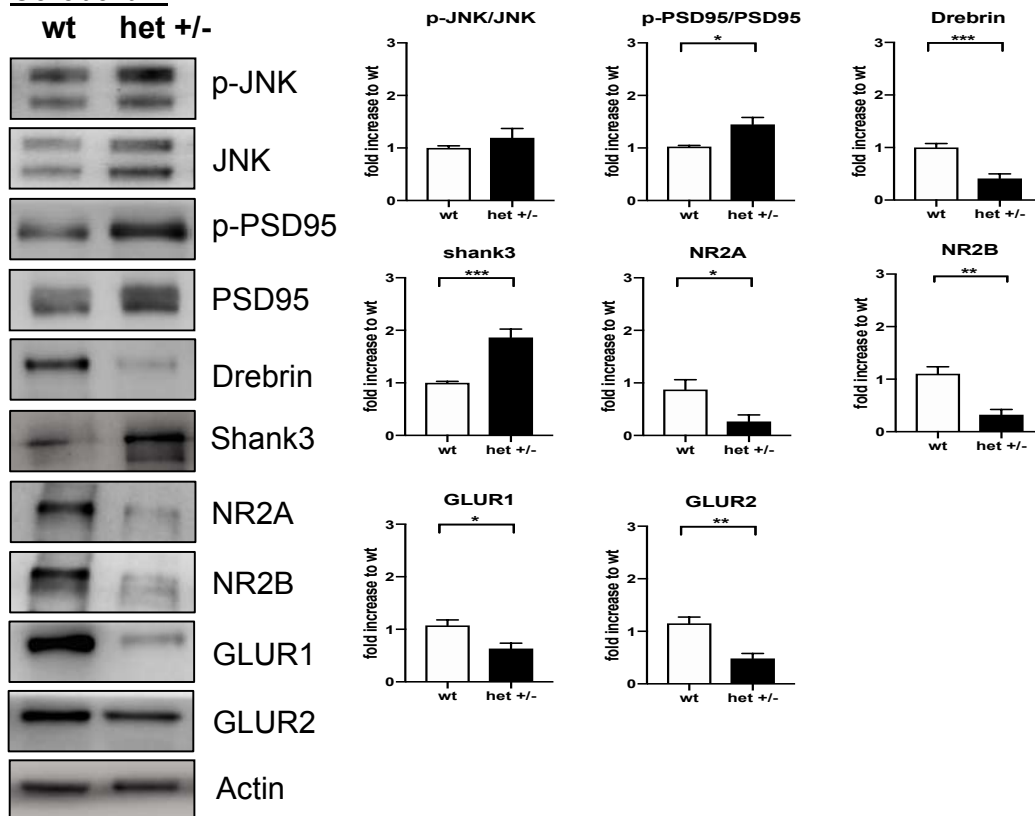


**Figure 30. Changes in JNK activation and PSD markers in cerebellum of *Ube3a*<sup>m-/p+</sup> at 7 weeks of age.** A) Representative western blots and relative quantifications changes in PSD biochemical marker levels. The p-PSD95/PSD95 ratio and Shank3 levels are higher in *Ube3a*<sup>m-/p+</sup> mice than wt, while Drebrin, NR2A, NR2B, GluR1 and GluR2 levels are lower in *Ube3a*<sup>m-/p+</sup> and wt mice.  $n=10$ . Genotypes are compared using *t*-tests. Statistical significance: \* $p < 0.05$ , \*\* $p < 0.01$ , \*\*\* $p < 0.001$ . Data are expressed as mean  $\pm$  SEM.

#### 4.2.3 *Ube3a*<sup>m-/p+</sup> mice present behavioural impairments at 7 weeks of age

*Ube3a*<sup>m-/p+</sup> PSD showed significant biomarker changes in the 3 different brain areas analysed. In order to correlate *Ube3a*<sup>m-/p+</sup> synaptic dysfunctions, demonstrated by the analysis of the post-synaptic enriched protein fraction of cortex, hippocampus, and cerebellum, to both cognitive and locomotor defects we examined cognitive impairment with the Novel Object Recognition Test (NORT) and locomotor defects with the Open Field and Rotarod tests.

In the NORT, *Ube3a*<sup>m-/p+</sup> mice had a significantly lower discrimination index (DI) (96%) than aged-matched wt mice (p<0.05, Fig. 31A). These data confirm the severe cognitive impairment in *Ube3a*<sup>m-/p+</sup> mice already at 7 weeks of age.

To investigate spontaneous locomotor and exploratory activity in *Ube3a*<sup>m-/p+</sup> we ran the Open Field test on the same animals. *Ube3a*<sup>m-/p+</sup> mice had significantly lower velocity (15%) and shorter distance moved (14%) than aged-matched wt mice (p<0.05, Fig. 31B). The total number of crossing was significantly lower too (21%) in *Ube3a*<sup>m-/p+</sup> than wt mice (p<0.05, Fig. 31B). These data confirm locomotor impairments in *Ube3a*<sup>m-/p+</sup> mice. Exploratory activity was measured as the time spent in the inner and the outer zone (Fig. 31B): *Ube3a*<sup>m-/p+</sup> mice spent more time (9%, p<0.01) in the outer zone of the arena but the time spent in the inner zone was no significantly different from aged-matched wt mice. In addition, *Ube3a*<sup>m-/p+</sup> mice also had an increased hypermobility state (95%, p<0.01, Fig. 31B) compared to age-matched wt mice. To summarize, *Ube3a*<sup>m-/p+</sup> mice showed a mild exploratory impairment at 7 weeks compared to wt mice but had a severe hypermobility symptom.

The *Ube3a*<sup>m-/p+</sup> locomotor impairment was then characterized in the Rotarod test. *Ube3a*<sup>m-/p+</sup> had a shorter (17%) latency to fall on the accelerated rod than to aged-matched wt mice, with significantly reduced locomotor ability at 7 weeks of age (p<0.05, Fig. 31C).

These results suggest that *Ube3a*<sup>m-/p+</sup> mice at 7 weeks of age present an important cognitive impairment while the locomotor defects seem milder than in aged-matched wt mice.

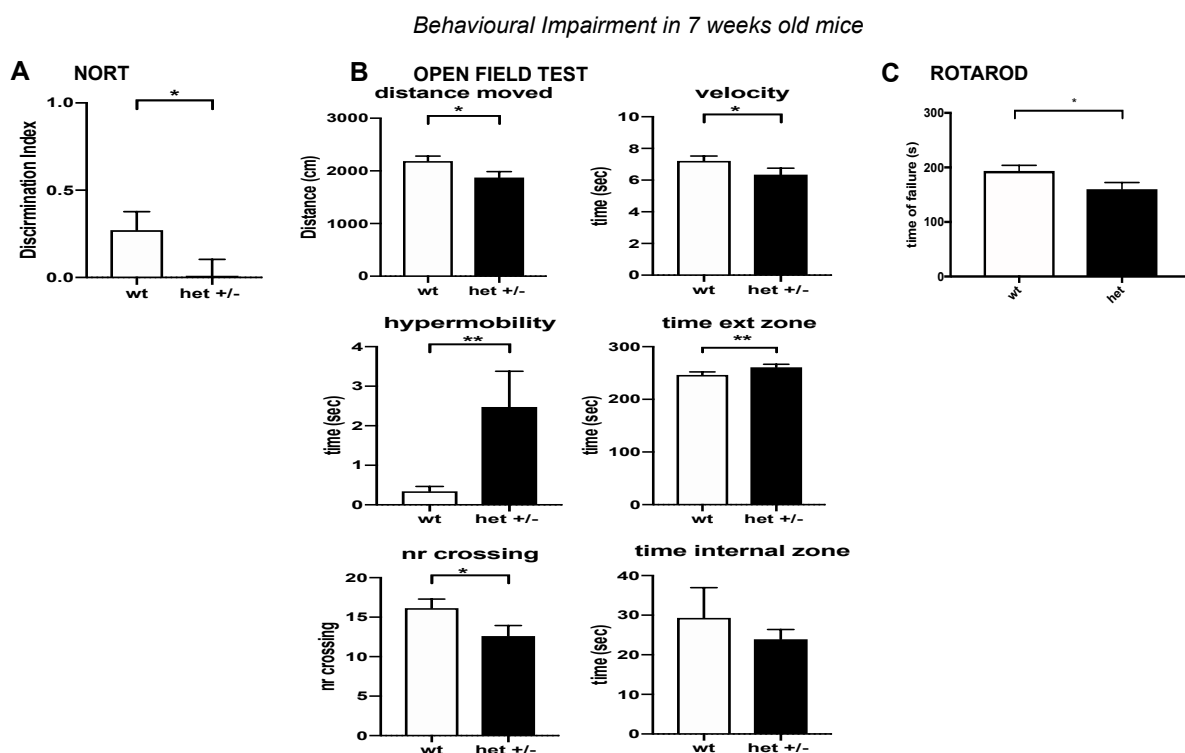


**Figure 31. 7-week-old *Ube3a*<sup>m-/p+</sup> mice show severe cognitive impairment and mild locomotor and exploratory defects.** *Ube3a*<sup>m-/p+</sup> mice give a lower DI in the NORT than aged-matched wt mice (A). The Open Field Test (B) shows the shorter distance moved, velocity and smaller number of crossing in *Ube3a*<sup>m-/p+</sup> mice than wt. *Ube3a*<sup>m-/p+</sup> mice also had increased hypermobility

and spent more time in the outer zone of the arena and less time in the inner zone (not significant). *Ube3a*<sup>m-/p+</sup> mice also had a shorter time to failure in the Rotarod test compared to wt mice (C). n=10. Genotypes were compared using t-tests. Statistical significance: \*p<0.05, \*\*p<0.01. Data are expressed as mean ± SEM.

#### 4.2.4 *Ube3a*<sup>m-/p+</sup> mice present changes in PSD biochemical markers and JNK activation in the post-synaptic element at 23 weeks of age

After the behavioural tests, we sacrificed animals and then characterized the synaptic dysfunction of *Ube3a*<sup>m-/p+</sup> mice at 23 weeks of age analysing the post-synaptic enriched protein fraction of cortex, hippocampus, and cerebellum.

Concerning the hippocampal post-synaptic elements, we found a strong JNK activation, proved by increased p-JNK/JNK ratio higher in *Ube3a*<sup>m-/p+</sup> than wt (49%, p<0.0001, Fig. 32). The p-PSD95/PSD95 ratio (22%), Shank3 (47%), NR2A (55%), NR2B (25%) and GLUR2 (56%) levels were significantly higher in *Ube3a*<sup>m-/p+</sup> than wt mice (p<0.01, p<0.001, p<0.001, p<0.01, p<0.0001, Fig. 32) while Drebrin (45%) and GLUR1 (47%) levels were lower than in wt mice (p<0.0001, Fig. 32).

#### Post-Synaptic Protein-enriched fraction of 23 weeks old mice

##### A Hippocampus

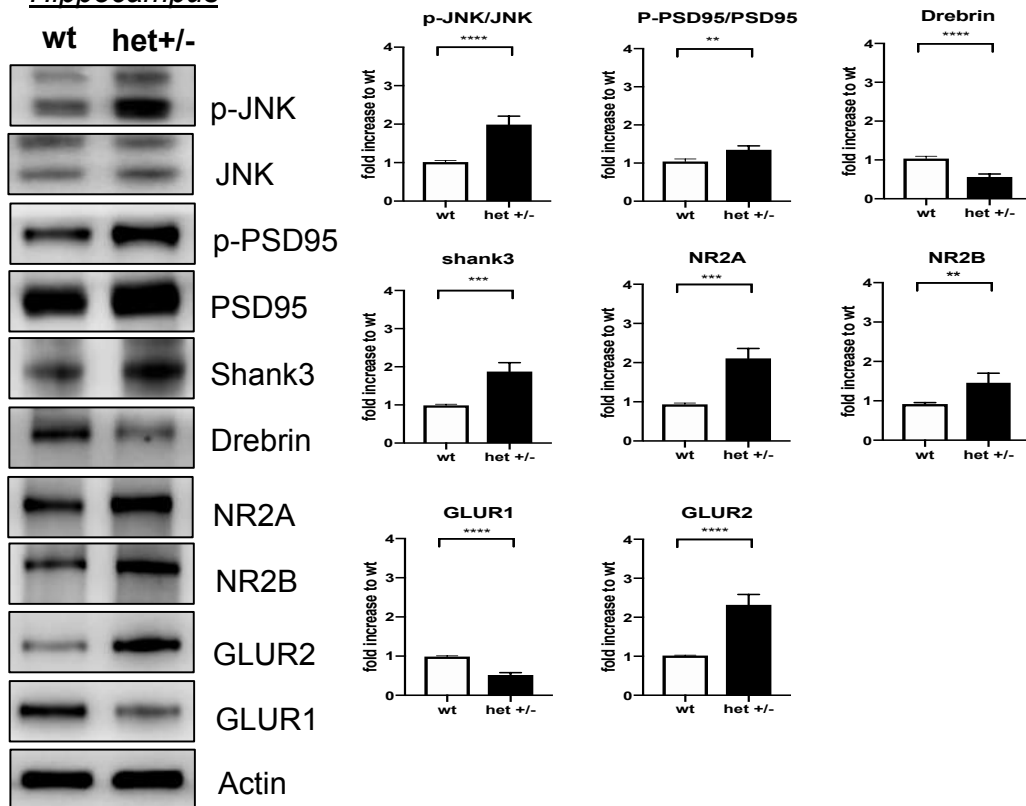


**Figure 32.** 23-week-old *Ube3a*<sup>m-/p+</sup> mice still present JNK activation and PSD alterations in the hippocampus. A) Representative western blots and relative quantifications showed JNK hyperactivation in the hippocampus TIF fraction of *Ube3a*<sup>m-/p+</sup> mice compared to wt mice. p-PSD95/PSD95 ratio, Shank3, NMDA-receptors and GLUR2 levels are higher in *Ube3a*<sup>m-/p+</sup> mice

than wt, while Drebrin and GLUR1 levels are lower in *Ube3a*<sup>m-/p+</sup> mice than wt. n=10. Genotypes are compared using t-tests. Statistical significance: \*\*p<0.01, \*\*\* p<0.001, \*\*\*\*p<0.0001. Data are expressed as mean ± SEM.

Also in cortex, JNK signalling was activated in *Ube3a*<sup>m-/p+</sup> compared to wt mice (p<0.0001, Fig. 33). The p-PSD95/PSD95 ratio and Shank3 levels were increased (p<0.0001, p<0.001, Fig. 33), while Drebrin, NR2A and GluR1 levels were significantly lower in *Ube3a*<sup>m-/p+</sup> than wt mice (p<0.01, p<0.05, p<0.05, Fig. 33). On the contrary, no differences were found in NR2B and GluR2 levels.

### Post-Synaptic Protein-enriched fraction of 23 weeks old mice

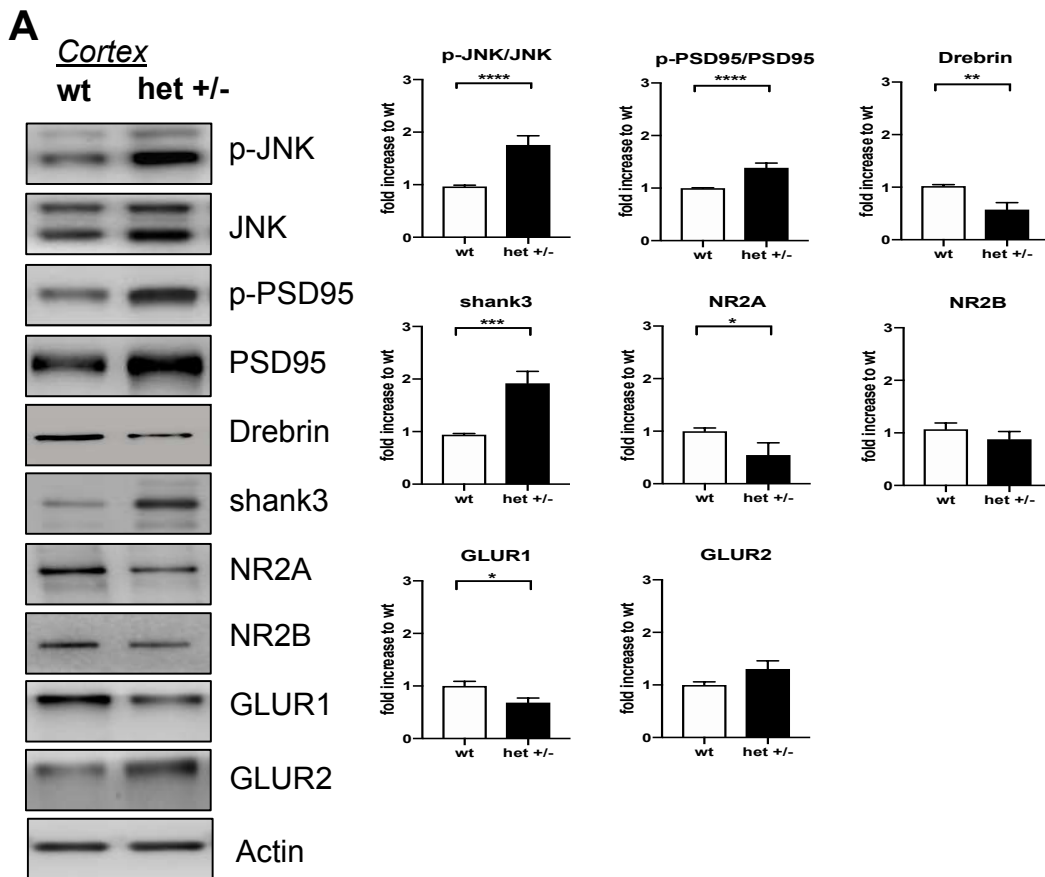


**Figure 33. 23-week-old *Ube3a*<sup>m-/p+</sup> mice still present JNK activation and PSD alterations in the cortex.** A) Representative western blots and relative quantifications showed JNK hyperactivation in the cortex TIF fraction of *Ube3a*<sup>m-/p+</sup> mice compared to wt mice. p-PSD95/PSD95 ratio, Shank3, NR2A and GLUR1 levels are higher in *Ube3a*<sup>m-/p+</sup> mice than wt, while Drebrin and GLUR1 levels are lower in *Ube3a*<sup>m-/p+</sup> mice than wt. n=10. Genotypes are compared using t-tests. Statistical significance: \*p<0.05, \*\*p<0.01, \*\*\* p<0.001, \*\*\*\*p<0.0001. Data are expressed as mean ± SEM.

Lastly, in the cerebellum, we did not find any changes in JNK activation but just a tendency to be increased in *Ube3a*<sup>m-/p+</sup> compared to wt mice. On the other hand, we observed a general deregulation of scaffold and protein levels: p-PSD95/PSD95 ratio and Shank3 levels were increased (p<0.05, p<0.001,

Fig. 34), while Drebrin, NR2A, NR2B, GluR1 and GluR2 levels were significantly lower in *Ube3a*<sup>m-/p+</sup> than wt mice ( $p < 0.001$ ,  $p < 0.05$ ,  $p < 0.01$ ,  $p < 0.05$ ,  $p < 0.01$ , Fig. 34).

### Post-Synaptic Protein-enriched fraction of 23 weeks old mice

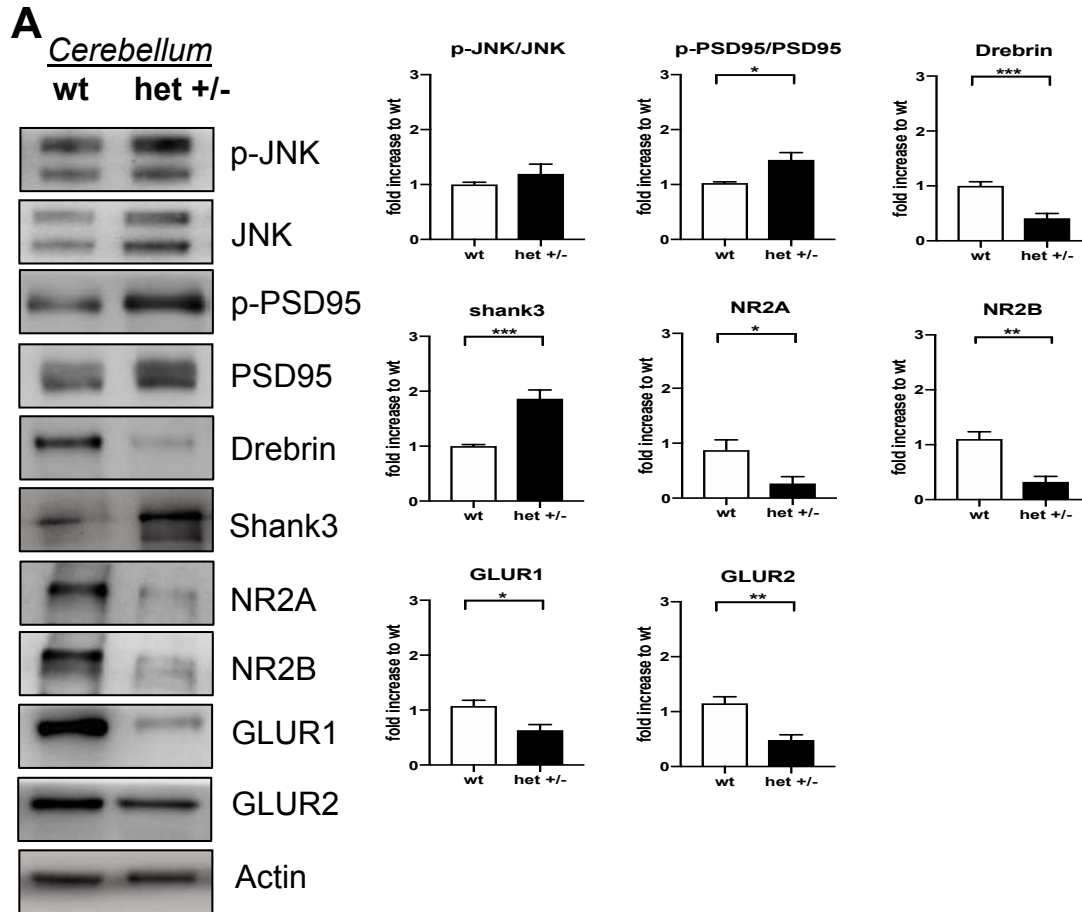


**Figure 34. 23-week-old *Ube3a*<sup>m-/p+</sup> mice present PSD alterations in cerebellum.** A) Representative western blots and relative quantifications showed increased levels of p-PSD95/PSD95 ratio and Shank3 and reduced levels of Drebrin, NR2A, NR2B, GLUR1 and GLUR2 in *Ube3a*<sup>m-/p+</sup> mice than wt.  $n = 10$ . Genotypes are compared using *t*-tests. Statistical significance: \* $p < 0.05$ , \*\* $p < 0.01$ , \*\*\* $p < 0.001$ . Data are expressed as mean  $\pm$  SEM.

#### 4.2.5 *Ube3a*<sup>m-/p+</sup> mice present behavioural impairments at 23 weeks of age

Cognitive and locomotor defects in *Ube3a*<sup>m-/p+</sup> mice were examined also at 23 weeks of age. In the NORT, *Ube3a*<sup>m-/p+</sup> mice had a significantly lower DI than aged-matched wt mice ( $p < 0.001$ , Fig. 35A). Wt mice had a DI of 0.272, and *Ube3a*<sup>m-/p+</sup> DI had -0.1352 while at 7 weeks it was 0.009422. These data indicate that *Ube3a*<sup>m-/p+</sup> cognitive impairments get worse with the progression of the AS pathology.

The Open Field test was run at 23 weeks to assess the spontaneous locomotor and exploratory activity in *Ube3a*<sup>m-/p+</sup> and wt mice. Surprisingly, *Ube3a*<sup>m-/p+</sup> mice did not significantly differ in velocity and distance moved from aged-matched wt mice (Fig. 35B), indicating no genotypic differences. However,

at 23 weeks the total number of crossings was significantly smaller (30%) in *Ube3a*<sup>m-/p+</sup> ( $p < 0.05$ , Fig. 35B).

As regards exploratory activity, the time spent by *Ube3a*<sup>m-/p+</sup> mice in the inner zone did not significantly differ from the time spent by aged-matched wt mice (Fig. 35B), while the time spent in the outer zone was higher ( $p < 0.05$ , Fig. 35B).

Finally, *Ube3a*<sup>m-/p+</sup> mice still presented an increased hypermobility (78%,  $p < 0.05$ , Fig. 35B) compared to age-matched wt mice. The *Ube3a*<sup>m-/p+</sup> mice locomotor impairment at 23 weeks was not significantly different from wt mice, although there were fewer crossings and the evident hypermobility symptoms persisted at this stage of the AS pathology of mice. *Ube3a*<sup>m-/p+</sup> locomotor impairment was further characterized in the Rotarod test. At 23 weeks *Ube3a*<sup>m-/p+</sup> mice still had a shorter latency time (13%) on the rod than aged-matched wt mice, with a significant decrease of locomotor ability at 23 weeks of age ( $p < 0.05$ , Fig. 35C).

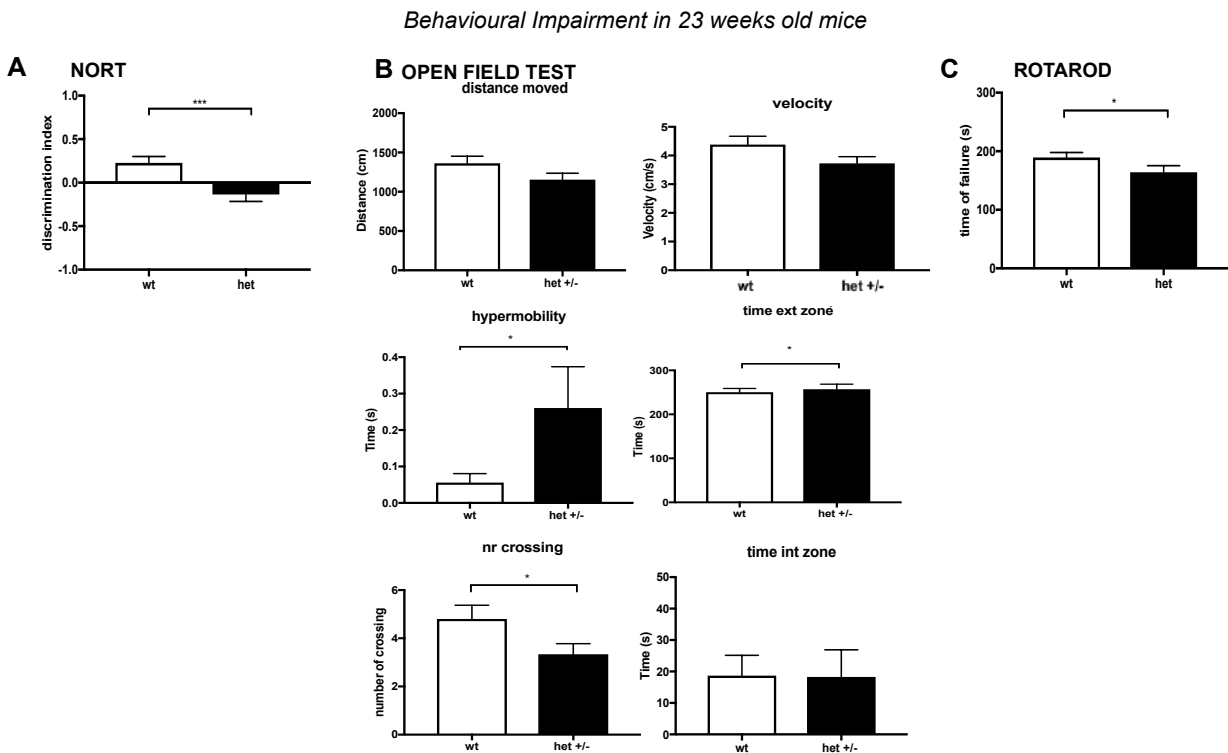


**Figure 35. Behavioural defect in 23-week-old *Ube3a*<sup>m-/p+</sup> mice.** *Ube3a*<sup>m-/p+</sup> mice show cognitive impairment indicated by a smaller DI in the NORT compared to aged-matched wt mice (A). The Open Field test (B) show no significant differences in distance, velocity, and time spent in the inner zone between wt and *Ube3a*<sup>m-/p+</sup> mice. *Ube3a*<sup>m-/p+</sup> mice had fewer crossings between the inner and outer zones of the arena and spent more time in the outer zone compared to wt mice. *Ube3a*<sup>m-/p+</sup> mice were also more hypermobile than wt. In the Rotarod test (C) *Ube3a*<sup>m-/p+</sup> mice had a shorten latency to fall on the rod than aged-matched wt mice.  $n=10$ . Genotypes were compared using *t*-tests. Statistical significance: \* $p < 0.05$ , \*\*\* $p < 0.001$ . Data are expressed as mean  $\pm$  SEM.

#### 4.2.6 Specific D-JNKI1 treatment prevents JNK signalling activation in 23 weeks old

##### **Ube3a<sup>m-/p+</sup> mice**

To determine the role of JNK in *Ube3a*<sup>m-/p+</sup> pathology we used the specific JNK inhibitor peptide, D-JNKI1, injected intraperitoneally every 4 weeks from 7 to 23 weeks of age, to inhibit JNK's action in *Ube3a*<sup>m-/p+</sup> mice and, as a control, in wt mice. Therefore, there were four groups: 1-D-JNKI1-treated wt 2-untreated wt mice and 3-D-JNKI1-treated *Ube3a*<sup>m-/p+</sup> and 4-untreated *Ube3a*<sup>m-/p+</sup> mice. D-JNKI1's inhibitory effect is measured as a reduction of p-JNK/JNK and p-c-Jun/c-Jun [371].

D-JNKI1 powerfully prevented JNK and c-Jun phosphorylation in the hippocampus (44%, p<0.0001; 51%, p<0.01, Fig. 36A), cortex (55%, p<0.0001; 30%, p<0.001% Fig. 36B), and cerebellum (26%, p<0.001; 40%, p<0.0001 Fig. 36C) in the treated compared to untreated *Ube3a*<sup>m-/p+</sup> mice but had no significant effect in wt mice.

These data confirm the efficacy of D-JNKI1 in the cortex, hippocampus, and cerebellum in-vivo and suggests there are no major side effects in control conditions.

D-JNK11 Chronic Treatment: Total Homogenate

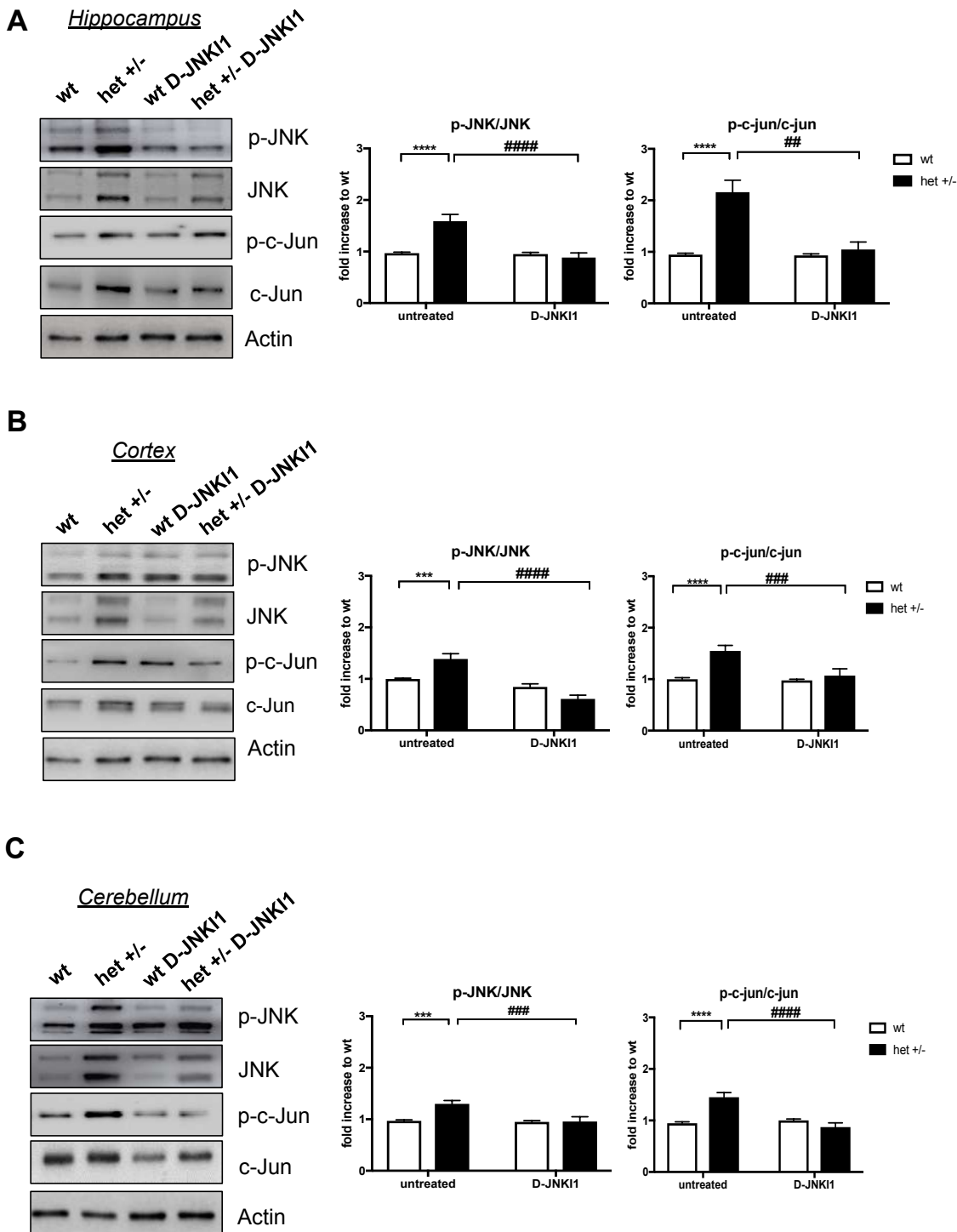


**Figure 36. D-JNK11 chronic treatment reduced JNK activation in the total homogenate of 23 weeks old *Ube3a*<sup>m-/p+</sup> mice.** Representative western blots and relative quantifications of A) hippocampus, B) cortex, C) cerebellum total homogenates show the higher p-JNK/JNK and p-c-Jun/c-Jun ratios in 23-week-old *Ube3a*<sup>m-/p+</sup> mice. D-JNK11 blocks the JNK signalling pathway activation. The treatment had no changes in wt mice. n=10. Significance differences from control \*\*\*p<0.001, \*\*\*\*p<0.0001; D-JNK11 treated vs untreated: ##p<0.01, ###p<0.001, ####p<0.0001. Two-way ANOVA, Tukey's post-hoc test. Data are expressed as mean ± SEM.

#### 4.2.7 D-JNK11 normalizes biochemical PSD changes in 23 weeks old *Ube3a*<sup>m-/p+</sup> mice

D-JNK11 normalized the biochemical changes in the post-synaptic element of the hippocampus, cortex, and cerebellum in *Ube3a*<sup>m-/p+</sup> mice. In the hippocampus D-JNK11 reduced the p-JNK/JNK and p-PSD95/PSD95 ratios (to 49% and 26%), ( $p < 0.0001$ ,  $p < 0.05$ , Fig. 37) compared to untreated *Ube3a*<sup>m-/p+</sup> mice. Shank3 and Drebrin levels were both regularized to control levels. D-JNK11 also normalized the levels of NR2B (72%,  $p < 0.01$ , Fig. 37), GLUR1 33% ( $p < 0.05$ , Fig. 37) and GLUR2 40% ( $p < 0.01$ , Fig. 37) compared to untreated *Ube3a*<sup>m-/p+</sup> mice, while there was no effect on NR2A. As regards D-JNK11 inhibition on wt mice, there were no significant changes in PSD markers, suggesting no major toxic effects.

**A**

Post-synaptic protein enriched fraction

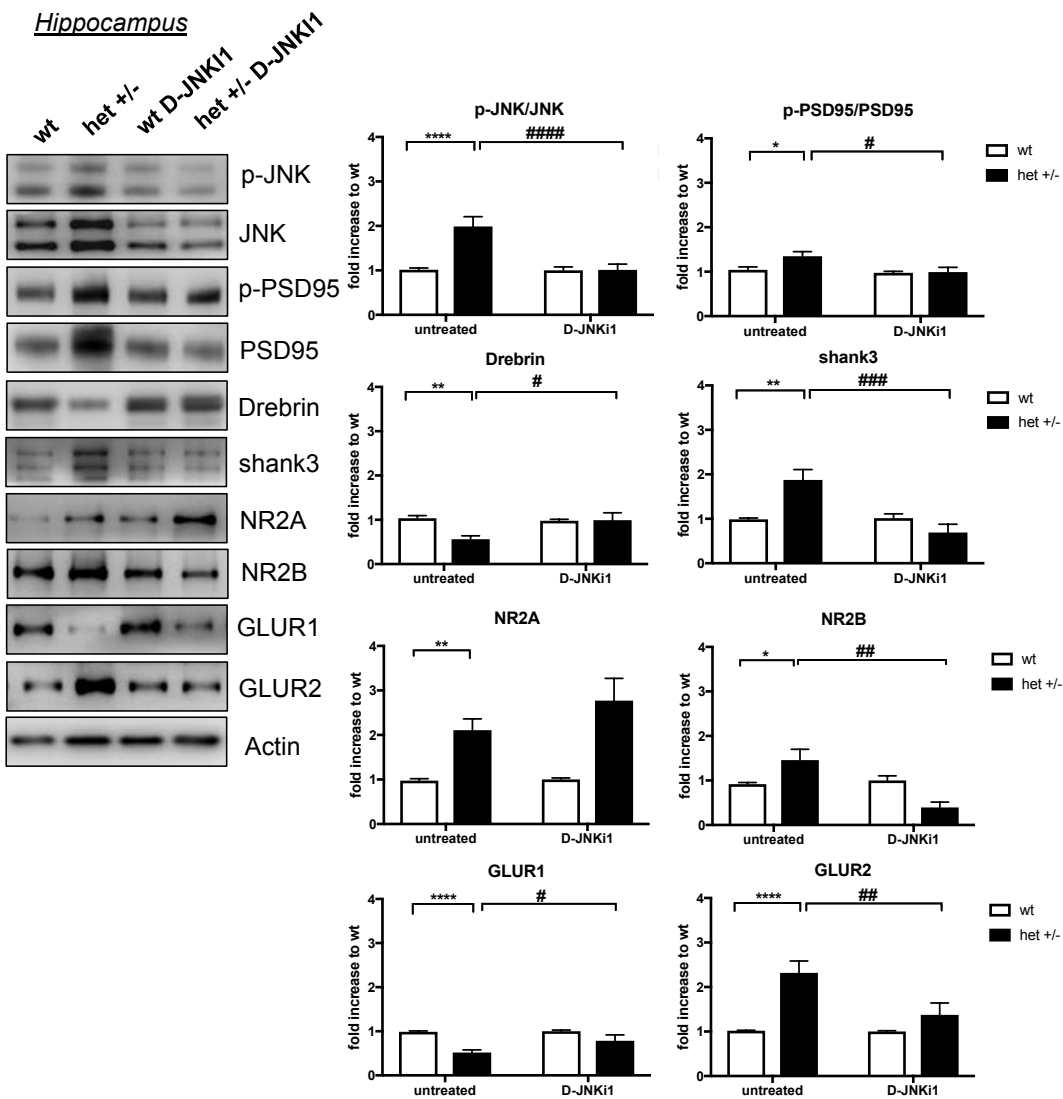


**Figure 37. D-JNK11 chronic treatment reduced JNK activation in the hippocampus TIF fraction of 23 weeks old *Ube3a*<sup>m-/p+</sup> mice.** (A) Representative western blots and quantifications show JNK activation in the hippocampus TIF fraction of *Ube3a*<sup>m-/p+</sup> mice at 23 weeks of age with higher levels of p-PSD95/PSD95, Shank3, NR2A, NR2B and GLUR2 then in wt mice. On the contrary, Drebrin and GLUR1 levels are reduced in *Ube3a*<sup>m-/p+</sup> mice to age-matched wt. D-JNK11 reduced JNK activation, the p-PSD95/PSD95

ratio, Shank3 and NR2B levels but raised Drebrin, GLUR1 and NR2A (not significant) levels in treated compared to untreated *Ube3a*<sup>m-/p+</sup> mice. The treatment did not cause any changes in wt. n=10. Significance differences from control \*p<0.05, \*\*p<0.01, \*\*\*p<0.0001; D-JNKI1 treated vs untreated: #p<0.05, ##p<0.01, ### p<0.001, #### p<0.0001. Two-way ANOVA, Tukey's post-hoc test. Data are expressed as mean ± SEM.

D-JNKI1 also rescued the biochemical changes observed in the cortex post-synaptic element of 23-week-old *Ube3a*<sup>m-/p+</sup> mice. Briefly, the treatment powerfully reduced (58%) the p-JNK/JNK ratio in the PSD of treated *Ube3a*<sup>m-/p+</sup> compared to untreated mice (p<0.001, Fig. 38). The p-PSD95/PSD95 ratio was lower (35%, p<0.01, Fig. 38) in treated *Ube3a*<sup>m-/p+</sup> compared to untreated *Ube3a*<sup>m-/p+</sup> mice (Fig. 38); Shank3 was lower as well (70%, p<0.0001, Fig. 38), while Drebrin did not significantly change. D-JNKI1 restored NMDA and AMPA receptor levels. NR2A decreased 64% (p<0.0001, Fig. 38), NR2B 49% (p<0.01, Fig. 38), GLUR1 39% (p<0.01, Fig. 38) and GLUR2 61% (p<0.0001, Fig. 38) in treated compared to untreated *Ube3a*<sup>m-/p+</sup> mice. D-JNKI1 normalized the biochemical marker levels of *Ube3a*<sup>m-/p+</sup> treated mice and had no significant effect in wt mice.

**A**

Post-Synaptic Protein enriched fraction

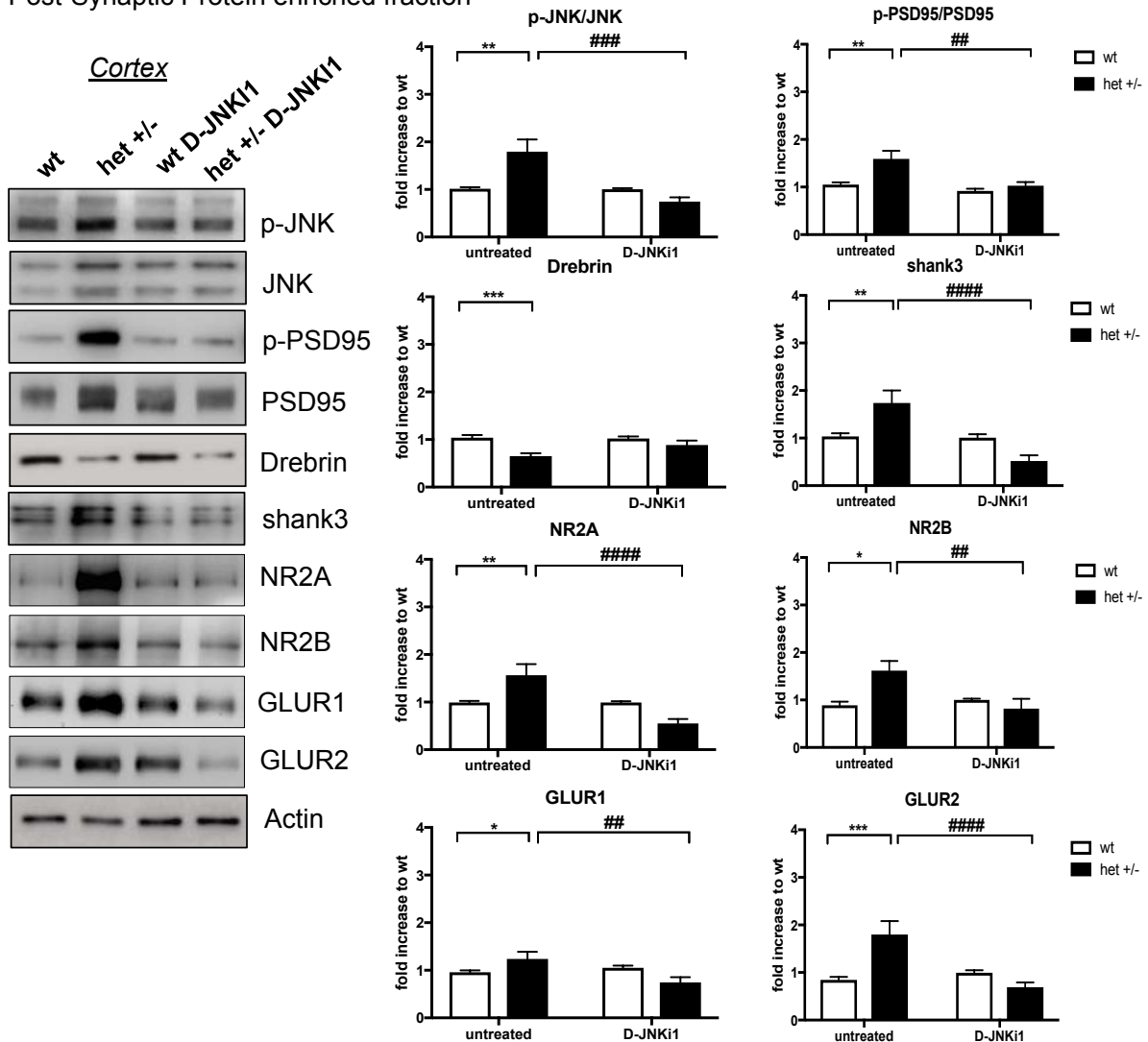


**Figure 38. D-JNKI1 chronic treatment reduced JNK activation in the cortex TIF fraction of 23 weeks old *Ube3a*<sup>m-/p+</sup> mice.** (A) Representative western blots and quantifications show JNK activation in the cortex TIF fraction of *Ube3a*<sup>m-/p+</sup> mice at 23 weeks of age with higher levels of p-PSD95/PSD95, Shank3, NR2A, NR2B, GLUR1 and GLUR2 then in wt mice. On the contrary, Drebrin levels are reduced in *Ube3a*<sup>m-/p+</sup> mice to age-matched wt. D-JNKI1 reduced JNK activation, the p-PSD95/PSD95 ratio, Shank3, NR2A, NR2B, GLUR1 and GLUR2 levels but raised Drebrin (not significant) levels in treated compared to untreated *Ube3a*<sup>m-/p+</sup> mice. The treatment did not cause any changes in wt. n=10. Significance differences from control \*p<0.05, \*\*p<0.01, \*\*\*p<0.001; D-JNKI1 treated vs untreated: ##p<0.01, ### p<0.001, #### p<0.0001. Two-way ANOVA, Tukey's post-hoc test. Data are expressed as mean ± SEM.

Finally, D-JNKI1 at 23 week normalized biochemical marker levels in the cerebellum of *Ube3a*<sup>m-/p+</sup> mice: p-JNK/JNK (38%) and p-PSD95/PSD95 (54%) ratios were lower in the post-synaptic enriched protein fraction of treated *Ube3a*<sup>m-/p+</sup> compared to untreated mice (p<0.001, p<0.0001, Fig. 39). Shank3 and Drebrin levels were both regularized, while the treatment raised the NMDA (70%, p<0.05 for NR2B, not significant for NR2A, Fig. 39) and AMPA receptor levels (GLUR1 62%, GLUR2 38%, p<0.0001, p<0.01 Fig. 39) compared to untreated mice. No significant effects were seen on treated wt mice (Fig. 39).

These data indicate that the D-JNK11 normalizes biochemical PSD alterations in-vivo in all the three brain areas studied.

**A**

Post-Synaptic Protein-enriched fraction

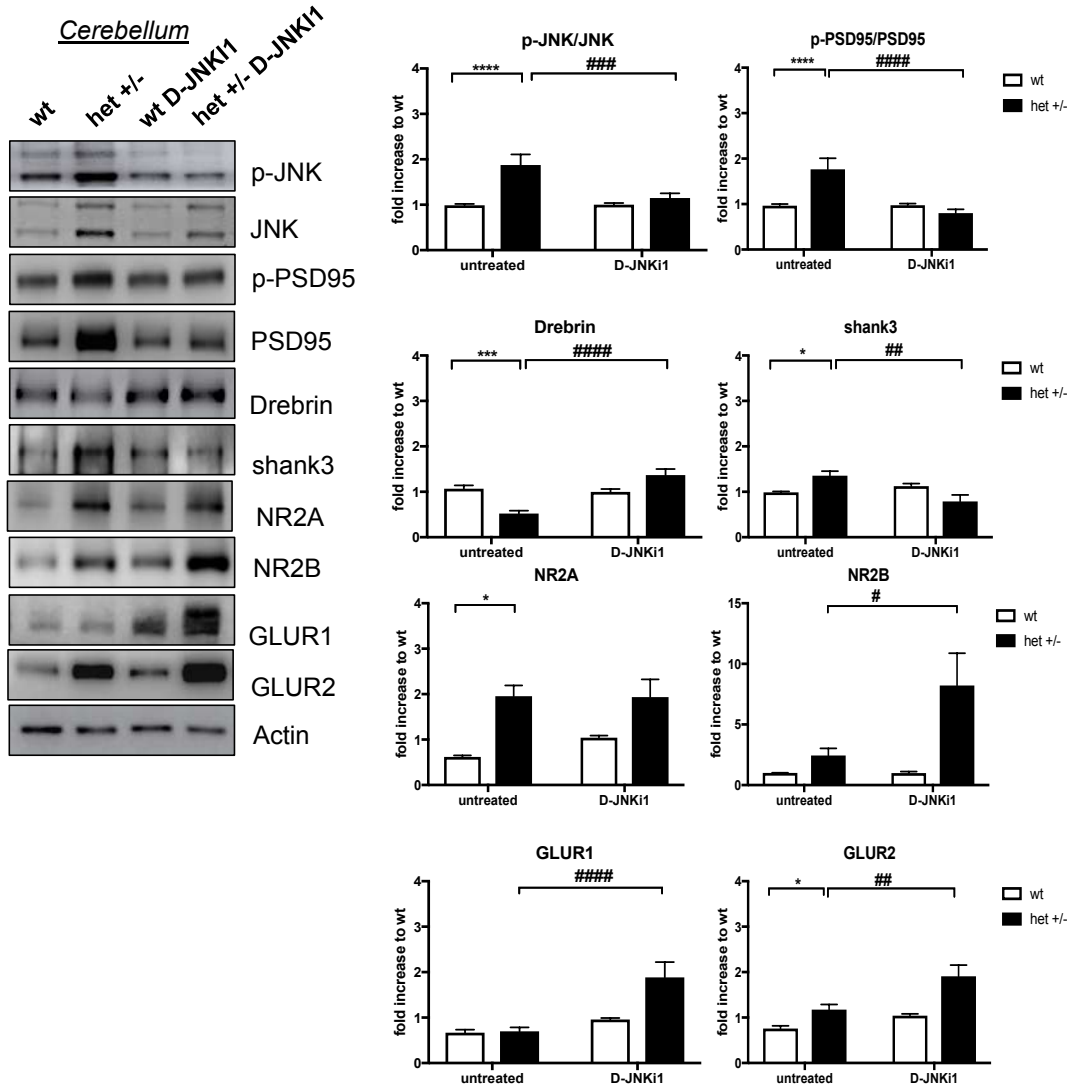


**Figure 39. D-JNK11 chronic treatment reduced JNK activation in the cerebellum TIF fraction of 23 weeks old *Ube3a*<sup>m-/p+</sup> mice.** (A) Representative western blots and quantifications show JNK activation in cerebellum TIF fraction of *Ube3a*<sup>m-/p+</sup> mice at 23 weeks of age with higher levels of p-PSD95/PSD95, Shank3, NR2A and GLUR2 then in wt mice. On the contrary, Drebrin levels are reduced in *Ube3a*<sup>m-/p+</sup> mice to age-matched wt. D-JNK11 reduced JNK activation, the p-PSD95/PSD95 ratio, Shank3 levels but raised Drebrin, NR2A, NR2B, GLUR1 and GLUR2 levels in treated compared to untreated *Ube3a*<sup>m-/p+</sup> mice. The treatment did not cause any changes in wt. n=10. Significance differences from control \*p<0.05, \*\*\*p<0.001, \*\*\*\*p<0.0001; D-JNK11 treated vs untreated: #p<0.05, ##p<0.01, ###p<0.001, ####p<0.0001. Two-way ANOVA, Tukey's post-hoc test. Data are expressed as mean ± SEM.

#### 4.2.8 D-JNKI1 rescues cognitive impairments but not locomotor defects

To evaluate the potential neuroprotective effect of D-JNKI1 on cognitive impairment we investigated untreated and treated *Ube3a*<sup>m-/p+</sup> and wt mice in the NORT during chronic treatment, once a month at the indicated times (from 7 to 23 weeks). The *Ube3a*<sup>m-/p+</sup> DI was always lower than aged-matched wt mice, and the genotypic difference increased with the severity of the AS-pathology as expected (159% p<0.0001, Fig. 40A1-A2). At 23 weeks the *Ube3a*<sup>m-/p+</sup> had a significantly lower DI than aged-matched wt mice. D-JNKI1 had no effect in wt in fact the two curves (continue and dotted) overlap (Fig. 40A4). However, with the chronic D-JNKI1 treatment we found a significant difference between treated *Ube3a*<sup>m-/p+</sup> and untreated mice; their performances were significantly better (144%) at 23 weeks of age, reaching an average DI of 0.31 compared to untreated *Ube3a*<sup>m-/p+</sup> (average DI of -0.1352, Fig. 40A3). D-JNKI1 rescued the cognitive impairment in *Ube3a*<sup>m-/p+</sup> mice.

D-JNKI1's effect on the locomotor defect was investigated in the Rotarod test. In the four groups previously described (untreated and treated wt and *Ube3a*<sup>m-/p+</sup> mice) from 7 to 23 weeks of age, there was an overall genotypic difference between wt and *Ube3a*<sup>m-/p+</sup> mice (p <0.0001, Fig. 40B1-B2). At the last time point, *Ube3a*<sup>m-/p+</sup> mice spent 13% less time on the rotating bar than wt mice Fig. 40B2). We found no significant effect in treated *Ube3a*<sup>m-/p+</sup> and untreated *Ube3a*<sup>m-/p+</sup> (Fig. 40B3). In conclusion chronic D-JNKI1 treatment had no positive effect on locomotor impairments.

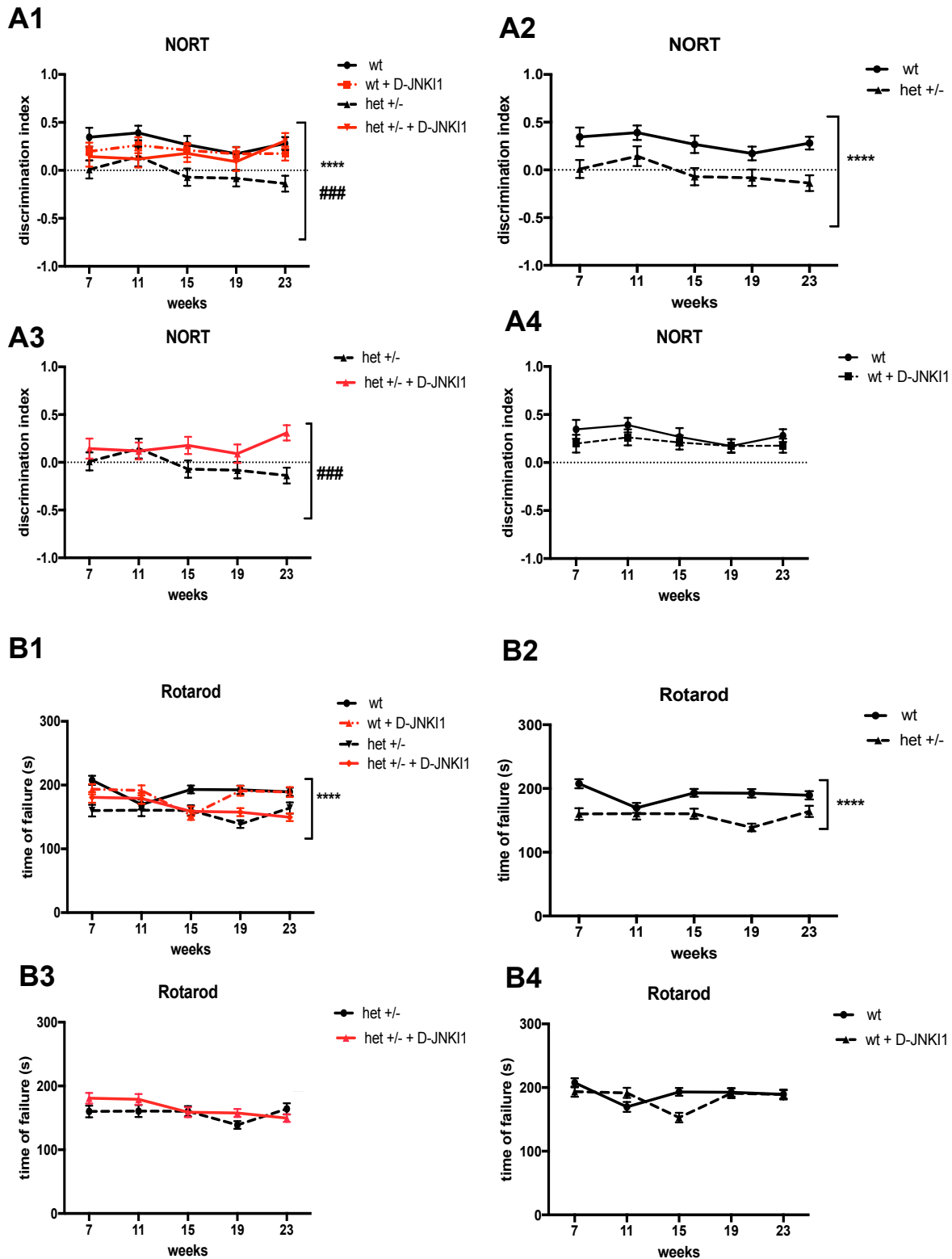


**Figure 40. D-JNK11 prevents cognitive impairments in *Ube3a*<sup>m-/p+</sup> mice in the Novel object recognition test but not locomotor impairments.** A1) Cognitive performances over time in treated and untreated *Ube3a*<sup>m-/p+</sup> and wt mice. A2) The discrimination index was significantly lower in *Ube3a*<sup>m-/p+</sup> mice (red line) than wt (black line). A3) DJNK11 treatment restored the cognitive impairment in treated *Ube3a*<sup>m-/p+</sup> (red line) mice compared to untreated *Ube3a*<sup>m-/p+</sup> mice (black line) at 23 weeks of age, with no significant effect on treated wt (dotted black line) compared to untreated wt mice (continuous black line) (A4). From 7 to 23 weeks of age, in the Rotarod test, treated and untreated, *Ube3a*<sup>m-/p+</sup> mice (dotted line) showed locomotor impairment compared to wt (continuous black line) (B1-B2). However, D-JNK11 did not induce any significant improvement in *Ube3a*<sup>m-/p+</sup> (red

line) compared to untreated *Ube3a*<sup>m-/p+</sup> mice (black line) (B3) or in wt (dotted black line) compared to untreated wt (continuous black line) (B4). n=10. Statistical significance: \*\*\*\*p<0.0001, ###p<0.001. Two-way ANOVA, Tukey's post-hoc test. Data are expressed as mean ± SEM.

## 4.3 JNK in a chronic disease: two Alzheimer in-vitro and in-vivo models

### 4.3.1 In-vivo model-5XFAD mice: JNK signalling pathway activation during time in the cortex and hippocampus total homogenate

In order to characterize JNK activation in 5xFAD mice, we performed Western Blot analysis on the total homogenate of cortex and hippocampus in three different time points: 4, 6 and 10 months of age.

We measured JNK activation, as the ratio between the phosphorylated and the total form of the kinases and its action on its elective target c-Jun and APP, using a specific antibody able to recognize the specific JNK phosphorylation site on this protein (T669).

At 4 months of age, representing an early phase of the disease, in the cortex, the JNK signalling was already activated. In fact, we observed a significant increase of P-JNK/JNK and P-c-Jun/c-Jun ratios (1.61- and 2.22-fold increase respectively,  $p < 0.01$ ;  $p < 0.05$ , Fig. 41A) together with augmented P-APP and APP levels (3,97- and 2,7-fold increase,  $p < 0.001$ ;  $p < 0.001$ , Fig. 41A) in tg vs wt mice. JNK activation persists during time also in the later phases. At 6 months of age, we found 1.72 fold increased ratio of P-JNK/JNK, 2.01 of P-c-Jun/c-Jun, 4,88 of P-APP and 2,12 of APP ( $p < 0.001$ ;  $p < 0.01$ ;  $p < 0.001$ ,  $p < 0.001$ , Fig. 41C) while at 10 months of age, P-JNK/JNK ratio was 5.81 fold increased in tg compared to wt mice, P-c-Jun/c-Jun 2.57, P-APP 3,72 and APP 1,58 ( $p < 0.05$ ;  $p < 0.05$ ;  $p < 0.05$ ;  $p < 0.05$ , Fig. 41E).

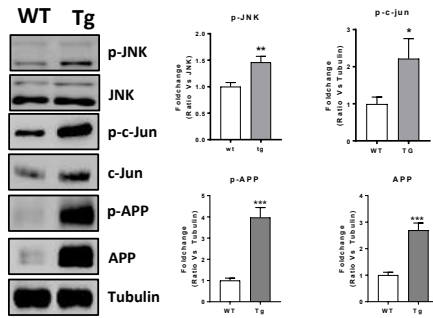
We also analysed JNK activation in the hippocampus. In the first time point analysed P-JNK/JNK is 1.46-fold increased in tg compared to wt mice, in line with 1.94 increased in c-Jun activation ( $p < 0.01$ ;  $p < 0.01$ , Fig. 41B). In addition, also P-APP and APP were increased in tg compared to wt mice (2,7- and 3,91-fold increase respectively,  $p < 0.001$ ;  $p < 0.001$ , Fig. 41B). At 6 months of age, JNK activation persists also in this area. In fact, P-JNK/JNK, P-APP and APP were significantly increased in tg compared to wt mice (1.28-, 1.19- and 3,37- fold change respectively,  $p < 0.05$ ;  $p < 0.001$ ;  $p < 0.001$ ;  $p < 0.001$ , Fig. 41D). Also in the last time point analysed, the signalling was still activated with 3.22-fold increase in P-JNK/JNK, 4,74 in P-APP and 2,27 in APP levels in tg compared to wt mice ( $p < 0.01$ ;  $p < 0.05$ ;  $p < 0.05$ , Fig. 41F).

Cortex Total Homogenate

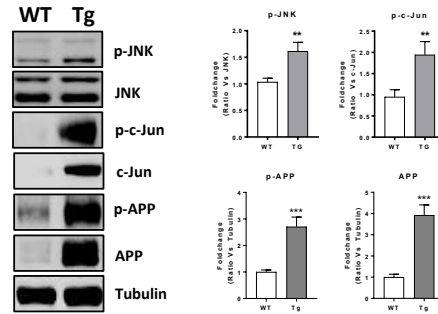
Hippocampus Total Homogenate

4 months

A

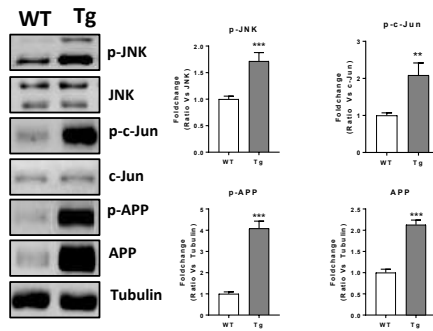


B

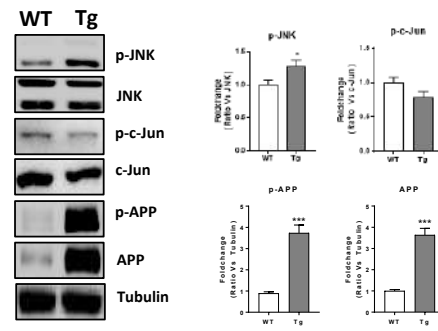


6 months

C

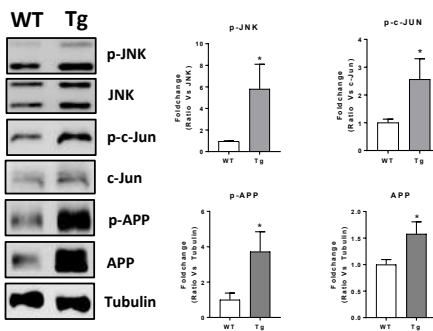


D



10 months

E



F

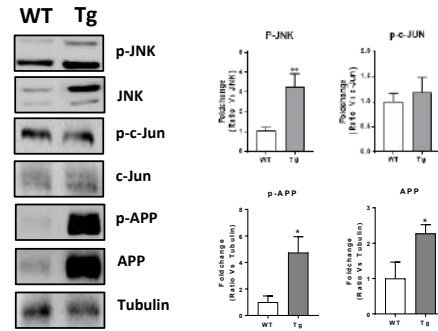


**Figure 41. JNK signalling pathway activation in cortex and hippocampus total homogenate of 4-, 6- and 10-months old mice.** Representative western blots and relative quantifications of total homogenate of A) 4 months old, C) 6 months old and E) 10 months old mice cortex and B) 4 months old, D) 6 months old and F) 10 months old mice hippocampus show higher level of p-JNK/JNK, p-c-Jun/c-Jun, P-APP and APP in 5x*FAD* *tg* vs *wt* mice. *n*=10. Genotypes are compared using *t*-tests. Statistical significance: \**p*<0.05, \*\**p*<0.01, \*\*\**p*<0.001. Data are expressed as mean ± SEM.

### 4.3.2 Cognitive Impairment and Synaptic Dysfunction in 4 months old 5xFAD mice

#### Radial Arms Water Maze

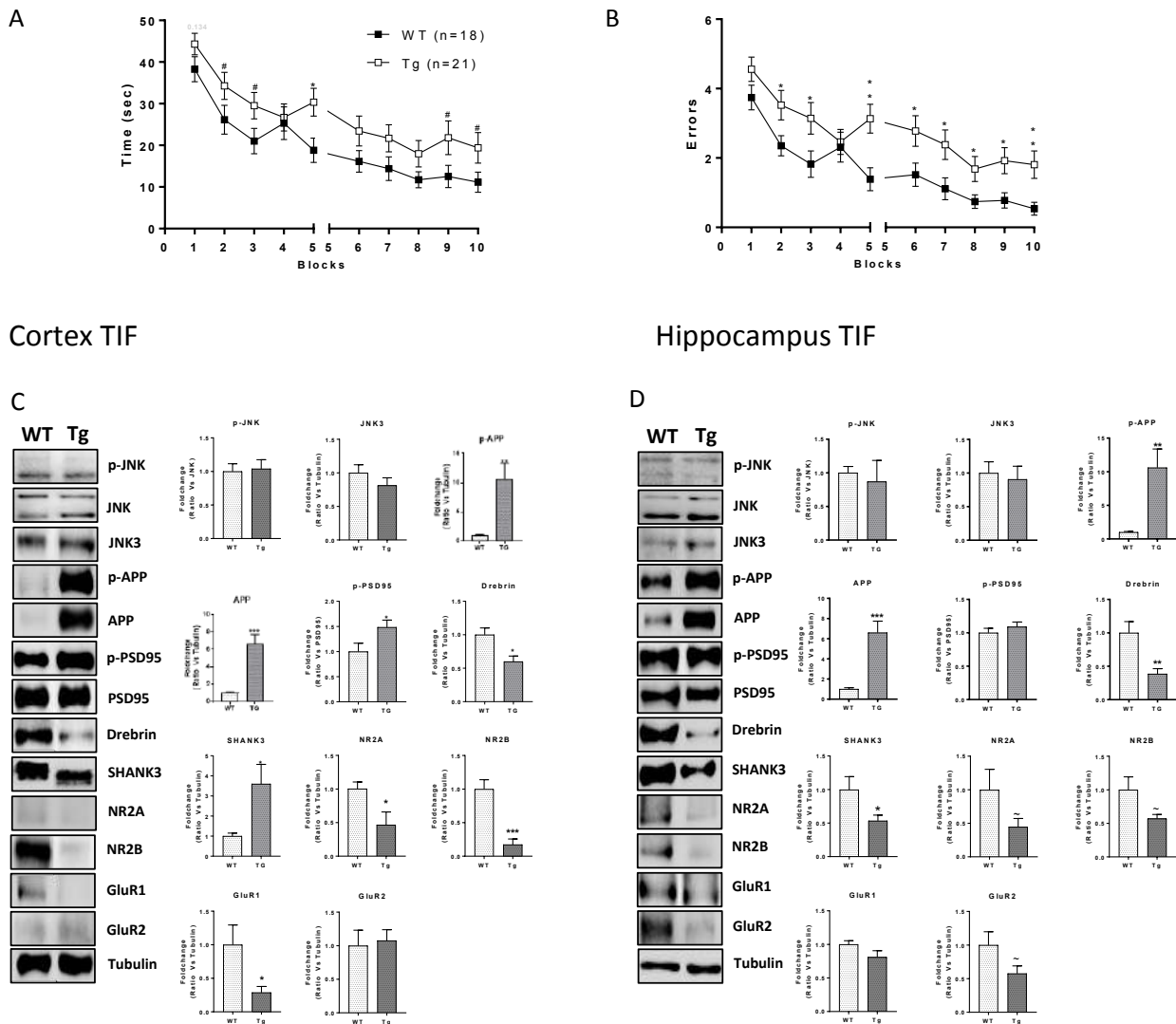


**Figure 42. Cognitive impairment and synaptic dysfunction in cortex and hippocampus of 4 months old mice.** A) Time and B) number of errors to find the submerged escape platform demonstrate the cognitive impairment in 5xFAD mice compared to wt. Representative western blots and relative quantifications of TIF C) cortex and D) hippocampus of 4 months old mice show reduced levels of some of the main markers of the excitatory synapses in tg compared to wt mice.  $n=10$ . Genotypes are compared using  $t$ -tests. Statistical significance:  $\#p<0.09$ ,  $*p<0.05$ ,  $**p<0.01$ . Data are expressed as mean +SEM.

In order to characterize the cognitive impairment in 5xFAD mice, we performed the Radial Arm Water Maze to measure the spatial navigation learning and memory, evaluating the time spent looking for the submerged escape platform and the number of errors made doing this task. Both mice groups, wt and tg, displayed a learning curve. Nevertheless,  $t$ -test performed on individual data points revealed that tg mice performed significantly worse compared to wt mice, suggesting an initial phase of cognitive impairment (Fig. 42A-B).

We then characterized the synaptic dysfunction in these mice, looking for the biochemical correlation with this initial impairment, by Western Blot analysis on the post-synaptic enriched protein fraction of cortex and hippocampus. Also in this cellular compartment we evaluated JNK signalling activation. In both areas analysed JNK signalling is not activated; in addition, we did not find any changes in JNK3 protein levels in tg compared to wt. On the contrary, we found increased P-APP and APP in the cortex (9.81- and 12.31-fold change) as well as in the hippocampus (10.61- and 6.59-fold change) of 5xFAD mice compared to wt ( $p < 0.01$ ;  $p < 0.001$ ;  $p < 0.01$ ;  $p < 0.001$ , Fig. 42C-D). In this time point, the analysis of the cortex of 5xFAD mice displayed a deregulation of the main scaffold protein of the excitatory synapses: P-PSD95/PSD95 ratio (1.49 fold change) and Shank3 (3.60 fold change) levels were increased in tg vs wt mice, while Drebrin (0.60), a marker for mature spines, was decreased ( $p < 0.05$ ;  $p < 0.05$ ;  $p < 0.05$ , Fig. 42C). Concerning the glutamate receptors levels, NR2A (0.46 fold change), NR2B (0.17 fold change) and GluR1 (0.29 fold change) levels were decreased in 5xFAD mice, but we did not find any differences in GluR2 levels between tg and wt mice ( $p < 0.05$ ;  $p < 0.001$ ;  $p < 0.05$ , Fig. 42C). On the contrary, in the hippocampus we found reduced Drebrin (0.39 fold change) and Shank3 (0.53 fold change) levels in tg compared to wt mice ( $p < 0.01$ ;  $p < 0.05$ , Fig. 42D) and only a tendency to be decreased in GluR2, NR2A, and NR2B ( $\sim p < 0.09$ ;  $\sim p < 0.09$ ;  $\sim p < 0.09$  Fig. 42D). Therefore, cortex and hippocampus displayed different vulnerability to neurodegeneration as proved by the biochemical analyses of the PSD region on the post-synaptic elements.

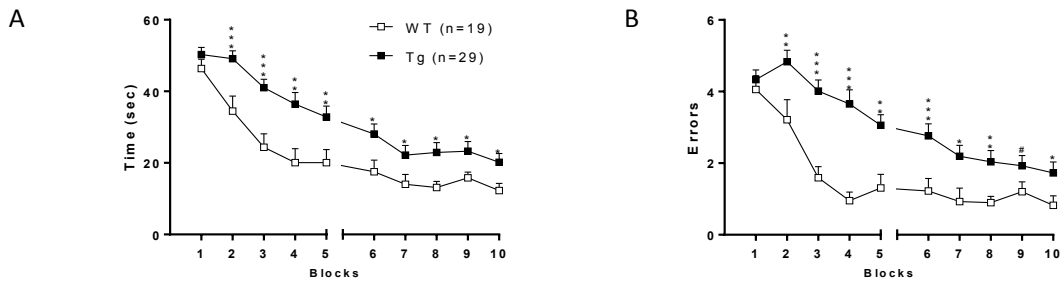
#### **4.3.3 Cognitive Impairment and Synaptic Dysfunction in 6 months old 5xFAD mice**

We then performed the same analysis described before on 6 months old mice in order to assess the progression of the disease. 5xFAD displayed a worsening in the learning and memory performances in the Radial Arm Water Maze compared to wt mice; in fact, they spent more time and made more errors to complete the task (Fig. 43A-B).

Concerning the biochemical evaluation of the synaptic dysfunction in the cortex, despite we did not find any differences in JNK activation, JNK3 levels were 1.33-fold increased in tg compared to wt mice ( $p < 0.01$ , Fig. 43C) and this is of relevance being JNK3 the most responsive isoform to stress stimuli in the brain.

In line with what observed at 4 months, P-APP and APP were increased (3.18 and 1.78 fold change) in 5xFAD mice compared to wt, as well as, Shank3 (0.27 fold change), NR2A (0.33 fold change), NR2B (0.28 fold change), GluR1 (0.06 fold change), and GluR2 (0.34 fold change) protein levels were strongly reduced in tg compared to wt mice ( $p < 0.01$ ;  $p < 0.001$ ;  $p < 0.01$ ;  $p < 0.001$ ;  $p < 0.01$ ;  $p < 0.01$ ;  $p < 0.05$ , Fig. 43C) demonstrating a strong impairment of the excitatory synapses.

## Radial Arms Water Maze



### Cortex TIF

### Hippocampus TIF

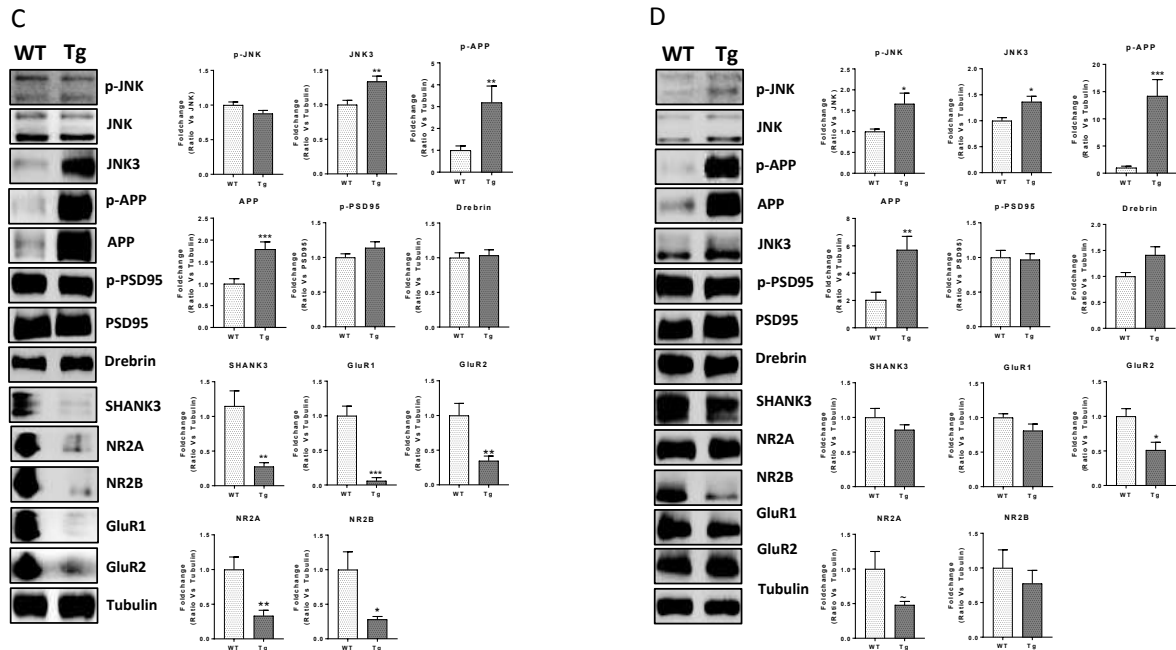


**Figure 43. Cognitive impairment and synaptic dysfunction in cortex and hippocampus of 6 months old mice.** A) Time and B) number of errors to find the submerged escape platform demonstrate the cognitive impairment in 5xFAD mice compared to wt. Representative western blots and relative quantifications of TIF C) cortex and D) hippocampus of 6 months old mice show increased JNK activation and JNK3 levels in the cortex and deregulated levels of some of the main markers of the excitatory synapses in tg compared to wt mice.  $n=10$ . Genotypes are compared using  $t$ -tests. Statistical significance:  $\sim p < 0.09$ ,  $*p < 0.05$ ,  $**p < 0.01$ ,  $***p < 0.001$ . Data are expressed as mean  $\pm$  SEM.

On the other hand, in the hippocampus we found increased P-JNK/JNK (1.66 foldchange) and JNK3 (1.37 foldchange) level together with augmented P-APP and APP (14.20 and 5.71 foldchange) in tg compared to wt mice ( $p < 0.05$ ;  $p < 0.05$ ;  $p < 0.001$ ;  $p < 0.01$ , Fig. 43D). Despite this, the hippocampus continues to prove to be a less vulnerable area; we observed only a statistically significant reduction of GluR2 (0.51 foldchange;  $p < 0.05$ , Fig. 43D), a tendency of reduction of NR2A and no changes in the levels of the other markers in tg vs. wt mice.

### 4.3.4 Cognitive Impairment and Synaptic Dysfunction in 10 months old 5xFAD mice

The last time point analysed was 10 months. At this age, 5xFAD displayed an almost flat learning curve demonstrating a great difficulty in completing the behavioural test task and therefore a great worsening of cognitive and mnemonic abilities compared to wt mice, which completed the test with performances that can be stackable on those of the previous time points (Fig. 44A-B).

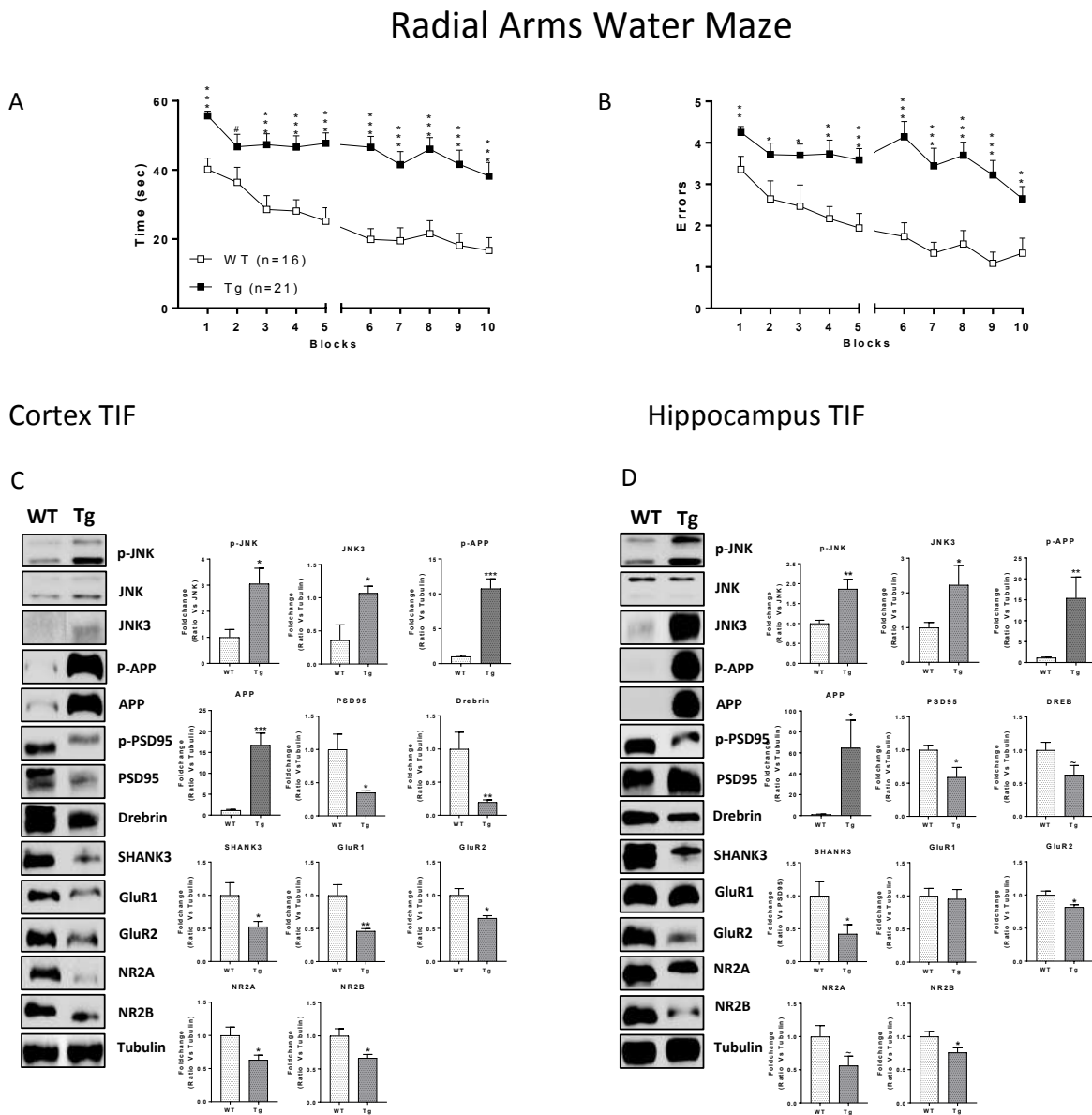


**Figure 44. Cognitive impairment and synaptic dysfunction in cortex and hippocampus of 10 months old mice.** A) Time and B) number of errors to find the submerged escape platform demonstrate the cognitive impairment in 5xFAD mice compared to wt. Representative western blots and relative quantifications of C) cortex and D) hippocampus TIF of 10 months old mice show increased JNK activation and JNK3 levels and reduced levels of some of the main markers of the excitatory synapses in tg compared to wt mice. n=10. Genotypes are compared using t-tests. Statistical significance: \*p<0.05, \*\*p<0.01, \*\*\*p<0.001. Data are expressed as mean + SEM.

Concerning the Western Blot analysis of the TIF fraction, in this latter time-point, we found JNK (cortex 3.05; hippocampus 1.87 foldchange) signalling activation and increased JNK3 (Ctx 2.98; H 2.23 foldchange) levels in both areas analysed (cortex:  $p < 0.05$ ;  $p < 0.05$ ; Fig. 5C; hippocampus:  $p < 0.01$ ;  $p < 0.05$ , Fig. 44C-D). In addition, also P-APP and APP were increased in tg compared to wt mice in both areas (cortex: 10.74- and 16.75-fold change;  $p < 0.001$ ;  $p < 0.001$ . Hippocampus: 15.38- and 64.77-fold change;  $p < 0.01$ ;  $p < 0.05$ , Fig. 44C-D). Concerning the deregulation of the PSD marker levels cortex and hippocampus still displayed several differences. In the cortex post-synaptic proteins enriched fraction, we found reduced level of all the markers analysed: PSD95 was 0.35 fold decreased, Drebrin 0.20. Shank3 0.53, NR2A 0.63, NR2B 0.66, GluR1 0.46 and GluR2 0.65 in tg compared to wt mice ( $p < 0.05$ ;  $p < 0.01$ ;  $p < 0.05$ ;  $p < 0.01$ ;  $p < 0.05$ ;  $p < 0.05$ ;  $p < 0.05$ , Fig. 44C), demonstrating a strong synaptic dysfunction well correlated with the performances in the behavioural test. Concerning the hippocampus, the synaptopathy results in the reduction of PSD95 (0.59 foldchange), Shank3 (0.42 foldchange), NR2B (0.76 foldchange) and GluR2 (0.82 foldchange) levels in tg compared to wt mice ( $p < 0.05$ ;  $p < 0.05$ ;  $p < 0.05$ ;  $p < 0.05$ ; Fig. 44D) and in reduced tendency for NR2A and Drebrin levels.

#### **4.3.5 JNK3 correlates with APP phosphorylation and cognitive decline**

In order to clarify the role of JNK3 in AD pathogenesis we performed several correlations between the biochemical and behavioural results.

Firstly, we found that P-APP/APP levels, measured in both cortex and hippocampus, correlate with cognitive impairment expressed as the time spent in completing the behavioural task (Fig. 45A). This is particularly important because phosphorylation of APP induced the production of A $\beta$  oligomers that, in turn, cause synaptic dysfunction that is reflected in the strong cognitive deficit displayed by 5XFAD tg mice.

Then, being JNK3 the key JNK's isoform that preferentially phosphorylates APP in T668, we correlated its levels with P-APP/APP ratio in the post-synaptic enriched protein fraction, confirming the strong relation between JNK3 and P-APP in the cortex as well as in the hippocampus of 5XFADtg mice at 4, 6 and 10 months of age, suggesting that JNK3 is the isoform more strongly implicated in the pathological phosphorylation of the APP (Fig. 45B).

Finally, having verified the correlation between P-APP/JNK3 and cognitive impairment, to strengthen the hypothesis that JNK3 is the isoform of JNK most involved in neurodegeneration, we correlated its levels with the time spent by mice finding the escape platform in the 6 AWM. As expected, JNK3 levels in the cortex and hippocampus TIF fraction are strongly correlated with the cognitive deficit (Fig. 45C).

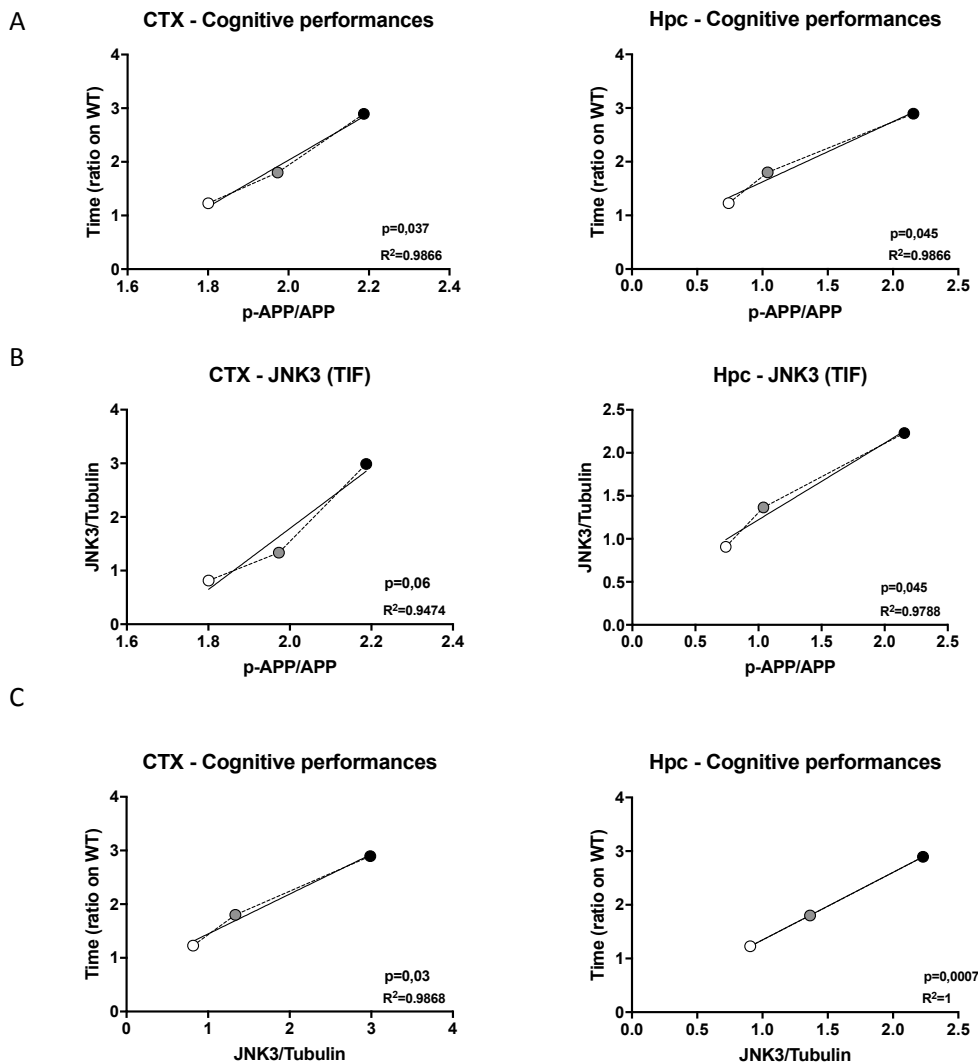


**Figure 45. Statistical Correlations of biochemical and behavioural analysis.** A) Statistical Correlations between cognitive dysfunction and P-APP/APP levels in the cortex (right) and hippocampus (left). B) Statistical Correlations between JNK3 and P-APP/APP levels in the tif fraction of both cortex (right) and hippocampus (left). C) Statistical Correlations between cognitive dysfunction and JNK3 levels in the tif fraction of cortex (right) and hippocampus (left). N=10.

#### 4.3.6 Specificity and toxicity of the specific JNK3 inhibitor peptide: d-SIMBA2

To test the possibility that JNK isoforms have different impact on AD and synaptic dysfunction development, we design a specific JNK3 inhibitor, being JNK3 the selective JNK isoform in the brain and the most reactive to stress stimuli[101]. The key challenges in this field are the selectivity profiles and the passage through the blood brain barrier, as well as the evaluation of the optimal therapeutic index[373]. To target JNK3, we took advantage of published evidence supporting that the scaffold protein  $\beta$ -arrestin2 can bind specifically to JNK3 and catalyse its activation, by recruiting the upstream kinases of the cascade[290,291]. We synthesized a peptide containing the  $\beta$ -arrestin2 sequence responsible for the binding to JNK3 and the d-TAT peptide sequence (D-form of the aminoacids of the TAT sequence), to allow penetration of the cell membrane and the blood brain barrier (BBB).

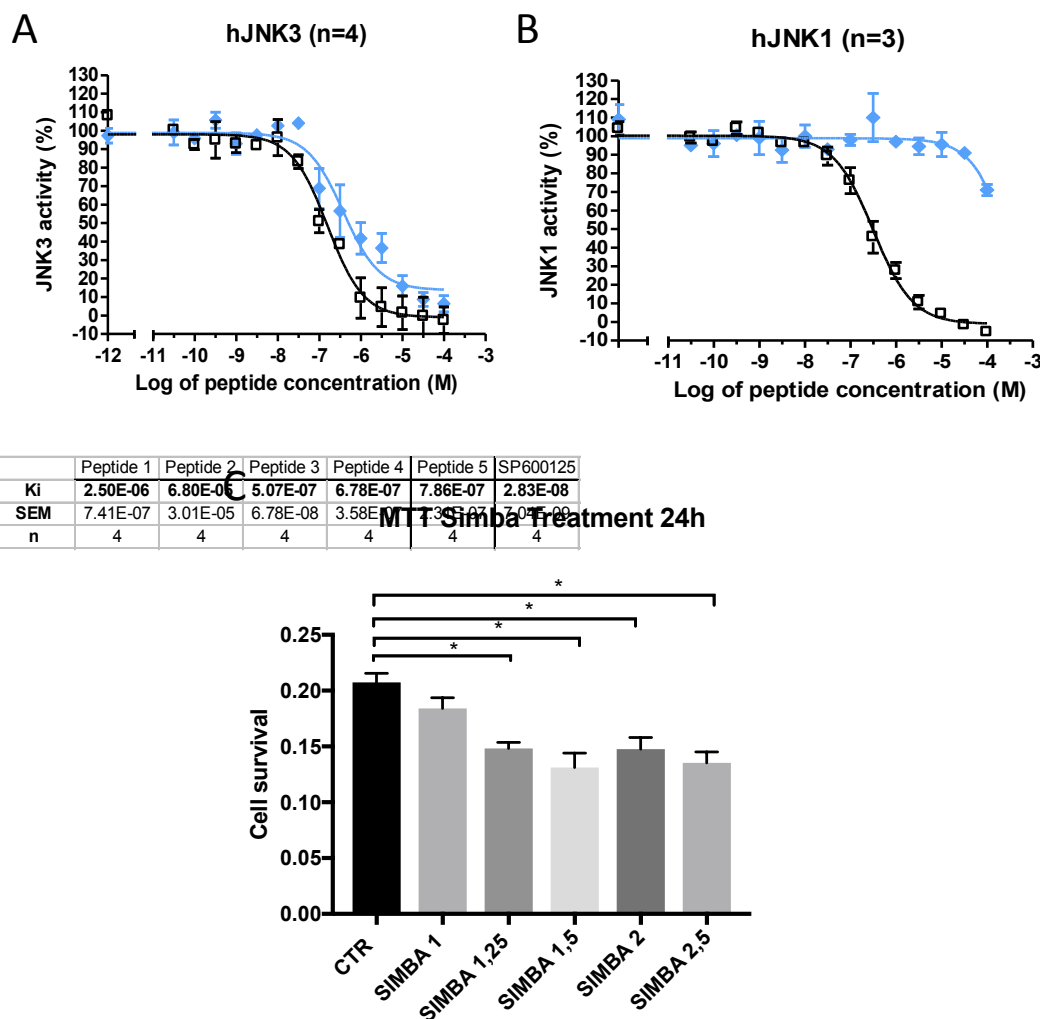


**Figure 46. Specificity and toxicity of dSIMBA2 peptide.** Alpha screen test showing the kinetics of inhibition of A) JNK3 and B) JNK1 phosphorylation following incubation with dSIMBA2 (blue curve) or SP600125 as control (black curve). SP600125 was able to reduce the kinase activity of all JNK isoforms, while dSIMBA2 was specific for JNK3 at low concentrations. C) Cell viability was assessed in primary neuronal culture treated with increasing dose of dSIMBA2 for 24 hours by MTT assay. Data are represented as mean  $\pm$  SEM of 3 independent experiments and were analysed with one-way ANOVA test, followed by post hoc test Turkey. Significance relative to ctr: \*  $p < 0.05$ ,  $n = 6$ ).

To assess dSIMBA2 specificity for JNK3 we performed the Alpha Screen Kinase Assay. Our data indicated that dSIMBA2 inhibited JNK3 activity in a dose dependent manner (blue line, Figure 46A). The ATP-competitive non-isoform selective JNK inhibitor SP600125 was used as a positive control (black line, Figure 46A). As shown in Figure 25A, dSIMBA2 achieved comparable levels of JNK3 inhibition under these assay conditions. We then tested the ability of dSIMBA2 to inhibit the other JNK isoforms. In particular, we focused on JNK1 because it shares the highest homology of sequence with JNK3 (about 91% of homology and 95% of similarity) compared to JNK2 (about 83% homology and 90%

similarity)[353] and is the other major isoform in the CNS. As expected, dSIMBA2 had no effect on JNK1 activity (Fig. 46B). This data was a first proof for dSIMBA2 specificity for JNK3.

Once the cell-free activity was established, the toxicity of the dSIMBA2 peptide was evaluated in-vitro on primary neuronal cultures. To this end, primary cortical neurons were treated, in control condition, with increasing doses of the peptide (1  $\mu$ M, 1.25 $\mu$ M, 1.5  $\mu$ M, 2  $\mu$ M and 2.5  $\mu$ M) for 24h. The toxicity was evaluated by MTT assay and expressed as survival rate. The results of the MTT assay (Figure 46C) show that concentrations higher than 1 $\mu$ M resulted toxic on primary neuronal cultures. On the contrary, 1  $\mu$ M did not induce significant toxicity. This dose was then chosen to continue in-vitro studies.

#### 4.3.5 Set-up of the in-vitro model of synaptopathy induced by A $\beta$ oligomers (ABO)

It is known that treatment with subtoxic dose of ABO induced changes in the synaptic organization with reduction in dendritic spines density and abnormal expression of scaffold proteins and neurotransmitter receptor levels[322,368]. We used a previous paradigm developed in the laboratory, with minor modifications. We were able to induce a strong synaptopathy of the excitatory synapses in absence of neuronal death. Primary cortical neurons from C57bl6 mice were treated with a dose of soluble ABO1–42 equal to 3 $\mu$ M for 3 hours. In order to assess JNK activation, ABO treated, and untreated neuronal culture were processed for biochemical analysis of the total homogenate as well as of the TIF fraction representing the post-synaptic proteins enriched fraction.

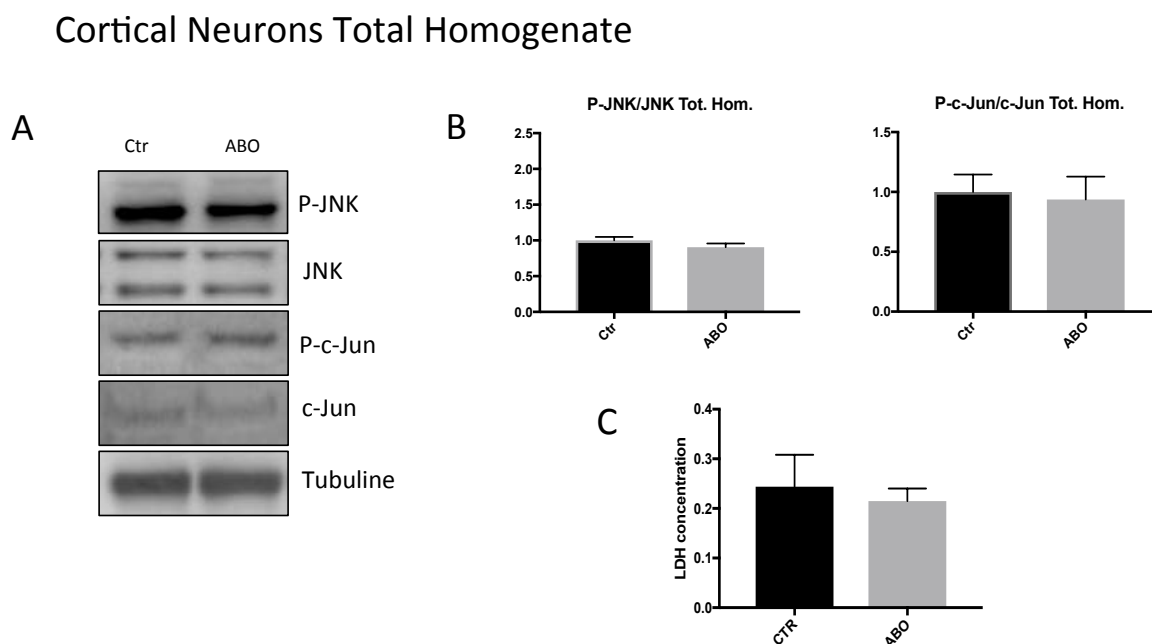


**Figure 47. Analysis of the total Homogenate of cortical primary neurons after ABO treatment. A) Western Blot and B) relative quantifications show that the treatment with ABO 3 $\mu$ M for 3h did not induce any changes in JNK activation in the total**

homogenate. C) LDH assay indicates that the ABO treatment did not induce neural death too. Data are shown as mean  $\pm$  SEM of 3 independent experiments and were analysed by Student's *t*-test followed by Tukey's post hoc test,  $n=12$ .

As expected, the biochemical analyses on the total homogenate (Fig. 47A-B) revealed that ABO did not induce any significant effects on the activation of JNK, measured as the ratio between the phosphorylated and the total form of the kinase, as well as on the phosphorylation levels of c-Jun. These results are in line with the LDH analysis, performed to monitor the cell death. In fact, there are no differences in the LDH release in the media of ctr and treated culture meaning that no cell death is induced by ABO (Fig. 47C).

### Cortical Neurons TIF

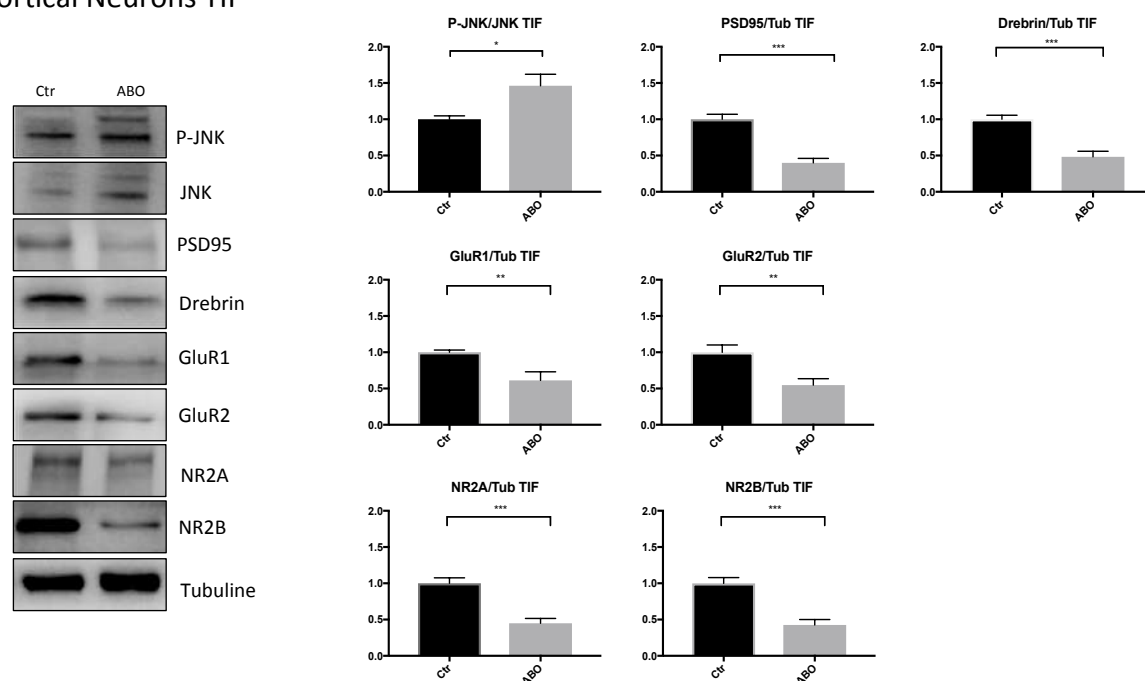


**Figure 48. Analysis of the Triton Insoluble Fraction (TIF) of cortical primary neurons after ABO treatment.** A) Western Blot and B) relative quantifications show that the treatment with ABO 3 $\mu$ M for 3h induced JNK activation and a general deregulation of scaffold proteins and neurotransmitters receptor levels. Significance relative to ctr: \* $p<0.05$ , \*\* $p<0.01$ , \*\*\* $p<0.001$ . Data are shown as mean  $\pm$  SEM of 3 independent experiments and were analysed by Student's *t*-test followed by Tukey's post hoc test,  $n=12$ .

We then analysed the post-synaptic protein enriched fraction of the same culture. In line with the experiments previous conducted in the laboratory[322], three hours after treatment with ABO1-42, the JNK signalling is strongly activated in treated compared to untreated cultures ( $p<0.05$ , Fig. 48). Furthermore, we analysed the level of two important scaffold proteins of the excitatory post-synaptic terminal: PSD95 and Drebrin, also a marker for mature spines. PSD95 and Drebrin levels were 40% and 48% lower in treated compared to untreated cultures ( $p < 0.001$ , Fig. 48). We also analysed AMPA and NMDA glutamate receptors levels finding a general reduction in their levels. GluR1 and GluR2 were 60%

and 54% and NR2A and NR2B 44% and 57% lower respectively in ABO treated compared to untreated cultures ( $p < 0.01$ ;  $p < 0.01$ ;  $p < 0.001$ ;  $p < 0.001$ , Fig. 48).

These data confirm that treatment with ABO1-42  $3\mu\text{M}$  for three hours induces a strong JNK signalling pathway activation and consequently the synaptopathy of the excitatory synapse in primary cortical neurons.

#### 4.3.6 dSIMBA2 neuroprotection in-vitro against ABO-induced synaptopathy

Having proved the activity, specificity, and the maximum non-toxic dose of the dSIMBA2 peptide, we lastly tested its neuroprotective effect in preventing the synaptic dysfunction in the in-vitro model of synaptopathy induced by ABO. To do this, primary cortical neuronal cultures were pre-treated with  $1\mu\text{M}$  of dSIMBA2 and after 30 minutes exposed to ABO stimulation for three hours.

#### Cortical Neurons Total Homogenate

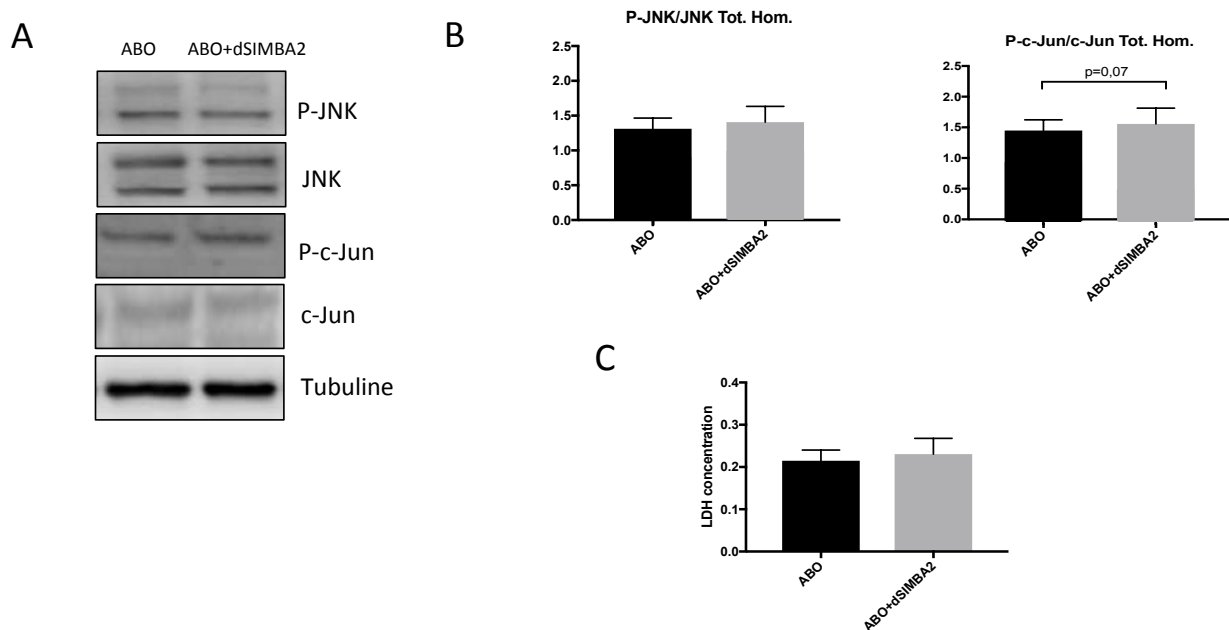


**Figure 49.** Analysis of the total homogenate of primary cortical neuronal cultures pre-treated with dSIMBA2 and ABO. A) Western Blot and B) relative quantifications show that the treatment with dSIMBA2  $1\mu\text{M}$  30 minutes before the ABO did not induce any changes in JNK activation nor neuronal death. Data are shown as mean  $\pm$  SEM of 3 independent experiments and were analysed by Student's *t*-test followed by Tukey's post hoc test,  $n=12$ .

We firstly analysed the effect of dSIMBA2 on the total homogenate of ABO treated cultures. In this model, as previously proved, ABO treatment does not induce JNK activation at this cellular level; consequently, the peptide does not induce statistically significant changes in JNK phosphorylation levels. However, interestingly, the activation of its elective target c-Jun shows a decreasing tendency in the dSIMBA2-

ABO treated compared to untreated cultures (Fig. 49A-B). Furthermore, to monitor the levels of neuronal death, and verify that the concomitant treatment of ABO and dSIMBA2 do not induce side effects in-vitro, we performed LDH assay. In line with previous results (see fig. 45 and 47), neither dSIMBA2-ABO nor ABO alone, at the concentrations used, are toxic (Fig. 49C).

### Cortical Neurons TIF

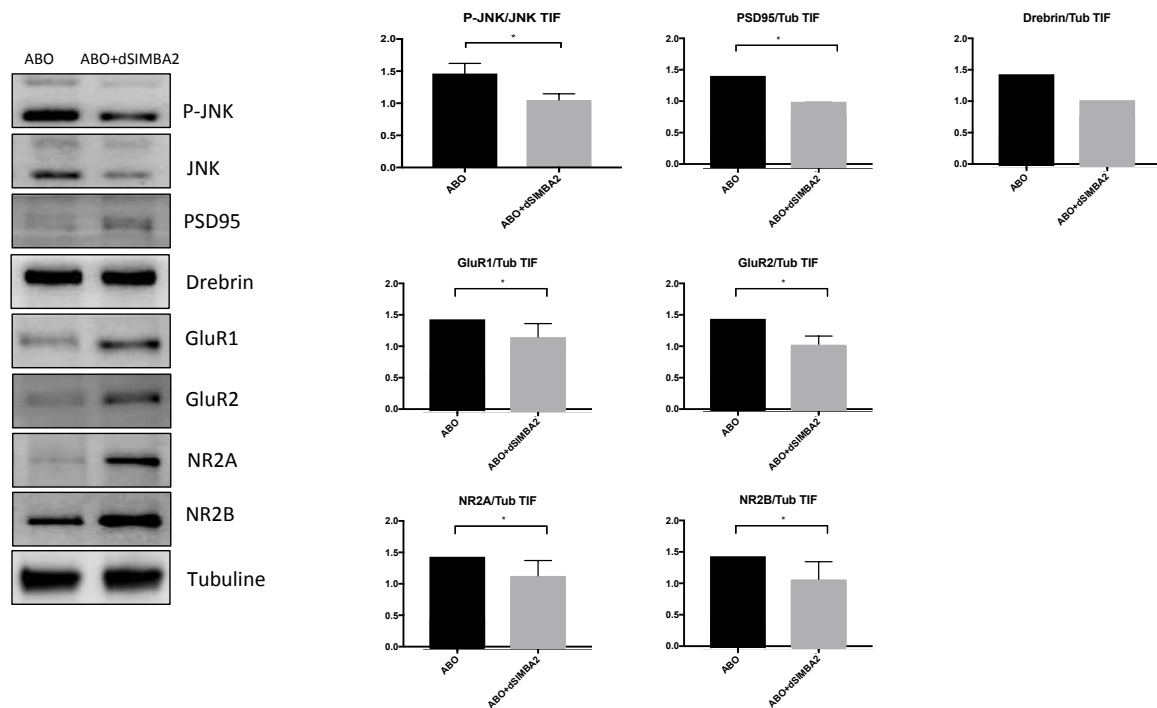


**Figure 50. dSIMBA2 protective effect against synaptopathy induced by ABO.** A) Western Blot and B) relative quantifications show that the treatment with dSIMBA2 1  $\mu$ M 30 minutes before the ABO reduced JNK activation and prevented the reduction in the excitatory post-synaptic markers. Significance relative to ctr: \*  $p < 0.05$ . Data are shown as mean  $\pm$  SEM of 3 independent experiments and were analysed by Student's *t*-test followed by Tukey's post hoc test,  $n = 12$ .

We then analysed the TIF of the same culture. dSIMBA2 pre-treatment induced a reduction equal to 72% of JNK activation in presence of ABO ( $p < 0.05$ , Fig. 50). In line, the peptide prevents the synaptic dysfunction induced by ABO; in fact, PSD95 levels were 50% ( $p < 0.05$ , Fig. 50), GluR1 53% ( $p < 0.05$ , Fig. 50), GluR2 54% ( $p < 0.05$ , Fig. 50), NR2A 40% ( $p < 0.05$ , Fig. 50) and NR2B 42% ( $p < 0.05$ , Fig. 50) higher compared to dSIMBA2 untreated cultures. Only Drebrin levels are not significantly increased in treated compared to untreated cultures.

These preliminary analyses confirm the neuroprotective effect of the SIMBA2 peptide against the synaptic dysfunction induced by ABO in-vitro and pave the way for the translation to the in-vivo model of AD.

## 5. Discussion

---

Neurological disorders are the first leading cause of disability and the second leading cause of death worldwide. Numbers that are expected to further increase as a result of population growth and aging. There is no way to escape from the fact that brain disorders are a major public health problem[374]. Researching the pathways and the mechanisms involved in the development of brain diseases are mandatory targets to explore in order to elucidate the causes and to improve diagnosis criteria, prevention strategies and treatments.

Although brain disorders present many different pathological/clinical manifestations, as well as origins and causes transduced by different intracellular molecular pathways, they all present synaptic dysfunction [101,375]. This phenomenon is characterized by deregulation of neurotransmitter release and uptake and consequent impairment of synaptic plasticity in both excitatory and inhibitory neurons. These serious anomalies at the synaptic level are then reflected on the behavior and on the higher cerebral functions. It is therefore crucial to understand the **intracellular mechanisms underlying synaptic modulation in order to design powerful neuroprotective strategies**. In this thesis, **we decided to examine synaptic dysfunction as a common neurodegenerative mechanism from neurodevelopmental** (Angelman and Rett syndromes) **to chronic neurodegenerative diseases** (Alzheimer Disease).

We discovered that the c-Jun N-terminal Kinase (JNK) signaling pathway, involved in stress response as well as in other different physiological functions, is a common actor in the synaptopathy of all these brain diseases.

From its discovery, over 30 years ago, JNK was firstly found to be strongly activated in response to stress stimuli playing crucial roles in apoptosis. Over time and with specific studies on knockout mice the importance of JNK has also been revealed in a number of physiological processes, particularly in the brain. In fact, besides regulating neuronal death, it is involved in brain morphogenesis and axodendritic design during development, synaptic plasticity and memory formation[224]. In addition, evidence in the literature shows its deregulation in various CNS pathologies but also in cancer and in autoimmune disease.

JNK modulates 3 major actions, very important specifically in neurons that are highly polarized cells. In different cellular compartments JNK plays diverse functions: 1 - at the pre-synaptic terminal, it regulates the zipping of the vesicles and the release of neurotransmitter[376]; 2 -at the post-synaptic level, it controls the correct organization of receptors and scaffold proteins in the active zone of the PSD region where takes place the reception of the neurotransmitter[250,320,323]; 3 -in the soma, it governs apoptotic, necrotic and autophagic neuronal deaths[377], acting on different targets and intracellular organelles. All these physiological mechanisms are vital and work in the same way in all the brain areas controlling, with the same mechanism, all the different functions of the brain. JNK, by regulating neurotransmitter release and contributing to the organization of the PSD region, plays also crucial role in driving the synaptic dysfunction process. This process, despite giving very different behavioral but also biochemical outcomes in different diseases, is underpinned by the same basic mechanisms in which

JNK is involved. Since it acts on these basic and shared mechanisms, by inhibiting the action of JNK, we have shown that it is possible to block the process and reverse the specific deficits of all the pathologies analyzed.

Therefore, JNK and its pathway, formed by a myriad of upstream activators and downstream targets, represent an intriguing subject to study in the CNS, especially knowing that kinases have become one of the most important targets in drug discovery. In fact, there are 68 FDA-approved drugs targeting different protein kinases, six of which were approved in the last year[378].

In the following chapter, we will discuss the obtained results in the characterization of JNK role in the synaptopathy associated to the three different diseases analysed, Rett, Angelman and Alzheimer, in order to better elucidate their significance in their specific contexts of neurodevelopmental and neurodegenerative diseases.

## 5.1 Rett Syndrome

MECP2 mutations can lead to a variety of neurological and psychiatric problems, the most known being RTT, through a plethora of molecular and neuronal consequences. Therefore, for RTT and other MECP2-related conditions it is important to discover the key intracellular pathways that can be targeted with drugs of high translational value [379].

We here examine stress-JNK pathway activation in three RTT models: the first, *Mecp2*-knock out male mice, represents a severe RTT-phenotype; the second, *Mecp2*-heterozygous female mice, is a milder phenotype model of this pathology but, importantly, replicates the X-linked RTT female mosaicism, and the third is a human model (hiPSCs differentiated neurons from female MECP2-RTT patients) important to assess the translational value of animal findings. The JNK pathway is activated in all three RTT models, indicating that *Mecp2* mutation, or its absence (*Mecp2*<sup>y/-</sup>), induces downstream activation of the JNK stress-signalling pathway in both mouse and human RTT models.

The specific JNK inhibition, by D-JNKI1, reverses RTT pathological phenotypes in all three models. This is the first demonstration that JNK plays a key role in RTT.

In particular, in symptomatic *Mecp2*<sup>y/-</sup> male mice, there is powerful JNK activation in the total homogenate and in the post-synaptic enriched fraction (TIF) of different brain areas. It is important to underline that synaptic abnormalities are closely correlated to the RTT symptomatology. Importantly, D-JNKI1 rescues the effects of the lack of *Mecp2*<sup>y/-</sup> in male mice, showing the most severe RTT phenotype, improving the general well-being conditions and significantly rescuing the behavioural defects and decreasing the apnea numbers. This effect is of note and has an important translational value, in fact, apnea occurs in 65 to 93% of all RTT patients [380,381]. Research in mouse models of RTT suggests that different areas in the ventrolateral medulla and pons give rise to different aspects of this breathing disorder [163] but it will be necessary to study D-JNKI1 effects in these areas to explain its action. Unfortunately, for ethical reasons, we could not study whether the treatment prolonged the

survival of male *Mecp2<sup>y/-</sup>* mice treated with the peptide. However, it is worth noting that chronic D-JNKI1 treatment significantly improves the overall well-being condition in *Mecp2<sup>y/-</sup>* mice. In correlation with these improvements, D-JNKI1 rescues the molecular disorganization of the PSD region of the post-synaptic element in *Mecp2<sup>y/-</sup>* mice by normalizing PSD95, PSD93, NMDA-r and AMPA-r, SHANK3 and Drebrin levels. The key role of JNK in the regulation of AMPA receptors membrane insertion [382] and in PSD95 stability [78] as well as the D-JNKI1 neuroprotective effect has been previously described in Alzheimer's diseases [366,367,383–386]. Here, for the first time, we link the *Mecp2* absence/truncation to the downstream activation of the JNK stress signalling pathway.

The link between MECP2 and AMPA receptors regulation was already known, in fact MECP2 recruits histone deacetylase to silence the transcription of *GluR1* and *GluR2*[387,388]. As a result, AMPAR regulation deficiencies have been implicated in the ASD characteristics associated with this condition[389]. In our *Mecp2<sup>y/-</sup>* model, both AMPA subunits display a tendency to be increased, and D-JNKI1 treatment restores their physiological levels.

Thus, in severe RTT phenotype, D-JNKI1's powerful neuroprotection is achieved by joint functional (breathing and behaviour) and biochemical effects (key players of degenerative intracellular pathways). These functional improvements are important because these are a disabling aspect of RTT syndrome that dramatically impacts the patient's quality of life.

D-JNKI1 effect was also observed in a second animal model, *Mecp2<sup>+/-Jae</sup>* female mice, which mimic a milder RTT phenotype, expressing both the mutated and wild-type *Mecp2* alleles, and thus replicating the somatic mosaicism reported in female RTT patients. *Mecp2<sup>+/-Jae</sup>* female mice present phosphorylation of c-Jun, indicating activation of the JNK stress pathway in the cortex, hippocampus, and cerebellum of symptomatic animals. Our data also provide the first indication that the molecular organization of the PSD is profoundly altered in *Mecp2<sup>+/-Jae</sup>* females. These mice had atypical scaffold protein levels: PSD95, PSD93 and SHANK3 were high, while Drebrin is low, suggesting again the disorganization of the PSD region. The dysfunctional spines and these alterations are closely correlated to powerful JNK activation in the post-synaptic elements. As previously seen in *Mecp2<sup>y/-</sup>*, in *Mecp2<sup>+/-Jae</sup>* mice too, chronic D-JNKI1 treatment improves behavioural impairments and rescue PSD alterations, compared to untreated *Mecp2<sup>+/-Jae</sup>* mutants. The *Mecp2<sup>+/-Jae</sup>* display different changes in biochemical marker levels in the PSD-region compared to *Mecp2<sup>y/-</sup>*, however these are both JNK-dependent. In fact, in both models, JNK specific inhibition restored their levels to wt animals. We speculate that this is due to the fact that JNK inhibition prevents its action on the PSD95 scaffold phosphorylation, avoiding receptors deregulation. In addition, this normalization is well correlated to improved functional outcomes. D-JNKI1 treatment in wt mice induced a significant increase of PSD95 and a reduction in SHANK3 levels in the PSD region of the post-synaptic element, however without a correlation with changes in the glutamate receptor levels, supporting the normal behaviour of control mice.

The differences found in the molecular dis-organization of excitatory synapses in *Mecp2<sup>y/-</sup>* and *Mecp2<sup>+/-Jae</sup>* and their comparison was never achieved before. The simplest hypothesis is that this is due to the

complete absence of *Mecp2* in *Mecp2*<sup>y/-</sup> male and by the presence of a mosaic-like expression of *Mecp2*<sup>+/-</sup> <sup>Jae</sup> in female. Along the same line, a previous work that have attempted to compare the morphological organization of dendrites and dendritic spines in *Mecp2*<sup>y/-</sup> male and *Mecp2*<sup>+/-</sup> female showed clear differences in several neuronal parameters between the two genotypes [390].

Importantly, this study reveals that both mouse strains present synaptic alterations leading to a common over-activation of JNK, both in the absence (*Mecp2*<sup>y/-</sup>) and in a mosaicism expression of *Mecp2* mutation and wild type allele (*Mecp2*<sup>+/-</sup> <sup>Jae</sup> mice) and the specific inhibition of JNK reverses RTT signs/symptoms in both mouse models.

Excitatory post-synaptic compartment anomalies have already been described in several neurological disorders associated with cognitive decline, including Alzheimer's but also in neurodevelopmental intellectual disabilities, autism spectrum disorders and in RTT as well [391–398]. Being synaptic dysfunction the first degenerative event in brain diseases and representing an important therapeutical window of intervention, potential treatment able to promote the maintenance of biochemical markers of the PSD region and to restore the activity of spines will offer one of the most exciting therapeutic agents against many different brain diseases. Since JNK specific inhibition prevents RTT synaptopathy and rescues behavioural and breathing defects, treatments that target the JNK pathway represent strong candidates against RTT and other neurodevelopmental disorders.

To verify the translational value of JNK inhibition in humans we studied neurons derived from iPSCs (hiPSCs) obtaining the first proof of principle of JNK's role in the Human RTT. The hiPSCs technology is important to discover druggable targets in human diseases and for testing the efficacy and specificity of new therapeutic compounds. We find JNK activation in hMECP2mut differentiated neurons and this correlates with an increased neuronal death, importantly, the isogenic hiPSCs show control levels of JNK and no cell death. The D-JNKI1 treatment of hMECP2mut neurons inhibits JNK activation and prevents neuronal death, indicating its clinical relevance. In this initial study, the characterization of neuronal cells is not complete since it is focused only on JNK signalling. It will be important, in future studies, to assess the molecular link between *Mecp2* and JNK. This could provide important information on how the *Mecp2* loss/mutation induces JNK activation.

Notably, the JNK pathway cross talks with other intracellular pathways already known and more characterized in RTT, such as PI3K/AKT/GSK3/NFκB[399–401] and BDNF[402]. It will be important, in future studies, to assess the molecular link between *Mecp2* and JNK. This could provide important information on how the *Mecp2* loss/mutation induces JNK activation. The connection between *Mecp2* and JNK pathway is a very intriguing issue; some indications from the literature showed that JNK inhibition, with SP600125 (chemical inhibitor), decreased the bindings of MeCP2 and histone-3 trimethyl K9 to the MOR promoter indicating a transcriptional regulation of MOR by JNK inhibition[403]. In addition, our unpublished results of the system biology analysis on MECP2 network identify JNK as a signaling pathway implicated in RETT synaptic dysfunction. Further investigations to identify the relation between *Mecp2* and stress JNK pathway are currently ongoing.

Currently, there is no cure for RTT, and medical management is aimed to provide symptomatic relief for patients through a multidisciplinary approach. Some of the medical concerns that need to be addressed in RTT patients include a few disorders, including breathing irregularities such as apnea, hyperventilation, and breath holding [404]. Successful management of these irregularities can be difficult, and sudden death in patients with RTT as result of an autonomic dysfunction is a potential risk factor. However, precautions should be taken to avoid medications that alter breathing patterns, for example, opioid medications [405]. Management of these conditions can substantially improve the quality of life of RTT patients and should not be overlooked [406]. In such as context, these findings are encouraging for further studies in animal models that overt breathing abnormalities focused on the efficacy of preventive administration of the D-JNKI1 inhibitor reducing breathing disorders and potentially encouraging to undertake clinical studies on brainstem modulation of breathing in patients with RTT.

Finally, we suggest that these results can open the real possibility to D-JNKI1 clinical application. Although there is no evidence of side effects of the D-JNKI1 inhibitor in mice [360,371,407,408] the passage to humans could lead to unwanted effects, in fact, chronic clinical studies, so far, are restricted to topical usage [409]. A chronic and systemic inhibition of the JNK pathway could generate side effects since JNKs family regulate a myriad of cellular functions, some not linked to the pathophysiology of diseases. We think that a possible solution can be to target just JNK3: the brain specific isoform of JNKs and the most responsive to stress stimulations [410].

## 5.2 Angelman Syndrome

The *Ube3a* maternal deficient mouse model recapitulates different pathological symptoms associated with AS syndrome including impaired hippocampal long-term potentiation and reduced dendritic spine density, together with cognitive and motor deficits and inducible seizures [176,361,411–413].

Although mutations in the UBE3A gene result in AS pathology, little is known yet about the role of UBE3A in the nervous system and/or how UBE3A mutation/loss induces neuronal degeneration, with consequent cognitive and locomotor impairments. The cellular mechanisms of the downstream effects of UBE3A loss in neurons are still lacking, thus there are still no effective treatments.

This study provides the first proof of principle of an important downstream JNK role in *Ube3a*<sup>m-/p+</sup> pathology. In fact, in *Ube3a*<sup>m-/p+</sup> mice presented high JNK activation in the soma and this activation persists during all the stages of the pathology, from the earlier, 7 weeks of age (a stage comparable to adolescence), to the adulthood (23 weeks), suggesting an important function of this stress pathway in AS. In addition, *Ube3a*<sup>m-/p+</sup> mice had higher levels of c-Jun, the elective JNK's target, than wt mice, indicating the activation of neuronal death pathway.

We also found that *Ube3a*<sup>m-/p+</sup> mice had changes in the PSD marker levels in the post-synaptic enriched protein fraction, suggesting more immature and disorganized dendritic spines. These generalized

alterations of the PSD markers in cortex, cerebellum and hippocampus, caused by the loss of UBE3A, are in line with the reduced dendritic spine density observed in AS patients [414] and AS mouse models [176,411,412,415,416]. With the PSD marker alterations in the post-synaptic element we also found powerful JNK activation, at 7 and at 23 weeks of age, confirmed by the specific increase of the p-PSD95/PSD95 ratio in the TIF, suggesting that JNK pathway is involved in synaptic dysfunction in AS, as reported in other brain disease models [385,417].

In addition, also AMPA receptors are deregulated. It is known, in fact, that Ube3A regulates excitatory synapse development by controlling the degradation of Arc, a synaptic protein that promotes the internalization of the AMPA sub-type of glutamate receptors. The disruption of Ube3A leads to an increase in Arc expression and a decrease in the number of AMPA receptors contributing to the cognitive dysfunction that occurs in Angelman Syndrome and possible other ASDs[418].

The synaptic defects in this mouse model are related with behavioural impairments: *Ube3a*<sup>m-/p+</sup> mice had cognitive deficits starting in the first phase of AS pathology (7 weeks), which then increased with age (23 weeks). On the other hand, the *Ube3a*<sup>m-/p+</sup> mice also show a locomotor impairment; however, these deficits did not increase with age (from 7 to 23 weeks) like the cognitive one, and instead remained constant in the Rotarod test. The OF test detected locomotor impairments only at 7 weeks of age, while at 23 weeks of age there was no genotypic difference between wt and *Ube3a*<sup>m-/p</sup> mice. However, despite this, *Ube3a*<sup>m-/p</sup> mice presented synaptic alterations in both the early and late stages of the pathology, suggesting that their motor defects are not highlighted by these tests, more sensitive and accurate behavioural tests are needed.

To determine the importance of JNK's role in this AS model, we chronically treated with D-JNKI1, specific inhibition of JNK, *Ube3a*<sup>m-/p+</sup> mice to see whether JNK inhibition blocked AS pathology and could offer a new pharmacological opportunity against AS.

D-JNKI1 treatment in *Ube3a*<sup>m-/p+</sup> mice, starting at 7 weeks of age and ending at 23 weeks of age, inhibited c-Jun phosphorylation in *Ube3a*<sup>m-/p+</sup> in all the brain areas studied in-vivo. It is well known that c-Jun is the elective target of JNK and, importantly, it is phosphorylated in response to many different stress stimuli. c-Jun is involved in multiple cellular processes like gene expression, apoptosis, metabolism and other critical physiological responses [419,420]. Notably, JNK inhibition (D-JNKI1) powerfully prevents the phosphorylation of c-Jun in the nuclei of cortical, hippocampal, and cerebellar neurons, avoiding their neurodegenerative pathway. In addition, the treatment also normalized the previously observed biochemical PSD alterations, and the p-JNK/JNK and p-PSD95/PSD95 ratios were reduced in all the brain areas.

The neuroprotection on the PSD is paired by the NORT results: D-JNKI1 rescued *Ube3a*<sup>m-/p+</sup> cognitive impairments to the control level. In fact, after chronic treatment with D-JNKI1 the treated-*Ube3a*<sup>m-/p+</sup> D.I. was 0.31, while the untreated *Ube3a*<sup>m-/p+</sup> DI was -0.1352, D-JNKI1 leading the *Ube3a*<sup>m-/p+</sup> performance closer to control level (wt DI was 0.272).

Both the biochemical and functional findings strengthen the neuroprotection obtained with D-JNKI1, giving hope for a possible clinical application. Last but not least, D-JNKI1 treatment in wt mice did not show any significant adverse effect. This is the first proof of concept that in the brain the E3 ubiquitin ligase UBE3A loss induces the downstream activation of the JNK stress signalling pathway. UBE3A and JNK link may be indirect but, evidence demonstrated that loss of *Ube3a* leads to significant increases in PP2A activity, the protein phosphatase 2A, a well known regulator of JNK activity[421] and dendritic spine morphology and synaptic transmission. However, more investigations are needed to clarify the role of JNK in Angelman Syndrome that still remains pivotal since, its specific inhibition prevents c-Jun phosphorylation, rescues the PSD alterations and the cognitive impairments in *Ube3a*<sup>m-/p+</sup> mice, tackling the pathology.

### 5.3 Alzheimer Disease

Alzheimer's disease is the most common form of age-associated neurodegeneration characterized by impairment in cognitive functions and pathologically defined by the accumulation of  $\beta$ -amyloid plaques and neurofibrillary tangles. Despite the efforts of basic and pharmacological research, no treatment is available to definitely cure the disease. The only drugs approved are the use of cholinesterase inhibitors (Donepezil, Galantamine and Rivastigmine), blockers of the NMDA-receptor (Memantine) and Aducanumab to enhance the clearance of A $\beta$  oligomers. Therefore, there is an enormous need for drugs capable to prevent or modify the disease progression, especially in the early phase of the pathology. At the same time, AD is a synaptopathy, and changes at the synaptic level occur in the very early phases of the pathology, when the symptoms are slight and can be trace back to the Mild Cognitive Impairment (MCI).

To characterize this process and JNK involvement in-vivo we used an AD mice model, the 5xFAD mouse, overexpressing APP and PSEN1, containing 5 familial AD mutations (APP KM670/671NL (Swedish), APP I716V (Florida), APP V717I (London), PSEN1 M146L, PSEN1 L286V), under the control of a Thy1 mini-gene. These mice show amyloid pathologies, with plaques deposition starting from 2–4 months of age, microgliosis and inflammation together with synaptic and neuronal loss. We chose this model because ~10% of all AD studies employ this strain, and it is considered as a benchmark reference model in this field [422].

Already at 4 months of age, we found that JNK is activated in the total lysate of cortex as well as of the hippocampus in tg mice, with augmented level of APP and P-APP in the JNK's specific phosphorylation site. Importantly, at this time-point, we did not observe strong behavioural impairment, but only augmented errors number in completing the mnemonic task. These results proved that JNK is already activated in a pre-symptomatic stage of the AD in mice attributable to the phase of MCI in humans.

JNK was activated also in later stages of the pathology, corresponding to 6 and 10 months of age. At this stage, amyloid plaques in 5xFAD progressively propagate in areas associated with the hippocampus such as the subiculum, the entorhinal cortex and are diffuse in all six layers of the cerebral cortex [423]. Accordingly, both APP and P-APP levels were increased in all time points and areas analysed confirming the strong amyloid pathology in 5XFAD mice and the JNK action on one of its crucial targets involved in the AD pathogenesis. On the contrary, the activation of the elective JNK target c-Jun resulted steadily increased in the cortex of tg mice but not in the hippocampus. c-Jun is involved in neuronal death and neuroinflammation [424], [425], [426] and this difference in its activation could be due to a different vulnerability between cortex and hippocampus being more active in the cortical neuronal population, and therefore causing greater damage to the cortex. This scenario would also in agreement with the evidence showing that the brain area most commonly affected by AD is the cerebral cortex, with particularly evident damage in the entorhinal cortex[427].

JNK activation during time is accompanied to a worsening of the behavioural performances in the Radial Arm Water Maze, corresponding to increased time and number of errors in completing the task.

JNK activation and exacerbation of memory impairment in these mice are in line with previous results on another AD mice model, simpler compared to 5XFAD, the CRND8 mice, in which the AD symptoms appear very early in the life span of the animals, making difficult the study of the progression of the mechanisms that lead to the mnemonic deficit [428]. Also in this model, JNK was precociously activated both in the total homogenate and in the TIF fraction together with abnormality in the PSD composition [407], [429]. In line, beyond the total lysate, we also found JNK activation in the dendritic spine compartment with strong abnormalities in both AMPA and NMDA glutamate receptors levels and deregulation of the main excitatory scaffold proteins like PSD95, Drebrin and Shank3 in both areas analysed.

Interestingly, some of these alterations are already present at 4 months of age, when the mice are almost asymptomatic. In particular, concerning AMPA receptors, in the presence of high concentrations of soluble oligomeric A $\beta$ , AMPA receptors are constantly endocytosed and removed[430] in a dose dependent manner. This is clear in the cortex of 5XFAD, where both GluR1 and GluR2 are progressively reduced over time. On the contrary, in the hippocampus are differently regulated. This could be due to a different vulnerability of these brain areas.

This data further supports the idea that AD starts with dysfunction of the synapses occurring in the very early stages of the disease. Acting in this phase, when the damages of the synapse are mild and reversible can improve the prognosis of the pathology.

JNK key role in AD was already proved and confirmed using D-JNKI1 in the CRND8 AD model, in which JNK inhibition ameliorate the phenotype and rescue the synaptic impairment from a biochemical and functional point of view as well[417], [431], [432] but also in 5XFAD model[339,339]. However, pan-JNK inhibition may lead to several side effects in long-term treatment. For this reason, we characterized the levels of JNK3, the brain specific isoform of JNK and the most responsive to stimuli, particularly in

the post-synaptic enriched protein fraction, where its activation has more detrimental effects. We discovered increased JNK3 levels in the TIF fraction starting from 6 month of age, and this increased persist also in the latter time point.

To evaluate this assumption of JNK3 as the isoform most involved in AD, we performed several correlations.

First, we demonstrated that APP phosphorylation in T669 (the specific JNK site) correlates with the cognitive decline in 5XFAD mice. This makes sense considering that phosphorylation promotes the amyloidogenic cleavage of APP enhancing the oligomers (A $\beta$ -oligomers) production that are the most toxicity species for the synapses in the brain parenchyma. A $\beta$  oligomers, in addition, participate in the creation of a toxic loop of JNK activation: JNK, promoting the amyloidogenic APP cleavage, augments the oligomer production that in turn stimulates JNK activation itself.

All JNK isoforms can phosphorylate APP, but several evidences in literature demonstrate that JNK3 is the major kinase involved in the **abnormal phosphorylation of APP at T668**. In fact, in primary neurons, levels and activity of JNK3 directly correlate with APP phosphorylation[433]. It because the module that regulates the A $\beta$  neurotoxicity is mainly due to MLK3-MKK7-JNK3 signal cascades[327] rather than JNK1/2 activation. In line with these observations, 5XFAD mice crossed with JNK3-/- showed dramatically reduced p-JNK signals. In addition, in these mice, insoluble A $\beta$ 42 levels were reduced dramatically compared to those in 5FAD/JNK3+/+[434]. **The importance of JNK3 in the pathogenesis of AD has not only been demonstrated in preclinical models but also in patients.**

Indeed, mRNA levels, as well as JNK3 protein levels are significantly over-expressed in the brain tissues of AD patients[435]. It is important to emphasize that a significant correlation was observed between the levels of A $\beta$ 42 and JNK3 in the human brain. This correlation is also highlighted by the co-localization between senile plaques and JNK3, suggesting that some JNK3 proteins can accumulate during the formation of amyloid aggregates[436]. These data strongly corroborate our results in which JNK3 levels correlates with P-APP and cognitive decline in 5XFAD mice.

We therefore speculate that inhibiting only JNK3 can represent a potential strategy in order to tackle synaptic dysfunction associated to AD.

To prove this hypothesis, in collaboration with prof. Falconi, we developed a cell permeable peptide, using a similar strategy to D-JNKI1 inhibitor, able to selectively inhibit JNK3: dSIMBA2.

We take advantage of the unique 38 aminoacids of JNK3, absent in JNK1 and JNK2, that selectively bind  $\beta$ -arrestin2[437], [438] to generate a cell permeable peptide able to prevent these specific protein-protein interactions.

This bioactive cargo dSIMBA2 introduces an excess of  $\beta$ -arrestin2 sequence that links JNK3, preventing the access of JNK3 to  $\beta$ -arrestin2 and to the other cellular targets presenting this binding sequence. This results in a competitive substrate-type mechanism of action.

After demonstrating the specificity of dSIMBA2 in inhibiting only JNK3 with Alpha screen assay, we tested its neuroprotective effects in an-in-vitro model of cortical primary neurons in which synaptic

dysfunction is induced by A $\beta$  oligomers. Oligomers have the ability to accumulate in the synaptic space and disrupting synaptic function[439], [440], causing reduction in the levels of the NR2A and NR2B subunits of NMDA receptors, GluR1 and GluR2 subunits of AMPAR, PSD-95 and Drebrin and loss of s dendritic[441], [442], [443].

As previously demonstrated[417], [444], also in this model subtoxic doses of A $\beta$  oligomers induces strong JNK activation and reduction in AMPA and NMDA receptor levels together with deregulation of scaffold proteins, in line with what we observed in the in-vivo 5XFAD model. This model mimics the first phase of the synaptic dysfunction, in fact in the total homogenate of the culture we did not observe JNK nor c-Jun activation. Our results inference that dSIMBA2 reduces JNK3 activation, even if this is an indirect evaluation. We speculate that, since JNK3 is the JNK isoform most expressed in the CNS and the most responsive to stress stimuli, the contribution of the other isoforms should be minor. Given the high homology of the phosphorylation sites on the three JNK isoforms, there are not available antibodies capable of recognizing only the phosphorylated JNK3, thus we inferred JNK3 activation as P-JNK/JNK ratio. The pre-treatment with dSIMBA2, blocks the synaptic dysfunction preventing the loss of receptors and scaffold protein in the excitatory synapses in-vitro proving a powerful neuroprotective effect.

Notwithstanding further experiments are necessary in order to better elucidate the mechanism of action of dSIMBA2, target engagement and stability, these encouraging results open the possibility to new strategies to treat not only AD but also many other synaptopathies. The specific inhibition of JNK3 isoform offers the advantage of acting only in the nervous tissue (not in the rest of the body) and preventing in this way only the pathological action mediated by the stress stimuli (JNK3 is the most responsive JNKs to stress-stimuli), thus preserving the physiological actions of the JNKs family, this will avoid the potential side effects of the inhibition of the ubiquitous action of JNK1 and 2.

In addition, JNK3 was found in the CSF of AD patients and its levels correlate to the cognitive decline [436]. This is particular interest because, in addition to reiterating JNK3 as a target, suggest that JNK3 is also biomarker of neurodegeneration. However, to date, further studies are currently in progress to clarify the potentiality of JNK3 as a biomarker of synaptic injury.

To conclude, the data obtained in this thesis participate in the reinforcement of JNK as a central actor in the degeneration mechanisms of the synapses that characterized both neurodevelopmental and neurodegenerative diseases.

In addition, it adds new elements to define JNK3, the most responsive JNK isoform to stress, as a key player in the AD, and an important target for the treatment of synaptic injury, potentially also in other brain illnesses.

In fact, developing new compounds able to inhibit one of the most responsive kinases to stress stimuli may be an intriguing field to explore, in light of the last reports of the FDA in the drug discovery matter[378].



## 6. References

---

1. Pacitti, D.; Privolizzi, R.; Bax, B.E. Organs to Cells and Cells to Organoids: The Evolution of in Vitro Central Nervous System Modelling. *Front. Cell. Neurosci.* **2019**, *13*, 129, doi:10.3389/fncel.2019.00129.
2. Chiaradia, I.; Lancaster, M.A. Brain Organoids for the Study of Human Neurobiology at the Interface of in Vitro and in Vivo. *Nat. Neurosci.* **2020**, *23*, 1496–1508, doi:10.1038/s41593-020-00730-3.
3. Lancaster, M.A. Brain Organoids: A New Frontier of Human Neuroscience Research. *Semin. Cell Dev. Biol.* **2021**, *111*, 1–3, doi:10.1016/j.semdb.2020.10.011.
4. Benson, D.L.; Huntley, G.W. Synapse Adhesion: A Dynamic Equilibrium Conferring Stability and Flexibility. *Curr. Opin. Neurobiol.* **2012**, *22*, 397–404, doi:10.1016/j.conb.2011.09.011.
5. Lepeta, K.; Lourenco, M.V.; Schweitzer, B.C.; Martino Adami, P.V.; Banerjee, P.; Catuara-Solarz, S.; de La Fuente Revenga, M.; Guillem, A.M.; Haidar, M.; Ijomone, O.M.; et al. Synaptopathies: Synaptic Dysfunction in Neurological Disorders - A Review from Students to Students. *J. Neurochem.* **2016**, *138*, 785–805, doi:10.1111/jnc.13713.
6. Croning, M.D.R.; Marshall, M.C.; McLaren, P.; Armstrong, J.D.; Grant, S.G.N. G2Cdb: The Genes to Cognition Database. *Nucleic Acids Res.* **2009**, *37*, D846–851, doi:10.1093/nar/gkn700.
7. Pirooznia, M.; Wang, T.; Avramopoulos, D.; Valle, D.; Thomas, G.; Huganir, R.L.; Goes, F.S.; Potash, J.B.; Zandi, P.P. SynaptomeDB: An Ontology-Based Knowledgebase for Synaptic Genes. *Bioinforma. Oxf. Engl.* **2012**, *28*, 897–899, doi:10.1093/bioinformatics/bts040.
8. Südhof, T.C. Towards an Understanding of Synapse Formation. *Neuron* **2018**, *100*, 276–293, doi:10.1016/j.neuron.2018.09.040.
9. Kantardzhieva, A.; Peppi, M.; Lane, W.S.; Sewell, W.F. Protein Composition of Immunoprecipitated Synaptic Ribbons. *J. Proteome Res.* **2012**, *11*, 1163–1174, doi:10.1021/pr2008972.
10. Siksou, L.; Rostaing, P.; Lechaire, J.-P.; Boudier, T.; Ohtsuka, T.; Fejtová, A.; Kao, H.-T.; Greengard, P.; Gundelfinger, E.D.; Triller, A.; et al. Three-Dimensional Architecture of Presynaptic Terminal Cytomatrix. *J. Neurosci. Off. J. Soc. Neurosci.* **2007**, *27*, 6868–6877, doi:10.1523/JNEUROSCI.1773-07.2007.
11. Ackermann, F.; Waites, C.L.; Garner, C.C. Presynaptic Active Zones in Invertebrates and Vertebrates. *EMBO Rep.* **2015**, *16*, 923–938, doi:10.15252/embr.201540434.
12. Löscher, W.; Gillard, M.; Sands, Z.A.; Kaminski, R.M.; Klitgaard, H. Synaptic Vesicle Glycoprotein 2A Ligands in the Treatment of Epilepsy and Beyond. *CNS Drugs* **2016**, *30*, 1055–1077, doi:10.1007/s40263-016-0384-x.
13. Yoon, T.-Y.; Munson, M. SNARE Complex Assembly and Disassembly. *Curr. Biol. CB* **2018**, *28*, R397–R401, doi:10.1016/j.cub.2018.01.005.
14. Ramakrishnan, N.A.; Drescher, M.J.; Drescher, D.G. The SNARE Complex in Neuronal and Sensory Cells. *Mol. Cell. Neurosci.* **2012**, *50*, 58–69, doi:10.1016/j.mcn.2012.03.009.
15. Hering, H.; Sheng, M. Dendritic Spines: Structure, Dynamics and Regulation. *Nat. Rev. Neurosci.* **2001**, *2*, 880–888, doi:10.1038/35104061.
16. Vallés, A.S.; Barrantes, F.J. Nanoscale Sub-Compartmentalization of the Dendritic Spine Compartment. *Biomolecules* **2021**, *11*, doi:10.3390/biom11111697.
17. Risher, W.C.; Ustunkaya, T.; Singh Alvarado, J.; Eroglu, C. Rapid Golgi Analysis Method for Efficient and Unbiased Classification of Dendritic Spines. *PLoS One* **2014**, *9*, e107591, doi:10.1371/journal.pone.0107591.
18. Arellano, J.I.; Benavides-Piccione, R.; Defelipe, J.; Yuste, R. Ultrastructure of Dendritic Spines: Correlation between Synaptic and Spine Morphologies. *Front. Neurosci.* **2007**, *1*, 131–143, doi:10.3389/neuro.01.1.1.010.2007.
19. Harris, K.M.; Stevens, J.K. Dendritic Spines of CA 1 Pyramidal Cells in the Rat Hippocampus: Serial Electron Microscopy with Reference to Their Biophysical Characteristics. *J. Neurosci. Off. J. Soc. Neurosci.* **1989**, *9*, 2982–2997.
20. Trommald, M.; Hulleberg, G. Dimensions and Density of Dendritic Spines from Rat Dentate Granule Cells Based on Reconstructions from Serial Electron Micrographs. *J. Comp. Neurol.* **1997**, *377*, 15–28, doi:10.1002/(sici)1096-9861(19970106)377:1<15::aid-cne3>3.0.co;2-m.
21. Matsuzaki, M.; Ellis-Davies, G.C.; Nemoto, T.; Miyashita, Y.; Iino, M.; Kasai, H. Dendritic Spine Geometry Is Critical for AMPA Receptor Expression in Hippocampal CA1 Pyramidal Neurons. *Nat. Neurosci.* **2001**, *4*, 1086–1092, doi:10.1038/nn736.
22. Noguchi, J.; Nagaoka, A.; Watanabe, S.; Ellis-Davies, G.C.R.; Kitamura, K.; Kano, M.; Matsuzaki, M.; Kasai, H. In Vivo Two-Photon Uncaging of Glutamate Revealing the Structure-Function Relationships of Dendritic Spines in the Neocortex of Adult Mice. *J. Physiol.* **2011**, *589*, 2447–2457, doi:10.1113/jphysiol.2011.207100.
23. Scheefhals, N.; MacGillavry, H.D. Functional Organization of Postsynaptic Glutamate Receptors. *Mol. Cell. Neurosci.* **2018**, *91*, 82–94, doi:10.1016/j.mcn.2018.05.002.

24. Bayés, A.; Collins, M.O.; Croning, M.D.R.; van de Lagemaat, L.N.; Choudhary, J.S.; Grant, S.G.N. Comparative Study of Human and Mouse Postsynaptic Proteomes Finds High Compositional Conservation and Abundance Differences for Key Synaptic Proteins. *PLoS One* **2012**, *7*, e46683, doi:10.1371/journal.pone.0046683.
25. Trinidad, J.C.; Thalhammer, A.; Specht, C.G.; Lynn, A.J.; Baker, P.R.; Schoepfer, R.; Burlingame, A.L. Quantitative Analysis of Synaptic Phosphorylation and Protein Expression. *Mol. Cell. Proteomics MCP* **2008**, *7*, 684–696, doi:10.1074/mcp.M700170-MCP200.
26. Wilkinson, B.; Coba, M.P. Molecular Architecture of Postsynaptic Interactomes. *Cell. Signal.* **2020**, *76*, 109782, doi:10.1016/j.cellsig.2020.109782.
27. Cohen, R.S.; Blomberg, F.; Berzins, K.; Siekevitz, P. The Structure of Postsynaptic Densities Isolated from Dog Cerebral Cortex. I. Overall Morphology and Protein Composition. *J. Cell Biol.* **1977**, *74*, 181–203, doi:10.1083/jcb.74.1.181.
28. Carlin, R.K.; Grab, D.J.; Cohen, R.S.; Siekevitz, P. Isolation and Characterization of Postsynaptic Densities from Various Brain Regions: Enrichment of Different Types of Postsynaptic Densities. *J. Cell Biol.* **1980**, *86*, 831–845, doi:10.1083/jcb.86.3.831.
29. Klauck, T.M.; Scott, J.D. The Postsynaptic Density: A Subcellular Anchor for Signal Transduction Enzymes. *Cell. Signal.* **1995**, *7*, 747–757, doi:10.1016/0898-6568(95)02003-9.
30. Ziff, E.B. Enlightening the Postsynaptic Density. *Neuron* **1997**, *19*, 1163–1174, doi:10.1016/s0896-6273(00)80409-2.
31. Bayés, A.; Grant, S.G.N. Neuroproteomics: Understanding the Molecular Organization and Complexity of the Brain. *Nat. Rev. Neurosci.* **2009**, *10*, 635–646, doi:10.1038/nrn2701.
32. Lowenthal, M.S.; Markey, S.P.; Dosemeci, A. Quantitative Mass Spectrometry Measurements Reveal Stoichiometry of Principal Postsynaptic Density Proteins. *J. Proteome Res.* **2015**, *14*, 2528–2538, doi:10.1021/acs.jproteome.5b00109.
33. Won, S.; Levy, J.M.; Nicoll, R.A.; Roche, K.W. MAGUKs: Multifaceted Synaptic Organizers. *Curr. Opin. Neurobiol.* **2017**, *43*, 94–101, doi:10.1016/j.conb.2017.01.006.
34. Coba, M.P.; Ramaker, M.J.; Ho, E.V.; Thompson, S.L.; Komiyama, N.H.; Grant, S.G.N.; Knowles, J.A.; Dulawa, S.C. Dlgap1 Knockout Mice Exhibit Alterations of the Postsynaptic Density and Selective Reductions in Sociability. *Sci. Rep.* **2018**, *8*, 2281, doi:10.1038/s41598-018-20610-y.
35. Li, J.; Zhang, W.; Yang, H.; Howrigan, D.P.; Wilkinson, B.; Souaiaia, T.; Evgrafov, O.V.; Genovese, G.; Clementel, V.A.; Tudor, J.C.; et al. Spatiotemporal Profile of Postsynaptic Interactomes Integrates Components of Complex Brain Disorders. *Nat. Neurosci.* **2017**, *20*, 1150–1161, doi:10.1038/nn.4594.
36. Li, J.; Wilkinson, B.; Clementel, V.A.; Hou, J.; O'Dell, T.J.; Coba, M.P. Long-Term Potentiation Modulates Synaptic Phosphorylation Networks and Reshapes the Structure of the Postsynaptic Interactome. *Sci. Signal.* **2016**, *9*, rs8, doi:10.1126/scisignal.aaf6716.
37. Malinow, R.; Malenka, R.C. AMPA Receptor Trafficking and Synaptic Plasticity. *Annu. Rev. Neurosci.* **2002**, *25*, 103–126, doi:10.1146/annurev.neuro.25.112701.142758.
38. Choquet, D.; Triller, A. The Dynamic Synapse. *Neuron* **2013**, *80*, 691–703, doi:10.1016/j.neuron.2013.10.013.
39. Lang, C.; Barco, A.; Zablow, L.; Kandel, E.R.; Siegelbaum, S.A.; Zakharenko, S.S. Transient Expansion of Synaptically Connected Dendritic Spines upon Induction of Hippocampal Long-Term Potentiation. *Proc. Natl. Acad. Sci. U. S. A.* **2004**, *101*, 16665–16670, doi:10.1073/pnas.0407581101.
40. Matsuzaki, M.; Honkura, N.; Ellis-Davies, G.C.R.; Kasai, H. Structural Basis of Long-Term Potentiation in Single Dendritic Spines. *Nature* **2004**, *429*, 761–766, doi:10.1038/nature02617.
41. Nägerl, U.V.; Eberhorn, N.; Cambridge, S.B.; Bonhoeffer, T. Bidirectional Activity-Dependent Morphological Plasticity in Hippocampal Neurons. *Neuron* **2004**, *44*, 759–767, doi:10.1016/j.neuron.2004.11.016.
42. Zhou, Q.; Homma, K.J.; Poo, M. Shrinkage of Dendritic Spines Associated with Long-Term Depression of Hippocampal Synapses. *Neuron* **2004**, *44*, 749–757, doi:10.1016/j.neuron.2004.11.011.
43. Gamlin, C.R.; Yu, W.-Q.; Wong, R.O.L.; Hoon, M. Assembly and Maintenance of GABAergic and Glycinergic Circuits in the Mammalian Nervous System. *Neural Develop.* **2018**, *13*, 12, doi:10.1186/s13064-018-0109-6.
44. Sassoè-Pognetto, M.; Frola, E.; Pugno, G.; Briatore, F.; Patrizi, A. Understanding the Molecular Diversity of GABAergic Synapses. *Front. Cell. Neurosci.* **2011**, *5*, 4, doi:10.3389/fncel.2011.00004.
45. Tyagarajan, S.K.; Fritschy, J.-M. Gephyrin: A Master Regulator of Neuronal Function? *Nat. Rev. Neurosci.* **2014**, *15*, 141–156, doi:10.1038/nrn3670.
46. Flores, C.E.; Méndez, P. Shaping Inhibition: Activity Dependent Structural Plasticity of GABAergic Synapses.

*Front. Cell. Neurosci.* **2014**, *8*, 327, doi:10.3389/fncel.2014.00327.

47. Markram, H.; Toledo-Rodriguez, M.; Wang, Y.; Gupta, A.; Silberberg, G.; Wu, C. Interneurons of the Neocortical Inhibitory System. *Nat. Rev. Neurosci.* **2004**, *5*, 793–807, doi:10.1038/nrn1519.

48. Petilla Interneuron Nomenclature Group; Ascoli, G.A.; Alonso-Nanclares, L.; Anderson, S.A.; Barrionuevo, G.; Benavides-Piccione, R.; Burkhalter, A.; Buzsáki, G.; Cauli, B.; Defelipe, J.; et al. Petilla Terminology: Nomenclature of Features of GABAergic Interneurons of the Cerebral Cortex. *Nat. Rev. Neurosci.* **2008**, *9*, 557–568, doi:10.1038/nrn2402.

49. McBain, C.J.; Fisahn, A. Interneurons Unbound. *Nat. Rev. Neurosci.* **2001**, *2*, 11–23, doi:10.1038/35049047.

50. Kandel, E. R., Schwartz, J. H., Jessell, T. M., Siegelbaum, S. A., Hudspeth, A. J., & Mack, S. *Principles of Neural Science (Fifth Edition)*; 2013;

51. Traynelis, S.F.; Wollmuth, L.P.; McBain, C.J.; Menniti, F.S.; Vance, K.M.; Ogden, K.K.; Hansen, K.B.; Yuan, H.; Myers, S.J.; Dingledine, R. Glutamate Receptor Ion Channels: Structure, Regulation, and Function. *Pharmacol. Rev.* **2010**, *62*, 405–496, doi:10.1124/pr.109.002451.

52. Baude, A.; Nusser, Z.; Roberts, J.D.; Mulvihill, E.; McIlhinney, R.A.; Somogyi, P. The Metabotropic Glutamate Receptor (mGluR1 Alpha) Is Concentrated at Perisynaptic Membrane of Neuronal Subpopulations as Detected by Immunogold Reaction. *Neuron* **1993**, *11*, 771–787, doi:10.1016/0896-6273(93)90086-7.

53. Nusser, Z.; Mulvihill, E.; Streit, P.; Somogyi, P. Subsynaptic Segregation of Metabotropic and Ionotropic Glutamate Receptors as Revealed by Immunogold Localization. *Neuroscience* **1994**, *61*, 421–427, doi:10.1016/0306-4522(94)90421-9.

54. MacGillavry, H.D.; Kerr, J.M.; Blanpied, T.A. Lateral Organization of the Postsynaptic Density. *Mol. Cell. Neurosci.* **2011**, *48*, 321–331, doi:10.1016/j.mcn.2011.09.001.

55. Tang, A.-H.; Chen, H.; Li, T.P.; Metzbower, S.R.; MacGillavry, H.D.; Blanpied, T.A. A Trans-Synaptic Nanocolumn Aligns Neurotransmitter Release to Receptors. *Nature* **2016**, *536*, 210–214, doi:10.1038/nature19058.

56. Hanley, J.G. Actin-Dependent Mechanisms in AMPA Receptor Trafficking. *Front. Cell. Neurosci.* **2014**, *8*, 381, doi:10.3389/fncel.2014.00381.

57. Kneussel, M.; Wagner, W. Myosin Motors at Neuronal Synapses: Drivers of Membrane Transport and Actin Dynamics. *Nat. Rev. Neurosci.* **2013**, *14*, 233–247, doi:10.1038/nrn3445.

58. Stefen, H.; Chaichim, C.; Power, J.; Fath, T. Regulation of the Postsynaptic Compartment of Excitatory Synapses by the Actin Cytoskeleton in Health and Its Disruption in Disease. *Neural Plast.* **2016**, *2016*, 2371970, doi:10.1155/2016/2371970.

59. Pérez-Otaño, I.; Luján, R.; Tavalin, S.J.; Plomann, M.; Modregger, J.; Liu, X.-B.; Jones, E.G.; Heinemann, S.F.; Lo, D.C.; Ehlers, M.D. Endocytosis and Synaptic Removal of NR3A-Containing NMDA Receptors by PACSIN1/Syndapin1. *Nat. Neurosci.* **2006**, *9*, 611–621, doi:10.1038/nn1680.

60. Racca, C.; Stephenson, F.A.; Streit, P.; Roberts, J.D.; Somogyi, P. NMDA Receptor Content of Synapses in Stratum Radiatum of the Hippocampal CA1 Area. *J. Neurosci. Off. J. Soc. Neurosci.* **2000**, *20*, 2512–2522.

61. Pelucchi, S.; Vandermeulen, L.; Pizzamiglio, L.; Aksan, B.; Yan, J.; Konietzny, A.; Bonomi, E.; Borroni, B.; Padovani, A.; Rust, M.B.; et al. Cyclase-Associated Protein 2 Dimerization Regulates Cofilin in Synaptic Plasticity and Alzheimer's Disease. *Brain Commun.* **2020**, *2*, fcaa086, doi:10.1093/braincomms/fcaa086.

62. Lei, S.; Czerwinska, E.; Czerwinski, W.; Walsh, M.P.; MacDonald, J.F. Regulation of NMDA Receptor Activity by F-Actin and Myosin Light Chain Kinase. *J. Neurosci. Off. J. Soc. Neurosci.* **2001**, *21*, 8464–8472.

63. Freche, D.; Pannasch, U.; Rouach, N.; Holcman, D. Synapse Geometry and Receptor Dynamics Modulate Synaptic Strength. *PloS One* **2011**, *6*, e25122, doi:10.1371/journal.pone.0025122.

64. Strack, S.; McNeill, R.B.; Colbran, R.J. Mechanism and Regulation of Calcium/Calmodulin-Dependent Protein Kinase II Targeting to the NR2B Subunit of the N-Methyl-D-Aspartate Receptor. *J. Biol. Chem.* **2000**, *275*, 23798–23806, doi:10.1074/jbc.M001471200.

65. Cheng, D.; Hoogenraad, C.C.; Rush, J.; Ramm, E.; Schlager, M.A.; Duong, D.M.; Xu, P.; Wijayawardana, S.R.; Hanfelt, J.; Nakagawa, T.; et al. Relative and Absolute Quantification of Postsynaptic Density Proteome Isolated from Rat Forebrain and Cerebellum. *Mol. Cell. Proteomics MCP* **2006**, *5*, 1158–1170, doi:10.1074/mcp.D500009-MCP200.

66. Chen, L.; Chetkovich, D.M.; Petralia, R.S.; Sweeney, N.T.; Kawasaki, Y.; Wenthold, R.J.; Brecht, D.S.; Nicoll, R.A. Stargazin Regulates Synaptic Targeting of AMPA Receptors by Two Distinct Mechanisms. *Nature* **2000**, *408*, 936–943, doi:10.1038/35050030.

67. Kim, E.; Sheng, M. PDZ Domain Proteins of Synapses. *Nat. Rev. Neurosci.* **2004**, *5*, 771–781, doi:10.1038/nrn1517.

68. Funke, L.; Dakoqi, S.; Brecht, D.S. Membrane-Associated Guanylate Kinases Regulate Adhesion and Plasticity at Cell Junctions. *Annu. Rev. Biochem.* **2005**, *74*, 219–245, doi:10.1146/annurev.biochem.74.082803.133339.
69. Gilman, S.R.; Iossifov, I.; Levy, D.; Ronemus, M.; Wigler, M.; Vitkup, D. Rare de Novo Variants Associated with Autism Implicate a Large Functional Network of Genes Involved in Formation and Function of Synapses. *Neuron* **2011**, *70*, 898–907, doi:10.1016/j.neuron.2011.05.021.
70. Kornau, H.C.; Schenker, L.T.; Kennedy, M.B.; Seeburg, P.H. Domain Interaction between NMDA Receptor Subunits and the Postsynaptic Density Protein PSD-95. *Science* **1995**, *269*, 1737–1740, doi:10.1126/science.7569905.
71. Elias, G.M.; Funke, L.; Stein, V.; Grant, S.G.; Brecht, D.S.; Nicoll, R.A. Synapse-Specific and Developmentally Regulated Targeting of AMPA Receptors by a Family of MAGUK Scaffolding Proteins. *Neuron* **2006**, *52*, 307–320, doi:10.1016/j.neuron.2006.09.012.
72. Lambert, J.T.; Hill, T.C.; Park, D.K.; Culp, J.H.; Zito, K. Protracted and Asynchronous Accumulation of PSD95-Family MAGUKs during Maturation of Nascent Dendritic Spines. *Dev. Neurobiol.* **2017**, *77*, 1161–1174, doi:10.1002/dneu.22503.
73. De Roo, M.; Klauser, P.; Mendez, P.; Poglia, L.; Muller, D. Activity-Dependent PSD Formation and Stabilization of Newly Formed Spines in Hippocampal Slice Cultures. *Cereb. Cortex N. Y. N 1991* **2008**, *18*, 151–161, doi:10.1093/cercor/bhm041.
74. Ehrlich, I.; Klein, M.; Rumpel, S.; Malinow, R. PSD-95 Is Required for Activity-Driven Synapse Stabilization. *Proc. Natl. Acad. Sci. U. S. A.* **2007**, *104*, 4176–4181, doi:10.1073/pnas.0609307104.
75. El-Husseini, A.E.; Schnell, E.; Chetkovich, D.M.; Nicoll, R.A.; Brecht, D.S. PSD-95 Involvement in Maturation of Excitatory Synapses. *Science* **2000**, *290*, 1364–1368.
76. Stein, V.; House, D.R.C.; Brecht, D.S.; Nicoll, R.A. Postsynaptic Density-95 Mimics and Occludes Hippocampal Long-Term Potentiation and Enhances Long-Term Depression. *J. Neurosci. Off. J. Soc. Neurosci.* **2003**, *23*, 5503–5506.
77. Vallejo, D.; Codocedo, J.F.; Inestrosa, N.C. Posttranslational Modifications Regulate the Postsynaptic Localization of PSD-95. *Mol. Neurobiol.* **2017**, *54*, 1759–1776, doi:10.1007/s12035-016-9745-1.
78. Kim, M.J.; Futai, K.; Jo, J.; Hayashi, Y.; Cho, K.; Sheng, M. Synaptic Accumulation of PSD-95 and Synaptic Function Regulated by Phosphorylation of Serine-295 of PSD-95. *Neuron* **2007**, *56*, 488–502, doi:10.1016/j.neuron.2007.09.007.
79. Pavlowsky, A.; Gianfelice, A.; Pallotto, M.; Zanchi, A.; Vara, H.; Khelifaoui, M.; Valnegri, P.; Rezai, X.; Bassani, S.; Brambilla, D.; et al. A Postsynaptic Signaling Pathway That May Account for the Cognitive Defect Due to IL1RAPL1 Mutation. *Curr. Biol. CB* **2010**, *20*, 103–115, doi:10.1016/j.cub.2009.12.030.
80. Nelson, C.D.; Kim, M.J.; Hsin, H.; Chen, Y.; Sheng, M. Phosphorylation of Threonine-19 of PSD-95 by GSK-3 $\beta$  Is Required for PSD-95 Mobilization and Long-Term Depression. *J. Neurosci. Off. J. Soc. Neurosci.* **2013**, *33*, 12122–12135, doi:10.1523/JNEUROSCI.0131-13.2013.
81. Aoki, C.; Sherpa, A.D. Making of a Synapse: Recurrent Roles of Drebrin A at Excitatory Synapses Throughout Life. *Adv. Exp. Med. Biol.* **2017**, *1006*, 119–139, doi:10.1007/978-4-431-56550-5\_8.
82. Mizui, T.; Kojima, N.; Yamazaki, H.; Katayama, M.; Hanamura, K.; Shirao, T. Drebrin E Is Involved in the Regulation of Axonal Growth through Actin-Myosin Interactions. *J. Neurochem.* **2009**, *109*, 611–622, doi:10.1111/j.1471-4159.2009.05993.x.
83. Sekino, Y.; Shirao, T. [Dynamics and function of actin-binding proteins in excitatory synapses]. *Tanpakushitsu Kakusan Koso.* **2006**, *51*, 350–356.
84. Yamazaki, H.; Kojima, N.; Kato, K.; Hirose, E.; Iwasaki, T.; Mizui, T.; Takahashi, H.; Hanamura, K.; Roppongi, R.T.; Koibuchi, N.; et al. Spikar, a Novel Drebrin-Binding Protein, Regulates the Formation and Stabilization of Dendritic Spines. *J. Neurochem.* **2014**, *128*, 507–522, doi:10.1111/jnc.12486.
85. Mizui, T.; Takahashi, H.; Sekino, Y.; Shirao, T. Overexpression of Drebrin A in Immature Neurons Induces the Accumulation of F-Actin and PSD-95 into Dendritic Filopodia, and the Formation of Large Abnormal Protrusions. *Mol. Cell. Neurosci.* **2005**, *30*, 630–638.
86. Sekino, Y.; Koganezawa, N.; Mizui, T.; Shirao, T. Role of Drebrin in Synaptic Plasticity. *Adv. Exp. Med. Biol.* **2017**, *1006*, 183–201, doi:10.1007/978-4-431-56550-5\_11.
87. Takizawa, H.; Hiroi, N.; Funahashi, A. Mathematical Modeling of Sustainable Synaptogenesis by Repetitive Stimuli Suggests Signaling Mechanisms in Vivo. *PLoS One* **2012**, *7*, e51000, doi:10.1371/journal.pone.0051000.
88. Worth, D.C.; Daly, C.N.; Geraldo, S.; Oozer, F.; Gordon-Weeks, P.R. Drebrin Contains a Cryptic F-Actin-Bundling Activity Regulated by Cdk5 Phosphorylation. *J. Cell Biol.* **2013**, *202*, 793–806, doi:10.1083/jcb.201303005.
89. Böckers, T.M.; Segger-Junius, M.; Iglauer, P.; Bockmann, J.; Gundelfinger, E.D.; Kreutz, M.R.; Richter, D.;

- Kindler, S.; Kreienkamp, H.-J. Differential Expression and Dendritic Transcript Localization of Shank Family Members: Identification of a Dendritic Targeting Element in the 3' Untranslated Region of Shank1 mRNA. *Mol. Cell. Neurosci.* **2004**, *26*, 182–190, doi:10.1016/j.mcn.2004.01.009.
90. Baron, M.K.; Boeckers, T.M.; Vaida, B.; Faham, S.; Gingery, M.; Sawaya, M.R.; Salyer, D.; Gundelfinger, E.D.; Bowie, J.U. An Architectural Framework That May Lie at the Core of the Postsynaptic Density. *Science* **2006**, *311*, 531–535, doi:10.1126/science.1118995.
91. Hayashi, M.K.; Tang, C.; Verpelli, C.; Narayanan, R.; Stearns, M.H.; Xu, R.-M.; Li, H.; Sala, C.; Hayashi, Y. The Postsynaptic Density Proteins Homer and Shank Form a Polymeric Network Structure. *Cell* **2009**, *137*, 159–171, doi:10.1016/j.cell.2009.01.050.
92. Boeckers, T.M.; Bockmann, J.; Kreutz, M.R.; Gundelfinger, E.D. ProSAP/Shank Proteins - a Family of Higher Order Organizing Molecules of the Postsynaptic Density with an Emerging Role in Human Neurological Disease. *J. Neurochem.* **2002**, *81*, 903–910, doi:10.1046/j.1471-4159.2002.00931.x.
93. Sheng, M.; Kim, E. The Shank Family of Scaffold Proteins. *J. Cell Sci.* **2000**, *113* (Pt 11), 1851–1856.
94. Gundelfinger, E.D.; Boeckers, T.M.; Baron, M.K.; Bowie, J.U. A Role for Zinc in Postsynaptic Density AsSAMbly and Plasticity? *Trends Biochem. Sci.* **2006**, *31*, 366–373, doi:10.1016/j.tibs.2006.05.007.
95. Roussignol, G.; Ango, F.; Romorini, S.; Tu, J.C.; Sala, C.; Worley, P.F.; Bockaert, J.; Fagni, L. Shank Expression Is Sufficient to Induce Functional Dendritic Spine Synapses in Aspiny Neurons. *J. Neurosci. Off. J. Soc. Neurosci.* **2005**, *25*, 3560–3570, doi:10.1523/JNEUROSCI.4354-04.2005.
96. Uemura, T.; Mori, H.; Mishina, M. Direct Interaction of GluRdelta2 with Shank Scaffold Proteins in Cerebellar Purkinje Cells. *Mol. Cell. Neurosci.* **2004**, *26*, 330–341, doi:10.1016/j.mcn.2004.02.007.
97. Qualmann, B.; Boeckers, T.M.; Jeromin, M.; Gundelfinger, E.D.; Kessels, M.M. Linkage of the Actin Cytoskeleton to the Postsynaptic Density via Direct Interactions of Abp1 with the ProSAP/Shank Family. *J. Neurosci. Off. J. Soc. Neurosci.* **2004**, *24*, 2481–2495, doi:10.1523/JNEUROSCI.5479-03.2004.
98. Vyas, Y.; Montgomery, J.M. The Role of Postsynaptic Density Proteins in Neural Degeneration and Regeneration. *Neural Regen. Res.* **2016**, *11*, 906–907, doi:10.4103/1673-5374.184481.
99. Ješko, H.; Ciešlik, M.; Gromadzka, G.; Adamczyk, A. Dysfunctional Proteins in Neuropsychiatric Disorders: From Neurodegeneration to Autism Spectrum Disorders. *Neurochem. Int.* **2020**, *141*, 104853, doi:10.1016/j.neuint.2020.104853.
100. Alexiou, A.; Nizami, B.; Khan, F.I.; Soursou, G.; Vairaktarakis, C.; Chatzichronis, S.; Tsiamis, V.; Mantzavinos, V.; Yarla, N.S.; Md Ashraf, G. Mitochondrial Dynamics and Proteins Related to Neurodegenerative Diseases. *Curr. Protein Pept. Sci.* **2018**, *19*, 850–857, doi:10.2174/1389203718666170810150151.
101. Musi, C.A.; Agrò, G.; Santarella, F.; Iervasi, E.; Borsello, T. JNK3 as Therapeutic Target and Biomarker in Neurodegenerative and Neurodevelopmental Brain Diseases. *Cells* **2020**, *9*, E2190, doi:10.3390/cells9102190.
102. Grzadzinski, R.; Huerta, M.; Lord, C. DSM-5 and Autism Spectrum Disorders (ASDs): An Opportunity for Identifying ASD Subtypes. *Mol. Autism* **2013**, *4*, 12, doi:10.1186/2040-2392-4-12.
103. Ali Rodriguez, R.; Joya, C.; Hines, R.M. Common Ribs of Inhibitory Synaptic Dysfunction in the Umbrella of Neurodevelopmental Disorders. *Front. Mol. Neurosci.* **2018**, *11*, 132, doi:10.3389/fnmol.2018.00132.
104. Delorme, R.; Ey, E.; Toro, R.; Leboyer, M.; Gillberg, C.; Bourgeron, T. Progress toward Treatments for Synaptic Defects in Autism. *Nat. Med.* **2013**, *19*, 685–694, doi:10.1038/nm.3193.
105. Sacai, H.; Sakoori, K.; Konno, K.; Nagahama, K.; Suzuki, H.; Watanabe, T.; Watanabe, M.; Uesaka, N.; Kano, M. Autism Spectrum Disorder-like Behavior Caused by Reduced Excitatory Synaptic Transmission in Pyramidal Neurons of Mouse Prefrontal Cortex. *Nat. Commun.* **2020**, *11*, 5140, doi:10.1038/s41467-020-18861-3.
106. Ebert, D.H.; Greenberg, M.E. Activity-Dependent Neuronal Signalling and Autism Spectrum Disorder. *Nature* **2013**, *493*, 327–337, doi:10.1038/nature11860.
107. Lahiri, D.K.; Sokol, D.K.; Erickson, C.; Ray, B.; Ho, C.Y.; Maloney, B. Autism as Early Neurodevelopmental Disorder: Evidence for an SAPP $\alpha$ -Mediated Anabolic Pathway. *Front. Cell. Neurosci.* **2013**, *7*, 94, doi:10.3389/fncel.2013.00094.
108. Spooren, W.; Lindemann, L.; Ghosh, A.; Santarelli, L. Synapse Dysfunction in Autism: A Molecular Medicine Approach to Drug Discovery in Neurodevelopmental Disorders. *Trends Pharmacol. Sci.* **2012**, *33*, 669–684, doi:10.1016/j.tips.2012.09.004.
109. Bowling, H.; Klann, E. Shaping Dendritic Spines in Autism Spectrum Disorder: MTORC1-Dependent Macroautophagy. *Neuron* **2014**, *83*, 994–996, doi:10.1016/j.neuron.2014.08.021.
110. Coley, A.A.; Gao, W.-J. PSD95: A Synaptic Protein Implicated in Schizophrenia or Autism? *Prog. Neuropsychopharmacol. Biol. Psychiatry* **2018**, *82*, 187–194, doi:10.1016/j.pnpbp.2017.11.016.

111. Hutsler, J.J.; Zhang, H. Increased Dendritic Spine Densities on Cortical Projection Neurons in Autism Spectrum Disorders. *Brain Res.* **2010**, *1309*, 83–94, doi:10.1016/j.brainres.2009.09.120.
112. Taoufik, E.; Kouroupi, G.; Zygogianni, O.; Matsas, R. Synaptic Dysfunction in Neurodegenerative and Neurodevelopmental Diseases: An Overview of Induced Pluripotent Stem-Cell-Based Disease Models. *Open Biol.* **2018**, *8*, doi:10.1098/rsob.180138.
113. Karahanoğlu, F.I.; Baran, B.; Nguyen, Q.T.H.; Meskaldji, D.-E.; Yendiki, A.; Vangel, M.; Santangelo, S.L.; Manoach, D.S. Diffusion-Weighted Imaging Evidence of Altered White Matter Development from Late Childhood to Early Adulthood in Autism Spectrum Disorder. *NeuroImage Clin.* **2018**, *19*, 840–847, doi:10.1016/j.nicl.2018.06.002.
114. Courchesne, E.; Pierce, K. Brain Overgrowth in Autism during a Critical Time in Development: Implications for Frontal Pyramidal Neuron and Interneuron Development and Connectivity. *Int. J. Dev. Neurosci. Off. J. Int. Soc. Dev. Neurosci.* **2005**, *23*, 153–170, doi:10.1016/j.ijdevneu.2005.01.003.
115. Matta, S.M.; Hill-Yardin, E.L.; Crack, P.J. The Influence of Neuroinflammation in Autism Spectrum Disorder. *Brain. Behav. Immun.* **2019**, *79*, 75–90, doi:10.1016/j.bbi.2019.04.037.
116. Voineagu, I.; Wang, X.; Johnston, P.; Lowe, J.K.; Tian, Y.; Horvath, S.; Mill, J.; Cantor, R.M.; Blencowe, B.J.; Geschwind, D.H. Transcriptomic Analysis of Autistic Brain Reveals Convergent Molecular Pathology. *Nature* **2011**, *474*, 380–384, doi:10.1038/nature10110.
117. Casanova, M.F.; El-Baz, A.; Vanbogaert, E.; Narahari, P.; Switala, A. A Topographic Study of Minicolumnar Core Width by Lamina Comparison between Autistic Subjects and Controls: Possible Minicolumnar Disruption Due to an Anatomical Element in-Common to Multiple Laminae. *Brain Pathol. Zurich Switz.* **2010**, *20*, 451–458, doi:10.1111/j.1750-3639.2009.00319.x.
118. McKavanagh, R.; Buckley, E.; Chance, S.A. Wider Minicolumns in Autism: A Neural Basis for Altered Processing? *Brain J. Neurol.* **2015**, *138*, 2034–2045, doi:10.1093/brain/awv110.
119. Perry, D.W.; Marston, G.M.; Hinder, S.A.; Munden, A.C.; Roy, A. The Phenomenology of Depressive Illness in People with a Learning Disability and Autism. *Autism Int. J. Res. Pract.* **2001**, *5*, 265–275, doi:10.1177/1362361301005003004.
120. Lee, M.; Martin-Ruiz, C.; Graham, A.; Court, J.; Jaros, E.; Perry, R.; Iversen, P.; Bauman, M.; Perry, E. Nicotinic Receptor Abnormalities in the Cerebellar Cortex in Autism. *Brain J. Neurol.* **2002**, *125*, 1483–1495, doi:10.1093/brain/awf160.
121. Fatemi, S.H.; Reutiman, T.J.; Folsom, T.D.; Thuras, P.D. GABA(A) Receptor Downregulation in Brains of Subjects with Autism. *J. Autism Dev. Disord.* **2009**, *39*, 223–230, doi:10.1007/s10803-008-0646-7.
122. Oblak, A.; Gibbs, T.T.; Blatt, G.J. Decreased GABAA Receptors and Benzodiazepine Binding Sites in the Anterior Cingulate Cortex in Autism. *Autism Res. Off. J. Int. Soc. Autism Res.* **2009**, *2*, 205–219, doi:10.1002/aur.88.
123. Purcell, A.E.; Jeon, O.H.; Zimmerman, A.W.; Blue, M.E.; Pevsner, J. Postmortem Brain Abnormalities of the Glutamate Neurotransmitter System in Autism. *Neurology* **2001**, *57*, 1618–1628, doi:10.1212/wnl.57.9.1618.
124. Fatemi, S.H.; Folsom, T.D. The Role of Fragile X Mental Retardation Protein in Major Mental Disorders. *Neuropharmacology* **2011**, *60*, 1221–1226, doi:10.1016/j.neuropharm.2010.11.011.
125. Ajram, L.A.; Pereira, A.C.; Durieux, A.M.S.; Velthuis, H.E.; Petrinovic, M.M.; McAlonan, G.M. The Contribution of [1H] Magnetic Resonance Spectroscopy to the Study of Excitation-Inhibition in Autism. *Prog. Neuropsychopharmacol. Biol. Psychiatry* **2019**, *89*, 236–244, doi:10.1016/j.pnpbp.2018.09.010.
126. Hegarty, J.P.; Zamzow, R.M.; Ferguson, B.J.; Christ, S.E.; Porges, E.C.; Johnson, J.D.; Beversdorf, D.Q. Beta-Adrenergic Antagonism Alters Functional Connectivity during Associative Processing in a Preliminary Study of Individuals with and without Autism. *Autism Int. J. Res. Pract.* **2020**, *24*, 795–801, doi:10.1177/1362361319868633.
127. Port, R.G.; Oberman, L.M.; Roberts, T.P. Revisiting the Excitation/Inhibition Imbalance Hypothesis of ASD through a Clinical Lens. *Br. J. Radiol.* **2019**, *92*, 20180944, doi:10.1259/bjr.20180944.
128. Bozzi, Y.; Provenzano, G.; Casarosa, S. Neurobiological Bases of Autism-Epilepsy Comorbidity: A Focus on Excitation/Inhibition Imbalance. *Eur. J. Neurosci.* **2018**, *47*, 534–548, doi:10.1111/ejn.13595.
129. de la Torre-Ubieta, L.; Won, H.; Stein, J.L.; Geschwind, D.H. Advancing the Understanding of Autism Disease Mechanisms through Genetics. *Nat. Med.* **2016**, *22*, 345–361, doi:10.1038/nm.4071.
130. Bourgeron, T. From the Genetic Architecture to Synaptic Plasticity in Autism Spectrum Disorder. *Nat. Rev. Neurosci.* **2015**, *16*, 551–563, doi:10.1038/nrn3992.
131. Kaizuka, T.; Takumi, T. Postsynaptic Density Proteins and Their Involvement in Neurodevelopmental Disorders. *J. Biochem. (Tokyo)* **2018**, *163*, 447–455, doi:10.1093/jb/mvy022.
132. Ebert, D.H.; Greenberg, M.E. Activity-Dependent Neuronal Signalling and Autism Spectrum Disorder. *Nature* **2013**, *493*, 327–337, doi:10.1038/nature11860.

133. Spooren, W.; Lindemann, L.; Ghosh, A.; Santarelli, L. Synapse Dysfunction in Autism: A Molecular Medicine Approach to Drug Discovery in Neurodevelopmental Disorders. *Trends Pharmacol. Sci.* **2012**, *33*, 669–684, doi:10.1016/j.tips.2012.09.004.
134. Jęško, H.; Cieślak, M.; Gromadzka, G.; Adamczyk, A. Dysfunctional Proteins in Neuropsychiatric Disorders: From Neurodegeneration to Autism Spectrum Disorders. *Neurochem. Int.* **2020**, *141*, 104853, doi:10.1016/j.neuint.2020.104853.
135. De Rubeis, S.; He, X.; Goldberg, A.P.; Poultney, C.S.; Samocha, K.; Cicek, A.E.; Kou, Y.; Liu, L.; Fromer, M.; Walker, S.; et al. Synaptic, Transcriptional and Chromatin Genes Disrupted in Autism. *Nature* **2014**, *515*, 209–215, doi:10.1038/nature13772.
136. Feyder, M.; Karlsson, R.-M.; Mathur, P.; Lyman, M.; Bock, R.; Momenan, R.; Munasinghe, J.; Scattoni, M.L.; Ihne, J.; Camp, M.; et al. Association of Mouse Dlg4 (PSD-95) Gene Deletion and Human DLG4 Gene Variation with Phenotypes Relevant to Autism Spectrum Disorders and Williams' Syndrome. *Am. J. Psychiatry* **2010**, *167*, 1508–1517, doi:10.1176/appi.ajp.2010.10040484.
137. State, M.W.; Levitt, P. The Conundrums of Understanding Genetic Risks for Autism Spectrum Disorders. *Nat. Neurosci.* **2011**, *14*, 1499–1506, doi:10.1038/nn.2924.
138. Nelson, A.D.; Bender, K.J. Dendritic Integration Dysfunction in Neurodevelopmental Disorders. *Dev. Neurosci.* **2021**, *43*, 201–221, doi:10.1159/000516657.
139. Percy, A.K. Rett Syndrome. Current Status and New Vistas. *Neurol. Clin.* **2002**, *20*, 1125–1141.
140. Moog, U.; Smeets, E.E.J.; van Roozendaal, K.E.P.; Schoenmakers, S.; Herbergs, J.; Schoonbrood-Lenssen, A.M.J.; Schrandt-Stumpel, C.T.R.M. Neurodevelopmental Disorders in Males Related to the Gene Causing Rett Syndrome in Females (MECP2). *Eur. J. Paediatr. Neurol. EJPN Off. J. Eur. Paediatr. Neurol. Soc.* **2003**, *7*, 5–12, doi:10.1016/s1090-3798(02)00134-4.
141. Bienvenu, T.; Carrié, A.; de Roux, N.; Vinet, M.C.; Jonveaux, P.; Couvert, P.; Villard, L.; Arzimanoglou, A.; Beldjord, C.; Fontes, M.; et al. MECP2 Mutations Account for Most Cases of Typical Forms of Rett Syndrome. *Hum. Mol. Genet.* **2000**, *9*, 1377–1384, doi:10.1093/hmg/9.9.1377.
142. Hagberg, B. Clinical Manifestations and Stages of Rett Syndrome. *Ment. Retard. Dev. Disabil. Res. Rev.* **2002**, *8*, 61–65, doi:10.1002/mrdd.10020.
143. Trevathan, E.; Naidu, S. The Clinical Recognition and Differential Diagnosis of Rett Syndrome. *J. Child Neurol.* **1988**, *3 Suppl*, S6-16.
144. Steffenburg, U.; Hagberg, G.; Hagberg, B. Epilepsy in a Representative Series of Rett Syndrome. *Acta Paediatr. Oslo Nor. 1992* **2001**, *90*, 34–39.
145. Stettner, G.M.; Huppke, P.; Brendel, C.; Richter, D.W.; Gärtner, J.; Dutschmann, M. Breathing Dysfunctions Associated with Impaired Control of Postinspiratory Activity in Mecp2-/- Knockout Mice. *J. Physiol.* **2007**, *579*, 863–876, doi:10.1113/jphysiol.2006.119966.
146. Tarquinio, D.C.; Hou, W.; Neul, J.L.; Kaufmann, W.E.; Glaze, D.G.; Motil, K.J.; Skinner, S.A.; Lee, H.-S.; Percy, A.K. The Changing Face of Survival in Rett Syndrome and MECP2-Related Disorders. *Pediatr. Neurol.* **2015**, *53*, 402–411, doi:10.1016/j.pediatrneurol.2015.06.003.
147. Neul, J.L.; Lane, J.B.; Lee, H.-S.; Geerts, S.; Barrish, J.O.; Annese, F.; Baggett, L.M.; Barnes, K.; Skinner, S.A.; Motil, K.J.; et al. Developmental Delay in Rett Syndrome: Data from the Natural History Study. *J. Neurodev. Disord.* **2014**, *6*, 20, doi:10.1186/1866-1955-6-20.
148. Neul, J.L.; Kaufmann, W.E.; Glaze, D.G.; Christodoulou, J.; Clarke, A.J.; Bahi-Buisson, N.; Leonard, H.; Bailey, M.E.S.; Schanen, N.C.; Zappella, M.; et al. Rett Syndrome: Revised Diagnostic Criteria and Nomenclature. *Ann. Neurol.* **2010**, *68*, 944–950, doi:10.1002/ana.22124.
149. Banerjee, A.; Miller, M.T.; Li, K.; Sur, M.; Kaufmann, W.E. Towards a Better Diagnosis and Treatment of Rett Syndrome: A Model Synaptic Disorder. *Brain J. Neurol.* **2019**, *142*, 239–248, doi:10.1093/brain/awy323.
150. Vashi, N.; Justice, M.J. Treating Rett Syndrome: From Mouse Models to Human Therapies. *Mamm. Genome Off. J. Int. Mamm. Genome Soc.* **2019**, *30*, 90–110, doi:10.1007/s00335-019-09793-5.
151. Weaving, L.S.; Ellaway, C.J.; Gécz, J.; Christodoulou, J. Rett Syndrome: Clinical Review and Genetic Update. *J. Med. Genet.* **2005**, *42*, 1–7, doi:10.1136/jmg.2004.027730.
152. Kishi, N.; Macklis, J.D. MECP2 Is Progressively Expressed in Post-Migratory Neurons and Is Involved in Neuronal Maturation Rather than Cell Fate Decisions. *Mol. Cell. Neurosci.* **2004**, *27*, 306–321, doi:10.1016/j.mcn.2004.07.006.
153. Durand, T.; De Felice, C.; Signorini, C.; Oger, C.; Bultel-Poncé, V.; Guy, A.; Galano, J.-M.; Leoncini, S.; Ciccoli, L.; Pecorelli, A.; et al. F(2)-Dihomo-Isoprostanol and Brain White Matter Damage in Stage 1 Rett Syndrome.

*Biochimie* **2013**, *95*, 86–90, doi:10.1016/j.biochi.2012.09.017.

154. Sceniak, M.P.; Lang, M.; Enomoto, A.C.; James Howell, C.; Hermes, D.J.; Katz, D.M. Mechanisms of Functional Hypoconnectivity in the Medial Prefrontal Cortex of *Mecp2* Null Mice. *Cereb. Cortex N. Y. N 1991* **2016**, *26*, 1938–1956, doi:10.1093/cercor/bhv002.

155. Chahil, G.; Bollu, P.C. Rett Syndrome. In *StatPearls*; StatPearls Publishing: Treasure Island (FL), 2018.

156. Nakai, N.; Takumi, T.; Nakai, J.; Sato, M. Common Defects of Spine Dynamics and Circuit Function in Neurodevelopmental Disorders: A Systematic Review of Findings From in Vivo Optical Imaging of Mouse Models. *Front. Neurosci.* **2018**, *12*, 412, doi:10.3389/fnins.2018.00412.

157. Landucci, E.; Brindisi, M.; Bianciardi, L.; Catania, L.M.; Daga, S.; Croci, S.; Frullanti, E.; Fallerini, C.; Butini, S.; Brogi, S.; et al. IPSC-Derived Neurons Profiling Reveals GABAergic Circuit Disruption and Acetylated  $\alpha$ -Tubulin Defect Which Improves after IHDAC6 Treatment in Rett Syndrome. *Exp. Cell Res.* **2018**, *368*, 225–235, doi:10.1016/j.yexcr.2018.05.001.

158. Dani, V.S.; Chang, Q.; Maffei, A.; Turrigiano, G.G.; Jaenisch, R.; Nelson, S.B. Reduced Cortical Activity Due to a Shift in the Balance between Excitation and Inhibition in a Mouse Model of Rett Syndrome. *Proc. Natl. Acad. Sci. U. S. A.* **2005**, *102*, 12560–12565, doi:10.1073/pnas.0506071102.

159. Meng, X.; Wang, W.; Lu, H.; He, L.-J.; Chen, W.; Chao, E.S.; Fiorotto, M.L.; Tang, B.; Herrera, J.A.; Seymour, M.L.; et al. Manipulations of MeCP2 in Glutamatergic Neurons Highlight Their Contributions to Rett and Other Neurological Disorders. *eLife* **2016**, *5*, doi:10.7554/eLife.14199.

160. Ure, K.; Lu, H.; Wang, W.; Ito-Ishida, A.; Wu, Z.; He, L.-J.; Sztainberg, Y.; Chen, W.; Tang, J.; Zoghbi, H.Y. Restoration of *Mecp2* Expression in GABAergic Neurons Is Sufficient to Rescue Multiple Disease Features in a Mouse Model of Rett Syndrome. *eLife* **2016**, *5*, doi:10.7554/eLife.14198.

161. Ogier, M.; Katz, D.M. Breathing Dysfunction in Rett Syndrome: Understanding Epigenetic Regulation of the Respiratory Network. *Respir. Physiol. Neurobiol.* **2008**, *164*, 55–63, doi:10.1016/j.resp.2008.04.005.

162. Medrihan, L.; Tantalaki, E.; Aramuni, G.; Sargsyan, V.; Dudanova, I.; Missler, M.; Zhang, W. Early Defects of GABAergic Synapses in the Brain Stem of a MeCP2 Mouse Model of Rett Syndrome. *J. Neurophysiol.* **2008**, *99*, 112–121, doi:10.1152/jn.00826.2007.

163. Ramirez, J.-M.; Ward, C.S.; Neul, J.L. Breathing Challenges in Rett Syndrome: Lessons Learned from Humans and Animal Models. *Respir. Physiol. Neurobiol.* **2013**, *189*, 280–287, doi:10.1016/j.resp.2013.06.022.

164. Viemari, J.-C.; Roux, J.-C.; Tryba, A.K.; Saywell, V.; Burnet, H.; Peña, F.; Zanella, S.; Bévingut, M.; Barthelemy-Requin, M.; Herzing, L.B.K.; et al. *Mecp2* Deficiency Disrupts Norepinephrine and Respiratory Systems in Mice. *J. Neurosci. Off. J. Soc. Neurosci.* **2005**, *25*, 11521–11530, doi:10.1523/JNEUROSCI.4373-05.2005.

165. Roux, J.-C.; Dura, E.; Villard, L. Tyrosine Hydroxylase Deficit in the Chemoafferent and the Sympathoadrenergic Pathways of the *Mecp2* Deficient Mouse. *Neurosci. Lett.* **2008**, *447*, 82–86, doi:10.1016/j.neulet.2008.09.045.

166. Chapleau, C.A.; Calfa, G.D.; Lane, M.C.; Albertson, A.J.; Larimore, J.L.; Kudo, S.; Armstrong, D.L.; Percy, A.K.; Pozzo-Miller, L. Dendritic Spine Pathologies in Hippocampal Pyramidal Neurons from Rett Syndrome Brain and after Expression of Rett-Associated MECP2 Mutations. *Neurobiol. Dis.* **2009**, *35*, 219–233, doi:10.1016/j.nbd.2009.05.001.

167. Madaan, M.; Mendez, M.D. Angelman Syndrome. In *StatPearls*; StatPearls Publishing: Treasure Island (FL), 2022.

168. Vu, T.H.; Hoffman, A.R. Imprinting of the Angelman Syndrome Gene, UBE3A, Is Restricted to Brain. *Nat. Genet.* **1997**, *17*, 12–13, doi:10.1038/ng0997-12.

169. Buiting, K.; Clayton-Smith, J.; Driscoll, D.J.; Gillissen-Kaesbach, G.; Kanber, D.; Schwinger, E.; Williams, C.; Horsthemke, B. Clinical Utility Gene Card for: Angelman Syndrome. *Eur. J. Hum. Genet. EJHG* **2015**, *23*, doi:10.1038/ejhg.2014.93.

170. Williams, C.A. The Behavioral Phenotype of the Angelman Syndrome. *Am. J. Med. Genet. C Semin. Med. Genet.* **2010**, *154C*, 432–437, doi:10.1002/ajmg.c.30278.

171. Williams, C.A.; Beaudet, A.L.; Clayton-Smith, J.; Knoll, J.H.; Kyllerman, M.; Laan, L.A.; Magenis, R.E.; Moncla, A.; Schinzel, A.A.; Summers, J.A.; et al. Angelman Syndrome 2005: Updated Consensus for Diagnostic Criteria. *Am. J. Med. Genet. A.* **2006**, *140*, 413–418, doi:10.1002/ajmg.a.31074.

172. Bindels-de Heus, K.G.C.B.; Mous, S.E.; Ten Hooven-Radstaake, M.; van Iperen-Kolk, B.M.; Navis, C.; Rietman, A.B.; Ten Hoopen, L.W.; Brooks, A.S.; ENCORE Expertise Center for AS; Elgersma, Y.; et al. An Overview of Health Issues and Development in a Large Clinical Cohort of Children with Angelman Syndrome. *Am. J. Med. Genet. A.* **2020**, *182*, 53–63, doi:10.1002/ajmg.a.61382.

173. Buiting, K.; Williams, C.; Horsthemke, B. Angelman Syndrome - Insights into a Rare Neurogenetic Disorder. *Nat. Rev. Neurol.* **2016**, *12*, 584–593, doi:10.1038/nrneuro.2016.133.
174. Bird, L.M. Angelman Syndrome: Review of Clinical and Molecular Aspects. *Appl. Clin. Genet.* **2014**, *7*, 93–104, doi:10.2147/TACG.S57386.
175. Kim, H.; Kunz, P.A.; Mooney, R.; Philpot, B.D.; Smith, S.L. Maternal Loss of Ube3a Impairs Experience-Driven Dendritic Spine Maintenance in the Developing Visual Cortex. *J. Neurosci. Off. J. Soc. Neurosci.* **2016**, *36*, 4888–4894, doi:10.1523/JNEUROSCI.4204-15.2016.
176. Yashiro, K.; Riday, T.T.; Condon, K.H.; Roberts, A.C.; Bernardo, D.R.; Prakash, R.; Weinberg, R.J.; Ehlers, M.D.; Philpot, B.D. Ube3a Is Required for Experience-Dependent Maturation of the Neocortex. *Nat. Neurosci.* **2009**, *12*, 777–783, doi:10.1038/nn.2327.
177. Koyavski, L.; Panov, J.; Simchi, L.; Rayi, P.R.; Sharvit, L.; Feuermann, Y.; Kaphzan, H. Sex-Dependent Sensory Phenotypes and Related Transcriptomic Expression Profiles Are Differentially Affected by Angelman Syndrome. *Mol. Neurobiol.* **2019**, *56*, 5998–6016, doi:10.1007/s12035-019-1503-8.
178. Kim, H.; Kunz, P.A.; Mooney, R.; Philpot, B.D.; Smith, S.L. Maternal Loss of Ube3a Impairs Experience-Driven Dendritic Spine Maintenance in the Developing Visual Cortex. *J. Neurosci. Off. J. Soc. Neurosci.* **2016**, *36*, 4888–4894, doi:10.1523/JNEUROSCI.4204-15.2016.
179. Wallace, M.L.; van Woerden, G.M.; Elgersma, Y.; Smith, S.L.; Philpot, B.D. Ube3a Loss Increases Excitability and Blunts Orientation Tuning in the Visual Cortex of Angelman Syndrome Model Mice. *J. Neurophysiol.* **2017**, *118*, 634–646, doi:10.1152/jn.00618.2016.
180. Zylka, M.J. Prenatal Treatment Path for Angelman Syndrome and Other Neurodevelopmental Disorders. *Autism Res. Off. J. Int. Soc. Autism Res.* **2020**, *13*, 11–17, doi:10.1002/aur.2203.
181. Tan, W.-H.; Bird, L.M. Angelman Syndrome: Current and Emerging Therapies in 2016. *Am. J. Med. Genet. C Semin. Med. Genet.* **2016**, *172*, 384–401, doi:10.1002/ajmg.c.31536.
182. Akhtar, A.; Andleeb, A.; Waris, T.S.; Bazzar, M.; Moradi, A.-R.; Awan, N.R.; Yar, M. Neurodegenerative Diseases and Effective Drug Delivery: A Review of Challenges and Novel Therapeutics. *J. Control. Release Off. J. Control. Release Soc.* **2021**, *330*, 1152–1167, doi:10.1016/j.jconrel.2020.11.021.
183. Przedborski, S.; Vila, M.; Jackson-Lewis, V. Neurodegeneration: What Is It and Where Are We? *J. Clin. Invest.* **2003**, *111*, 3–10, doi:10.1172/JCI17522.
184. Shrivastava, A.N.; Aperia, A.; Melki, R.; Triller, A. Physico-Pathologic Mechanisms Involved in Neurodegeneration: Misfolded Protein-Plasma Membrane Interactions. *Neuron* **2017**, *95*, 33–50, doi:10.1016/j.neuron.2017.05.026.
185. Lashuel, H.A.; Overk, C.R.; Oueslati, A.; Masliah, E. The Many Faces of  $\alpha$ -Synuclein: From Structure and Toxicity to Therapeutic Target. *Nat. Rev. Neurosci.* **2013**, *14*, 38–48, doi:10.1038/nrn3406.
186. Goedert, M. The Significance of Tau and Alpha-Synuclein Inclusions in Neurodegenerative Diseases. *Curr. Opin. Genet. Dev.* **2001**, *11*, 343–351, doi:10.1016/s0959-437x(00)00200-8.
187. Tyebji, S.; Hannan, A.J. Synaptopathic Mechanisms of Neurodegeneration and Dementia: Insights from Huntington's Disease. *Prog. Neurobiol.* **2017**, *153*, 18–45, doi:10.1016/j.pneurobio.2017.03.008.
188. Wang, Y.-C.; Lauwers, E.; Verstreken, P. Presynaptic Protein Homeostasis and Neuronal Function. *Curr. Opin. Genet. Dev.* **2017**, *44*, 38–46, doi:10.1016/j.gde.2017.01.015.
189. Olivero, P.; Lozano, C.; Sotomayor-Zárate, R.; Meza-Concha, N.; Arancibia, M.; Córdova, C.; González-Arriagada, W.; Ramírez-Barrantes, R.; Marchant, I. Proteostasis and Mitochondrial Role on Psychiatric and Neurodegenerative Disorders: Current Perspectives. *Neural Plast.* **2018**, *2018*, 6798712, doi:10.1155/2018/6798712.
190. Klaipts, C.L.; Jayaraj, G.G.; Hartl, F.U. Pathways of Cellular Proteostasis in Aging and Disease. *J. Cell Biol.* **2018**, *217*, 51–63, doi:10.1083/jcb.201709072.
191. Colpo, G.D.; Ribeiro, F.M.; Rocha, N.P.; Teixeira, A.L. Chapter 42 - Animal Models for the Study of Human Neurodegenerative Diseases. In *Animal Models for the Study of Human Disease (Second Edition)*; Conn, P.M., Ed.; Academic Press, 2017; pp. 1109–1129 ISBN 978-0-12-809468-6.
192. Cui, H.; Hayashi, A.; Sun, H.-S.; Belmares, M.P.; Cobey, C.; Phan, T.; Schweizer, J.; Salter, M.W.; Wang, Y.T.; Tasker, R.A.; et al. PDZ Protein Interactions Underlying NMDA Receptor-Mediated Excitotoxicity and Neuroprotection by PSD-95 Inhibitors. *J. Neurosci. Off. J. Soc. Neurosci.* **2007**, *27*, 9901–9915, doi:10.1523/JNEUROSCI.1464-07.2007.
193. Hill, M.D.; Goyal, M.; Menon, B.K.; Nogueira, R.G.; McTaggart, R.A.; Demchuk, A.M.; Poppe, A.Y.; Buck, B.H.; Field, T.S.; Dowlatsahi, D.; et al. Efficacy and Safety of Nerinetide for the Treatment of Acute Ischaemic Stroke (ESCAPE-NA1): A Multicentre, Double-Blind, Randomised Controlled Trial. *Lancet Lond. Engl.* **2020**, *395*, 878–887,

doi:10.1016/S0140-6736(20)30258-0.

194. Gardoni, F.; Sgobio, C.; Pendolino, V.; Calabresi, P.; Di Luca, M.; Picconi, B. Targeting NR2A-Containing NMDA Receptors Reduces L-DOPA-Induced Dyskinesias. *Neurobiol. Aging* **2012**, *33*, 2138–2144, doi:10.1016/j.neurobiolaging.2011.06.019.

195. Kaur, D.; Behl, T.; Sehgal, A.; Singh, S.; Sharma, N.; Bungau, S. Multifaceted Alzheimer's Disease: Building a Roadmap for Advancement of Novel Therapies. *Neurochem. Res.* **2021**, *46*, 2832–2851, doi:10.1007/s11064-021-03415-w.

196. Ju, Y.; Tam, K.Y. Pathological Mechanisms and Therapeutic Strategies for Alzheimer's Disease. *Neural Regen. Res.* **2022**, *17*, 543–549, doi:10.4103/1673-5374.320970.

197. Nelson, P.T.; Braak, H.; Markesbery, W.R. Neuropathology and Cognitive Impairment in Alzheimer Disease: A Complex but Coherent Relationship. *J. Neuropathol. Exp. Neurol.* **2009**, *68*, 1–14, doi:10.1097/NEN.0b013e3181919a48.

198. Porsteinsson, A.P.; Isaacson, R.S.; Knox, S.; Sabbagh, M.N.; Rubino, I. Diagnosis of Early Alzheimer's Disease: Clinical Practice in 2021. *J. Prev. Alzheimers Dis.* **2021**, *8*, 371–386, doi:10.14283/jpad.2021.23.

199. Iacono, D.; O'Brien, R.; Resnick, S.M.; Zonderman, A.B.; Pletnikova, O.; Rudow, G.; An, Y.; West, M.J.; Crain, B.; Troncoso, J.C. Neuronal Hypertrophy in Asymptomatic Alzheimer Disease. *J. Neuropathol. Exp. Neurol.* **2008**, *67*, 578–589, doi:10.1097/NEN.0b013e3181772794.

200. Driscoll, I.; Troncoso, J. Asymptomatic Alzheimer's Disease: A Prodrome or a State of Resilience? *Curr. Alzheimer Res.* **2011**, *8*, 330–335, doi:10.2174/156720511795745348.

201. FINDER, V.H.; GLOCKSHUBER, R. Amyloid-Beta Aggregation. *Neurodegener. Dis.* **2007**, *4*, 13–27, doi:10.1159/000100355.

202. Blanchard, J.W.; Victor, M.B.; Tsai, L.-H. Dissecting the Complexities of Alzheimer Disease with in Vitro Models of the Human Brain. *Nat. Rev. Neurol.* **2022**, *18*, 25–39, doi:10.1038/s41582-021-00578-6.

203. Ibanez, L.; Cruchaga, C.; Fernández, M.V. Advances in Genetic and Molecular Understanding of Alzheimer's Disease. *Genes* **2021**, *12*, 1247, doi:10.3390/genes12081247.

204. Perl, D.P. Neuropathology of Alzheimer's Disease. *Mt. Sinai J. Med. N. Y.* **2010**, *77*, 32–42, doi:10.1002/msj.20157.

205. Fein, J.A.; Sokolow, S.; Miller, C.A.; Vinters, H.V.; Yang, F.; Cole, G.M.; Gyllys, K.H. Co-Localization of Amyloid Beta and Tau Pathology in Alzheimer's Disease Synaptosomes. *Am. J. Pathol.* **2008**, *172*, 1683–1692, doi:10.2353/ajpath.2008.070829.

206. Ittner, L.M.; Götz, J. Amyloid- $\beta$  and Tau—a Toxic Pas de Deux in Alzheimer's Disease. *Nat. Rev. Neurosci.* **2011**, *12*, 65–72, doi:10.1038/nrn2967.

207. Wu, M.; Zhang, M.; Yin, X.; Chen, K.; Hu, Z.; Zhou, Q.; Cao, X.; Chen, Z.; Liu, D. The Role of Pathological Tau in Synaptic Dysfunction in Alzheimer's Diseases. *Transl. Neurodegener.* **2021**, *10*, 45, doi:10.1186/s40035-021-00270-1.

208. Haass, C.; Selkoe, D.J. Soluble Protein Oligomers in Neurodegeneration: Lessons from the Alzheimer's Amyloid Beta-Peptide. *Nat. Rev. Mol. Cell Biol.* **2007**, *8*, 101–112, doi:10.1038/nrm2101.

209. Holtzman, D.M.; Morris, J.C.; Goate, A.M. Alzheimer's Disease: The Challenge of the Second Century. *Sci. Transl. Med.* **2011**, *3*, 77sr1, doi:10.1126/scitranslmed.3002369.

210. Haass, C.; Willem, M. Secreted APP Modulates Synaptic Activity: A Novel Target for Therapeutic Intervention? *Neuron* **2019**, *101*, 557–559, doi:10.1016/j.neuron.2019.01.058.

211. Thinakaran, G.; Koo, E.H. Amyloid Precursor Protein Trafficking, Processing, and Function. *J. Biol. Chem.* **2008**, *283*, 29615–29619, doi:10.1074/jbc.R800019200.

212. Cirrito, J.R.; Yamada, K.A.; Finn, M.B.; Sloviter, R.S.; Bales, K.R.; May, P.C.; Schoepp, D.D.; Paul, S.M.; Mennerick, S.; Holtzman, D.M. Synaptic Activity Regulates Interstitial Fluid Amyloid-Beta Levels in Vivo. *Neuron* **2005**, *48*, 913–922, doi:10.1016/j.neuron.2005.10.028.

213. Grothe, M.; Heinsen, H.; Teipel, S. Longitudinal Measures of Cholinergic Forebrain Atrophy in the Transition from Healthy Aging to Alzheimer's Disease. *Neurobiol. Aging* **2013**, *34*, 1210–1220, doi:10.1016/j.neurobiolaging.2012.10.018.

214. Xu, Y.; Zhao, M.; Han, Y.; Zhang, H. GABAergic Inhibitory Interneuron Deficits in Alzheimer's Disease: Implications for Treatment. *Front. Neurosci.* **2020**, *14*, 660, doi:10.3389/fnins.2020.00660.

215. Rudy, J.W. Variation in the Persistence of Memory: An Interplay between Actin Dynamics and AMPA Receptors. *Brain Res.* **2015**, *1621*, 29–37, doi:10.1016/j.brainres.2014.12.009.

216. Guerrero-Muñoz, M.J.; Gerson, J.; Castillo-Carranza, D.L. Tau Oligomers: The Toxic Player at Synapses in

- Alzheimer's Disease. *Front. Cell. Neurosci.* **2015**, *9*, 464, doi:10.3389/fncel.2015.00464.
217. Cargnello, M.; Roux, P.P. Activation and Function of the MAPKs and Their Substrates, the MAPK-Activated Protein Kinases. *Microbiol. Mol. Biol. Rev. MMBR* **2011**, *75*, 50–83, doi:10.1128/MMBR.00031-10.
218. Boulton, T.G.; Yancopoulos, G.D.; Gregory, J.S.; Slaughter, C.; Moomaw, C.; Hsu, J.; Cobb, M.H. An Insulin-Stimulated Protein Kinase Similar to Yeast Kinases Involved in Cell Cycle Control. *Science* **1990**, *249*, 64–67, doi:10.1126/science.2164259.
219. Yan, L.; Carr, J.; Ashby, P.R.; Murry-Tait, V.; Thompson, C.; Arthur, J.S.C. Knockout of ERK5 Causes Multiple Defects in Placental and Embryonic Development. *BMC Dev. Biol.* **2003**, *3*, 11, doi:10.1186/1471-213X-3-11.
220. Jiang, Y.; Chen, C.; Li, Z.; Guo, W.; Gegner, J.A.; Lin, S.; Han, J. Characterization of the Structure and Function of a New Mitogen-Activated Protein Kinase (P38beta). *J. Biol. Chem.* **1996**, *271*, 17920–17926, doi:10.1074/jbc.271.30.17920.
221. Cuadrado, A.; Nebreda, A.R. Mechanisms and Functions of P38 MAPK Signalling. *Biochem. J.* **2010**, *429*, 403–417, doi:10.1042/BJ20100323.
222. Krishna, M.; Narang, H. The Complexity of Mitogen-Activated Protein Kinases (MAPKs) Made Simple. *Cell. Mol. Life Sci. CMLS* **2008**, *65*, 3525–3544, doi:10.1007/s00018-008-8170-7.
223. Antoniou, X.; Borsello, T. The JNK Signalling Transduction Pathway in the Brain. *Front. Biosci. Elite Ed.* **2012**, *4*, 2110–2120, doi:10.2741/528.
224. Coffey, E.T. Nuclear and Cytosolic JNK Signalling in Neurons. *Nat. Rev. Neurosci.* **2014**, *15*, 285–299, doi:10.1038/nrn3729.
225. Chang, L.; Karin, M. Mammalian MAP Kinase Signalling Cascades. *Nature* **2001**, *410*, 37–40, doi:10.1038/35065000.
226. Kyriakis, J.M.; Avruch, J. Mammalian Mitogen-Activated Protein Kinase Signal Transduction Pathways Activated by Stress and Inflammation. *Physiol. Rev.* **2001**, *81*, 807–869, doi:10.1152/physrev.2001.81.2.807.
227. Urano, F.; Wang, X.; Bertolotti, A.; Zhang, Y.; Chung, P.; Harding, H.P.; Ron, D. Coupling of Stress in the ER to Activation of JNK Protein Kinases by Transmembrane Protein Kinase IRE1. *Science* **2000**, *287*, 664–666, doi:10.1126/science.287.5453.664.
228. Fleming, Y.; Armstrong, C.G.; Morrice, N.; Paterson, A.; Goedert, M.; Cohen, P. Synergistic Activation of Stress-Activated Protein Kinase 1/c-Jun N-Terminal Kinase (SAPK1/JNK) Isoforms by Mitogen-Activated Protein Kinase Kinase 4 (MKK4) and MKK7. *Biochem. J.* **2000**, *352 Pt 1*, 145–154.
229. Manning, A.M.; Davis, R.J. Targeting JNK for Therapeutic Benefit: From Junk to Gold? *Nat. Rev. Drug Discov.* **2003**, *2*, 554–565, doi:10.1038/nrd1132.
230. Lee, H.W.; Choi, H.Y.; Joo, K.M.; Nam, D.-H. Tumor Progression Locus 2 (Tpl2) Kinase as a Novel Therapeutic Target for Cancer: Double-Sided Effects of Tpl2 on Cancer. *Int. J. Mol. Sci.* **2015**, *16*, 4471–4491, doi:10.3390/ijms16034471.
231. Tanoue, T.; Nishida, E. Docking Interactions in the Mitogen-Activated Protein Kinase Cascades. *Pharmacol. Ther.* **2002**, *93*, 193–202, doi:10.1016/S0163-7258(02)00188-2.
232. López, J.M. Digital Kinases: A Cell Model for Sensing, Integrating and Making Choices. *Commun. Integr. Biol.* **2010**, *3*, 146–150, doi:10.4161/cib.3.2.10365.
233. Bagowski, C.P.; Besser, J.; Frey, C.R.; Ferrell, J.E. The JNK Cascade as a Biochemical Switch in Mammalian Cells: Ultrasensitive and All-or-None Responses. *Curr. Biol. CB* **2003**, *13*, 315–320, doi:10.1016/s0960-9822(03)00083-6.
234. Waetzig, V.; Zhao, Y.; Herdegen, T. The Bright Side of JNKs-Multitalented Mediators in Neuronal Sprouting, Brain Development and Nerve Fiber Regeneration. *Prog. Neurobiol.* **2006**, *80*, 84–97, doi:10.1016/j.pneurobio.2006.08.002.
235. Zhao, Y.; Herdegen, T. Cerebral Ischemia Provokes a Profound Exchange of Activated JNK Isoforms in Brain Mitochondria. *Mol. Cell. Neurosci.* **2009**, *41*, 186–195, doi:10.1016/j.mcn.2009.02.012.
236. Zhao, Y.; Spigolon, G.; Bonny, C.; Culman, J.; Vercelli, A.; Herdegen, T. The JNK Inhibitor D-JNKI-1 Blocks Apoptotic JNK Signaling in Brain Mitochondria. *Mol. Cell. Neurosci.* **2012**, *49*, 300–310, doi:10.1016/j.mcn.2011.12.005.
237. Harris, C.A.; Johnson, E.M. BH3-Only Bcl-2 Family Members Are Coordinately Regulated by the JNK Pathway and Require Bax to Induce Apoptosis in Neurons. *J. Biol. Chem.* **2001**, *276*, 37754–37760, doi:10.1074/jbc.M104073200.
238. Putcha, G.V.; Le, S.; Frank, S.; Besirli, C.G.; Clark, K.; Chu, B.; Alix, S.; Youle, R.J.; LaMarche, A.; Maroney, A.C.; et al. JNK-Mediated BIM Phosphorylation Potentiates BAX-Dependent Apoptosis. *Neuron* **2003**, *38*,

899–914, doi:10.1016/s0896-6273(03)00355-6.

239. Lei, K.; Davis, R.J. JNK Phosphorylation of Bim-Related Members of the Bcl2 Family Induces Bax-Dependent Apoptosis. *Proc. Natl. Acad. Sci. U. S. A.* **2003**, *100*, 2432–2437, doi:10.1073/pnas.0438011100.

240. Okuno, S.; Saito, A.; Hayashi, T.; Chan, P.H. The C-Jun N-Terminal Protein Kinase Signaling Pathway Mediates Bax Activation and Subsequent Neuronal Apoptosis through Interaction with Bim after Transient Focal Cerebral Ischemia. *J. Neurosci.* **2004**, *24*, 7879–7887, doi:10.1523/JNEUROSCI.1745-04.2004.

241. Yang, G.; Zhou, X.; Zhu, J.; Liu, R.; Zhang, S.; Coquinco, A.; Chen, Y.; Wen, Y.; Kojic, L.; Jia, W.; et al. JNK3 Couples the Neuronal Stress Response to Inhibition of Secretory Trafficking. *Sci. Signal.* **2013**, *6*, ra57, doi:10.1126/scisignal.2003727.

242. Yang, G.; Cynader, M.S. Regulation of Protein Trafficking: JNK3 at the Golgi Complex. *Cell Cycle* **2014**, *13*, 5–6, doi:10.4161/cc.27019.

243. Meur, A.M.-L. JNK Gives Axons a Second Chance. *J. Neurosci.* **2006**, *26*, 12104–12105, doi:10.1523/JNEUROSCI.4216-06.2006.

244. Holtmaat, A.; De Paola, V.; Wilbrecht, L.; Knott, G.W. Imaging of Experience-Dependent Structural Plasticity in the Mouse Neocortex in Vivo. *Behav. Brain Res.* **2008**, *192*, 20–25, doi:10.1016/j.bbr.2008.04.005.

245. Hollos, P.; John, J.M.; Lehtonen, J.V.; Coffey, E.T. Optogenetic Control of Spine-Head JNK Reveals a Role in Dendritic Spine Regression. *eNeuro* **2020**, *7*, ENEURO.0303-19.2019, doi:10.1523/ENEURO.0303-19.2019.

246. Komulainen, E.; Varidakis, A.; Kuleskaya, N.; Mohammad, H.; Sourander, C.; Rauvala, H.; Coffey, E.T. Impact of JNK and Its Substrates on Dendritic Spine Morphology. *Cells* **2020**, *9*, E440, doi:10.3390/cells9020440.

247. Zhu, Y.; Pak, D.; Qin, Y.; McCormack, S.G.; Kim, M.J.; Baumgart, J.P.; Velamoor, V.; Auberson, Y.P.; Osten, P.; van Aelst, L.; et al. Rap2-JNK Removes Synaptic AMPA Receptors during Depotential. *Neuron* **2005**, *46*, 905–916, doi:10.1016/j.neuron.2005.04.037.

248. Kim, M.J.; Futai, K.; Jo, J.; Hayashi, Y.; Cho, K.; Sheng, M. Synaptic Accumulation of PSD-95 and Synaptic Function Regulated by Phosphorylation of Serine-295 of PSD-95. *Neuron* **2007**, *56*, 488–502, doi:10.1016/j.neuron.2007.09.007.

249. Thomas, G.M.; Lin, D.-T.; Nuriya, M.; Haganir, R.L. Rapid and Bi-Directional Regulation of AMPA Receptor Phosphorylation and Trafficking by JNK. *EMBO J.* **2008**, *27*, 361–372, doi:10.1038/sj.emboj.7601969.

250. Edbauer, D.; Cheng, D.; Batterton, M.N.; Wang, C.-F.; Duong, D.M.; Yaffe, M.B.; Peng, J.; Sheng, M. Identification and Characterization of Neuronal Mitogen-Activated Protein Kinase Substrates Using a Specific Phosphomotif Antibody. *Mol. Cell. Proteomics MCP* **2009**, *8*, 681–695, doi:10.1074/mcp.M800233-MCP200.

251. Kunde, S.-A.; Rademacher, N.; Tzschach, A.; Wiedersberg, E.; Ullmann, R.; Kalscheuer, V.M.; Shoichet, S.A. Characterisation of de Novo MAPK10/JNK3 Truncation Mutations Associated with Cognitive Disorders in Two Unrelated Patients. *Hum. Genet.* **2013**, *132*, 461–471, doi:10.1007/s00439-012-1260-5.

252. Zhang, Y.; Zhou, L.; Miller, C.A. A Splicing Variant of a Death Domain Protein That Is Regulated by a Mitogen-Activated Kinase Is a Substrate for c-Jun N-Terminal Kinase in the Human Central Nervous System. *Proc. Natl. Acad. Sci. U. S. A.* **1998**, *95*, 2586–2591, doi:10.1073/pnas.95.5.2586.

253. Lindwall, C.; Kanje, M. Retrograde Axonal Transport of JNK Signaling Molecules Influence Injury Induced Nuclear Changes in P-c-Jun and ATF3 in Adult Rat Sensory Neurons. *Mol. Cell. Neurosci.* **2005**, *29*, 269–282, doi:10.1016/j.mcn.2005.03.002.

254. Crocker, S.J.; Lamba, W.R.; Smith, P.D.; Callaghan, S.M.; Slack, R.S.; Anisman, H.; Park, D.S. C-Jun Mediates Axotomy-Induced Dopamine Neuron Death in Vivo. *Proc. Natl. Acad. Sci. U. S. A.* **2001**, *98*, 13385–13390, doi:10.1073/pnas.231177098.

255. Yuan, Z.; Gong, S.; Luo, J.; Zheng, Z.; Song, B.; Ma, S.; Guo, J.; Hu, C.; Thiel, G.; Vinson, C.; et al. Opposing Roles for ATF2 and C-Fos in c-Jun-Mediated Neuronal Apoptosis. *Mol. Cell. Biol.* **2009**, *29*, 2431–2442, doi:10.1128/MCB.01344-08.

256. Ham, J.; Eilers, A.; Whitfield, J.; Neame, S.J.; Shah, B. C-Jun and the Transcriptional Control of Neuronal Apoptosis. *Biochem. Pharmacol.* **2000**, *60*, 1015–1021, doi:10.1016/s0006-2952(00)00372-5.

257. Desagher, S.; Severac, D.; Lipkin, A.; Bernis, C.; Ritchie, W.; Le Digarcher, A.; Journot, L. Genes Regulated in Neurons Undergoing Transcription-Dependent Apoptosis Belong to Signaling Pathways Rather than the Apoptotic Machinery. *J. Biol. Chem.* **2005**, *280*, 5693–5702, doi:10.1074/jbc.M408971200.

258. Ham, J.; Babij, C.; Whitfield, J.; Pfarr, C.M.; Lallemand, D.; Yaniv, M.; Rubin, L.L. A C-Jun Dominant Negative Mutant Protects Sympathetic Neurons against Programmed Cell Death. *Neuron* **1995**, *14*, 927–939, doi:10.1016/0896-6273(95)90331-3.

259. Behrens, A.; Sibilias, M.; Wagner, E.F. Amino-Terminal Phosphorylation of c-Jun Regulates Stress-Induced

- Apoptosis and Cellular Proliferation. *Nat. Genet.* **1999**, *21*, 326–329, doi:10.1038/6854.
260. Vaden, J.H.; Bhattacharyya, B.J.; Chen, P.-C.; Watson, J.A.; Marshall, A.G.; Phillips, S.E.; Wilson, J.A.; King, G.D.; Miller, R.J.; Wilson, S.M. Ubiquitin-Specific Protease 14 Regulates c-Jun N-Terminal Kinase Signaling at the Neuromuscular Junction. *Mol. Neurodegener.* **2015**, *10*, 3, doi:10.1186/1750-1326-10-3.
261. Schellino, R.; Boido, M.; Borsello, T.; Vercelli, A. Pharmacological C-Jun NH2-Terminal Kinase (JNK) Pathway Inhibition Reduces Severity of Spinal Muscular Atrophy Disease in Mice. *Front. Mol. Neurosci.* **2018**, *11*, 308, doi:10.3389/fnmol.2018.00308.
262. Morrison, D.K.; Davis, R.J. Regulation of MAP Kinase Signaling Modules by Scaffold Proteins in Mammals. *Annu. Rev. Cell Dev. Biol.* **2003**, *19*, 91–118, doi:10.1146/annurev.cellbio.19.111401.091942.
263. Bonny, C.; Nicod, P.; Waeber, G. IB1, a JIP-1-Related Nuclear Protein Present in Insulin-Secreting Cells. *J. Biol. Chem.* **1998**, *273*, 1843–1846, doi:10.1074/jbc.273.4.1843.
264. Whitmarsh, A.J. The JIP Family of MAPK Scaffold Proteins. *Biochem. Soc. Trans.* **2006**, *34*, 828–832, doi:10.1042/BST0340828.
265. Kelkar, N.; Standen, C.L.; Davis, R.J. Role of the JIP4 Scaffold Protein in the Regulation of Mitogen-Activated Protein Kinase Signaling Pathways. *Mol. Cell. Biol.* **2005**, *25*, 2733–2743, doi:10.1128/MCB.25.7.2733-2743.2005.
266. Verhey, K.J.; Meyer, D.; Deehan, R.; Blenis, J.; Schnapp, B.J.; Rapoport, T.A.; Margolis, B. Cargo of Kinesin Identified as Jip Scaffold Proteins and Associated Signaling Molecules. *J. Cell Biol.* **2001**, *152*, 959–970.
267. Matsuda, S.; Yasukawa, T.; Homma, Y.; Ito, Y.; Niikura, T.; Hiraki, T.; Hirai, S.; Ohno, S.; Kita, Y.; Kawasumi, M.; et al. C-Jun N-Terminal Kinase (JNK)-Interacting Protein-1b/Islet-Brain-1 Scaffolds Alzheimer's Amyloid Precursor Protein with JNK. *J. Neurosci.* **2001**, *21*, 6597–6607, doi:10.1523/JNEUROSCI.21-17-06597.2001.
268. Dhanasekaran, D.N.; Kashef, K.; Lee, C.M.; Xu, H.; Reddy, E.P. Scaffold Proteins of MAP-Kinase Modules. *Oncogene* **2007**, *26*, 3185–3202, doi:10.1038/sj.onc.1210411.
269. Davis, R.J. Signal Transduction by the JNK Group of MAP Kinases. *Cell* **2000**, *103*, 239–252, doi:10.1016/s0092-8674(00)00116-1.
270. Yasuda, J.; Whitmarsh, A.J.; Cavanagh, J.; Sharma, M.; Davis, R.J. The JIP Group of Mitogen-Activated Protein Kinase Scaffold Proteins. *Mol. Cell. Biol.* **1999**, *19*, 7245–7254, doi:10.1128/MCB.19.10.7245.
271. Drerup, C.M.; Nechiporuk, A.V. JNK-Interacting Protein 3 Mediates the Retrograde Transport of Activated c-Jun N-Terminal Kinase and Lysosomes. *PLoS Genet.* **2013**, *9*, e1003303, doi:10.1371/journal.pgen.1003303.
272. Kelkar, N.; Gupta, S.; Dickens, M.; Davis, R.J. Interaction of a Mitogen-Activated Protein Kinase Signaling Module with the Neuronal Protein JIP3. *Mol. Cell. Biol.* **2000**, *20*, 1030–1043, doi:10.1128/MCB.20.3.1030-1043.2000.
273. Dong, Z.; Zhou, L.; Del Villar, K.; Ghanavati, M.; Tashjian, V.; Miller, C.A. JIP1 Regulates Neuronal Apoptosis in Response to Stress. *Mol. Brain Res.* **2005**, *134*, 282–293, doi:10.1016/j.molbrainres.2004.10.039.
274. Pellet, J.B.; Haefliger, J.A.; Staple, J.K.; Widmann, C.; Welker, E.; Hirling, H.; Bonny, C.; Nicod, P.; Catsicas, S.; Waeber, G.; et al. Spatial, Temporal and Subcellular Localization of Islet-Brain 1 (IB1), a Homologue of JIP-1, in Mouse Brain. *Eur. J. Neurosci.* **2000**, *12*, 621–632, doi:10.1046/j.1460-9568.2000.00945.x.
275. Borsello, T.; Centeno, C.; Riederer, I.M.; Haefliger, J.-A.; Riederer, B.M. Phosphorylation-Dependent Dimerization and Subcellular Localization of Islet-Brain 1/c-Jun N-Terminal Kinase-Interacting Protein 1. *J. Neurosci. Res.* **2007**, *85*, 3632–3641, doi:10.1002/jnr.21435.
276. Bonny, C.; Oberson, A.; Negri, S.; Sauser, C.; Schorderet, D.F. Cell-Permeable Peptide Inhibitors of JNK: Novel Blockers of  $\beta$ -Cell Death. *Diabetes* **2001**, *50*, 77–82, doi:10.2337/diabetes.50.1.77.
277. Repici, M.; Chen, X.; Morel, M.-P.; Doulazmi, M.; Sclip, A.; Cannaya, V.; Veglianesi, P.; Kraftsik, R.; Mariani, J.; Borsello, T.; et al. Specific Inhibition of the JNK Pathway Promotes Locomotor Recovery and Neuroprotection after Mouse Spinal Cord Injury. *Neurobiol. Dis.* **2012**, *46*, 710–721, doi:10.1016/j.nbd.2012.03.014.
278. Suckfuell, M.; Lisowska, G.; Domka, W.; Kabacinska, A.; Morawski, K.; Bodlaj, R.; Klimak, P.; Kostrica, R.; Meyer, T. Efficacy and Safety of AM-111 in the Treatment of Acute Sensorineural Hearing Loss: A Double-Blind, Randomized, Placebo-Controlled Phase II Study. *Otol. Neurotol. Off. Publ. Am. Otol. Soc. Am. Neurotol. Soc. Eur. Acad. Otol. Neurotol.* **2014**, *35*, 1317–1326, doi:10.1097/MAO.0000000000000466.
279. Barr, R.K.; Kendrick, T.S.; Bogoyevitch, M.A. Identification of the Critical Features of a Small Peptide Inhibitor of JNK Activity\*. *J. Biol. Chem.* **2002**, *277*, 10987–10997, doi:10.1074/jbc.M107565200.
280. Heo, Y.-S.; Kim, S.-K.; Seo, C.I.; Kim, Y.K.; Sung, B.-J.; Lee, H.S.; Lee, J.I.; Park, S.-Y.; Kim, J.H.; Hwang, K.Y.; et al. Structural Basis for the Selective Inhibition of JNK1 by the Scaffolding Protein JIP1 and SP600125. *EMBO J.* **2004**, *23*, 2185–2195, doi:10.1038/sj.emboj.7600212.
281. Namgung, U.; Xia, Z. Arsenite-Induced Apoptosis in Cortical Neurons Is Mediated by c-Jun N-Terminal

- Protein Kinase 3 and P38 Mitogen-Activated Protein Kinase. *J. Neurosci. Off. J. Soc. Neurosci.* **2000**, *20*, 6442–6451.
282. Pan, J.; Pei, D.-S.; Yin, X.-H.; Hui, L.; Zhang, G.-Y. Involvement of Oxidative Stress in the Rapid Akt1 Regulating a JNK Scaffold during Ischemia in Rat Hippocampus. *Neurosci. Lett.* **2006**, *392*, 47–51, doi:10.1016/j.neulet.2005.08.057.
283. Kennedy, N.J.; Martin, G.; Ehrhardt, A.G.; Cavanagh-Kyros, J.; Kuan, C.-Y.; Rakic, P.; Flavell, R.A.; Treistman, S.N.; Davis, R.J. Requirement of JIP Scaffold Proteins for NMDA-Mediated Signal Transduction. *Genes Dev.* **2007**, *21*, 2336–2346, doi:10.1101/gad.1563107.
284. Beeler, N.; Riederer, B.M.; Waeber, G.; Abderrahmani, A. Role of the JNK-Interacting Protein 1/Islet Brain 1 in Cell Degeneration in Alzheimer Disease and Diabetes. *Brain Res. Bull.* **2009**, *80*, 274–281, doi:10.1016/j.brainresbull.2009.07.006.
285. Goodman, O.B.; Krupnick, J.G.; Santini, F.; Gurevich, V.V.; Penn, R.B.; Gagnon, A.W.; Keen, J.H.; Benovic, J.L. Beta-Arrestin Acts as a Clathrin Adaptor in Endocytosis of the Beta2-Adrenergic Receptor. *Nature* **1996**, *383*, 447–450, doi:10.1038/383447a0.
286. Srivastava, A.; Gupta, B.; Gupta, C.; Shukla, A.K. Emerging Functional Divergence of  $\beta$ -Arrestin Isoforms in GPCR Function. *Trends Endocrinol. Metab. TEM* **2015**, *26*, 628–642, doi:10.1016/j.tem.2015.09.001.
287. Zurkovsky, L.; Sedaghat, K.; Ahmed, M.R.; Gurevich, V.V.; Gurevich, E.V. Arrestin-2 and Arrestin-3 Differentially Modulate Locomotor Responses and Sensitization to Amphetamine. *Neuropharmacology* **2017**, *121*, 20–29, doi:10.1016/j.neuropharm.2017.04.021.
288. Gurevich, E.V.; Gurevich, V.V. Arrestins: Ubiquitous Regulators of Cellular Signaling Pathways. *Genome Biol.* **2006**, *7*, 236, doi:10.1186/gb-2006-7-9-236.
289. Zhan, X.; Kook, S.; Gurevich, E.V.; Gurevich, V.V. Arrestin-Dependent Activation of JNK Family Kinases. *Handb. Exp. Pharmacol.* **2014**, *219*, 259–280, doi:10.1007/978-3-642-41199-1\_13.
290. McDonald, P.H.; Chow, C.W.; Miller, W.E.; Laporte, S.A.; Field, M.E.; Lin, F.T.; Davis, R.J.; Lefkowitz, R.J. Beta-Arrestin 2: A Receptor-Regulated MAPK Scaffold for the Activation of JNK3. *Science* **2000**, *290*, 1574–1577, doi:10.1126/science.290.5496.1574.
291. Guo, C.; Whitmarsh, A.J. The  $\beta$ -Arrestin-2 Scaffold Protein Promotes c-Jun N-Terminal Kinase-3 Activation by Binding to Its Nonconserved N Terminus. *J. Biol. Chem.* **2008**, *283*, 15903–15911, doi:10.1074/jbc.M710006200.
292. Chen, W.-K.; Yeap, Y.Y.C.; Bogoyevitch, M.A. The JNK1/JNK3 Interactome--Contributions by the JNK3 Unique N-Terminus and JNK Common Docking Site Residues. *Biochem. Biophys. Res. Commun.* **2014**, *453*, 576–581, doi:10.1016/j.bbrc.2014.09.122.
293. Willoughby, E.A.; Collins, M.K. Dynamic Interaction between the Dual Specificity Phosphatase MKP7 and the JNK3 Scaffold Protein Beta-Arrestin 2. *J. Biol. Chem.* **2005**, *280*, 25651–25658, doi:10.1074/jbc.M501926200.
294. Gupta, S.; Barrett, T.; Whitmarsh, A.J.; Cavanagh, J.; Sluss, H.K.; Dérjard, B.; Davis, R.J. Selective Interaction of JNK Protein Kinase Isoforms with Transcription Factors. *EMBO J.* **1996**, *15*, 2760–2770.
295. Xie, X.; Gu, Y.; Fox, T.; Coll, J.T.; Fleming, M.A.; Markland, W.; Caron, P.R.; Wilson, K.P.; Su, M.S. Crystal Structure of JNK3: A Kinase Implicated in Neuronal Apoptosis. *Struct. Lond. Engl.* **1993**, *1998*, *6*, 983–991, doi:10.1016/s0969-2126(98)00100-2.
296. Kook, S.; Zhan, X.; Kaoud, T.S.; Dalby, K.N.; Gurevich, V.V.; Gurevich, E.V. Arrestin-3 Binds c-Jun N-Terminal Kinase 1 (JNK1) and JNK2 and Facilitates the Activation of These Ubiquitous JNK Isoforms in Cells via Scaffolding. *J. Biol. Chem.* **2013**, *288*, 37332–37342, doi:10.1074/jbc.M113.510412.
297. Lee, J.K.; Tam, J.W.; Tsai, M.J.; Tsai, S.Y. Identification of Cis- and Trans-Acting Factors Regulating the Expression of the Human Insulin Receptor Gene. *J. Biol. Chem.* **1992**, *267*, 4638–4645, doi:10.1016/S0021-9258(18)42881-5.
298. Lu, X.; Nemoto, S.; Lin, A. Identification of C-Jun NH2-Terminal Protein Kinase (JNK)-Activating Kinase 2 as an Activator of JNK but Not P38\*. *J. Biol. Chem.* **1997**, *272*, 24751–24754, doi:10.1074/jbc.272.40.24751.
299. Mohit, A.A.; Martin, J.H.; Miller, C.A. P493F12 Kinase: A Novel MAP Kinase Expressed in a Subset of Neurons in the Human Nervous System. *Neuron* **1995**, *14*, 67–78, doi:10.1016/0896-6273(95)90241-4.
300. Lee, J.K.; Park, J.; Lee, Y.D.; Lee, S.H.; Han, P.L. Distinct Localization of SAPK Isoforms in Neurons of Adult Mouse Brain Implies Multiple Signaling Modes of SAPK Pathway. *Brain Res. Mol. Brain Res.* **1999**, *70*, 116–124, doi:10.1016/s0169-328x(99)00136-9.
301. Coffey, E.T.; Smiciene, G.; Hongisto, V.; Cao, J.; Brecht, S.; Herdegen, T.; Courtney, M.J. C-Jun N-Terminal Protein Kinase (JNK) 2/3 Is Specifically Activated by Stress, Mediating c-Jun Activation, in the Presence of Constitutive JNK1 Activity in Cerebellar Neurons. *J. Neurosci. Off. J. Soc. Neurosci.* **2002**, *22*, 4335–4345, doi:20026401.

302. Brecht, S.; Kirchhof, R.; Chromik, A.; Willesen, M.; Nicolaus, T.; Raivich, G.; Wessig, J.; Waetzig, V.; Goetz, M.; Claussen, M.; et al. Specific Pathophysiological Functions of JNK Isoforms in the Brain. *Eur. J. Neurosci.* **2005**, *21*, 363–377, doi:10.1111/j.1460-9568.2005.03857.x.
303. Tararuk, T.; Ostman, N.; Li, W.; Björkblom, B.; Padzik, A.; Zdrojewska, J.; Hongisto, V.; Herdegen, T.; Konopka, W.; Courtney, M.J.; et al. JNK1 Phosphorylation of SCG10 Determines Microtubule Dynamics and Axodendritic Length. *J. Cell Biol.* **2006**, *173*, 265–277, doi:10.1083/jcb.200511055.
304. Chen, J.-T.; Lu, D.-H.; Chia, C.-P.; Ruan, D.-Y.; Sabapathy, K.; Xiao, Z.-C. Impaired Long-Term Potentiation in c-Jun N-Terminal Kinase 2-Deficient Mice. *J. Neurochem.* **2005**, *93*, 463–473, doi:10.1111/j.1471-4159.2005.03037.x.
305. Zeke, A.; Misheva, M.; Reményi, A.; Bogoyevitch, M.A. JNK Signaling: Regulation and Functions Based on Complex Protein-Protein Partnerships. *Microbiol. Mol. Biol. Rev. MMBR* **2016**, *80*, 793–835, doi:10.1128/MMBR.00043-14.
306. Kuan, C.Y.; Yang, D.D.; Samanta Roy, D.R.; Davis, R.J.; Rakic, P.; Flavell, R.A. The Jnk1 and Jnk2 Protein Kinases Are Required for Regional Specific Apoptosis during Early Brain Development. *Neuron* **1999**, *22*, 667–676, doi:10.1016/s0896-6273(00)80727-8.
307. Conze, D.; Krahl, T.; Kennedy, N.; Weiss, L.; Lumsden, J.; Hess, P.; Flavell, R.A.; Le Gros, G.; Davis, R.J.; Rincón, M. C-Jun NH(2)-Terminal Kinase (JNK)1 and JNK2 Have Distinct Roles in CD8(+) T Cell Activation. *J. Exp. Med.* **2002**, *195*, 811–823, doi:10.1084/jem.20011508.
308. Myers, A.K.; Meechan, D.W.; Adney, D.R.; Tucker, E.S. Cortical Interneurons Require Jnk1 to Enter and Navigate the Developing Cerebral Cortex. *J. Neurosci. Off. J. Soc. Neurosci.* **2014**, *34*, 7787–7801, doi:10.1523/JNEUROSCI.4695-13.2014.
309. Kuan, C.-Y.; Whitmarsh, A.J.; Yang, D.D.; Liao, G.; Schloemer, A.J.; Dong, C.; Bao, J.; Banasiak, K.J.; Haddad, G.G.; Flavell, R.A.; et al. A Critical Role of Neural-Specific JNK3 for Ischemic Apoptosis. *Proc. Natl. Acad. Sci. U. S. A.* **2003**, *100*, 15184–15189, doi:10.1073/pnas.2336254100.
310. Li, Q.M.; Tep, C.; Yune, T.Y.; Zhou, X.Z.; Uchida, T.; Lu, K.P.; Yoon, S.O. Opposite Regulation of Oligodendrocyte Apoptosis by JNK3 and Pin1 after Spinal Cord Injury. *J. Neurosci. Off. J. Soc. Neurosci.* **2007**, *27*, 8395–8404, doi:10.1523/JNEUROSCI.2478-07.2007.
311. de Lemos, L.; Junyent, F.; Verdaguer, E.; Folch, J.; Romero, R.; Pallàs, M.; Ferrer, I.; Auladell, C.; Camins, A. Differences in Activation of ERK1/2 and P38 Kinase in Jnk3 Null Mice Following KA Treatment. *J. Neurochem.* **2010**, *114*, 1315–1322, doi:10.1111/j.1471-4159.2010.06853.x.
312. Colombo, A.; Bastone, A.; Ploia, C.; Sclip, A.; Salmona, M.; Forloni, G.; Borsello, T. JNK Regulates APP Cleavage and Degradation in a Model of Alzheimer’s Disease. *Neurobiol. Dis.* **2009**, *33*, 518–525, doi:10.1016/j.nbd.2008.12.014.
313. Shoichet, S.A.; Duprez, L.; Hagens, O.; Waetzig, V.; Menzel, C.; Herdegen, T.; Schweiger, S.; Dan, B.; Vamos, E.; Ropers, H.-H.; et al. Truncation of the CNS-Expressed JNK3 in a Patient with a Severe Developmental Epileptic Encephalopathy. *Hum. Genet.* **2006**, *118*, 559–567, doi:10.1007/s00439-005-0084-y.
314. Shukkur, E.A.; Shimohata, A.; Akagi, T.; Yu, W.; Yamaguchi, M.; Murayama, M.; Chui, D.; Takeuchi, T.; Amano, K.; Subramhanya, K.H.; et al. Mitochondrial Dysfunction and Tau Hyperphosphorylation in Ts1Cje, a Mouse Model for Down Syndrome. *Hum. Mol. Genet.* **2006**, *15*, 2752–2762, doi:10.1093/hmg/ddl211.
315. Kernohan, K.D.; McBride, A.; Hartley, T.; Rojas, S.K.; Care4Rare Canada Consortium; Dymont, D.A.; Boycott, K.M.; Dyack, S. P21 Protein-Activated Kinase 1 Is Associated with Severe Regressive Autism, and Epilepsy. *Clin. Genet.* **2019**, *96*, 449–455, doi:10.1111/cge.13618.
316. Pavlowsky, A.; Gianfelice, A.; Pallotto, M.; Zanchi, A.; Vara, H.; Khelfaoui, M.; Valnegri, P.; Rezai, X.; Bassani, S.; Brambilla, D.; et al. A Postsynaptic Signaling Pathway That May Account for the Cognitive Defect Due to IL1RAPL1 Mutation. *Curr. Biol. CB* **2010**, *20*, 103–115, doi:10.1016/j.cub.2009.12.030.
317. Ziats, M.N.; Rennert, O.M. Expression Profiling of Autism Candidate Genes during Human Brain Development Implicates Central Immune Signaling Pathways. *PLoS One* **2011**, *6*, e24691, doi:10.1371/journal.pone.0024691.
318. Yarza, R.; Vela, S.; Solas, M.; Ramirez, M.J. C-Jun N-Terminal Kinase (JNK) Signaling as a Therapeutic Target for Alzheimer’s Disease. *Front. Pharmacol.* **2015**, *6*, 321, doi:10.3389/fphar.2015.00321.
319. Salminen, A.; Kaarniranta, K.; Kauppinen, A.; Ojala, J.; Haapasalo, A.; Soininen, H.; Hiltunen, M. Impaired Autophagy and APP Processing in Alzheimer’s Disease: The Potential Role of Beclin 1 Interactome. *Prog. Neurobiol.* **2013**, *106–107*, 33–54, doi:10.1016/j.pneurobio.2013.06.002.
320. Sclip, A.; Tozzi, A.; Abaza, A.; Cardinetti, D.; Colombo, I.; Calabresi, P.; Salmona, M.; Welker, E.; Borsello,

- T. C-Jun N-Terminal Kinase Has a Key Role in Alzheimer Disease Synaptic Dysfunction in Vivo. *Cell Death Dis.* **2014**, *5*, e1019, doi:10.1038/cddis.2013.559.
321. Sclip, A.; Antoniou, X.; Colombo, A.; Camici, G.G.; Pozzi, L.; Cardinetti, D.; Feligioni, M.; Veglianese, P.; Bahlmann, F.H.; Cervo, L.; et al. C-Jun N-Terminal Kinase Regulates Soluble A $\beta$  Oligomers and Cognitive Impairment in AD Mouse Model. *J. Biol. Chem.* **2011**, *286*, 43871–43880, doi:10.1074/jbc.M111.297515.
322. Sclip, A.; Arnaboldi, A.; Colombo, I.; Veglianese, P.; Colombo, L.; Messa, M.; Mancini, S.; Cimini, S.; Morelli, F.; Antoniou, X.; et al. Soluble A $\beta$  Oligomer-Induced Synaptopathy: C-Jun N-Terminal Kinase's Role. *J. Mol. Cell Biol.* **2013**, *5*, 277–279, doi:10.1093/jmcb/mjt015.
323. Costello, D.A.; Herron, C.E. The Role of C-Jun N-Terminal Kinase in the A Beta-Mediated Impairment of LTP and Regulation of Synaptic Transmission in the Hippocampus. *Neuropharmacology* **2004**, *46*, 655–662, doi:10.1016/j.neuropharm.2003.11.016.
324. Zhao, Y.; Kuca, K.; Wu, W.; Wang, X.; Nepovimova, E.; Musilek, K.; Wu, Q. Hypothesis: JNK Signaling Is a Therapeutic Target of Neurodegenerative Diseases. *Alzheimers Dement. n/a*, doi:10.1002/alz.12370.
325. Petrov, D.; Luque, M.; Pedrós, I.; Ettcheto, M.; Abad, S.; Pallàs, M.; Verdaguer, E.; Auladell, C.; Folch, J.; Camins, A. Evaluation of the Role of JNK1 in the Hippocampus in an Experimental Model of Familial Alzheimer's Disease. *Mol. Neurobiol.* **2016**, *53*, 6183–6193, doi:10.1007/s12035-015-9522-6.
326. Kimberly, W.T.; Zheng, J.B.; Town, T.; Flavell, R.A.; Selkoe, D.J. Physiological Regulation of the  $\beta$ -Amyloid Precursor Protein Signaling Domain by c-Jun N-Terminal Kinase JNK3 during Neuronal Differentiation. *J. Neurosci.* **2005**, *25*, 5533–5543, doi:10.1523/JNEUROSCI.4883-04.2005.
327. Xu, Y.; Hou, X.-Y.; Liu, Y.; Zong, Y.-Y. Different Protection of K252a and N-Acetyl-L-Cysteine against Amyloid-Beta Peptide-Induced Cortical Neuron Apoptosis Involving Inhibition of MLK3-MKK7-JNK3 Signal Cascades. *J. Neurosci. Res.* **2009**, *87*, 918–927, doi:10.1002/jnr.21909.
328. Yoon, S.O.; Park, D.J.; Ryu, J.C.; Ozer, H.G.; Tep, C.; Shin, Y.J.; Lim, T.H.; Pastorino, L.; Kunwar, A.J.; Walton, J.C.; et al. JNK3 Perpetuates Metabolic Stress Induced by A $\beta$  Peptides. *Neuron* **2012**, *75*, 824–837, doi:10.1016/j.neuron.2012.06.024.
329. Chang, L.; Jones, Y.; Ellisman, M.H.; Goldstein, L.S.B.; Karin, M. JNK1 Is Required for Maintenance of Neuronal Microtubules and Controls Phosphorylation of Microtubule-Associated Proteins. *Dev. Cell* **2003**, *4*, 521–533, doi:10.1016/s1534-5807(03)00094-7.
330. Ploia, C.; Antoniou, X.; Sclip, A.; Grande, V.; Cardinetti, D.; Colombo, A.; Canu, N.; Benussi, L.; Ghidoni, R.; Forloni, G.; et al. JNK Plays a Key Role in Tau Hyperphosphorylation in Alzheimer's Disease Models. *J. Alzheimers Dis. JAD* **2011**, *26*, 315–329, doi:10.3233/JAD-2011-110320.
331. Buccarello, L.; Musi, C.A.; Turati, A.; Borsello, T. The Stress C-Jun N-Terminal Kinase Signaling Pathway Activation Correlates with Synaptic Pathology and Presents A Sex Bias in P301L Mouse Model of Tauopathy. *Neuroscience* **2018**, *393*, 196–205, doi:10.1016/j.neuroscience.2018.09.049.
332. Yoshida, H.; Hastie, C.J.; McLauchlan, H.; Cohen, P.; Goedert, M. Phosphorylation of Microtubule-Associated Protein Tau by Isoforms of c-Jun N-Terminal Kinase (JNK). *J. Neurochem.* **2004**, *90*, 352–358, doi:10.1111/j.1471-4159.2004.02479.x.
333. Sato, S.; Tatebayashi, Y.; Akagi, T.; Chui, D.-H.; Murayama, M.; Miyasaka, T.; Planel, E.; Tanemura, K.; Sun, X.; Hashikawa, T.; et al. Aberrant Tau Phosphorylation by Glycogen Synthase Kinase-3 $\beta$  and JNK3 Induces Oligomeric Tau Fibrils in COS-7 Cells. *J. Biol. Chem.* **2002**, *277*, 42060–42065, doi:10.1074/jbc.M202241200.
334. Medhi, B.; Chakrabarty, M. Insulin Resistance: An Emerging Link in Alzheimer's Disease. *Neurol. Sci. Off. J. Ital. Neurol. Soc. Ital. Soc. Clin. Neurophysiol.* **2013**, *34*, 1719–1725, doi:10.1007/s10072-013-1454-1.
335. Shieh, J.C.-C.; Huang, P.-T.; Lin, Y.-F. Alzheimer's Disease and Diabetes: Insulin Signaling as the Bridge Linking Two Pathologies. *Mol. Neurobiol.* **2020**, *57*, 1966–1977, doi:10.1007/s12035-019-01858-5.
336. Zhu, X.; Raina, A.K.; Rottkamp, C.A.; Aliev, G.; Perry, G.; Boux, H.; Smith, M.A. Activation and Redistribution of C-Jun N-Terminal Kinase/Stress Activated Protein Kinase in Degenerating Neurons in Alzheimer's Disease. *J. Neurochem.* **2001**, *76*, 435–441, doi:10.1046/j.1471-4159.2001.00046.x.
337. Zhu, X.; Raina, A.K.; Lee, H.-G.; Chao, M.; Nunomura, A.; Tabaton, M.; Petersen, R.B.; Perry, G.; Smith, M.A. Oxidative Stress and Neuronal Adaptation in Alzheimer Disease: The Role of SAPK Pathways. *Antioxid. Redox Signal.* **2003**, *5*, 571–576, doi:10.1089/152308603770310220.
338. Wang, D.; Fei, Z.; Luo, S.; Wang, H. MiR-335-5p Inhibits  $\beta$ -Amyloid (A $\beta$ ) Accumulation to Attenuate Cognitive Deficits Through Targeting c-Jun-N-Terminal Kinase 3 in Alzheimer's Disease. *Curr. Neurovasc. Res.* **2020**, *17*, 93–101, doi:10.2174/1567202617666200128141938.
339. Gourmaud, S.; Paquet, C.; Dumurgier, J.; Pace, C.; Bouras, C.; Gray, F.; Laplanche, J.-L.; Meurs, E.F.;

Mouton-Liger, F.; Hugon, J. Increased Levels of Cerebrospinal Fluid JNK3 Associated with Amyloid Pathology: Links to Cognitive Decline. *J. Psychiatry Neurosci. JPN* **2015**, *40*, 151–161, doi:10.1503/jpn.140062.

340. Paquet, C.; Dumurgier, J.; Hugon, J. Pro-Apoptotic Kinase Levels in Cerebrospinal Fluid as Potential Future Biomarkers in Alzheimer's Disease. *Front. Neurol.* **2015**, *6*, 168, doi:10.3389/fneur.2015.00168.

341. Hunot, S.; Vila, M.; Teismann, P.; Davis, R.J.; Hirsch, E.C.; Przedborski, S.; Rakic, P.; Flavell, R.A. JNK-Mediated Induction of Cyclooxygenase 2 Is Required for Neurodegeneration in a Mouse Model of Parkinson's Disease. *Proc. Natl. Acad. Sci. U. S. A.* **2004**, *101*, 665–670, doi:10.1073/pnas.0307453101.

342. de Los Reyes Corrales, T.; Losada-Pérez, M.; Casas-Tintó, S. JNK Pathway in CNS Pathologies. *Int. J. Mol. Sci.* **2021**, *22*, 3883, doi:10.3390/ijms22083883.

343. de Lemos, L.; Junyent, F.; Camins, A.; Castro-Torres, R.D.; Folch, J.; Olloquequi, J.; Beas-Zarate, C.; Verdaguier, E.; Auladell, C. Neuroprotective Effects of the Absence of JNK1 or JNK3 Isoforms on Kainic Acid-Induced Temporal Lobe Epilepsy-Like Symptoms. *Mol. Neurobiol.* **2018**, *55*, 4437–4452, doi:10.1007/s12035-017-0669-1.

344. Guan, Q.-H.; Pei, D.-S.; Liu, X.-M.; Wang, X.-T.; Xu, T.-L.; Zhang, G.-Y. Neuroprotection against Ischemic Brain Injury by SP600125 via Suppressing the Extrinsic and Intrinsic Pathways of Apoptosis. *Brain Res.* **2006**, *1092*, 36–46, doi:10.1016/j.brainres.2006.03.086.

345. Bogoyevitch, M.A.; Arthur, P.G. Inhibitors of C-Jun N-Terminal Kinases: JuNK No More? *Biochim. Biophys. Acta* **2008**, *1784*, 76–93, doi:10.1016/j.bbapap.2007.09.013.

346. Repici, M.; Borsello, T. JNK Pathway as Therapeutic Target to Prevent Degeneration in the Central Nervous System. *Adv. Exp. Med. Biol.* **2006**, *588*, 145–155, doi:10.1007/978-0-387-34817-9\_13.

347. Borsello, T.; Clarke, P.G.H.; Hirt, L.; Vercelli, A.; Repici, M.; Schorderet, D.F.; Bogousslavsky, J.; Bonny, C. A Peptide Inhibitor of C-Jun N-Terminal Kinase Protects against Excitotoxicity and Cerebral Ischemia. *Nat. Med.* **2003**, *9*, 1180–1186, doi:10.1038/nm911.

348. Borsello, T.; Bonny, C. Use of Cell-Permeable Peptides to Prevent Neuronal Degeneration. *Trends Mol. Med.* **2004**, *10*, 239–244, doi:10.1016/j.molmed.2004.03.008.

349. Björkblom, B.; Ostman, N.; Hongisto, V.; Komarovski, V.; Filén, J.-J.; Nyman, T.A.; Kallunki, T.; Courtney, M.J.; Coffey, E.T. Constitutively Active Cytoplasmic C-Jun N-Terminal Kinase 1 Is a Dominant Regulator of Dendritic Architecture: Role of Microtubule-Associated Protein 2 as an Effector. *J. Neurosci. Off. J. Soc. Neurosci.* **2005**, *25*, 6350–6361, doi:10.1523/JNEUROSCI.1517-05.2005.

350. Antoniou, X.; Falconi, M.; Di Marino, D.; Borsello, T. JNK3 as a Therapeutic Target for Neurodegenerative Diseases. *J. Alzheimers Dis. JAD* **2011**, *24*, 633–642, doi:10.3233/JAD-2011-091567.

351. Siddiqui, M.A.; Reddy, P.A. Small Molecule JNK (c-Jun N-Terminal Kinase) Inhibitors. *J. Med. Chem.* **2010**, *53*, 3005–3012, doi:10.1021/jm9003279.

352. Schnieders, M.J.; Kaoud, T.S.; Yan, C.; Dalby, K.N.; Ren, P. Computational Insights for the Discovery of Non-ATP Competitive Inhibitors of MAP Kinases. *Curr. Pharm. Des.* **2012**, *18*, 1173–1185, doi:10.2174/138161212799436368.

353. Modi, V.; Dunbrack, R.L. A Structurally-Validated Multiple Sequence Alignment of 497 Human Protein Kinase Domains. *Sci. Rep.* **2019**, *9*, 19790, doi:10.1038/s41598-019-56499-4.

354. Koch, P.; Gehringer, M.; Laufer, S.A. Inhibitors of C-Jun N-Terminal Kinases: An Update. *J. Med. Chem.* **2015**, *58*, 72–95, doi:10.1021/jm501212r.

355. Lu, H.; Zhou, Q.; He, J.; Jiang, Z.; Peng, C.; Tong, R.; Shi, J. Recent Advances in the Development of Protein-Protein Interactions Modulators: Mechanisms and Clinical Trials. *Signal Transduct. Target. Ther.* **2020**, *5*, 1–23, doi:10.1038/s41392-020-00315-3.

356. Kaoud, T.S.; Yan, C.; Mitra, S.; Tseng, C.-C.; Jose, J.; Taliaferro, J.M.; Tuohetahunttila, M.; Devkota, A.; Sammons, R.; Park, J.; et al. From in Silico Discovery to Intra-Cellular Activity: Targeting JNK-Protein Interactions with Small Molecules. *ACS Med. Chem. Lett.* **2012**, *3*, 721–725, doi:10.1021/ml300129b.

357. Taoufik, E.; Kouroupi, G.; Zygogianni, O.; Matsas, R. Synaptic Dysfunction in Neurodegenerative and Neurodevelopmental Diseases: An Overview of Induced Pluripotent Stem-Cell-Based Disease Models. *Open Biol.* **2018**, *8*, 180138, doi:10.1098/rsob.180138.

358. Porte, B.; Marguerit, G.; Thomasseau, S.; Paquet, C.; Hugon, J. Dose-Dependent Neuroprotective Effect of the JNK Inhibitor Brimapitide in 5xFAD Transgenic Mice. *Brain Res.* **2020**, *1727*, 146587, doi:10.1016/j.brainres.2019.146587.

359. Gourmaud, S.; Thomas, P.; Thomasseau, S.; Tible, M.; Abadie, C.; Paquet, C.; Hugon, J. Brimapitide Reduced Neuronal Stress Markers and Cognitive Deficits in 5XFAD Transgenic Mice. *J. Alzheimers Dis. JAD* **2018**, *63*, 665–674, doi:10.3233/JAD-171099.

360. Musi, C.A.; Agrò, G.; Buccarello, L.; Camuso, S.; Borsello, T. JNK Signaling Activation in the Ube3a Maternal Deficient Mouse Model: Its Specific Inhibition Prevents Post-Synaptic Protein-Enriched Fraction Alterations and Cognitive Deficits in Angelman Syndrome Model. *Neurobiol. Dis.* **2020**, *140*, 104812, doi:10.1016/j.nbd.2020.104812.
361. Jiang, Y.H.; Armstrong, D.; Albrecht, U.; Atkins, C.M.; Noebels, J.L.; Eichele, G.; Sweatt, J.D.; Beaudet, A.L. Mutation of the Angelman Ubiquitin Ligase in Mice Causes Increased Cytoplasmic P53 and Deficits of Contextual Learning and Long-Term Potentiation. *Neuron* **1998**, *21*, 799–811, doi:10.1016/s0896-6273(00)80596-6.
362. Hotta, A.; Cheung, A.Y.L.; Farra, N.; Garcha, K.; Chang, W.Y.; Pasceri, P.; Stanford, W.L.; Ellis, J. EOS Lentiviral Vector Selection System for Human Induced Pluripotent Stem Cells. *Nat. Protoc.* **2009**, *4*, 1828–1844, doi:10.1038/nprot.2009.201.
363. Takahashi, K.; Tanabe, K.; Ohnuki, M.; Narita, M.; Ichisaka, T.; Tomoda, K.; Yamanaka, S. Induction of Pluripotent Stem Cells from Adult Human Fibroblasts by Defined Factors. *Cell* **2007**, *131*, 861–872, doi:10.1016/j.cell.2007.11.019.
364. Amenduni, M.; De Filippis, R.; Cheung, A.Y.L.; Disciglio, V.; Epistolato, M.C.; Ariani, F.; Mari, F.; Mencarelli, M.A.; Hayek, Y.; Renieri, A.; et al. IPS Cells to Model CDKL5-Related Disorders. *Eur. J. Hum. Genet. EJHG* **2011**, *19*, 1246–1255, doi:10.1038/ejhg.2011.131.
365. Livide, G.; Patriarchi, T.; Amenduni, M.; Amabile, S.; Yasui, D.; Calcagno, E.; Lo Rizzo, C.; De Falco, G.; Ulivieri, C.; Ariani, F.; et al. GluD1 Is a Common Altered Player in Neuronal Differentiation from Both MECP2-Mutated and CDKL5-Mutated IPS Cells. *Eur. J. Hum. Genet. EJHG* **2015**, *23*, 195–201, doi:10.1038/ejhg.2014.81.
366. Sclip, A.; Tozzi, A.; Abaza, A.; Cardinetti, D.; Colombo, I.; Calabresi, P.; Salmona, M.; Welker, E.; Borsello, T. C-Jun N-Terminal Kinase Has a Key Role in Alzheimer Disease Synaptic Dysfunction in Vivo. *Cell Death Dis.* **2014**, *5*, e1019, doi:10.1038/cddis.2013.559.
367. Sclip, A.; Arnaboldi, A.; Colombo, I.; Veglianesi, P.; Colombo, L.; Messa, M.; Mancini, S.; Cimini, S.; Morelli, F.; Antoniou, X.; et al. Soluble A $\beta$  Oligomer-Induced Synaptopathy: C-Jun N-Terminal Kinase's Role. *J. Mol. Cell Biol.* **2013**, *5*, 277–279, doi:10.1093/jmcb/mjt015.
368. Massignan, T.; Cimini, S.; Stincardini, C.; Cerovic, M.; Vanni, I.; Elezgarai, S.R.; Moreno, J.; Stravalaci, M.; Negro, A.; Sangiovanni, V.; et al. A Cationic Tetrapyrrole Inhibits Toxic Activities of the Cellular Prion Protein. *Sci. Rep.* **2016**, *6*, 23180, doi:10.1038/srep23180.
369. Calfa, G.; Percy, A.K.; Pozzo-Miller, L. Experimental Models of Rett Syndrome Based on Mecp2 Dysfunction. *Exp. Biol. Med. Maywood NJ* **2011**, *236*, 3–19, doi:10.1258/ebm.2010.010261.
370. Gardoni, F.; Schrama, L.H.; Kamal, A.; Gispen, W.H.; Cattabeni, F.; Di Luca, M. Hippocampal Synaptic Plasticity Involves Competition between Ca<sup>2+</sup>/Calmodulin-Dependent Protein Kinase II and Postsynaptic Density 95 for Binding to the NR2A Subunit of the NMDA Receptor. *J. Neurosci. Off. J. Soc. Neurosci.* **2001**, *21*, 1501–1509.
371. Borsello, T.; Clarke, P.G.H.; Hirt, L.; Vercelli, A.; Repici, M.; Schorderet, D.F.; Bogousslavsky, J.; Bonny, C. A Peptide Inhibitor of C-Jun N-Terminal Kinase Protects against Excitotoxicity and Cerebral Ischemia. *Nat. Med.* **2003**, *9*, 1180–1186, doi:10.1038/nm911.
372. Bonny, C.; Oberson, A.; Negri, S.; Sauser, C.; Schorderet, D.F. Cell-Permeable Peptide Inhibitors of JNK: Novel Blockers of Beta-Cell Death. *Diabetes* **2001**, *50*, 77–82.
373. Ahmed, T.; Zulfiqar, A.; Arguelles, S.; Rasekhan, M.; Nabavi, S.F.; Silva, A.S.; Nabavi, S.M. Map Kinase Signaling as Therapeutic Target for Neurodegeneration. *Pharmacol. Res.* **2020**, *160*, 105090, doi:10.1016/j.phrs.2020.105090.
374. Feigin, V.L.; Vos, T.; Nichols, E.; Owolabi, M.O.; Carroll, W.M.; Dichgans, M.; Deuschl, G.; Parmar, P.; Brainin, M.; Murray, C. The Global Burden of Neurological Disorders: Translating Evidence into Policy. *Lancet Neurol.* **2020**, *19*, 255–265, doi:10.1016/S1474-4422(19)30411-9.
375. Lepeta, K.; Lourenco, M.V.; Schweitzer, B.C.; Martino Adami, P.V.; Banerjee, P.; Catuara-Solarz, S.; de La Fuente Revenga, M.; Guillem, A.M.; Haidar, M.; Ijomone, O.M.; et al. Synaptopathies: Synaptic Dysfunction in Neurological Disorders - A Review from Students to Students. *J. Neurochem.* **2016**, *138*, 785–805, doi:10.1111/jnc.13713.
376. Biggi, S.; Buccarello, L.; Sclip, A.; Lippiello, P.; Tonna, N.; Rumio, C.; Di Marino, D.; Miniaci, M.C.; Borsello, T. Evidence of Presynaptic Localization and Function of the C-Jun N-Terminal Kinase. *Neural Plast.* **2017**, *2017*, 6468356, doi:10.1155/2017/6468356.
377. Borsello, T.; Croquelois, K.; Hornung, J.-P.; Clarke, P.G.H. N-Methyl-d-Aspartate-Triggered Neuronal Death in Organotypic Hippocampal Cultures Is Endocytic, Autophagic and Mediated by the c-Jun N-Terminal Kinase Pathway. *Eur. J. Neurosci.* **2003**, *18*, 473–485, doi:10.1046/j.1460-9568.2003.02757.x.

378. Roskoski, R. Properties of FDA-Approved Small Molecule Protein Kinase Inhibitors: A 2020 Update. *Pharmacol. Res.* **2020**, *152*, 104609, doi:10.1016/j.phrs.2019.104609.
379. Katz, D.M.; Bird, A.; Coenraads, M.; Gray, S.J.; Menon, D.U.; Philpot, B.D.; Tarquinio, D.C. Rett Syndrome: Crossing the Threshold to Clinical Translation. *Trends Neurosci.* **2016**, *39*, 100–113, doi:10.1016/j.tins.2015.12.008.
380. Katz, D.M.; Dutschmann, M.; Ramirez, J.-M.; Hilaire, G. Breathing Disorders in Rett Syndrome: Progressive Neurochemical Dysfunction in the Respiratory Network after Birth. *Respir. Physiol. Neurobiol.* **2009**, *168*, 101–108, doi:10.1016/j.resp.2009.04.017.
381. Weese-Mayer, D.E.; Lieske, S.P.; Boothby, C.M.; Kenny, A.S.; Bennett, H.L.; Silvestri, J.M.; Ramirez, J.-M. Autonomic Nervous System Dysregulation: Breathing and Heart Rate Perturbation During Wakefulness in Young Girls with Rett Syndrome. *Pediatr. Res.* **2006**, *60*, 443–449, doi:10.1203/01.pdr.0000238302.84552.d0.
382. Thomas, G.M.; Lin, D.-T.; Nuriya, M.; Haganir, R.L. Rapid and Bi-Directional Regulation of AMPA Receptor Phosphorylation and Trafficking by JNK. *EMBO J.* **2008**, *27*, 361–372, doi:10.1038/sj.emboj.7601969.
383. Sclip, A.; Antoniou, X.; Colombo, A.; Camici, G.G.; Pozzi, L.; Cardinetti, D.; Feligioni, M.; Veglianese, P.; Bahlmann, F.H.; Cervo, L.; et al. C-Jun N-Terminal Kinase Regulates Soluble A $\beta$  Oligomers and Cognitive Impairment in AD Mouse Model. *J. Biol. Chem.* **2011**, *286*, 43871–43880, doi:10.1074/jbc.M111.297515.
384. Buccarello, L.; Sclip, A.; Sacchi, M.; Castaldo, A.M.; Bertani, I.; ReCecconi, A.; Maestroni, S.; Zerbini, G.; Nucci, P.; Borsello, T. The C-Jun N-Terminal Kinase Plays a Key Role in Ocular Degenerative Changes in a Mouse Model of Alzheimer Disease Suggesting a Correlation between Ocular and Brain Pathologies. *Oncotarget* **2017**, *8*, 83038–83051, doi:10.18632/oncotarget.19886.
385. Buccarello, L.; Musi, C.A.; Turati, A.; Borsello, T. The Stress C-Jun N-Terminal Kinase Signaling Pathway Activation Correlates with Synaptic Pathology and Presents A Sex Bias in P301L Mouse Model of Tauopathy. *Neuroscience* **2018**, *393*, 196–205, doi:10.1016/j.neuroscience.2018.09.049.
386. Cimini, S.; Sclip, A.; Mancini, S.; Colombo, L.; Messa, M.; Cagnotto, A.; Di Fede, G.; Tagliavini, F.; Salmona, M.; Borsello, T. The Cell-Permeable A $\beta$ 1-6A2VTAT(D) Peptide Reverts Synaptopathy Induced by A $\beta$ 1-42wt. *Neurobiol. Dis.* **2016**, *89*, 101–111, doi:10.1016/j.nbd.2015.12.013.
387. Qiu, Z.; Sylwestrak, E.L.; Lieberman, D.N.; Zhang, Y.; Liu, X.-Y.; Ghosh, A. The Rett Syndrome Protein MeCP2 Regulates Synaptic Scaling. *J. Neurosci. Off. J. Soc. Neurosci.* **2012**, *32*, 989–994, doi:10.1523/JNEUROSCI.0175-11.2012.
388. Hou, Y.-Y.; Cai, Y.-Q.; Pan, Z.Z. Persistent Pain Maintains Morphine-Seeking Behavior after Morphine Withdrawal through Reduced MeCP2 Repression of GluA1 in Rat Central Amygdala. *J. Neurosci. Off. J. Soc. Neurosci.* **2015**, *35*, 3689–3700, doi:10.1523/JNEUROSCI.3453-14.2015.
389. Niescier, R.F.; Lin, Y.-C. The Potential Role of AMPA Receptor Trafficking in Autism and Other Neurodevelopmental Conditions. *Neuroscience* **2021**, *479*, 180–191, doi:10.1016/j.neuroscience.2021.09.013.
390. Belichenko, P.V.; Wright, E.E.; Belichenko, N.P.; Masliah, E.; Li, H.H.; Mobley, W.C.; Francke, U. Widespread Changes in Dendritic and Axonal Morphology in Mecp2-Mutant Mouse Models of Rett Syndrome: Evidence for Disruption of Neuronal Networks. *J. Comp. Neurol.* **2009**, *514*, 240–258, doi:10.1002/cne.22009.
391. Bourgeron, T. A Synaptic Trek to Autism. *Curr. Opin. Neurobiol.* **2009**, *19*, 231–234, doi:10.1016/j.conb.2009.06.003.
392. Chapleau, C.A.; Larimore, J.L.; Theibert, A.; Pozzo-Miller, L. Modulation of Dendritic Spine Development and Plasticity by BDNF and Vesicular Trafficking: Fundamental Roles in Neurodevelopmental Disorders Associated with Mental Retardation and Autism. *J. Neurodev. Disord.* **2009**, *1*, 185–196, doi:10.1007/s11689-009-9027-6.
393. Fiala, J.C.; Spacek, J.; Harris, K.M. Dendritic Spine Pathology: Cause or Consequence of Neurological Disorders? *Brain Res. Brain Res. Rev.* **2002**, *39*, 29–54, doi:10.1016/s0165-0173(02)00158-3.
394. Fukuda, T.; Itoh, M.; Ichikawa, T.; Washiyama, K.; Goto, Y. Delayed Maturation of Neuronal Architecture and Synaptogenesis in Cerebral Cortex of Mecp2-Deficient Mice. *J. Neuropathol. Exp. Neurol.* **2005**, *64*, 537–544, doi:10.1093/jnen/64.6.537.
395. Garey, L. When Cortical Development Goes Wrong: Schizophrenia as a Neurodevelopmental Disease of Microcircuits. *J. Anat.* **2010**, *217*, 324–333, doi:10.1111/j.1469-7580.2010.01231.x.
396. Levenga, J.; Willemsen, R. Perturbation of Dendritic Protrusions in Intellectual Disability. *Prog. Brain Res.* **2012**, *197*, 153–168, doi:10.1016/B978-0-444-54299-1.00008-X.
397. Penzes, P.; Cahill, M.E.; Jones, K.A.; VanLeeuwen, J.-E.; Woolfrey, K.M. Dendritic Spine Pathology in Neuropsychiatric Disorders. *Nat. Neurosci.* **2011**, *14*, 285–293, doi:10.1038/nn.2741.
398. Zhao, X.; Pak, C.; Smrt, R.D.; Jin, P. Epigenetics and Neural Developmental Disorders: Washington DC, September 18 and 19, 2006. *Epigenetics* **2007**, *2*, 126–134, doi:10.4161/epi.2.2.4236.

399. Ricciardi, S.; Boggio, E.M.; Grosso, S.; Lonetti, G.; Forlani, G.; Stefanelli, G.; Calcagno, E.; Morello, N.; Landsberger, N.; Biffo, S.; et al. Reduced AKT/MTOR Signaling and Protein Synthesis Dysregulation in a Rett Syndrome Animal Model. *Hum. Mol. Genet.* **2011**, *20*, 1182–1196, doi:10.1093/hmg/ddq563.
400. Jorge-Torres, O.C.; Szczesna, K.; Roa, L.; Casal, C.; Gonzalez-Sommermeier, L.; Soler, M.; Velasco, C.D.; Martínez-San Segundo, P.; Petazzi, P.; Sáez, M.A.; et al. Inhibition of Gsk3b Reduces Nfkb1 Signaling and Rescues Synaptic Activity to Improve the Rett Syndrome Phenotype in Mecp2-Knockout Mice. *Cell Rep.* **2018**, *23*, 1665–1677, doi:10.1016/j.celrep.2018.04.010.
401. Kishi, N.; MacDonald, J.L.; Ye, J.; Molyneaux, B.J.; Azim, E.; Macklis, J.D. Reduction of Aberrant NF-KB Signalling Ameliorates Rett Syndrome Phenotypes in Mecp2-Null Mice. *Nat. Commun.* **2016**, *7*, 10520, doi:10.1038/ncomms10520.
402. Li, W.; Pozzo-Miller, L. BDNF Deregulation in Rett Syndrome. *Neuropharmacology* **2014**, *76 Pt C*, 737–746, doi:10.1016/j.neuropharm.2013.03.024.
403. Wagley, Y.; Hwang, C.K.; Lin, H.-Y.; Kam, A.F.Y.; Law, P.-Y.; Loh, H.H.; Wei, L.-N. Inhibition of C-Jun NH2-Terminal Kinase Stimulates Mu Opioid Receptor Expression via P38 MAPK-Mediated Nuclear NF-KB Activation in Neuronal and Non-Neuronal Cells. *Biochim. Biophys. Acta* **2013**, *1833*, 1476–1488, doi:10.1016/j.bbamcr.2013.02.017.
404. Chahil, G.; Bollu, P.C. Rett Syndrome. In *StatPearls*; StatPearls Publishing: Treasure Island (FL), 2020.
405. Cosentino, L.; Vigli, D.; Franchi, F.; Laviola, G.; De Filippis, B. Rett Syndrome before Regression: A Time Window of Overlooked Opportunities for Diagnosis and Intervention. *Neurosci. Biobehav. Rev.* **2019**, *107*, 115–135, doi:10.1016/j.neubiorev.2019.05.013.
406. Singh, J.; Lanzarini, E.; Santosh, P. Autonomic Dysfunction and Sudden Death in Patients with Rett Syndrome: A Systematic Review. *J. Psychiatry Neurosci. JPN* **2020**, *45*, 150–181, doi:10.1503/jpn.190033.
407. Scip, A.; Tozzi, A.; Abaza, A.; Cardinetti, D.; Colombo, I.; Calabresi, P.; Salmona, M.; Welker, E.; Borsello, T. C-Jun N-Terminal Kinase Has a Key Role in Alzheimer Disease Synaptic Dysfunction in Vivo. *Cell Death Dis.* **2014**, *5*, e1019, doi:10.1038/cddis.2013.559.
408. Scip, A.; Antoniou, X.; Colombo, A.; Camici, G.G.; Pozzi, L.; Cardinetti, D.; Feligioni, M.; Veglianese, P.; Bahlmann, F.H.; Cervo, L.; et al. C-Jun N-Terminal Kinase Regulates Soluble A $\beta$  Oligomers and Cognitive Impairment in AD Mouse Model. *J. Biol. Chem.* **2011**, *286*, 43871–43880, doi:10.1074/jbc.M111.297515.
409. Staecker, H.; Jokovic, G.; Karpishchenko, S.; Kienle-Gogolok, A.; Krzyzaniak, A.; Lin, C.-D.; Navratil, P.; Tzvetkov, V.; Wright, N.; Meyer, T. Efficacy and Safety of AM-111 in the Treatment of Acute Unilateral Sudden Deafness-A Double-Blind, Randomized, Placebo-Controlled Phase 3 Study. *Otol. Neurotol. Off. Publ. Am. Otol. Soc. Am. Neurotol. Soc. Eur. Acad. Otol. Neurotol.* **2019**, *40*, 584–594, doi:10.1097/MAO.0000000000002229.
410. Yang, D.D.; Kuan, C.Y.; Whitmarsh, A.J.; Rincón, M.; Zheng, T.S.; Davis, R.J.; Rakic, P.; Flavell, R.A. Absence of Excitotoxicity-Induced Apoptosis in the Hippocampus of Mice Lacking the Jnk3 Gene. *Nature* **1997**, *389*, 865–870, doi:10.1038/39899.
411. Dindot, S.V.; Antalffy, B.A.; Bhattacharjee, M.B.; Beaudet, A.L. The Angelman Syndrome Ubiquitin Ligase Localizes to the Synapse and Nucleus, and Maternal Deficiency Results in Abnormal Dendritic Spine Morphology. *Hum. Mol. Genet.* **2008**, *17*, 111–118, doi:10.1093/hmg/ddm288.
412. Sato, M.; Stryker, M.P. Genomic Imprinting of Experience-Dependent Cortical Plasticity by the Ubiquitin Ligase Gene Ube3a. *Proc. Natl. Acad. Sci. U. S. A.* **2010**, *107*, 5611–5616, doi:10.1073/pnas.1001281107.
413. Weeber, E.J.; Jiang, Y.-H.; Elgersma, Y.; Varga, A.W.; Carrasquillo, Y.; Brown, S.E.; Christian, J.M.; Mirnikjoo, B.; Silva, A.; Beaudet, A.L.; et al. Derangements of Hippocampal Calcium/Calmodulin-Dependent Protein Kinase II in a Mouse Model for Angelman Mental Retardation Syndrome. *J. Neurosci. Off. J. Soc. Neurosci.* **2003**, *23*, 2634–2644.
414. Jay, V.; Becker, L.E.; Chan, F.W.; Perry, T.L. Puppet-like Syndrome of Angelman: A Pathologic and Neurochemical Study. *Neurology* **1991**, *41*, 416–422, doi:10.1212/wnl.41.3.416.
415. Cooper, B.; Schneider, S.; Bohl, J.; Jiang, Y. hui; Beaudet, A.; Vande Pol, S. Requirement of E6AP and the Features of Human Papillomavirus E6 Necessary to Support Degradation of P53. *Virology* **2003**, *306*, 87–99, doi:10.1016/s0042-6822(02)00012-0.
416. Wallace, M.L.; Burette, A.C.; Weinberg, R.J.; Philpot, B.D. Maternal Loss of Ube3a Produces an Excitatory/Inhibitory Imbalance through Neuron Type-Specific Synaptic Defects. *Neuron* **2012**, *74*, 793–800, doi:10.1016/j.neuron.2012.03.036.
417. Scip, A.; Tozzi, A.; Abaza, A.; Cardinetti, D.; Colombo, I.; Calabresi, P.; Salmona, M.; Welker, E.; Borsello, T. C-Jun N-Terminal Kinase Has a Key Role in Alzheimer Disease Synaptic Dysfunction in Vivo. *Cell Death Dis.*

2014, 5, e1019, doi:10.1038/cddis.2013.559.

418. Greer, P.L.; Hanayama, R.; Bloodgood, B.L.; Mardinly, A.R.; Lipton, D.M.; Flavell, S.W.; Kim, T.-K.; Griffith, E.C.; Waldon, Z.; Maehr, R.; et al. The Angelman Syndrome Protein Ube3A Regulates Synapse Development by Ubiquitinating Arc. *Cell* **2010**, *140*, 704–716, doi:10.1016/j.cell.2010.01.026.

419. Cy, K.; Dd, Y.; Dr, S.R.; Rj, D.; P, R.; Ra, F. The Jnk1 and Jnk2 Protein Kinases Are Required for Regional Specific Apoptosis During Early Brain Development Available online: [https://pubmed.ncbi.nlm.nih.gov/10230788/?from\\_single\\_result=The+Jnk1+and+Jnk2+protein+kinases+are+required+for+regional+specific+apoptosis+during+early+brain+development](https://pubmed.ncbi.nlm.nih.gov/10230788/?from_single_result=The+Jnk1+and+Jnk2+protein+kinases+are+required+for+regional+specific+apoptosis+during+early+brain+development) (accessed on 27 November 2019).

420. Dd, Y.; Cy, K.; Aj, W.; M, R.; Ts, Z.; Rj, D.; P, R.; Ra, F. Absence of Excitotoxicity-Induced Apoptosis in the Hippocampus of Mice Lacking the Jnk3 Gene Available online: [https://pubmed.ncbi.nlm.nih.gov/9349820/?from\\_single\\_result=Absence+of+excitotoxicity-induced+apoptosis+in+the+hippocampus+of+mice+lacking+the+Jnk3+gene](https://pubmed.ncbi.nlm.nih.gov/9349820/?from_single_result=Absence+of+excitotoxicity-induced+apoptosis+in+the+hippocampus+of+mice+lacking+the+Jnk3+gene) (accessed on 27 November 2019).

421. Wang, J.; Lou, S.-S.; Wang, T.; Wu, R.-J.; Li, G.; Zhao, M.; Lu, B.; Li, Y.-Y.; Zhang, J.; Cheng, X.; et al. UBE3A-Mediated PTPA Ubiquitination and Degradation Regulate PP2A Activity and Dendritic Spine Morphology. *Proc. Natl. Acad. Sci. U. S. A.* **2019**, *116*, 12500–12505, doi:10.1073/pnas.1820131116.

422. Forner, S.; Kawauchi, S.; Balderrama-Gutierrez, G.; Kramár, E.A.; Matheos, D.P.; Phan, J.; Javonillo, D.I.; Tran, K.M.; Hingco, E.; da Cunha, C.; et al. Systematic Phenotyping and Characterization of the 5xFAD Mouse Model of Alzheimer's Disease. *Sci. Data* **2021**, *8*, 270, doi:10.1038/s41597-021-01054-y.

423. Girard, S.D.; Jacquet, M.; Baranger, K.; Migliorati, M.; Escoffier, G.; Bernard, A.; Khrestchatsky, M.; Féron, F.; Rivera, S.; Roman, F.S.; et al. Onset of Hippocampus-Dependent Memory Impairments in 5XFAD Transgenic Mouse Model of Alzheimer's Disease. *Hippocampus* **2014**, *24*, 762–772, doi:10.1002/hipo.22267.

424. Nijboer, C.H.; Bonestroo, H.J.C.; Zijlstra, J.; Kavelaars, A.; Heijnen, C.J. Mitochondrial JNK Phosphorylation as a Novel Therapeutic Target to Inhibit Neuroinflammation and Apoptosis after Neonatal Ischemic Brain Damage. *Neurobiol. Dis.* **2013**, *54*, 432–444, doi:10.1016/j.nbd.2013.01.017.

425. Badshah, H.; Ali, T.; Rehman, S.; Amin, F.; Ullah, F.; Kim, T.H.; Kim, M.O. Protective Effect of Lupeol Against Lipopolysaccharide-Induced Neuroinflammation via the P38/c-Jun N-Terminal Kinase Pathway in the Adult Mouse Brain. *J. Neuroimmune Pharmacol.* **2016**, *11*, 48–60, doi:10.1007/s11481-015-9623-z.

426. Anfinogenova, N.D.; Quinn, M.T.; Schepetkin, I.A.; Atochin, D.N. Alarmins and C-Jun N-Terminal Kinase (JNK) Signaling in Neuroinflammation. *Cells* **2020**, *9*, 2350, doi:10.3390/cells9112350.

427. Baranger, K.; Giannoni, P.; Girard, S.D.; Girot, S.; Gaven, F.; Stephan, D.; Migliorati, M.; Khrestchatsky, M.; Bockaert, J.; Marchetti-Gauthier, E.; et al. Chronic Treatments with a 5-HT<sub>4</sub> Receptor Agonist Decrease Amyloid Pathology in the Entorhinal Cortex and Learning and Memory Deficits in the 5xFAD Mouse Model of Alzheimer's Disease. *Neuropharmacology* **2017**, *126*, 128–141, doi:10.1016/j.neuropharm.2017.08.031.

428. Kitazawa, M.; Medeiros, R.; Laferla, F.M. Transgenic Mouse Models of Alzheimer Disease: Developing a Better Model as a Tool for Therapeutic Interventions. *Curr. Pharm. Des.* **2012**, *18*, 1131–1147, doi:10.2174/138161212799315786.

429. Giovannini, M.G.; Cerbai, F.; Bellucci, A.; Melani, C.; Grossi, C.; Bartolozzi, C.; Nosi, D.; Casamenti, F. Differential Activation of Mitogen-Activated Protein Kinase Signalling Pathways in the Hippocampus of CRND8 Transgenic Mouse, a Model of Alzheimer's Disease. *Neuroscience* **2008**, *153*, 618–633, doi:10.1016/j.neuroscience.2008.02.061.

430. Guntupalli, S.; Jang, S.E.; Zhu, T.; Haganir, R.L.; Widagdo, J.; Anggono, V. GluA1 Subunit Ubiquitination Mediates Amyloid- $\beta$ -Induced Loss of Surface  $\alpha$ -Amino-3-Hydroxy-5-Methyl-4-Isioxazolepropionic Acid (AMPA) Receptors. *J. Biol. Chem.* **2017**, *292*, 8186–8194, doi:10.1074/jbc.M116.774554.

431. Colombo, A.; Bastone, A.; Ploia, C.; Scip, A.; Salmona, M.; Forloni, G.; Borsello, T. JNK Regulates APP Cleavage and Degradation in a Model of Alzheimer's Disease. *Neurobiol. Dis.* **2009**, *33*, 518–525, doi:10.1016/j.nbd.2008.12.014.

432. Ploia, C.; Antoniou, X.; Scip, A.; Grande, V.; Cardinetti, D.; Colombo, A.; Canu, N.; Benussi, L.; Ghidoni, R.; Forloni, G.; et al. JNK Plays a Key Role in Tau Hyperphosphorylation in Alzheimer's Disease Models. *J. Alzheimers Dis. JAD* **2011**, *26*, 315–329, doi:10.3233/JAD-2011-110320.

433. Kimberly, W.T.; Zheng, J.B.; Town, T.; Flavell, R.A.; Selkoe, D.J. Physiological Regulation of the  $\beta$ -Amyloid Precursor Protein Signaling Domain by c-Jun N-Terminal Kinase JNK3 during Neuronal Differentiation. *J. Neurosci.* **2005**, *25*, 5533–5543, doi:10.1523/JNEUROSCI.4883-04.2005.

434. Yoon, S.O.; Park, D.J.; Ryu, J.C.; Ozer, H.G.; Tep, C.; Shin, Y.J.; Lim, T.H.; Pastorino, L.; Kunwar, A.J.; Walton, J.C.; et al. JNK3 Perpetuates Metabolic Stress Induced by Abeta Peptides. *Neuron* **2012**, *75*, 824–837,

doi:10.1016/j.neuron.2012.06.024.

435. Wang, S.; Li, K.; Zhao, S.; Zhang, X.; Yang, Z.; Zhang, J.; Zhang, T. Early-Stage Dysfunction of Hippocampal Theta and Gamma Oscillations and Its Modulation of Neural Network in a Transgenic 5xFAD Mouse Model. *Neurobiol. Aging* **2020**, *94*, 121–129, doi:10.1016/j.neurobiolaging.2020.05.002.

436. Gourmaud, S.; Paquet, C.; Dumurgier, J.; Pace, C.; Bouras, C.; Gray, F.; Laplanche, J.-L.; Meurs, E.F.; Mouton-Liger, F.; Hugon, J. Increased Levels of Cerebrospinal Fluid JNK3 Associated with Amyloid Pathology: Links to Cognitive Decline. *J. Psychiatry Neurosci. JPN* **2015**, *40*, 151–161, doi:10.1503/jpn.140062.

437. Guo, C.; Whitmarsh, A.J. The  $\beta$ -Arrestin-2 Scaffold Protein Promotes c-Jun N-Terminal Kinase-3 Activation by Binding to Its Nonconserved N Terminus \*. *J. Biol. Chem.* **2008**, *283*, 15903–15911, doi:10.1074/jbc.M710006200.

438. McDonald, P.H.; Chow, C.W.; Miller, W.E.; Laporte, S.A.; Field, M.E.; Lin, F.T.; Davis, R.J.; Lefkowitz, R.J. Beta-Arrestin 2: A Receptor-Regulated MAPK Scaffold for the Activation of JNK3. *Science* **2000**, *290*, 1574–1577, doi:10.1126/science.290.5496.1574.

439. Gasparini, L.; Dityatev, A. Beta-Amyloid and Glutamate Receptors. *Exp. Neurol.* **2008**, *212*, 1–4, doi:10.1016/j.expneurol.2008.03.005.

440. Parameshwaran, K.; Dhanasekaran, M.; Suppiramaniam, V. Amyloid Beta Peptides and Glutamatergic Synaptic Dysregulation. *Exp. Neurol.* **2008**, *210*, 7–13, doi:10.1016/j.expneurol.2007.10.008.

441. Almeida, C.G.; Tampellini, D.; Takahashi, R.H.; Greengard, P.; Lin, M.T.; Snyder, E.M.; Gouras, G.K. Beta-Amyloid Accumulation in APP Mutant Neurons Reduces PSD-95 and GluR1 in Synapses. *Neurobiol. Dis.* **2005**, *20*, 187–198, doi:10.1016/j.nbd.2005.02.008.

442. Balducci, C.; Beeg, M.; Stravalaci, M.; Bastone, A.; Sclip, A.; Biasini, E.; Tapella, L.; Colombo, L.; Manzoni, C.; Borsello, T.; et al. Synthetic Amyloid- $\beta$  Oligomers Impair Long-Term Memory Independently of Cellular Prion Protein. *Proc. Natl. Acad. Sci.* **2010**, doi:10.1073/pnas.0911829107.

443. Lacor, P.N.; Buniel, M.C.; Furlow, P.W.; Clemente, A.S.; Velasco, P.T.; Wood, M.; Viola, K.L.; Klein, W.L. A $\beta$  Oligomer-Induced Aberrations in Synapse Composition, Shape, and Density Provide a Molecular Basis for Loss of Connectivity in Alzheimer's Disease. *J. Neurosci.* **2007**, *27*, 796–807, doi:10.1523/JNEUROSCI.3501-06.2007.

444. Massignan, T.; Cimini, S.; Stincardini, C.; Cerovic, M.; Vanni, I.; Elezgarai, S.R.; Moreno, J.; Stravalaci, M.; Negro, A.; Sangiovanni, V.; et al. A Cationic Tetrapyrrole Inhibits Toxic Activities of the Cellular Prion Protein. *Sci. Rep.* **2016**, *6*, 23180, doi:10.1038/srep23180.

## Publications:

1. *JNK signaling provides a novel therapeutic target for Rett syndrome.*

**Musi CA**, Castaldo AM, Valsecchi AE, Cimini S, Morello N, Pizzo R, Renieri A, Meloni I, Bonati M, Giustetto M, Borsello T. *BMC Biol.* 2021 Dec 16;19(1):256. doi: 10.1186/s12915-021-01190-2. PMID: 34911542 Free PMC article. PMID: 34794851

2. *Common pathways in dementia and diabetic retinopathy: understanding the mechanisms of diabetes-related cognitive decline.*

Little K, Llorián-Salvador M, Scullion S, Hernández C, Simó-Servat O, Del Marco A, Bosma E, Vargas-Soria M, Carranza-Naval MJ, Van Bergen T, Galbiati S, Viganò I, **Musi CA**, Schlingemann R, Feyen J, Borsello T, Zerbini G, Klaassen I, Garcia-Alloza M, Simó R, Stitt AW; RECOGNISED consortium (GA 847749). *Trends Endocrinol Metab.* 2022 Jan;33(1):50-71. doi: 10.1016/j.tem.2021.10.008. Epub 2021 Nov 15. PMID: 34794851 Review. PMID: 34459572

3. *Super-resolution study of PIAS SUMO E3-ligases in hippocampal and cortical neurons.*

Conz A, **Musi CA**, Russo L, Borsello T, Colnaghi L. *Eur J Histochem.* 2021 Aug 11;65(s1):3241. doi: 10.4081/ejh.2021.3241. PMID: 34459572 Free PMC article. PMID: 33113832

4. *Neuronal Localization of SENP Proteins with Super Resolution Microscopy.*

Colnaghi L, Conz A, Russo L, **Musi CA**, Fioriti L, Borsello T, Salmona M. *Brain Sci.* 2020 Oct 25;10(11):778. doi: 10.3390/brainsci10110778. PMID: 33113832 Free PMC article. PMID: 32998477

5. *JNK3 as Therapeutic Target and Biomarker in Neurodegenerative and Neurodevelopmental Brain Diseases.*

**Musi CA**, Agrò G, Santarella F, Iervasi E, Borsello T. *Cells.* 2020 Sep 28;9(10):2190. doi: 10.3390/cells9102190. PMID: 32998477 Free PMC article. Review. PMID: 32087286

6. *JNK signaling activation in the Ube3a maternal deficient mouse model: its specific inhibition prevents post-synaptic protein-enriched fraction alterations and cognitive deficits in Angelman Syndrome model.*

**Musi CA**, Agrò G, Buccarello L, Camuso S, Borsello T. *Neurobiol Dis.* 2020 Jul;140:104812. doi: 10.1016/j.nbd.2020.104812. Epub 2020 Feb 19. PMID: 32087286. PMID: 30315879

7. *The Stress c-Jun N-terminal Kinase Signaling Pathway Activation Correlates with Synaptic Pathology and Presents A Sex Bias in P301L Mouse Model of Tauopathy.*

Buccarello L, **Musi CA**, Turati A, Borsello T. *Neuroscience.* 2018 Nov 21;393:196-205. doi:10.1016/j.neuroscience.2018.09.049. Epub 2018 Oct 11. PMID: 30315879